The Role of SAMSN1 in Multiple Myeloma

Natasha Lauren Friend

Myeloma Research Laboratory
Adelaide Medical School
Faculty of Health and Medical Sciences
The University of Adelaide
&
Cancer Theme
South Australian Health and Medical Research Institute
(SAHMRI)

A thesis submitted to the University of Adelaide
for the degree of Doctor of Philosophy
August 2019

TABLE OF CONTENTS

ABSTRACT

Multiple myeloma (MM) is a haematological malignancy characterised by the uncontrolled clonal proliferation of neoplastic plasma cells (PCs) within the bone marrow (BM). Our group previously identified a homozygous deletion of *Samsn1*, a gene encoding a putative adaptor protein, in the genome of the MM-prone C57BL/KaLwRij mouse strain. In addition, the re-expression of Samsn1 in the C57BL/KaLwRij-derived 5TGM1 MM PC line was shown to inhibit tumour growth *in vivo*. Furthermore, *SAMSN1* expression was found to be down-regulated in the PCs of MM patients compared to healthy controls. Collectively, these data suggested that *SAMSN1* may be a novel tumour suppressor gene in MM.

The fact that *Samsn1*$^{-/-}$ C57BL/KaLwRij mice develop MM with late onset and incomplete penetrance suggested that *Samsn1* loss may co-operate with another lesion to drive disease development. In this thesis, bioinformatic analysis revealed that the down-regulation of the tumour suppressor *GLIPR1* was significantly associated with reduced *SAMSN1* expression in the PCs of MM patients. *Glipr1* expression was found to be absent in 5TGM1 cells and its re-introduction reduced tumour growth *in vivo*, although this did not reach statistical significance. In addition, *Samsn1* and *Glipr1* double knockout mice were generated and monitored for clonal PC expansions for one year. These mice were not found to display enhanced PC abnormalities compared to wildtype mice, suggesting that the concomitant loss of *Samsn1* and *Glipr1* is insufficient to promote MM development within this timeframe.

Although Samsn1 was previously shown to negatively regulate the proliferation and cytoskeletal remodelling of activated B cells, the mechanism(s) by which it inhibited 5TGM1 tumour formation was yet to be determined. In this thesis, Samsn1 was found to inhibit the growth of metastatic, but not primary, 5TGM1 tumours following intratibial injection into C57BL/KaLwRij mice but had no effect on the BM homing of 5TGM1 cells *in vivo*. These data suggest that Samsn1 may promote the action of anti-tumour factors from within the BM microenvironment. In addition, Samsn1 was found to not inhibit 5TGM1 tumour growth in immunodeficient mice and to promote the cytotoxicity of C57BL/KaLwRij-derived $CD8^+$ T cells towards 5TGM1 cells. These findings suggest that Samsn1 may enhance immune system-mediated targeting of MM PCs. Notably, Samsn1 was found to inhibit 5TGM1 tumour growth in immunocompetent C57BL/*Samsn1*$^{-/-}$ mice, but not wildtype C57BL/6 mice, and anti-Samsn1 antibodies were detected in the serum of a *Samsn1*$^{-/-}$ mouse. These data suggest that the increased immunogenicity of Samsn1-

expressing 5TGM1 cells in C57BL/KaLwRij mice may be due to the presence of adaptive immune cells that recognise Samsn1 as a foreign antigen in this *Samsn1*$^{-/-}$ mouse strain. As SAMSN1-specific immune cells will be deleted by tolerance processes in patients, the findings from the 5TGM1/KaLwRij model no longer support a potential tumour suppressor role for SAMSN1 in human MM. Given that SAMSN1 levels were found to have no effect on the growth of human MM cell lines *in vitro* or *in vivo*, the current weight of evidence suggests that *SAMSN1* is unlikely to be an important tumour suppressor gene in MM.

DECLARATION

I certify that this work contains no material which has been accepted for the award of any other degree or diploma in my name in any university or other tertiary institution and, to the best of my knowledge and belief, contains no material previously published or written by another person, except where due reference has been made in the text. In addition, I certify that no part of this work will, in the future, be used in a submission in my name for any other degree or diploma in any university or other tertiary institution without the prior approval of the University of Adelaide and where applicable, any partner institution responsible for the joint award of this degree.

I give permission for the digital version of my thesis to be made available on the web, via the University's digital research repository, the Library Search and also through web search engines, unless permission has been granted by the University to restrict access for a period of time. I acknowledge the support I have received for my research through the provision of an Australian Government Research Training Program Scholarship.

Signed:

.....

Natasha Friend Date: 29th August 2019

ACKNOWLEDGEMENTS

Firstly, I would like to thank my supervisors Prof Andrew Zannettino and Dr Duncan Hewett for all your guidance and support throughout my PhD studies and in the preparation of this thesis. Andrew, thank you for giving me the opportunity to undertake my PhD studies in the Myeloma Research Laboratory with you and your fantastic team. I am particularly appreciative of your well-considered and timely reviewing of my thesis during a very busy period. I feel extremely fortunate to have had the pleasure of also being supervised by the always knowledgeable and patient Duncan. Your constant encouragement, understanding and sense of humour has been indispensable in getting me to this point.

Thank you to all my colleagues in the Myeloma Research Laboratory and the Mesenchymal Stem Cell Laboratory for your assistance and friendship throughout my candidature. You are a very special group of kind and talented people, who it was a pleasure to learn from, work alongside and hang out with. Special thanks to Bill and Jacquie for your assistance with animal work, Kate for your help with bioinformatics, Sally for your technical assistance with histology and Steve for your advice regarding co-immunoprecipitation. Many thanks also to Duncan, Vicki, Elyse, Kim and Khatora for giving so generously of your time to masterfully assist with my big mouse days.

Undoubtedly, one of the highlights of my PhD experience has been the friendships I have formed with the other students within the laboratory. You have been incredibly caring, generous and loyal allies who have helped me through the difficult times. Thank you to Krzysztof, Ankit and Chee Man for your advice, understanding and for showing us all how it's done. Many thanks also to Mara, Khatora and Alanah for your invaluable friendship and for listening to me ramble on at lunchtime or on the train. Special thanks to Kim, my partner in crime from the beginning, I could not have hoped for a more supportive, humble and inspiring companion on this rollercoaster ride of a PhD. Thank you all for indulging my penchant for green tea ice-cream and karaoke, and I can't wait to see all the amazing things you will achieve in your lives and careers.

Many other people outside of the laboratory have made an important contribution to this project. Thank you to Dr Mark Van der Hoek and the staff of the David Gunn Genomics Facility at SAHMRI for your assistance with generating RNA-seq data. Thanks to Dr Chung Hoow Kok and Dr Jimmy Breen for your help with bioinformatics and to Sophie Kogoj for

your assistance with histology. Thanks also to Prof Paul Thomas, Melissa White, Sandie Piltz and the team at the South Australian Genome Editing Facility for your help in generating the *Glipr1* knockout mice. In addition, I am very grateful to the always obliging Randall Grose and Sophie Watts of the SAHMRI Flow Cytometry Facility for your invaluable assistance in experimental planning and execution. Furthermore, I must express my thanks to the dedicated staff of the SAHMRI Bioresources Facility, particularly Nicole, Rianna and Carly, for your help with animal work. Special thanks also to the Bioresources veterinarian Dr Lewis Vaughan for your incredible patience and understanding during my training. I would also like to acknowledge the financial support I received from the M F & M H Joyner Scholarship in Medicine and George Fraser Supplementary Scholarship.

On a personal note, I am very thankful for the kindness and encouragement I received from my amazing friends over the past four years, especially Eloise, Ashleigh, Thomas, Eboni, Hollie and Amelia. Thank you for always caring, never judging and always bringing a smile to my face. I would also like to thank all the members of my extended family for your love and understanding over the past few years. In particular, I wish to express my gratitude to Gran for your unwavering belief in me always.

Finally, I can never express how grateful I am for the unconditional love and support I received from my parents Robert and Vicki over the past four years and throughout my studies. While you may have not always understood the details of what I was up to in the laboratory, you always understood when I was struggling and went above and beyond to help me get back on track. Without a doubt, I would never have reached this point without both of you and I feel that this thesis is very much our achievement. Love you loads.

Thank you!

ABBREVIATIONS

αMEM	Minimum Essential Medium Eagle, Alpha Modification
AID	activation-induced cytidine deaminase
ANOVA	analysis of variance
ASCT	autologous stem cell transplant
ATCC	American Type Culture Collection
BCR	B cell receptor
BLI	bioluminescence imaging
BM	bone marrow
BMMNC	bone marrow mononuclear cell
BMSC	bone marrow stromal cell
CAR	chimeric antigen receptor
cDNA	complementary DNA
CNA	copy number alteration
CPM	copies per million
CRAB	hypercalcemia, renal insufficiency, anaemia and bone lesions
CTL	cytotoxic T lymphocyte
CXCL	chemokine (C-X-C motif) ligand
DAVID	Database for Annotation, Visualization and Integrated Discovery
DMEM	Dulbecco's Modified Eagle Medium
DNA	deoxyribonucleic acid
dNTP	deoxyribonucleotide triphosphate
EMD	extramedullary disease
EV	empty vector
F-actin	filamentous actin
FCS	fetal calf serum
FDA	Food and Drug Administration
FDR	false discovery rate
FLC	free light chain
FMO	fluorescence minus one
GEP	gene expression profiling
GFP	green fluorescent protein
gRNA	guide RNA
GWAS	genome-wide association study

HDAC	histone deacetylase
HDT	high dose therapy
HEK	human embryonic kidney
HMCL	human myeloma cell line
i.t.	intratibial
i.v.	intravenous
IgH	immunoglobulin heavy chain
IgM	immunoglobulin M
IHC	immunohistochemistry
IL	interleukin
IMDM	Iscove's Modified Dulbecco's Medium
IMiD	immunomodulatory imide drug
IP	immunoprecipitation
ISS	International Staging System
KD	knockdown
LIMMA	linear models for microarray data
MACS	magnetic-activated cell sorting
MFI	mean fluorescence intensity
MGUS	monoclonal gammopathy of undetermined significance
MHC	major histocompatibility complex
miRNA	microRNA
MM	multiple myeloma
MRI	magnetic resonance imaging
mRNA	messenger RNA
mSMART	Mayo Stratification of Myeloma and Risk-Adapted Therapy
NDMM	newly diagnosed multiple myeloma
NF	nuclease free
NF-κB	nuclear factor κ-light-chain-enhancer of activated B cells
NGS	next generation sequencing
NK	natural killer
NSG	NOD SCID gamma
NTC	no template control
OS	overall survival
PAGE	polyacrylamide gel electrophoresis
PB	peripheral blood

PBS	phosphate buffered saline
PC	plasma cell
PCL	plasma cell leukemia
PCR	polymerase chain reaction
PFS	progression free survival
RIPA	radioimmunoprecipitation assay
RISS	Revised International Staging System
RMA	robust multi-array average
RNA	ribonucleic acid
RPMI	Roswell Park Memorial Institute
RT	reverse transcription
SAM	sterile alpha motif
SD	standard deviation
SDS	sodium dodecyl sulphate
SEM	standard error of the mean
SH3	src homology 3
SMM	smouldering multiple myeloma
SNP	single nucleotide polymorphism
SPEP	serum protein electrophoresis
TrHBMEC	transformed human bone marrow endothelial cell
TTP	time to progression
USA	United States of America
VCD	Velcade (bortezomib), cyclophosphamide and dexamethasone
VRD	Velcade (bortezomib), Revlimid (lenalidomide) and dexamethasone
WES	whole exome sequencing
WT	wildtype

PUBLICATIONS

Scientific Manuscripts

1. **Friend N.**, Noll J.E., Panagopoulos V., Hewett D.R., Zannettino A.C.W. (2019). Investigating the role of SAMSN1 in multiple myeloma. *Manuscript in preparation*.

2. **Friend N.**, Noll J.E., Vandyke K., Oppermann K.S., Clark K.C., Hewett D.R., Zannettino A.C.W. (2019). Investigating the role of GLIPR1 in multiple myeloma. *Manuscript in preparation*.

3. Hewett D.R., Vandyke K., Lawrence D.M., **Friend N.**, Noll J.E., Geoghegan J., Croucher P.I., Zannettino A.C.W. (2017). DNA Barcoding reveals habitual clonal dominance of myeloma plasma cells in the bone marrow microenvironment. *Neoplasia*, 19(4):972-81.

Conference Proceedings

1. **Friend N.**, Panagopoulos V., Hewett D.R. & Zannettino A.C.W. (2018). Investigating the tumour suppressor role of SAMSN1 in multiple myeloma. *SAHMRI Scientific Showcase 2018.* Adelaide, Australia, November 2018. Poster presentation.

2. **Friend N.**, Panagopoulos V., Hewett D.R. & Zannettino A.C.W. (2018). SAMSN1 inhibits the metastasis of multiple myeloma cells via an immune-dependent mechanism. *Florey Postgraduate Conference 2018*. Adelaide, Australia, September 2018. Poster presentation.

3. **Friend N.**, Noll J.E., Panagopoulos V., Hewett D.R. & Zannettino A.C.W. (2018). SAMSN1 inhibits the metastasis of multiple myeloma cells via an immune-dependent mechanism. *SA ASMR Scientific Meeting 2018*. Adelaide, Australia, June 2018. Oral presentation.

4. **Friend N.**, Noll J.E., Panagopoulos V., Hewett D.R. & Zannettino A.C.W. (2018). SAMSN1 inhibits the metastasis of multiple myeloma cells. *New Directions in*

Leukemia Research Meeting 2018. Brisbane, Australia, March 2018. Poster Presentation.

5. **Friend N.**, Noll J.E., Panagopoulos V., Kok C.H., Hewett D.R. & Zannettino A.C.W. (2017). SAMSN1 inhibits the metastasis of multiple myeloma cells. *SAHMRI Scientific Showcase 2017*. Adelaide, Australia, November 2017. Poster presentation.

6. **Friend N.**, Noll J.E., Panagopoulos V., Kok C.H., Hewett D.R. & Zannettino A.C.W. (2017). SAMSN1 inhibits the metastasis of multiple myeloma cells. *Florey Postgraduate Conference 2017*. Adelaide, Australia, September 2017. Poster presentation.

7. **Friend N.**, Noll J.E., Panagopoulos V., Kok C.H., Hewett D.R. & Zannettino A.C.W. (2017). SAMSN1 inhibits the metastasis of multiple myeloma cells. *SA ASMR Scientific Meeting 2017*. Adelaide, Australia, June 2017. Oral presentation.

8. **Friend N.**, Clark K.C., Noll J.E., Vandyke K., Kok C.H., Hewett D.R. & Zannettino A.C.W. (2016). Investigating the role of *SAMSN1* and *GLIPR1* in multiple myeloma. *SA ASMR Scientific Meeting 2016*. Adelaide, Australia, June 2016. Oral presentation.

1 INTRODUCTION

1.1 Multiple myeloma: Clinical description

Multiple myeloma (MM) is a haematological malignancy of plasma cells (PCs), the terminally-differentiated and antibody-producing cells of the B cell lineage. This cancer is characterised by the clonal expansion of neoplastic PCs within the bone marrow (BM), which produce large amounts of a non-functional monoclonal immunoglobulin, also known as a paraprotein/M protein, that can be detected in blood serum and urine (light chain only)[1]. MM displays a high degree of heterogeneity both biologically (underlying genetic abnormalities) and clinically (response to treatment and outcome)[2]. There are premalignant PC proliferative disorders associated with MM and the disease can also progress to more advanced stages with inferior prognosis. Although recent treatment advances have improved the outcomes for MM patients, the majority of patients relapse with refractory disease and thus MM remains largely incurable[3].

1.1.1 Epidemiology

MM accounts for ~10% of haematological malignancies and ~1% of all cancers[1,4]. In Australia, 1,885 new cases of MM were diagnosed in 2015, with an age standardised incidence rate of 6.9 cases per 100,000[5]. The incidence of MM is higher in developed countries, such as Australia, the United States of America (USA) and the United Kingdom, which is likely due to increased awareness and better diagnostic capabilities[1]. MM is primarily a disease of older adults, with a median age at diagnosis of 71.5 years in Australia[5]. The adjusted prevalence rates of MM among males are ~50% higher than those among females[5,6]. There are also disparities in the incidence of MM according to ethnicity, with MM found to occur twice as frequently in people with African heritage compared to Caucasians[6]. The median overall survival (OS) for MM is ~6 years[7], which is consistent with the most recently reported Australian five-year relative survival rate of 50.7% (2011-2015)[5].

1.1.2 Clinical manifestations

The major clinical manifestations of MM are due to either the direct effects of expanded clonal PCs within the BM or indirect effects of their by-products on other organs. The major cause of morbidity for MM is bone disease, which causes pain and pathologic fractures in ~60% of cases[8]. The bone disease results from lytic lesions, which are generated due to the increased number and activity of bone-resorptive osteoclasts and the decreased number and activity of bone-forming osteoblasts within the BM[8]. These abnormalities can be attributed

to the altered production of key signalling molecules involved in bone homeostasis, including receptor activator of nuclear factor-κB ligand (RANKL)[9-11], osteoprotegerin (OPG)[10,11], stromal-derived factor-1α (SDF-1α/CXCL12)[12] and dickkopf-related protein 1 (DKK1)[13], by MM PCs and/or BM stromal cells (BMSCs). A related clinical feature of MM is high levels of calcium in the blood (hypercalcemia), which occurs as a result of osteolysis[14]. This complication arises in approximately one third of MM cases and can cause a range of symptoms, including nausea and confusion[14]. Hypercalcemia and the large amount of MM PC-derived free monoclonal immunoglobulin light chains (FLC) in the blood promotes the development of renal insufficiency, which occurs in ~20-40% of MM patients[15]. In addition, anaemia occurs in almost all MM patients, which can cause debilitating fatigue[16]. The reduction in red blood cell number has been attributed to a number of factors, including marrow replacement by tumour cells, decreased erythropoietin production from impaired kidneys and/or cytokine-mediated marrow suppression[16]. Together hypercalcemia, renal insufficiency, anaemia and bone lesions constitute the common set of clinical manifestations of MM known as the CRAB features[17]. Furthermore, another major cause of morbidity and mortality in MM is infection, which is attributable to the immune suppression present in almost all MM patients due to underlying disease biology and/or therapy[18].

1.1.3 Disease stages

1.1.3.1 Monoclonal gammopathy of undetermined significance

All cases of malignant MM are preceded by the premalignant, asymptomatic condition monoclonal gammopathy of undetermined significance (MGUS), characterised by a clonal proliferation of PCs in the BM[19,20]. For a diagnosis of MGUS three criteria must be met: (1) serum monoclonal protein < 3 g/dL, (2) clonal BM PCs < 10% and (3) absence of end-organ damage, such as the CRAB features, that is related to the PC dyscrasia (Table 1.1)[21]. MGUS is a common disorder in older individuals, with an estimated prevalence of 3-4% in people over 50 years of age[22,23]. The risk of progression from MGUS to overt MM is a persistent 1% per year, but the time to progression (TTP) is highly variable, with the majority of MGUS cases never progressing to symptomatic disease[24,25]. Currently, it is not possible to accurately predict if, or when, MGUS will progress on an individual level, but markers of increased abnormal PC bulk (M protein ≥ 1.5g/dL and serum FLC ratio > 1.65) have been associated with an increased risk of progression[25,26]. A recent study found that the lifetime risk of progression to MM was 30% for MGUS patients who have both elevated M protein and an

Table 1.1: International Myeloma Working Group diagnostic criteria for MM and related PC disorders[21,27].

Monoclonal gammopathy of undetermined significance (MGUS)	All 3 criteria must be met: • Serum monoclonal protein (non-IgM type) < 3 g/dL • Clonal BM PCs < 10% • Absence of end-organ damage such as hypercalcemia, renal insufficiency, anaemia, and bone lesions (CRAB) that can be attributed to the PC proliferative disorder
Smouldering multiple myeloma (SMM)	Both criteria must be met: • Serum monoclonal protein ≥ 3 g/dL, or urinary monoclonal protein > 500 mg per 24 hours and/or clonal BM PCs 10%-60% • Absence of myeloma defining events (MDEs) or amyloidosis
Multiple myeloma (MM)	Both criteria must be met: • Clonal BM PCs ≥ 10% or biopsy-proven bony or extramedullary plasmacytoma • Any one or more of the following MDEs: o Evidence of end organ damage that can be attributed to the underlying PC proliferative disorder, specifically: ▪ Hypercalcemia: serum calcium > 0.25 mM (> 1 mg/dL) higher than the upper limit of normal or > 2.75 mM (>11 mg/dL) ▪ Renal insufficiency: creatinine clearance < 40 mL per minute or serum creatinine > 2 mg/dL ▪ Anaemia: haemoglobin value of > 2 g/dL below the lower limit of normal or a haemoglobin value < 10 g/dL ▪ Bone lesions: one or more osteolytic lesions on skeletal radiography, computed tomography, or positron emission tomography-CT o Clonal BM PCs ≥ 60% o Involved:uninvolved serum FLC ratio ≥ 100 (involved FLC level must be ≥ 100 mg/L) o ≥ 2 focal lesions on magnetic resonance imaging (MRI) studies (at least 5 mm in size)
Secondary plasma cell leukaemia (PCL)	Both criteria must be met: • Meet the criteria for a diagnosis of MM • Peripheral blood PC count of 2×10^9/L or > 20% of the differential white blood cell count

abnormal FLC ratio, 20% for those who have one of these factors and only 7% for those who have neither risk factor[25]. The recommended management of MGUS patients is ongoing monitoring for disease progression, the frequency of which depends on their risk stratification[28,29].

1.1.3.2 Smouldering MM

Smouldering MM (SMM) is an intermediate disease stage between MGUS and MM that is still an asymptomatic PC proliferative disorder but is more advanced than MGUS (Table 1.1)[21,30]. SMM is a clinically-defined entity that includes patients with asymptomatic, early MM, who rapidly progress to end organ damage, and more indolent MGUS-like cases, who have a much lower rate of disease progression[31]. Consistent with this, the risk of progression for SMM patients is 10% per year for the first five years post-diagnosis but decreases to 3% per year over the next five years and 1.5% per year thereafter[30]. This means that 50% of SMM cases, probably those with asymptomatic malignancy, progress to MM in the first five years post-diagnosis, while one third of SMM cases, most likely those with biological premalignancy, do not progress within the first 10 years[30]. Several factors have been found to predict for a high risk of progression in SMM patients, including BM PCs > 20%[30], evolving M protein levels[32,33], an abnormal PC immunophenotype[34], serum FLC ratio ≥ 8[35] and suppression of ≥ 2 uninvolved immunoglobulins (immunoparesis)[30,34].

Studies showed that SMM patients with ≥ 60% clonal BM PCs[36,37], a serum FLC ratio ≥ 100[37,38] and ≥ 2 focal lesions on MRI[39,40] had an ~80% risk of progressing to symptomatic MM within two years. In addition, the first randomised trial in which early treatment was assessed in high-risk SMM patients found that it increased the TTP and OS of these patients[41,42]. Consequently, the 10-15% of SMM patients that had one or more of these biomarkers, and thus an ultra-high-risk of progression, were reclassified as having MM requiring treatment in 2014[21]. For the remaining SMM patients, a recent study found that BM PCs > 20%, M protein > 2 g/dL and a serum FLC ratio > 20 were independent predictors of progression to MM, which led to the development of the Mayo "20-2-20" risk stratification system[43]. SMM patients with two or more of the "20-2-20" risk factors (~36%) were found to have an ~50% risk of progressing to MM within two years and thus were classified as high-risk[43]. The current standard of care for SMM involves the close monitoring of patients for disease progression[29]. Interestingly, this diligent follow-up may be responsible

for the finding that the OS of MM patients with a prior diagnosis of SMM was higher compared to those with a prior diagnosis of MGUS[44].

1.1.3.3 Multiple myeloma

The updated diagnostic criteria for MM stipulate that patients must have ≥ 10% clonal BM PCs and at least one myeloma-defining event (MDE), which consist of characteristic end-organ damage (CRAB features, section 1.1.2) and the three new biomarkers of progressive asymptomatic disease (section 1.1.3.2; Table 1.1)[21]. Notably, the current description of MM does not include a measure of M protein, as 15-20% of MM cases only produce immunoglobulin light chains and 3% of MM patients have non-secretory disease[16,45]. The risk stratification of newly diagnosed MM patients was previously based on the International Staging System (ISS), which used two measures of tumour burden, β2-microglobulin and serum albumin levels, to generate three risk groups (Table 1.2)[46]. A Revised ISS (RISS) was subsequently proposed that had improved prognostic power due to the addition of two factors related to disease biology, serum lactate dehydrogenase levels and high-risk cytogenetic abnormalities (sections 1.2.3 and 1.2.4.3; Table 1.2)[47]. In addition, there is the Mayo Stratification of Myeloma and Risk-Adapted Therapy (mSMART) staging system, which takes into account additional cytogenetic/genetic factors and gene expression profiling (GEP, section 1.2.5; Table 1.2)[48,49].

1.1.3.4 Plasma cell leukaemia and extramedullary disease

MM continues to progress post diagnosis, as is evidenced by the inevitable relapse of symptomatic and refractory disease following treatment[1]. In the later stages of MM, the malignant PCs can lose their dependence on the BM microenvironment and can be found growing at other sites in the body[50]. MM PCs can undergo a leukemic progression, resulting in many tumour cells being present in the peripheral circulation, which is known as plasma cell leukaemia (PCL)[51,52]. The current diagnostic criteria for PCL are ≥ 20% circulating PCs and/or > 2 x 10^9 PC/L in the peripheral blood, which occurs in 1-2% of MM patients (Table 1.1)[27]. The median TTP from a diagnosis of MM to PCL is 31 months[53] and PCL is associated with a very inferior prognosis[54,55]. Recent studies have found that cases with circulating PCs ≥ 5% have a similarly poor prognosis compared to cases with circulating PCs ≥ 20%, suggesting that the diagnostic criteria for PCL should be revised[55-57]. MM PCs can also infiltrate other anatomical sites distant to the BM and adjacent soft tissue, which is known as extramedullary disease (EMD)[58]. The frequency of EMD in relapsed MM patients

Table 1.2: Common risk stratification systems for MM patients.

System	Variables	Stages
International Staging System (ISS)[46]	Serum albumin and β2m levels	•I: serum albumin ≥ 3.5 g/dL and β2m < 3.5 mg/dL •II: neither stage I nor III •III: β2m > 5.5 mg/dL
Revised International Staging System (RISS)[47]	Serum albumin, β2m, LDH levels and high-risk cytogenetics (del(17p), t(4;14) or t(14;16))	•I: ISS stage I, LDH normal, and no high-risk cytogenetics •II: neither stage I nor stage III •III: ISS stage III plus abnormal LDH or high-risk cytogenetics
mSMART risk staging[48,49]	RISS, high-risk genetic abnormalities, GEP	•Standard risk: no high-risk factors •High risk: RISS III, t(4;14), t(14;16), t(14;20), del(17p), *TP53* mutation, gain 1q, GEP high-risk signature

β2m = β2-microglobulin, del = deletion, LDH = lactate dehydrogenase, GEP = gene expression profiling, mSMART = Mayo Stratification of Myeloma and Risk-Adapted Therapy.

is 6-16% and the most common extramedullary sites of MM PC growth include the lung, pleura, liver and central nervous system[59-63]. Relapsed patients with EMD also have a significantly poorer prognosis compared to other relapsed patients, with a median survival of 5-16 months from EMD diagnosis[61-63]. Notably, most human myeloma cell lines (HMCLs) are derived from relapsed MM patients with PCL or EMD and thus grow independently of BM-derived factors *in vitro*[64].

1.1.4 Treatment

The outcomes for MM patients have improved significantly over the past 15 years and can largely be attributed to the increased use of autologous stem cell transplants (ASCT) and the introduction of new classes of drugs, particularly proteasome inhibitors and immunomodulatory imide drugs (IMiDs)[65,66]. Proteasome inhibitors, including first-generation bortezomib (Velcade), directly target MM PCs through enhancing the existing high levels of endoplasmic reticulum stress in these secretory cells, which induces a terminal unfolded protein response and apoptosis[67]. Conversely, IMiDs, including first generation thalidomide and second generation lenalidomide (Revlimid), primarily act indirectly by promoting anti-myeloma activity of T cells and natural killer (NK) cells[68,69]. This is achieved through the binding of IMiDs to the E3 ligase Cereblon in immune cells, which causes rapid ubiquitination and degradation of the transcription factors Ikaros and Aiolos[70,71].

The initial induction phase of treatment for newly diagnosed MM patients involves 4-6 rounds of therapy, which is typically a triplet regimen consisting of Velcade, Revlimid and the corticosteroid dexamethasone (VRD) in the USA[4]. However, the most commonly used induction regimen in Australia contains Velcade, cyclophosphamide (chemotherapy) and dexamethasone (VCD), as the Australian Pharmaceutical Benefits Scheme does not allow the concurrent use of a proteasome inhibitor and an IMiD[72]. Eligible patients are then recommended to receive high dose therapy (HDT) coupled with ASCT, which has been shown to significantly improve OS[73-75]. Finally, following HDT-ASCT, or additional cycles of therapy for transplant-ineligible patients, maintenance therapy with an IMiD is recommended, as it has been shown to improve progression-free survival (PFS) and OS[76,77]. Lenalidomide is the standard of care for maintenance therapy in the USA, whereas thalidomide is the only IMiD listed for this purpose in Australia[4,72].

Although the TTP greatly varies, MM patients almost invariably relapse and the salvage treatment employed is dependent upon factors related to treatment (prior response, resistance), disease (risk group stratification) and the patient (age, co-morbidities and performance status)[78]. Several new drugs have recently been approved by the Food and Drug Administration (FDA) for the treatment of relapsed MM and promise to further improve patient outcomes[78]. These include the next-generation proteasome inhibitors carfilzomib[79,80] and ixazomib[81,82], the third generation IMiD pomalidomide[83,84], the histone deacetylase (HDAC) inhibitor panobinostat[85,86], and the monoclonal antibodies daratumumab[87,88] and elotuzumab[89]. Furthermore, there are many emerging options for the treatment of MM currently in clinical trials, including chimeric antigen receptor (CAR) T cell therapies targeting B cell maturation antigen (BCMA)[90] and the B cell lymphoma 2 (Bcl-2) inhibitor venetoclax[91,92].

1.2 Genetic aetiology of MM

1.2.1 Normal PC development

Early B cells are derived from haematopoietic stem cells in the BM and undergo rearrangement of their immunoglobulin genes to produce a functional B cell receptor (BCR)[93]. Mature B cells expressing a BCR on their surface then migrate to secondary lymphoid organs, including lymph nodes and spleen[94]. Upon encountering their cognate antigen in the periphery, mature B cells are activated and proliferate rapidly within a germinal centre[95]. Here activated B cells undergo several processes, including affinity maturation and class-switch recombination, that produce B cells expressing a high affinity BCR with different effector functions. These processes involve the generation of DNA double-stranded breaks at the immunoglobulin heavy chain (IgH) locus, which are generated by activation-induced cytidine deaminase (AID)[96]. The resultant B cells can then differentiate into either memory B cells or antibody-secreting PCs, which is mediated by the altered expression of a few key transcription factors, including interferon regulatory factor 4 (IRF4) and PR domain zinc finger protein 1 (PRDM1)[97]. Following differentiation, PCs migrate to the BM and establish themselves in specific niches that support their long-term quiescence and survival[97].

1.2.2 Inherited genetic variation

Familial aggregation of PC disorders, including MM and MGUS, has been reported over several decades[98-100]. In addition, large scale case-control studies found that there was a two to three-fold increased risk of PC disorders in first degree relatives of MGUS/MM patients[101-103]. Furthermore, the increased risk of MGUS/MM in people with African heritage compared to Caucasians was maintained when socioeconomic status was considered[6]. Together, these data suggested that there was inheritable susceptibility to developing MGUS and MM. Large-scale genome-wide association studies (GWAS) provided the first unambiguous evidence that this was the case by identifying common genetic variants that were enriched in MM patients compared with healthy controls[104-108]. To date 23 single nucleotide polymorphisms (SNPs) have been identified that are independent risk loci for MM[104-108]. Most of these SNPs are in non-coding regions of the genome, which suggests that they affect the regulation of gene expression[107]. Investigations of the candidate causal genes associated with these SNPs found that most were linked to four functions: chromatin remodelling (*SP3*, *ABCF2*, *CBX7*), regulation of cell cycle and genomic stability (*CEP120*, *POT1*, *CDKN2A*), B cell development (*ELL2*, *PRDM1*, *TNFRSF13B*) and apoptosis/autophagy (*CDCA7L*, *WAC*, *RFWD3*, *KLF2*)[107]. Hence, dysregulation of these processes may be involved in the pathogenesis of PC proliferative disorders, however, functional validation is required. Notably, a recent study identified lysine-specific demethylase 1 (*KDM1A*) as an autosomal dominant MM germline predisposition gene, suggesting that rare inherited variants also contribute to the development of MGUS/MM[109].

1.2.3 Primary genetic events

The development of MM is a multi-step process that involves the accumulation of acquired genetic lesions within PCs (Figure 1.1)[110]. The majority of MM patients have one of two types of cytogenetic abnormality that, in most cases, are mutually exclusive and present in the entire population of clonal PCs: hyperdiploidy (≥ 48 chromosomes) and translocations involving the IgH locus on chromosome 14 (14q32)[111,112]. The fact that these genomic lesions are found at a similar frequency in MGUS patients compared to MM patients suggests that they are primary genetic events that initiate PC immortalisation[113-115]. However, as hyperdiploidy and IgH translocations are present in MGUS patients that never progress to MM, these lesions are likely to be necessary, but not sufficient, for the development of overt malignancy[116]. Despite this, primary genetic events were found to have prognostic significance for newly diagnosed MM patients[117-119].

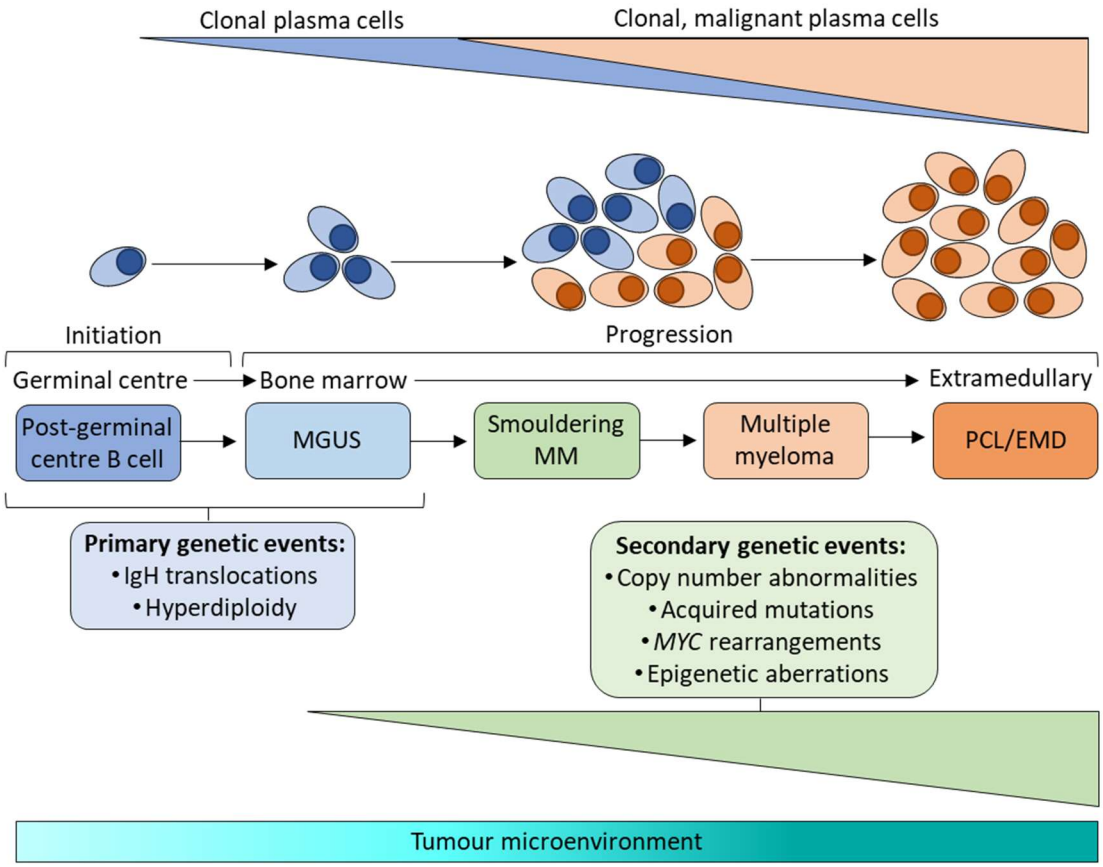

Figure 1.1: Initiation and progression of MM. The initiation of MM development is caused by a primary genetic event in a post-germinal centre B cell, which differentiates into a PC that resides in the BM. The benign clonal proliferation of this abnormal PC within the BM results in MGUS. The subsequent progression of disease to malignant MM is due to the acquisition of secondary genetic lesions and changes to the tumour microenvironment. As the disease progresses further, the neoplastic PCs can become independent of the BM, leading to PCL or EMD. Adapted from Kumar *et al.*, 2017[1]. MGUS = monoclonal gammopathy of undetermined significance, PCL = plasma cell leukaemia, EMD = extramedullary disease.

The primary cytogenetic event in ~40% of MM patients is a translocation between the IgH locus and one of five recurrent partner chromosomes (4, 6, 11, 14 and 20)[120-122]. The breakpoints of these translocations indicate that most are caused by an error in chromosomal reassembly following the AID-mediated generation of DNA double stranded breaks at the IgH locus during class switch recombination[123,124]. The translocations juxtapose a proto-oncogene(s) on the partner chromosome to the powerful IgH enhancer, resulting in its overexpression[93]. The most common IgH translocation is t(11;14) (q13;q32), which is found in ~18%[125-127] of MM patients at diagnosis and is considered to be of standard risk[49]. This chromosomal rearrangement results in the overexpression of the cyclin D1 (*CCND1*) gene, which, along with other D-group cyclins, is required for progression through G1 phase of the cell cycle[123,124].

The second most prevalent translocation is t(4;14) (p15;q32), which is detected in ~13% of newly diagnosed MM cases[125-127]. This rearrangement results in the overexpression of the nuclear receptor binding SET domain protein 2 (*NSD2*) gene, which encodes a histone methyltransferase, in all cases and the fibroblast growth factor receptor 3 (*FGFR3*) gene, which encodes a tyrosine kinase, in ~70% of cases[118,128]. The up-regulation of *NSD2* causes epigenetic reprogramming and thus gene expression changes that alter the adhesion, increase the proliferation and enhance the survival of PCs, including increasing the expression of the cyclin D2 (*CCND2*) gene[129,130]. While t(4;14) was initially considered to be a high-risk feature[117-119], the emergence of clinical trial results showing that bortezomib treatment negated/attenuated the poor patient outcomes associated with t(4;14)[131-134] led to its re-classification as an intermediate-risk factor[48,135]. However, in the latest version (v3.0) of the mSMART risk stratification guidelines, t(4;14) was reinstated as a high-risk abnormality[49]. This may be due to the fact that t(4;14) was found to be an independent predictor of poor prognosis in recent large clinical trials in which MM patients were treated with novel therapies[121,127].

Another two recurrent primary IgH translocations are t(14;16) (q32;q23) and t(14;20) (q32;q11), which are found in ~4% and ~1% of MM patients, respectively[125-127]. Both t(14;16) and t(14;20) result in the overexpression of an oncogenic MAF transcription factor (MAF or MAFB, respectively), which causes up-regulation of a range of genes, including *CCND2*[129,136-139]. The MAFs were also found to increase the expression of cytidine deaminase apolipoprotein B mRNA editing enzyme catalytic subunit (*APOBEC*) genes,

resulting in an increased mutational burden that may contribute to the poor prognosis associated these translocations in MM[121,125]. Finally, the standard risk translocation t(6;14)(p21;q32) is present in ~1%[125-127] of MM cases and causes direct overexpression of the cyclin D3 (*CCND3*) gene[129,140].

The primary genetic event in ~55% of MM patients is hyperdiploidy[120-122], which is caused by multiple trisomies of the odd-numbered chromosomes 3, 5, 7, 9, 11, 15, 19 and/or 21[111,115,141-143]. The mechanism by which these trisomies occur remains to be elucidated, but it has been suggested that they are gained in a single catastrophic event involving the mis-segregation of chromosomes at mitosis[144]. In the absence of high-risk secondary genetic events, patients with hyperdiploidy are of standard risk[49,121]. Similar to the recurrent IgH translocations, hyperdiploidy also results in increased expression of D group cyclins, specifically cyclin D1 and cyclin D2[121,129]. Notably, hyperdiploidy and recurrent IgH translocations converge to directly, or indirectly, upregulate D-group cyclins (Figure 1.2). Therefore, deregulation of the G1-S cell cycle transition appears to be an early and unifying pathogenic event that drives the development of MGUS[129].

1.2.4 Secondary genetic events

Secondary genetic events are thought to promote the transition from MGUS/SMM to MM and the progression from newly diagnosed MM to refractory MM/EMD/PCL[110]. Genetic lesions that have a higher frequency in MM patients compared to MGUS patients are generally considered to be secondary events[2]. Several different types of secondary genetic events are thought to contribute to malignant transformation in MM, including DNA mutations, translocations and copy number alterations (CNAs)[145].

1.2.4.1 DNA mutations

The advent of massively parallel next-generation sequencing (NGS) of DNA has enabled the mutational spectrum of MM PCs to be assessed in large cohorts of patients[146]. Genes that are found to be affected by non-synonymous mutations more frequently than predicted from the background mutation rate are classified as being recurrently mutated, suggesting that they are drivers of MM development[147,148]. The NGS studies of newly diagnosed MM have revealed the absence of a universal driver mutation and instead demonstrated a high degree of interpatient heterogeneity[120,122,147-149]. Only a few recurrently mutated genes were found to be affected in greater than 10% of MM patients, but there was a “long tail” of genes that

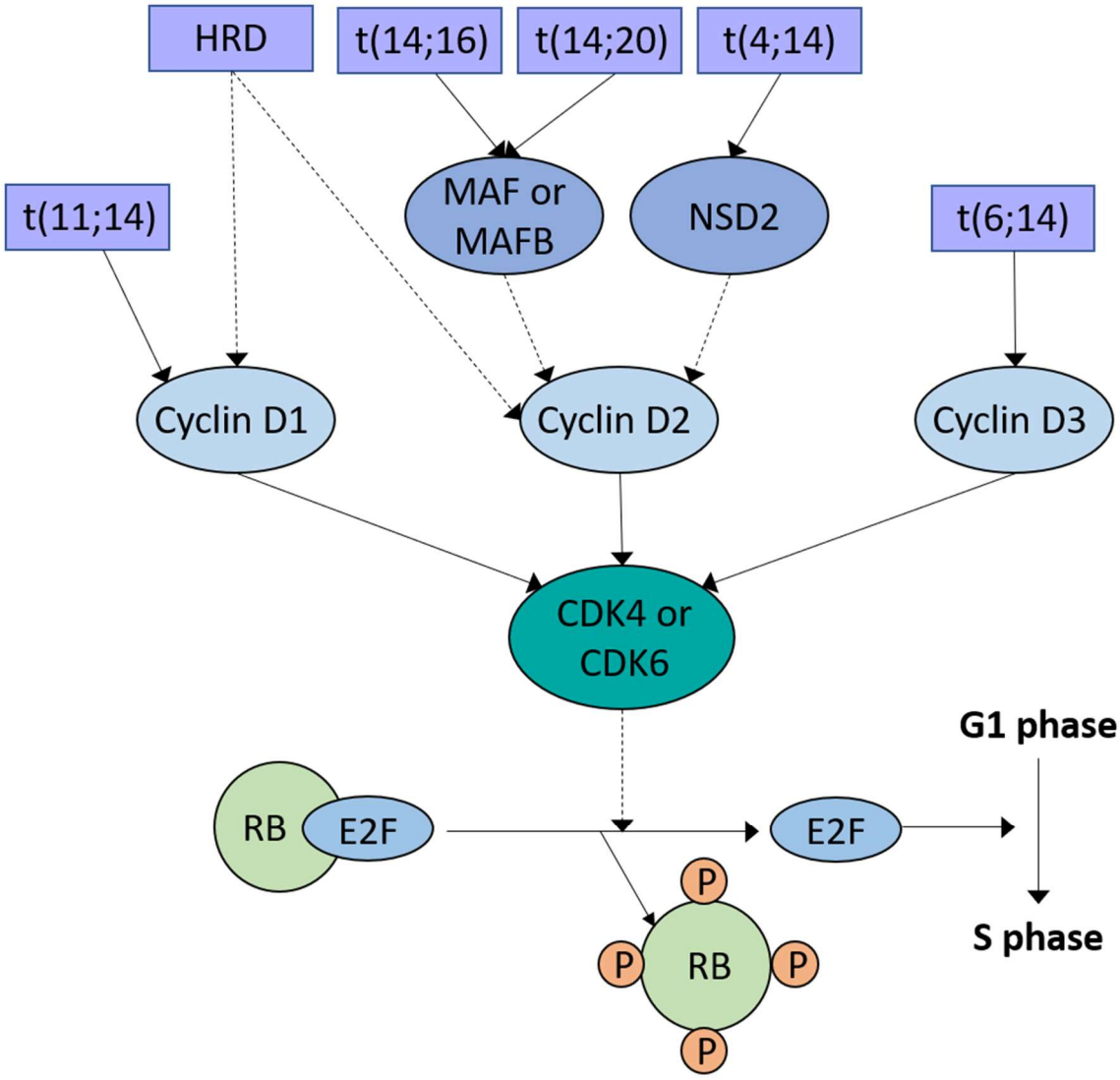

Figure 1.2: Primary cytogenetic events converge to dysregulate the G1/S cell cycle checkpoint. MM initiating events, translocations involving the IgH locus and hyperdiploidy (HRD), either directly (indicated by solid lines) or indirectly (indicated by dashed lines) lead to the up-regulation of cyclin D1, cyclin D2 or cyclin D3. These D-group cyclins can all form complexes with cyclin-dependent kinase 4 (CDK4) and CDK6, which phosphorylate the retinoblastoma protein (RB), leading to its dissociation from the transcription factor E2F. This enables E2F to drive the transcription of genes required for progression through the G1/S cell cycle checkpoint. Adapted from Pawlyn *et al.,* 2017[50].

were recurrently mutated at a frequency below 5%[120,122,147-149]. Up until recently, 16 genes had been identified as recurrently mutated in at least one whole exome sequencing (WES) study of MM patients (Figure 1.3)[120,148,149]. However, in the largest WES study of newly diagnosed MM patients to date (n = 1,273)[122], a combination of frequency and function-based approaches led to the identification of an additional 47 mutated driver genes[122].

The MM mutated driver genes cluster in particular pathways, suggesting that the dysregulation of these functions promotes disease progression[120,122,150]. Approximately 50% of MM patients have an oncogenic mutation in a gene involved in the pro-proliferative MEK/ERK signalling pathway, including *KRAS* (~20%), *NRAS* (~20%) and *BRAF* (~7%)[120,122,148-150]. Two MM driver genes with a relatively high mutation frequency are the RNA exonuclease *DIS3* (~10%) and the non-canonical poly(A) polymerase *FAM46C* (~9%), which are both involved in RNA processing[120,148,149]. FAM46C was demonstrated to be a tumour suppressor that inhibits the proliferation and survival of MM PCs[151,152], but the role of DIS3 in MM PCs remains to be determined[122]. In addition, negative regulators of the nuclear factor κ-light-chain-enhancer of activated B cells (NF-κB) signalling pathway are affected by inactivating mutations in ~11% of MM patients, including *TRAF3* (~5%) and *CYLD* (~3%)[120,122,148-150]. This leads to aberrant activation of the NF-κB pathway, which promotes the survival of MM PCs[153,154]. Furthermore, ~24% of MM cases harbour a mutation in an epigenetic regulator, including *HIST1H1E* (~4%), *ARID1A* (~2%) and *KMT2B* (~2%), and ~5% have a mutation in a gene involved in B cell development, including *IRF4* (~3%) and *PRDM1* (~2%)[122]. DNA mutations were found to be of little prognostic value in MM[127,150] with the notable exception of mutations in the crucial tumour suppressor gene *TP53* (~5%), which have consistently been associated with poor patient outcomes[120,150,155]. However, several studies have shown that having an increased number of driver mutations, irrespective of the genes involved, is associated with reduced survival in newly diagnosed MM patients[127,150].

1.2.4.2 Secondary translocations: MYC abnormalities

Chromosomal translocations that are not associated with class switch recombination are another type of secondary genetic event that is present in the PCs of MM patients. Most secondary translocations involve the *MYC* oncogene at 8q24 and are found in ~20% of newly diagnosed MM patients[125,156-159]. The immunoglobulin genes constitute ~40% of MYC translocation partners and other recurrent partner genes include *FAM46C* (9.5%), *FOXO3*

	Walker 2018 % (n=1273)	Walker 2015 % (n=463)	Lohr 2014 % (n=203)	Bolli 2014 % (n=67)	Function
KRAS	22	21	23	20	MEK/ERK
NRAS	17	19	20	20	MEK/ERK
DIS3	10	9	11		RNA processing
FAM46C	9	6	11	10	RNA processing
BRAF	8	7	6	12	MEK/ERK
TP53	6	3	8	12	DNA damage response
TRAF3	5	4	5		NF-κB
SP140	2			6	Unknown
HIST1H1E	4	3			Epigenetic
CYLD	3	2	2		NF-κB
MAX	3	2			Transcription factor
IRF4	3	3			B cell development
LTB	2	3		4	Immune response
PRDM1	2		5		B cell development
RB1	2		3		Cell cycle
ACTG1	3		2		Cytoskeleton

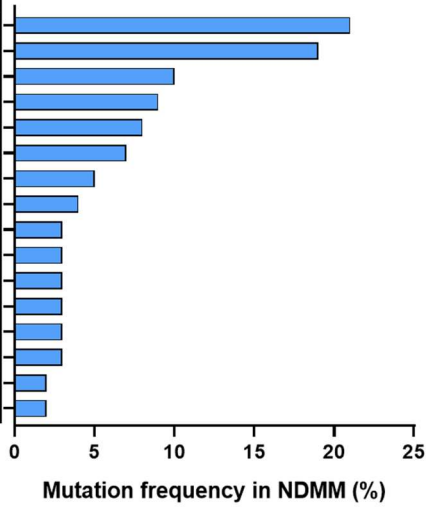

Figure 1.3: Recurrently mutated genes in patients with newly diagnosed MM. The frequency of DNA mutations in the 16 genes that were found to be significantly mutated in at least two of the four WES studies of newly diagnosed MM (NDMM) patients to date are listed[120,122,148,149]. The function of each gene is also shown and the average mutation frequency across all four studies is displayed by the bars (right). Adapted from Manier *et al.* 2017[145].

(6%) and *BMP6* (3.5%)[125]. These translocations invariably juxtapose the *MYC* locus to a superenhancer associated with the partner gene, resulting in significant overexpression of *MYC*[156-158]. Other chromosomal rearrangements, including gains and inversions, have been identified at the *MYC* locus, such that *MYC* rearrangements are found in ~50% of MM patients[158]. In addition, two thirds of MM patients were found to have a MYC activation gene expression signature, suggesting that there are alternative mechanisms by which MYC is aberrantly activated in MM[160]. Regarding prognostic significance, translocation/gain of *MYC* was found to be associated with significantly reduced PFS and OS of MM patients[125,127,150,157]. While some studies also found *MYC* rearrangements to be an independent negative prognostic factor in MM[125,157], the most recent studies have not confirmed this in multivariate analyses[127,150]. Interestingly, a recent study showed that 1.5% of MM patients have a non-*MYC* secondary translocation that generates a fusion gene predicted to cause activation of oncogenic kinases involved in the MEK/ERK or NF-κB signalling pathways[161].

1.2.4.3 Copy number alterations

CNAs, which are gains or losses of genomic regions ranging from a few kilobases up to whole chromosome arms, are common secondary genetic events in MM[145]. Recurrent CNAs most likely constitute driver events and thus one or more of the genes in the minimally affected region may be important for the pathogenesis of MM[145]. Deletions are thought to aid in MM development by disrupting an allele of one or more tumour suppressor genes in the lost region, leading to their inactivation by haploinsufficiency or in combination with a mutation/deletion of the second allele[145]. A recent study found that loss of heterozygosity > 4.6% across the genome was found to be associated with a significantly poorer prognosis in MM patients, suggesting that increased CNA-mediated tumour suppressor disruption promotes disease progression[127]. Conversely, recurrent copy number gains are thought to contribute to the pathogenesis of MM by increasing the expression of important oncogenes that promote PC growth and survival[145].

Deletion of all or part of the long arm of chromosome 13, del(13q), is present in the PCs of ~45% of newly diagnosed MM patients[119-122,162,163]. It is likely that del(13q) disrupts multiple tumour suppressor genes, but there are several pieces of evidence to suggest that *RB1* is a key target: (1) it is located in a minimally deleted region at 13q14.2[122,162], (2) it is significantly under-expressed in del(13q) cases[162] and (3) it is recurrently mutated in ~2%

of patients[120,122,148]. Other putative tumour suppressor genes affected by del(13q) include *DIS3* and metabolism-associated *TGDS*, which were also found to be recurrently mutated in MM[122]. While del(13q) was originally found to confer a poor prognosis[117,119], subsequent studies found that this adverse impact on MM patient outcome was nullified when the association of del(13q) with high-risk cytogenetic lesions, such as t(4;14), were taken into account[120,127,162].

Other recurrent chromosomal deletions in MM involve the long arm of chromosomes 14 and 16, which are present in ~14% and ~19% of patients, respectively[120-122]. The negative regulators of the NF-κB pathway *TRAF3* and *CYLD* are likely to be the critical tumour suppressor genes targeted by del(14q) and del(16q), respectively, as they are affected by recurrent mutations and homozygous deletions[120,122,148,162]. Biallelic inactivation of *TRAF3* and *CYLD* has been found to occur in 5.2% and 2.6% of MM cases, respectively[122], but was not found to impact the prognosis of MM patients[120,127,162]. Another commonly deleted region in MM is the short arm of chromosome 1, some portion of which is lost in ~25% of patients[120,122,162]. Commonly deleted regions of 1p include 1p32.3 and 1p12, which are lost in ~9% and ~15% of newly diagnosed MM cases, respectively[120,122,162,164]. Pro-apoptotic *FAF1* (1p32.3), negative cell cycle regulator *CDKN2C* (1p32.3) and recurrently mutated *FAM46C* (1p12) were found to be affected by homozygous deletions, suggesting that these are at least some of the target tumour suppressor genes on 1p[162]. Deletions of 1p32 and 1p12 have been associated with impaired OS[120,121,162,164,165] but were not found to be independent negative prognostic factors[49,127].

There are two recurrent CNAs that have been identified as robust independent negative prognostic factors for OS in newly diagnosed MM[145]. One is the gain of the long arm of chromosome 1, which is present in ~35% of MM patients[120-122,162] and was shown to be an independent predictor of inferior outcome[120,127,162,166]. However, recent studies found that only amplification of 1q21 (≥ 4 copies) was significantly associated with inferior OS, suggesting that quantifying the copy number of 1q21 is key for identifying a very high-risk group of MM patients[120,127]. The minimally gained region at 1q21 contains several candidate oncogenes[162], including the cyclin dependent kinase activator *CKS1B* that has been shown to promote the growth and survival of human MM cell lines *in vitro*[166-168]. In a recent study, an RNA interference screen of 78 genes at 1q21 showed that the down-regulation of known MM survival factor *MCL1* and five other genes (*UBAP2L*, *INTS3*, *LASS2*, *KRTCAP2*, and

ILF2) impaired HMCL proliferation and survival *in vitro*[169]. Of these genes, 1q21 amplification-driven overexpression of *ILF2* (interleukin enhancer binding factor 2) was found to promote HMCL survival *in vivo* by enhancing DNA damage repair and thus tolerance of genomic instability, suggesting that *ILF2* overexpression may also be involved in the pathogenesis of 1q21 gains[169].

The second recurrent CNA that is consistently found to be an independent adverse prognostic factor for MM patients is deletion of the short arm of chromosome 17, del(17p)[117,119-121,162]. This deletion is present in ~9% of MM patients and the main target is thought to be *TP53*[120,122,162]. A significant negative correlation between the percentage of PCs harbouring del(17p) and the OS of MM patients has been shown, but there is a lack of consensus on the optimum percentage cut-off that should be used to identify high-risk patients[170-173]. Importantly, recent studies have found that the inferior prognosis associated with del(17p) is attributable to those patients that have biallelic inactivation of *TP53*, which occurs in ~40% of cases with del(17p)[127,170]. Hence, it has been suggested that the mutational, as well as the copy number, status of *TP53* must be determined in order to accurately identify MM patients with truly high-risk disease[127].

1.2.5 Gene expression changes

Global gene expression profiling (GEP), initially using microarray and later RNA sequencing technology, revealed that the transcriptome of MM PCs is significantly different to normal and MGUS PCs[174-177]. Interestingly, the difference in the transcriptome between normal and MGUS PCs was found to be greater than the difference between MGUS and MM PCs, suggesting that primary genetic events have a greater impact on gene expression than secondary events[175,177]. Genes differentially expressed in MM PCs were found to cluster in pathways relevant to disease, including cell cycle, apoptosis and MYC activation[160,174,178]. Hierarchical clustering of MM cases based on their transcriptome identified up to 11 different subgroups, which reflects the molecular heterogeneity evident in MM[179,180]. Most of the subgroups are strongly correlated with primary cytogenetic abnormalities but some are also associated with clinical features[179,180]. For example, the low bone lesion subgroup is characterised by low or no incidence of bone lesions, which is likely due to reduced expression of *DKK1*[179,180]. Notably, a number of these subgroups were found to be associated with high-risk disease, including the t(4;14)-associated NSD2 subgroup and the t(14;16) and t(14;20)-associated MAF/MAFB subgroups[179-181]. Further to this, GEP has been used to

identify certain gene expression signatures, consisting of between 4 and 92 genes, which are independent prognostic factors in MM[182-189]. While there is minimal overlap between the genes included in these signatures, a recent study found that simply averaging two of the existing signatures could reliably predict MM patient outcome[190]. Despite the predictive power of these signatures, GEP is not currently performed in general clinical practice due to issues with standardisation and unknown relevance to different therapeutic regimens[191].

1.2.6 Epigenetic aberrations

Although the aberrant gene expression pattern in MM has been well characterised, the dysregulation of epigenetic mechanisms, including DNA methylation, histone modifications and microRNA expression, that contribute to these changes remains poorly understood. The fact that approximately a quarter of newly diagnosed MM patients have a driver mutation in an epigenetic gene that functions in histone acetylation (*CREBBP*, *EP300*), histone methylation (*KDM6A*, *KMT2B*, *KMT2C*, *SETD2*), DNA methylation (*DNMT3A*, *IDH1*, *IDH2*, *TET2*), or chromatin remodelling (*ARID1A*, *ARID2*) highlights the importance of epigenetic aberrations to the pathogenesis of MM[122,192]. Regarding DNA methylation, studies comparing the DNA methylome of normal or MGUS PCs to MM PCs have consistently shown that MM is characterised by widespread hypomethylation[193-196], which is associated with genomic instability in cancer[197]. In addition, MM cases were found to have focal regions of gene-specific DNA hypermethylation embedded within the hypomethylation pattern[194-196]. Hypermethylation of CpG sites was found in the promoters of tumour suppressor genes, leading to their decreased expression, and was associated with adverse outcomes for some genes[194,198]. Another study found that hypermethylation of intronic enhancer regions was a feature of MM, resulting in reduced expression of the cognate genes[196]. Notably, the levels and patterns of DNA methylation in MM were found to be highly heterogeneous, which may be associated with the different primary cytogenetic lesions[194,196].

Another layer of epigenetic regulation of gene expression is the post-translational modification of histones, which modulates the structure of chromatin. The relevance of aberrant histone modification in the development of MM is highlighted by the pathogenic nature of up-regulating the H3K36 methyltransferase NSD2 in t(4;14) cases, which has been shown to significantly alter the histone methylation pattern and transcriptome of MM PCs[130]. Similar to the poor prognosis associated with NSD2 overexpression, up-regulation of

another histone methyltransferase, enhancer of zeste homologue 2 (EZH2), was also found to be associated with worse outcomes for MM patients[199,200]. EZH2 inhibitors were shown to cause cell cycle arrest and apoptosis of MM PCs *in vitro*, indicating that the maintenance of epigenetic deregulation is crucial for the growth and survival of tumour cells[200]. In addition, the expression of class I HDACs has been found to be increased in MM PCs compared to normal PCs and higher expression of HDAC1 in MM was shown to be associated with significantly shorter PFS and OS[201]. The HDAC inhibitor panobinostat was demonstrated to have anti-MM activity *in vitro*[202] and significantly prolong the PFS of relapsed/refractory patients in combination with bortezomib and dexamethasone[203], suggesting that aberrant HDAC activity is a key contributor to the growth and survival of MM PCs. Furthermore, a recent study found that there is widespread conversion of normally heterochromatic regions to active euchromatin in MM PCs, suggesting that chromatin decondensation contributes to the development of MM[204].

MicroRNAs (miRNAs) are small (18–22 nucleotides) endogenous non-coding RNAs that post-transcriptionally regulate gene expression in a sequence-specific manner. An important role for miRNA-mediated regulation of gene expression in the development of MM is suggested by the finding that MM PCs have a miRNA signature that is distinct from MGUS PCs and normal PCs[205-208]. For example, the oncogenic *miR17-92* cluster was found to be significantly up-regulated and the tumour suppressor miRNAs *mir-15a* and *mir-16* were found to be significantly down-regulated in MM PCs[205-208]. The oncogenic/tumour suppressor role of these miRNAs was confirmed by the finding that *miR-19a/b* antagonists and *mir15-a* or *mir-16* mimics inhibit the growth of HMCLs *in vivo*[205,206]. In addition, the tumour suppressor *let-7* family of miRNAs, the targets of which include *MYC, KRAS* and *CCND1,* was found to be down-regulated in MM, and a *let-7b* mimic reduced MM tumour growth *in vivo*[209]. The activity of the key tumour suppressor TP53 may also be regulated by miRNAs, as the expression of *miR-192, -194,* and *-215* were found to be reduced in MM compared to MGUS, leading to increased levels of the TP53 inhibitor MDM2[210]. Notably, the miRNA expression profile in circulating exosomes was shown to be significantly different in MM patients compared to healthy controls[211]. For example, *let-7b* levels were significantly reduced in the MM exosomes, and low *let-7b* was associated with an adverse outcome in MM patients[211]. Hence, profiling circulating exosomal miRNAs may be a novel non-invasive risk stratification approach for newly diagnosed MM patients.

1.2.7 Clonal heterogeneity and evolution

In addition to the considerable interpatient heterogeneity of genetic driver events in MM, NGS studies have revealed that there is also significant intrapatient heterogeneity[148,149,212-216]. MM tumours were shown to be composed of multiple genetically heterogeneous subpopulations of cells called subclones, with a median of six subclones present at diagnosis per patient[217]. These subclones share a common pool of clonal mutations, which likely represent lesions that occurred early in disease development, but also harbour distinct subclonal mutations, which likely occurred later in MM progression[148,149,212-216]. Many secondary genetic events that are considered key drivers of MM development can be clonal or subclonal, including *KRAS* and *NRAS* mutations, suggesting that they can occur at various stages of disease[148,149]. In addition, NGS analysis of MM tumour samples collected from separate sites within a patient at the same timepoint has revealed that 75% of patients display spatial heterogeneity[218]. Some MM patients were found to have subclones harbouring high-risk genetic drivers, such as biallelic inactivation of *TP53,* in some BM sites but not others[218]. Hence, the current practice of performing genetic analyses on BM samples from a single site may lead to inaccurate risk classification, and thus sub-optimal clinical management, of MM patients.

The subclonal architecture of a tumour can evolve over time and this is thought to occur in a Darwinian manner in which subclones compete with one another for growth and survival under selective pressures, such as immune surveillance and treatment[219]. Analyses of the subclonal structure of paired tumour samples collected from the same MM patient prior to treatment and at relapse has revealed several patterns of clonal evolution[149,214,217,220,221]. Approximately two thirds of MM patients exhibit branching evolution, which is characterised by both the loss of some subclones and the gain of other subclones with novel mutations[217]. A pattern of linear evolution is observed in ~20% of cases in which genetic lesions are gained but there is no apparent loss of clones[217]. Both of these patterns of evolution are most commonly seen in patients who achieve a deep response to treatment and result from the emergence of minor, pre-existing resistant subclones[217]. In the remaining ~15% of patients there is no change in the subclones at relapse, which is termed a stable evolutionary pattern[217]. In a recent study, stable evolution was only observed in cases that did not achieve a complete response to therapy, suggesting that a dominant, innately-resistant clone was present at diagnosis[217]. In those patients with branching or linear evolution, an increase in mutational load was observed at relapse due to the emergence of

novel clones that had additional acquired lesions, including gain of 1q, biallelic inactivation of *TP53* and *MYC* translocations[217,220,221]. Notably, studies in which MM patients were treated uniformly showed that there was no unifying mutation that emerged, suggesting that resistance/relapse occurs through multiple mechanisms[217,220]. Hence, in order to effectively achieve long-term control of MM and prevent relapse, therapies will need to target clonal drivers or be used in combination.

1.2.8 Oncogene dependencies

The increasing numbers of newly diagnosed MM patients undergoing in-depth genetic analysis has enabled the relationships, or oncogenic dependencies, between driver events to be comprehensively assessed[120,122,150]. Recent studies have revealed patterns of co-occurring and mutually exclusive cytogenetic events, CNAs and mutations in MM patients, with primary IgH translocations and hyperdiploidy events found to have positive and negative associations with distinct secondary genetic hits (Table 1.3)[120,122,150]. These data suggest that the selective advantage of emergent genetic hits is predetermined by existing lesions in clonal PCs[122]. In most MM tumours, *KRAS* and *NRAS* mutations were found to exhibit mutual exclusivity[120,148,150] and, when they did co-occur in a patient, they were shown to be within separate subclones of the tumour[216]. This is consistent with mutations in either of these genes causing activation of the MAPK/ERK pathway and thus being functionally redundant[148,216].

Some of the most significant positive associations were found to be between primary IgH translocations and mutations within the partner oncogene on derivative chromosome 14[120,122,125]. While the mutational signature suggests that the partner genes were altered by AID, the mutations were non-randomly distributed in the genes, suggesting that they are likely to be co-operative driver, not passenger, events[125]. Another common type of positive association was the co-occurrence of a CNA and a mutation that collaborated to cause the biallelic inactivation of a tumour suppressor gene, including del(17p) and *TP53* mutation, del(13q) and *DIS3* mutation and del(16q) and *CYLD* mutation[122,150]. The potential mechanism of co-operativity between other significantly co-occurring lesions, such as hyperdiploidy and *FAM46C* mutations, are not immediately apparent and require further investigation[122]. Furthermore, specific mutations within a gene were shown to have a variable frequency between cytogenetic subgroups, for example, *BRAF*^{D594N} was uniquely

Table 1.3: Oncogenic dependencies between primary and secondary genetic events in MM. The secondary translocations, gene mutations (indicated by gene names) and CNAs that were found to significantly co-occur (positive association) or be mutually exclusive (negative association) with primary cytogenetic events in newly diagnosed MM patients. Data from Walker *et al.*, 2018[122].

Primary event	**Secondary events**	
	Positive association	**Negative association**
Hyperdiploidy	t(*MYC*), *FAM46C*, +6p	*IRF4*, *PRKD2*, *CCND1*, *DIS3*, *MAX*, -4p, -13q, -14q
t(4;14)	*FGFR3*, *DIS3*, *PRKD2*, -1p, -4p, -11q, -12p, -13q, -14q, +1q	*NRAS*, t(*MYC*), -16q
t(11;14)	*CCND1*, *IRF4*	t(*MYC*), -1p, -4p, -8p, -13q, -14q, -16q, +1q, +6p
t(14;16)	*BRAF*, *DIS3*, *TRAF2*, -13q, +1q	-
t(14;20)	-	-
t(6;14)	-14q, -16q	-

predominant in the t(14;16) subgroup, whereas *BRAF*^{V600E} was the most common variant in the other subgroups[122]. This suggests that distinct mutations within the same gene may vary in their mechanism of action and thus the selective advantage they confer on different genetic backgrounds.

1.2.9 Progression from MGUS/SMM to MM

Understanding the mechanisms by which disease progresses from asymptomatic MGUS and SMM to overt MM is crucial for identifying key therapeutic targets that promote malignancy. With respect to primary cytogenetic events, both MGUS and SMM patients with t(4;14) or hyperdiploidy were found to have an increased risk of disease progression, despite the fact that hyperdiploid MM is considered to be of standard risk[43,222-224]. Notably, many of the recurrent mutations, CNAs and cytogenetic rearrangements in MM that are generally considered to be secondary events are also found at the MGUS/SMM stages, albeit at a lower frequency[114,225-228]. Such lesions, including gain 1q and del(13q)[228], may further prime immortalised PCs for malignant transformation but are unlikely to drive disease progression to overt MM[229]. Conversely, there are some lesions that are absent or found at a very low frequency in MGUS patients, such as *TP53* mutations/deletions and *MYC* rearrangements, which likely constitute genuine drivers of progression to overt MM[226,228]. A small number of NGS studies have examined paired MGUS/SMM and MM samples from the same patient, showing that the transition to overt malignancy is associated with an altered pattern, but not load, of mutations and CNAs[215,230-232]. There was no gene or pathway found to be universally disrupted during the progression from asymptomatic to symptomatic disease, suggesting that there are varied molecular mechanisms by which the transition from MGUS to MM occurs[231,232]. Mutations in several genes that are recurrently affected in MM were found to be associated with the MGUS/SMM to MM transition, including *KRAS*, *DIS3*, *SP140*, *TRAF3*, *PRDM1* and *IRF4*, suggesting that these lesions may be key drivers of disease progression[232]. However, the potential role of *KRAS* mutations in driving malignant transformation is undermined by the fact that they were also found in MGUS patients[232] and were not associated with reduced TTP[228].

NGS studies of PCs from MGUS/SMM patients have shown that there is a similar degree of clonal heterogeneity present compared to MM PCs, suggesting that disease evolution is already occurring at early stages of the disease[215,230-232]. Paired MGUS/SMM and MM analyses have revealed that stable or branching patterns of clonal evolution are present

during the transition from MGUS/SMM to MM[231,232]. The evidence of a stable evolutionary pattern in some patients indicates that the clones capable of causing symptomatic disease are already present at pre-symptomatic stages of disease[231,232]. This finding suggests that PC-extrinsic factors, such as inhibition of microenvironment-mediated growth control, may play an important role in promoting malignant transformation. Consistent with this, primary MGUS PCs were shown to be capable of progressive expansion in the BM of a humanised mouse strain, with different minor subclones reproducibly emerging in the xenotransplant compared to the baseline tumour sample[233]. However, branching evolution was also observed in the MGUS/SMM to MM transition, which was associated with a longer TTP compared to stable evolution[231]. This suggests that the acquisition of additional genetic drivers is required to enable malignant transformation in some patients. Overall, it is likely that the progression from asymptomatic MGUS/SMM to overt MM requires the accumulation of specific PC-intrinsic driver lesions, as well as changes to PC-extrinsic factors in the BM microenvironment.

1.2.10 Transgenic mouse models of MM

Transgenic mouse models are important tools for demonstrating the driver status of recurrent genetic abnormalities in malignancy. However, many of the transgenic mice that were generated to model MM have been of limited relevance because the transgenes investigated were not observed to be mutated or dysregulated in the PCs of MM patients[234,235], and/or the transgenes were expressed in early B cells, resulting in lymphomas and extra-medullary plasmacytomas rather than an MM-like disease[236,237]. For example, overexpression of *Maf*, in the B cell lineage resulted in the development of B cell lymphomas, not MM, in aged mice[238]. That said, a proportion of the *Maf* mice did display some clinical features of MM, such as increased M protein levels and a plasmablastic phenotype[238]. While the phenotype of these mice suggested that *MAF* overexpression promotes B cell tumorigenesis, its exact role in promoting the development of MM remains to be completely elucidated.

A transgenic mouse model that faithfully recapitulates the key aspects of MM disease is the Vk*MYC model. In C57BL/6 mice harbouring the Vk*MYC transgene, MYC overexpression is sporadically activated by somatic hypermutation and thus only occurs in post-germinal centre B cells[239]. The resulting PC proliferative disorder has an indolent disease course and shares many of the biological and clinical features of human MM, including BM localisation of tumour, progressive increases in M protein, kidney damage

and bone lesions[239]. The malignant nature of the expanded PCs was confirmed by their ability to be successfully transplanted into syngeneic mice[239]. Crucially, overexpression of MYC by the Vk*MYC transgene did not cause MM in the Balb/c mouse strain, which, unlike the C57BL/6 strain, are not prone to developing MGUS[158]. These data strongly suggest that the up-regulation of MYC can cause the progression from MGUS to MM, as was hypothesised from the prevalence of MYC activation in MM PCs but not MGUS PCs[160]. To continue improving the understanding of MM disease biology, further *in vivo* exploration of the role played by one, or a combination of co-occurring, putative driver mutations in the development of MM is warranted.

1.3 SAMSN1

1.3.1 Gene, mRNA and protein

SAM domain, SH3 domain and nuclear localization signals 1 (*SAMSN1),* also known as *SASH2*/*NASH1*/*HACS1*/*SLy2*, was first identified in a study of genes expressed in MM and is localised on human chromosome 21 (q11.2)[240]. There are three verified transcript variants of *SAMSN1* and the canonical sequence encodes a 373 amino acid protein isoform[241]. The SAMSN1 protein contains an N-terminal nuclear localisation sequence, a src homology 3 (SH3) domain in the middle of the protein and a sterile alpha motif (SAM) domain toward the C-terminus of the protein[240,242]. Both SH3 and SAM domains are protein interaction modules, with SH3 binding to proline-rich regions and SAM binding to both SAM and non-SAM domains[240,242]. The co-occurrence of SH3 and SAM domains in a protein like SAMSN1 often indicates that it has an adaptor or scaffolding function[241]. *SAMSN1* is expressed highly in the haematopoietic compartment, including peripheral blood lymphocytes, immune tissues and the BM, and to a lesser extent in other tissues, including the heart, lung and brain[240,242]. Despite the presence of a nuclear localisation signal, SAMSN1 was found to primarily localise to the cytoplasm[240]. SAMSN1 belongs to the SH3 domain protein expressed in the lymphocyte (SLy) family of proteins that also contains SASH3 (SLY/HACS2), which is highly homologous to SAMSN1, and SASH1, which contains an additional SAM domain (Figure 1.4)[240,242]. *SASH3* is located on the X chromosome and is expressed exclusively in lymphocytes[243], whereas *SASH1* is ubiquitously expressed and found on the long arm of chromosome 6[244]. The genes encoding this family of proteins have orthologues in rodents, birds, reptiles and ray-finned fish, suggesting that they are highly evolutionarily conserved and thus have important functions[245].

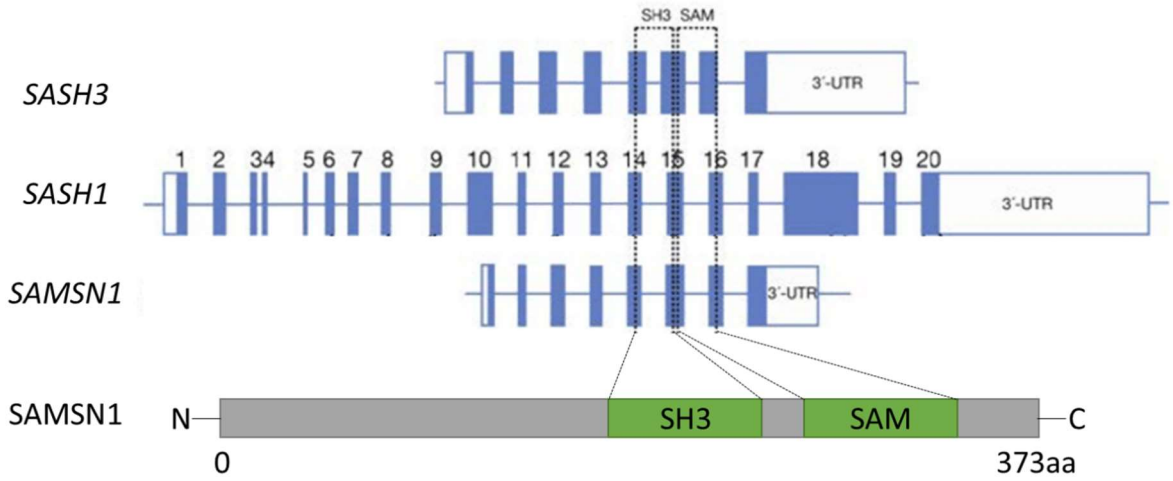

Figure 1.4: SLY family of proteins. A schematic representation of the *SASH3*, *SASH1* and *SAMSN1* mRNA transcripts and the SAMSN1 protein. The location of the conserved SH3 and SAM domains are highlighted. Adapted from Weidmann, 2015[246].

1.3.2 Functions in normal cells

SAMSN1 was shown to be significantly up-regulated in human and mouse splenic B cells following treatment with IL-4 and other B cell activators, including anti-IgM and anti-CD40[241]. This induction of SAMSN1 was found to involve multiple signalling molecules, including signal transducer and activator of transcription 6 (STAT6), phosphoinositide 3-kinase (PI3K), protein kinase C (PKC), and NF-κB[241]. In addition, in primary murine B cells, *Samsn1* mRNA expression was found to be increased in activated germinal centre B cells in comparison to resting mature B cells[247]. Notably, the overexpression of *Samsn1* in murine B cells was found to inhibit proliferation in response to activating stimuli[241]. Together, these data suggest that SAMSN1 is induced by BCR stimulation and negatively regulates the resultant activation of B cells. In keeping with this observation, Samsn1 was found to affect the function of B and T cells from *Samsn1* knockout/transgenic mice compared to wildtype (WT) mice, despite the size of B and T cell populations in the BM and spleen not being affected[245,248,249]. Increased B cell and T cell proliferation *in vitro* and enhanced humoral immune responses *in vivo* were observed in *Samsn1*$^{-/-}$ mice compared to WT mice[245]. In contrast, *Samsn1* transgenic mice were found to have reduced serum IgM levels at baseline, and following immunisation, compared to WT mice[248]. Together, these data suggest that SAMSN1 is an immunoinhibitory adaptor in normal B and T lymphocytes. Interestingly, functional deletion of homologous *Sash3* in mice resulted in decreased lymphocyte function, suggesting that, in contrast to SAMSN1, SASH3 promotes activation of adaptive immunity.

In relation to the mechanism by which SAMSN1 attenuates B cell responses, SAMSN1 was found to associate with tyrosine phosphorylated proteins in the BJAB B cell lymphoma cell line following BCR stimulation[241]. In addition, a yeast two-hybrid screen identified paired immunoglobulin-like receptor B (PIR-B), a negative regulator of B cell activation that is phosphorylated following BCR engagement[250], as a putative interaction partner of SAMSN1[241]. This was supported by the finding that the overexpressed cytoplasmic tail of PIR-B bound to endogenous SAMSN1 in BJAB cells, although an association between endogenous PIR-B and Samsn1 in primary murine B cells was not detected[241]. These data suggest that SAMSN1's inhibition of B cell activation may be mediated by binding to PIR-B and enhancing negative regulation of BCR signalling. In addition, SAMSN1 has been implicated in the epigenetic control of gene expression[251]. When overexpressed in Jurkat acute T cell lymphoma cells and human embryonic kidney (HEK) 293T cells, SAMSN1, while found predominantly in the cytoplasm, was also present in the nucleus, with the

subcellular localisation shown to be controlled by interactions with 14-3-3 proteins[251]. In the nuclei of these cells, overexpressed SAMSN1 co-immunoprecipitated with overexpressed Sin3-associated polypeptide 30 (SAP30) and HDAC1[251], which are both members of the Sin3 transcriptional co-repressor complex[252]. In addition, the presence of overexpressed SAMSN1 in lysates from HEK293T cells increased the deacetylase activity of overexpressed HDAC1 *in vitro*[251]. Although there are no reports of these findings being replicated with endogenously expressed proteins in normal B cells, these data suggest that SAMSN1 may be capable of directly modulating gene expression in B cells, resulting in the inhibition of adaptive immune responses.

Another mechanism by which SAMSN1 may mediate its immunoinhibitory effects has also been proposed. Overexpression of SAMSN1 in HeLa cervical adenocarcinoma cells was found to cause morphological changes, including increased formation of actin-rich membrane ruffles in which SAMSN1 co-localised with polymerised F-actin[249]. This SAMSN1-mediated remodelling of the actin cytoskeleton was demonstrated to be dependent on the SH3 domain of SAMSN1 and the activity of the small Rho GTPase Rac1[249], which is known to control the formation of branched actin structures in membrane ruffles[253,254]. In addition, SAMSN1 was found to interact in an SH3-dependent manner with cortactin, an activator of Arp2/3 complex-mediated actin polymerization[255], suggesting that SAMSN1 may affect cytoskeletal remodelling by modulating the activity of cortactin[249]. Furthermore, SAMSN1 was shown to enhance the spreading of HeLa cells on a gelatin-coated surface[249]. In contrast, B cells from Samsn1 transgenic mice exhibited significantly reduced cell spreading on an anti-IgM-coated surface compared to B cells from WT mice[249]. In the primary B cells from the transgenic mice, Samsn1 was demonstrated to bind endogenous Hs1, the lymphocyte-specific homologue of cortactin[256]. The difference in the effect of Samsn1 on cell spreading between HeLa and murine B cells may relate to the contrasting properties of normal motile B lymphocytes and transformed epithelial HeLa cells, including the cell type-specific differences in the proteins that interact with SAMSN1/Samsn1. Notably, cell spreading is crucial for maximising the interaction of lymphocytes with antigen, which promotes immune cell activation[257]. Hence, these data suggest that SAMSN1 may negatively regulate adaptive immune responses by inhibiting cytoskeletal remodelling-dependent immune synapse formation. Notably, fellow SLY family member SASH1 has also been found to interact with cortactin and modulate actin cytoskeletal remodelling, resulting in increased cell adhesion and decreased cell migration[258,259].

1.3.3 Role in cancer

1.3.3.1 Identification as a putative tumour suppressor in MM

SAMSN1 has recently been implicated as having a tumour suppressor role in MM. The first piece of evidence suggesting this came from a comparative study of the closely-related C57BL/KaLwRij (KaLwRij) and C57BL/6 mouse strains[260,261]. Both the C57BL/6 and KaLwRij strains develop an MGUS-like benign clonal PC proliferative disorder at the same rate of ~60-70% by two years old[262], but KaLwRij mice are unique in their ability to spontaneously develop MM, albeit at a low frequency of ~0.5% in mice over two years old[263,264]. Hence, any genetic differences between the two strains of mice may contribute to the predisposition of KaLwRij mice to develop MM, which may also be relevant to the pathogenesis of human MM. Transcriptomic analysis of the BM from both mouse strains revealed that one of the most differentially expressed genes was *Samsn1*, which was found to be 52-fold down-regulated in the BM of KaLwRij mice compared to WT C57BL/6 mice[260]. In fact, the expression of *Samsn1* was shown to be completely lost in the BM of KaLwRij mice, including normal PCs, and in all the other cells/tissues tested[260]. This loss of *Samsn1* expression was found to be caused by a 180 kb homozygous deletion on chromosome 16 in the KaLwRij genome, which entirely encompasses *Samsn1* but not any other genes[260]. This finding was confirmed in a subsequent study, which through SNP array profiling found that the *Samsn1* deletion was the most striking structural variant in the genome of KaLwRij mice compared to WT mice[261]. These findings suggested that the loss of *Samsn1* may contribute to the capability of KaLwRij mice to progress from MGUS to MM.

The potential role of *Samsn1* as a tumour suppressor gene in murine MM was assessed using an immunocompetent 5T murine model of MM (5TMM). The 5TMM model is based on the finding that the transplantation of diseased BM from aged KaLwRij mice intravenously (i.v.) into young syngeneic recipients resulted in the development of MM, which recapitulated many features of human MM, including PC tumour growth in the BM, paraprotein production and lytic bone disease[263,264]. Subsequently, distinct MM cell lines were generated from different KaLwRij donor mice, including the 5T2[263-266], 5T33vv[264], 5T33vt[267]and 5TGM1 (5T33 subclone)[268] lines. The 5T2 and 5T33vv lines can only be passaged *in vivo*, while the 5T33vt and 5TGM1 cell lines are readily cultivated *in vitro*, enabling them to be genetically modified and maximising their utility for *in vivo* studies[269,270]. Using the 5TGM1/KaLwRij MM model, the enforced re-expression of Samsn1 in 5TGM1 cells was

found to significantly inhibit MM tumour development and associated bone disease compared to control 5TGM1 cells *in vivo*[260]. This suggested that the loss of *Samsn1* promotes MM development in the KaLwRij model of murine MM. In relation to human MM, *in silico* analysis of microarray gene expression data from PCs revealed that the expression of *SAMSN1* was significantly lower in MM patients compared to PCs from MGUS patients and normal controls[260]. In addition, reduced *SAMSN1* expression was found to be significantly associated with adverse clinical parameters in MM patients, including increased tumour burden and lower OS[260]. Together, these data suggested that *SAMSN1* may also be a tumour suppressor gene in human MM and a reduction in its expression may promote the transition from MGUS to MM.

1.3.3.2 Role in other malignancies

SAMSN1 was found to have reduced expression, and was thus implicated as a tumour suppressor gene, in several malignancies besides MM. The first description of reduced *SAMSN1* expression was in lung cancer, in which loss of heterozygosity at 21q21 is a common abnormality[271]. *SAMSN1* was one of eight genes located within a homozygously deleted region on 21q21 in a lung cancer cell line, but was the only gene with expression levels that were decreased in all the lung cancer cell lines tested compared to normal lung tissue[271]. This suggested that *SAMSN1* may be a key target of the 21q21 deletion and thus a tumour suppressor gene in lung cancer[271]. In addition, ulcerative colitis patients with colon cancer were found to have significantly lower expression of *SAMSN1* compared to those patients without cancer, suggesting that SAMSN1 may inhibit the transition from pre-neoplastic lesions to overt malignancy in colorectal cancer[272]. Furthermore, *SAMSN1* mRNA expression was found to be lower in cancerous tissues compared to normal adjacent tissue from gastric cancer and hepatocellular carcinoma patients[273,274]. Low *SAMSN1* expression in these cancers was found to be associated with increased tumour size and decreased OS, suggesting that *SAMSN1* may also be a tumour suppressor gene in gastric cancer and hepatocellular carcinoma[273,274]. In contrast, another study found that the expression of *SAMSN1* was increased in glioma compared to normal brain tissue and high expression of *SAMSN1* was associated with reduced survival for patients with glioblastoma multiforme[275]. This suggests that the role of SAMSN1 in malignancy may be cell-type specific. Notably, fellow SLY protein family member *SASH1* was also shown to be down-regulated and associated with adverse clinical features in a range of cancers, including breast cancer[244], colon cancer[276] and osteosarcoma[277].

1.3.3.3 Mechanism of disruption in cancer

In relation to the mechanism by which the expression of *SAMSN1* is reduced in cancers, ~30% of human lung cancers have a 21q deletion, suggesting that deletion may be at least one way by which the expression of *SAMSN1* is reduced in this malignancy [278]. However, gain, not loss, of the long arm of chromosome 21 is a recurrent CNA in MM patients and thus the down-regulation of *SAMSN1* expression is likely to occur by another mechanism[162]. In addition, DNA mutation is unlikely to be the cause of reduced *SAMSN1* expression in MM PCs, as only one *SAMSN1* mutation has been identified in NGS studies of cancers, which was a nonsense mutation in a patient with angioimmunoblastic T cell lymphoma[279]. However, DNA methylation at specific CpG sites in the *SAMSN1* promoter were found to correspond with *SAMSN1* expression levels in most human MM cell lines[260]. In addition, treatment with the DNA de-methylating agent 5-aza-2′-deoxycytidine was able to significantly increase *SAMSN1* expression in many of the HMCLs with *SAMSN1* promoter hypermethylation[260]. Hypermethylation of the *SAMSN1* promoter and associated reduced expression of *SAMSN1* was also observed in hepatocellular carcinoma cell lines[273]. This suggests that aberrant hypermethylation of the *SAMSN1* promoter may be a key mechanism by which *SAMSN1* expression is reduced in MM and other malignancies[260,273]. While a correlation between *SAMSN1* methylation and expression is yet to be established in MM patient samples, the potential down-regulation of *SAMSN1* by promoter hypermethylation is consistent with the known hypermethylation of tumour suppressor genes in MM PCs[194,198].

1.3.3.4 Mechanism of action in cancer

To date there has been limited investigation of the potential mechanisms by which SAMSN1 suppresses cancers, including MM. Given that SAMSN1 has been shown to inhibit the proliferation of normal B cells following BCR stimulation[241,245] it is conceivable that SAMSN1 may limit the proliferation of MM PCs. While another group found that Samsn1 significantly reduced the proliferation of 5TGM1 cells under basal conditions[261], our group observed reduced proliferation of Samsn1-expressing 5TGM1 cells only when they were co-cultured with KaLwRij-derived BMSCs *in vitro*[260]. Our group also showed that Samsn1-expressing 5TGM1 cells and SAMSN1-expressing HMCLs display increased adhesion to BM stroma *in vitro*[260]. Interestingly, overexpression of SAMSN1 in human lung cancer cell lines was not found to affect cell proliferation *in vitro*[271]. Collectively, these data suggest that SAMSN1's suppression of MM development may be mediated, at least in part, by

limiting the proliferation of MM PCs, potentially in a BM microenvironment-dependent manner. Notably, SASH1 has been shown to have a range of tumour suppressor effects in epithelial cancer cells, including inhibiting the proliferation, viability and migration/invasion of malignant cells[277,280,281]. This suggests that there may be mechanisms beyond attenuating proliferation that contribute to the tumour suppressor effect of SAMSN1 in MM. Importantly, despite KaLwRij mice being *Samsn1*$^{-/-}$, they only develop spontaneous MM with a long latency and low penetrance[263,264]. This suggests that *Samsn1* loss is necessary, but not sufficient, to cause MM in KaLwRij mice. Hence, it is likely that *SAMSN1* down-regulation co-operates with other genetic/epigenetic "hits" to drive the development of malignant PCs.

1.4 Summary and aims

MM is the second most common haematological malignancy in adults, which is characterized by the clonal expansion of malignant PCs in the BM[1]. Recent genomic studies have revealed that MM is a genetically heterogenous disease and the genetic aberrations that drive MM development and progression are incompletely understood[120,122,232]. It was previously revealed that *Samsn1* is homozygously deleted in the KaLwRij mouse strain[260], which can develop an MM-like malignancy in old age[263,264]. In addition, the re-expression of Samsn1 in the KaLwRij-derived 5TGM1 MM PC line significantly inhibited tumour development following i.v. inoculation into syngeneic KaLwRij mice[260]. This suggests that Samsn1, a putative adaptor protein that has been shown to negatively regulate B cell responses[241,245], is a tumour suppressor in the context of murine MM. However, the fact that MM only develops in *Samsn1*$^{-/-}$ KaLwRij mice with late onset and incomplete penetrance[264] suggests that *Samsn1* loss must co-operate with other acquired genetic changes to promote the development of MM. In relation to human MM, *SAMSN1* expression was found to be significantly reduced in the PCs from MM patients compared to healthy controls and *SAMSN1* down-regulation was shown to be significantly associated with increased PC burden and reduced OS[260,261]. These data are consistent with SAMSN1 also potentially having a tumour suppressor role in the context of human MM. However, the functional role of SAMSN1 in human MM cells has not yet been empirically investigated. Furthermore, the underlying molecular mechanism(s) by which Samsn1/SAMSN1 suppresses MM remains to be determined.

The studies in this thesis were designed to address the following aims:

1. Identify and investigate potential genetic aberrations that may co-operate with the down-regulation of *SAMSN1* to promote the development and/or progression of MM.
2. Determine the mechanism(s) by which Samsn1 inhibits 5TGM1 tumour growth *in vivo*.
3. Investigate the functional role of SAMSN1 in human MM cells.

2 MATERIALS AND METHODS

2.1 Molecular biology

2.1.1 RNA techniques

2.1.1.1 RNA-sequencing

Total RNA was extracted from 5TGM1 cells using the RNeasy Mini Kit and the RNase-Free DNase Set (QIAGEN), according to the manufacturer's instructions. RNA quantity was determined using the Qubit™ RNA BR Assay Kit and Qubit™ 2 Fluorometer (Thermo Fisher Scientific), according to the manufacturer's instructions. RNA quality was determined using the RNA 6000 Nano kit on the Bioanalyzer 2200 (Agilent) and all samples had an RNA integrity number > 8. Library construction and RNA-sequencing with the NextSeq® 500 (Illumina) were performed by the David Gunn Genomics Facility (SAHMRI, Adelaide). RNA-seq libraries were prepared using NEXTflex™ Rapid Directional mRNA-Seq Kit Bundle with RNA-Seq Barcodes and poly(A) beads (BIOO Scientific), according to the manufacturer's instructions. Initial raw read processing was performed using an in-house pipeline developed at SAHMRI. Briefly, raw single-end FASTQ reads were aligned to the GRCh38/mm10 version of the mouse genome using the transcriptome algorithm STAR. After alignment, mapped sequence reads were summarised to the mm10 gene intervals using the tool featureCounts, available through the package RSubread. Quality control assessment was performed using FastQC, followed by data filtering for low counts. Differential gene expression analysis was then undertaken using limma-voom in R v3.5.1. Gene ontology analysis was performed using the Database for Annotation, Visualization and Integrated Discovery (DAVID) v6.8 available at <https://david.ncifcrf.gov/home.jsp>[282].

2.1.1.2 Total RNA isolation

Total RNA was isolated from purified primary mouse CD138^{+} PCs using the All Prep DNA/RNA Micro Kit (QIAGEN). Total RNA from cell lines was extracted from 5-10 x 10^6 cells using TRIzol™ Reagent (Invitrogen). Briefly, cells were lysed in 1 mL TRIzol™ and 0.2 mL of chloroform was added. The TRIzol™ and chloroform were mixed by vigorous shaking and incubated for 3 minutes at room temperature. Samples were centrifuged at 12,000 x g and 4°C for 5 minutes to separate phases, and the RNA-containing aqueous phase was collected. Total RNA was precipitated by the addition of 0.5 mL isopropanol and 2 µL (20µg) ribonuclease-free glycogen (Roche) and incubated at room temperature for 10 minutes. The RNA was pelleted by centrifugation at 12,000 x g and 4°C for 15 minutes and then washed with 75% (v/v) ethanol. The RNA was resuspended in UltraPure™ DNase/RNase-Free Distilled Water (nuclease-free (NF) water; Invitrogen) and incubated at

60°C for 10 minutes to facilitate solubilisation. The concentration of RNA in solution was determined by measuring the absorption at 260 nm on a NanoDrop™ 8000 Spectrophotometer (Thermo Fisher Scientific). RNA was stored at -80°C.

2.1.1.3 Reverse transcription polymerase chain reaction

To qualitatively assess messenger RNA (mRNA) levels, reverse transcription polymerase chain reaction (RT-PCR) was performed. Firstly, total RNA (2 µg) was reverse transcribed into single-stranded complementary DNA (cDNA) using SuperScript™ IV Reverse Transcriptase (Invitrogen). The RNA sample was resuspended in a total volume of 11 µL with NF water and 1 µL each of random hexamers (50µM), oligo$(dT)_{20}$ (50µM) and deoxyribonucleotide triphosphate (dNTP) mix (10 mM) were added. The solution was incubated at 65°C for 5 minutes and immediately chilled on ice for at least 2 minutes. A mix containing 5 µL of 5x RT buffer, 1 µL of 0.1 M DTT and 1 µL of SuperScript™ IV enzyme (200 U) was then added to the denatured RNA. This reaction mixture was incubated for 10 minutes at 23°C, 10 minutes at 55°C and 10 minutes at 80°C. It was then diluted to a total volume of 0.1 mL with NF water and either used immediately for downstream applications or stored at –20°C. Negative control minus reverse transcriptase reactions were performed concurrently for all samples.

PCR was then performed using AmpliTaq Gold™ DNA Polymerase (Thermo Fisher Scientific), with each 25 µL reaction containing 2 µL of cDNA, 0.2 mM dNTPs, 1.5 mM $MgCl_2$, 0.5 µM forward primer, 0.5 µM reverse primer, 1x PCR Buffer II and 1.25 U DNA polymerase in NF water. No template control (NTC) reactions were performed for each target gene and primer sequences are listed in Table 2.1. Reactions were performed on a Veriti™ Thermal Cycler (Thermo Fisher Scientific) using the following cycling parameters: 95°C for 10 minutes; 35 cycles of 95°C for 15 seconds, 55°C for 30 seconds and 72°C for 1 minute; and 72°C for 5 minutes. The PCR products were then visualised by agarose gel electrophoresis. A gel was cast containing 2 % (w/v) agarose in TAE buffer (40 mM Tris base, 20 mM acetic acid and 1 mM ethylenediamine tetraacetic acid (EDTA)) and 1:10,000 GelRed® (Biotium) for DNA visualisation. The PCR products (10 µL) were mixed with 6x Gel Loading Dye (New England BioLabs), loaded into the gel, resolved by electrophoresis and visualised using a Gel Doc™ XR+ Imager (Bio-Rad).

2.1.1.4 Quantitative reverse transcription polymerase chain reaction

To quantitatively assess mRNA levels, quantitative reverse transcription polymerase chain reaction (RT-qPCR) was performed. Firstly, RT of total RNA was performed as described in section 2.1.1.3. Secondly, qPCR was performed, with each 15 µL reaction containing 2 µL of cDNA, 1x RT^2 SYBR® Green qPCR Mastermix (QIAGEN), 0.5 µM forward primer, 0.5 µM reverse primer in NF water in a 96-well clear PCR plate (Bio-Rad). Primer sequences are listed in Table 2.1. All cDNA samples were analysed in triplicate and minus reverse transcriptase and NTC reactions were included for each sample and target gene, respectively. Reactions were performed on the CFX Connect™ Real-Time PCR Detection System (Bio-Rad) using the following cycling parameters: 50°C for 2 minutes; 95°C for 15 minutes; 40 cycles of 95°C for 15 seconds, 60°C for 25 seconds and 72°C for 10 seconds; and 72°C for 3 minutes. A melt curve was then performed in which there was an incremental increase of 0.5°C/5 seconds from 65°C to 95°C. Standard curves were generated to determine the reaction efficiency of each primer pair. Normalisation and relative expression analysis were performed, with the reaction efficiency taken into account, using Q-Gene software[283].

Table 2.1: RT-PCR and RT-qPCR primer sequences.

Gene	Species	Forward/reverse primer sequences (*5' - 3'*)
Glipr1 ex1-2	Mouse	TCACAACCAGCTTCGGTCAA/ GTGAATGCAGCTGTGGGTTG
Glipr1 ex3-4	Mouse	AGGTTGTTTGGGCAGACAGT/ TTTTGGGCAATCACTGCACG
Actb/ACTB	Mouse/Human	TTGCTGACAGGATGCAGAAG/ AAGGGTGTAAAACGCAGCTC
Samsn1	Mouse	TTCACGCCAAGTCCCTATGAC/ TTCCCATTGGTGTTTTGCAGATA
SAMSN1	Human	TCCCTCAAAGCCAGTGACTC/ GCCACAGAATGGTCCTGAAT
B2M	Human	AGGCTATCCAGCGTACTCCA/ CGGCAGGCATACTCATCTTT
Tex101	Mouse	ACTGCCAGGTGAGTCAAACC/ GACGGTCCTGGTTCCATCTG
Negr1	Mouse	ATGTGACGCAGGAGCACTT/ CCATACTGGGCTGTACTTGGA

2.1.2 DNA techniques

2.1.2.1 Restriction enzyme digest

Restriction digests of DNA were routinely performed by digesting 1 µg of DNA with 10 units of restriction enzyme (New England BioLabs) in the supplied digestion buffer and in a total reaction volume of 50 µL. The reaction was incubated at the optimum temperature

for 1 hour. The restriction enzyme was then inactivated by heat, where applicable, or the products were immediately resolved by agarose gel electrophoresis, as described in section 2.1.1.3, and gel purified using the UltraClean® 15 DNA Purification Kit (MO BIO Laboratories), according to the manufacturer's instructions.

2.1.2.2 Ligation

Ligations were routinely carried out in a total volume of 10 µL, containing insert and vector DNA at an insert:vector molar ratio of 3:1, 1x T4 DNA Ligase Reaction Buffer and 1 µL (400 U) of T4 DNA ligase (New England BioLabs). The ligation reaction mix was incubated at 4°C overnight. A negative control reaction containing no insert was also performed to assess the levels of vector re-ligation.

2.1.2.3 Preparation of chemically competent *E. coli* JM109 cells

Frozen *Escherichia coli* JM109 cells were streaked onto a LB agar plate, made using Difco LB Broth Lennox and Bacto™ Agar (BD Biosciences), and incubated at 37°C overnight. A single colony was inoculated into 10 mL of LB broth and grown in a 37°C shaking incubator overnight. This starter culture was used to inoculate 200 mL of LB broth and was grown in a 37°C shaking incubator until the culture reached OD_{600} = 0.6. The bacteria were incubated on ice for 30 minutes, then pelleted at 3,000 x g and 4°C for 5 minutes. The cell pellet was then resuspended in 25 mL of ice-cold 0.1 M $MgCl_2$ and pelleted again. The bacteria were resuspended in 8 mL of ice-cold 0.1 M $CaCl_2$ and 15% (v/v) glycerol and incubated on ice for 1 hour. Aliquots were frozen and stored at -80°C until required.

2.1.2.4 Transformation of competent cells

A 100 µL frozen aliquot of chemically competent *E. coli* JM109 cells per ligation were incubated on ice for 5 minutes. The ligation reaction was added to a 100 µL aliquot of bacterial cells, mixed gently and incubated on ice for 30 minutes. The cells were then heat-shocked at 42°C for 2 minutes and placed back on ice for 5 minutes. Following this, 200 µL of LB broth was added to the cells and incubated for 30 minutes in a 37°C shaking incubator. The cells were then spread onto a LB agar plate containing 100 µg/mL ampicillin (Sigma-Aldrich) and incubated at 37°C overnight. Transformed colonies were picked and used to inoculate LB broth for subsequent plasmid purification.

2.1.2.5 Purification of plasmid DNA from bacteria

For small scale plasmid DNA extractions from bacteria, buffers P1, P2 and P3 (QIAGEN) were used to perform alkaline lysis-based mini-preps, according to the manufacturer's instructions. For medium scale plasmid DNA extractions from bacteria, the PureLink™ HiPure Plasmid Filter Midiprep Kit (Invitrogen) and PureLink™ HiPure Precipitator Modules (Invitrogen) were used to perform midi-preps, according to the manufacturer's instructions.

2.1.2.6 Sanger sequencing

Plasmids/linear DNA fragments and appropriate primers were provided to the Australian Genome Research Facility (AGRF), which undertook the Sanger sequencing reactions and generated sequencing chromatograms. Analysis of the sequencing data was performed using the publicly available chromatogram viewer Chromas v2.6.2 (Technelysium) and the multiple sequence alignment tool ClustalX v2.1 (Science Foundation Ireland).

2.1.2.7 Generation of expression vectors

HA-tagged *Samsn1* overexpression vector

A sequence encoding a HA-tag followed by a stop codon was inserted between the *Nde*I and *Xho*I restriction enzyme sites in the retroviral pRUFimCH2 vector[260]. The murine *Samsn1* coding sequence was then amplified from C57BL/6 splenocyte-derived cDNA by PCR such that the product contained the *Samsn1* open reading frame with the start codon forming part of one *Nde*I site and the stop codon replaced by a second *Nde*I site. The *Nde*I-flanked *Samsn1* insert and the HA-tag-containing pRUFimCH2 vector were then *Nde*I digested and ligated to generate the pRUFimCH2.Samsn1-HA vector, which encodes Samsn1 with an in-frame C-terminal HA tag.

Glipr1 overexpression vector

To generate a *Glipr1* overexpression vector, the *Glipr1* coding sequence was amplified from C57BL/6 thymus-derived cDNA and subcloned into the pRUFimCH2 retroviral vector to generate pRUFimCH2.Glipr1, as previously described[260].

SAMSN1 overexpression vector

A retroviral overexpression vector for *SAMSN1*, pRUFiG2.SAMSN1, was previously generated[260].

SAMSN1 gRNA expression vectors

The MIT CRISPR design tool (http://crispr.mit.edu) was used to select two guide RNAs (gRNAs) targeting exon 4 of *SAMSN1*. The sequences of gRNA #1 and #2 were *5'*-GGTCACTGTTTCTATATGGG-*3'* and *5'*-GAGACTATCCATGGAGTCAC-*3'*, respectively. To clone the individual gRNAs, 24 bp complementary oligonucleotides containing the gRNA sequence and a 4-bp overhang (forward: TCCC and reverse: AAAC) were annealed and phosphorylated. The gRNA containing double-stranded DNA fragments were cloned into the *Bsmb*I-digested pFH1tUTG lentiviral vector [284], which was kindly provided by Assoc Prof Marco Herold (WEHI, Australia).

2.1.2.8 Heteroduplex mobility assay

DNA was extracted and purified from CRISPR-targeted cells using a DNeasy® kit (QIAGEN). PCR was performed to amplify a 1.1 kb region encompassing exon 4 of *SAMSN1* using primers F: 5'-CTAGGTGGCAAGCATGGTATTAGATTTG-3' and R: 5'-AGAAAGAAAGAGACAGAGAATGGAGCAG-3'. The products were subjected to heteroduplex formation in which they were incubated at 95°C for 5 minutes and the temperature was then reduced to 85°C at a ramp rate of 51%, followed by a decrease to 25°C at a ramp rate of 2.6%. The products were resolved by gel electrophoresis within a 12% acrylamide gel in 1x TBE buffer (100 mM Tris base, 100 mM boric acid, 2 mM EDTA) and post-stained with GelRed® (Biotium) to enable DNA visualisation using a Gel Doc™ XR+ Imager (Bio-Rad).

2.1.3 Protein techniques

2.1.3.1 Preparation of whole cell lysates

Cells were washed in ice-cold 1x phosphate buffered saline (PBS, Sigma-Aldrich) and then resuspended in an appropriate volume of radioimmunoprecipitation assay (RIPA) buffer (1% NP-40 (v/v), 20 mM HEPES, 150 mM NaCl, 10% glycerol (v/v), 2 mM Na_3VO_4, 10 mM $Na_4P_2O_7$, 2 mM NaF, and 1x cOmplete™ EDTA-free Protease Inhibitor Cocktail (Roche)) by vortexing. Samples were incubated on ice for 30 minutes with occasional vortexing. The lysates were then centrifuged at 20,000 x g at 4°C for 20 minutes and the supernatant was collected. The protein concentration in the cleared whole cell lysate was determined using the *RC DC*™ Protein Assay Kit (Bio-Rad), according to manufacturer's instructions. Protein lysates were stored at -80°C.

2.1.3.2 Western blotting

An appropriate amount of protein lysate was mixed with reducing buffer (50 mM Tris-HCl pH 7.4, 10% glycerol (v/v), 2% sodium dodecyl sulphate (SDS) (w/v), 0.02% bromophenol blue (w/v) and 5% β-mercaptoethanol (v/v)) and denatured by boiling for 4 minutes. Proteins were loaded into 10% SDS-polyacrylamide gel electrophoresis (PAGE) gels in Tris-Glycine-SDS running buffer (0.3% (w/v) Tris-HCl, 1.44% (w/v) glycine and 0.1% (w/v) SDS). To resolve the proteins, gel electrophoresis was performed using the Mini-PROTEAN™ III System (Bio-Rad). Proteins were transferred from the gel to a nitrocellulose 0.45 µm membrane (Bio-Rad) using the Mini Trans-Blot® Electrophoretic Transfer Cell (Bio-Rad). The transfer was performed in transfer buffer (192 mM Tris, 25 mM glycine, 20% methanol (v/v) and 0.02% (w/v) SDS) at 100 V and 4°C for 1 hour. Following the transfer, the membrane was incubated with membrane blocking buffer (5% (w/v) skim milk powder in 1x TBST buffer (50 mM Tris-HCl pH 7.5, 150 mM NaCl and 0.1% TWEEN 20)) at room temperature for 1 hour. The blocked membrane was then probed with primary antibody (Table 2.2) at an optimised concentration in membrane blocking buffer with rocking and at 4°C overnight. For blots expected to have low signal intensity, the primary antibody was diluted in Solution 1 from the SignalBoost™ Immunoreaction Enhancer Kit (Merck). Following 3 washes in TBST, the blot was incubated with an appropriate DyLight-680/800-conjugated secondary antibody (Thermo Fisher Scientific) diluted 1:10,000 in TBST, or Solution 2 from the enhancer kit, with rocking and at room temperature in the dark for 1 hour. The blot was again washed 3 times in TBST and then imaged using the Odyssey® CLx Imager (LI-COR). Quantitative analysis of band intensity was performed using ImageJ software (http://fiji.sc).

Table 2.2: Primary antibodies used for Western blotting.

Target	Source	Concentration	Company	Catalogue no.
GLIPR1	Polyclonal goat	1:250	R&D Systems	AF4468
HA-tag	Monoclonal mouse	1:1,000	Cell Signalling Technology	2367S
HS1	Polyclonal rabbit	1:1,000	Cell Signalling Technology	4557
pHS1	Polyclonal rabbit	1:1,000	Cell Signalling Technology	4507
SAMSN1	Polyclonal rabbit	1:500	Sigma-Aldrich	HPA010645
HSP90	Polyclonal rabbit	1:2,500	Santa Cruz Biotechnology	7947
β-Actin	Monoclonal mouse	1:5,000	Sigma-Aldrich	A1978

2.1.3.3 Co-immunoprecipitation

5TGM1 cells (2 x 10^7) were washed twice in ice-cold 1x PBS and lysed in 1 mL of immunoprecipitation (IP) lysis buffer (50 mM Tris-HCl pH 7.4, 150 mM NaCl, 10% glycerol (v/v), 2 mM Na_3VO_4, 1x cOmplete™ Protease Inhibitor Cocktail (Roche) and 1% NP-40/CHAPS (v/v)) for 30 minutes under rotation at 4°C. The lysate was cleared by centrifugation, as described in section 2.1.3.1, added to 50 µL packed volume of anti-HA antibody-conjugated agarose (clone 3F10, rat IgG1; Roche) and incubated under rotation and at 4°C for 2 hours. The agarose was then washed 5 times in 1 mL of IP lysis buffer and the associated proteins were eluted by boiling with 50 µL of 2x reducing buffer for 5 minutes. The supernatant was collected and split into two fractions (10% and 90% of the total volume), which were separately subjected to SDS-PAGE along with pre-IP and post-IP controls, as described in section 2.1.3.2. To assess the success of the IP, lanes of the gel containing pre-IP, post-IP and 10% of the eluates were transferred to a nitrocellulose membrane and subjected to Western blotting using an anti-HA-tag primary antibody, as described in section 2.1.3.2. The remaining portion of the gel containing most of the co-IP eluates was fixed and stained with SYPRO™ Ruby Protein Gel Stain (Invitrogen), according to the manufacturer's instructions, and then imaged using a Gel Doc™ XR+ Imager (Bio-Rad).

2.2 Cell culture techniques

2.2.1 Maintenance of cells in culture

All cell lines were maintained in a humidified environment at 37°C in the presence of 5% CO_2 and were manipulated within a class II biological safety cabinet. Unless otherwise specified, all cell culture reagents were sourced from Sigma-Aldrich and all media were supplemented with 2 mM L-glutamine, 100 U/mL penicillin, 100 µg/mL streptomycin, 1 mM sodium pyruvate, and 10 mM HEPES buffer. All cell lines were tested for mycoplasma infection using a MycoAlert™ Mycoplasma Detection Kit (Lonza) prior to use and were maintained in culture for a maximum of 4 weeks.

2.2.1.1 Mouse myeloma 5TGM1 cell line

The murine MM 5TGM1 PC line was originally kindly provided by Assoc Prof Claire Edwards (University of Oxford, UK). 5TGM1 cells expressing both green fluorescent protein (GFP) and luciferase were previously generated using the retroviral expression vector NES-TGL[285]. To generate a basal 5TGM1 cell line with enhanced BM tropism,

5TGM1 cells were previously injected i.v. into C57BL/KaLwRij (KaLwRij) mice (section 2.3.5.1) and those present in the long bones of the hind limbs were purified and expanded. 5TGM1 cells were maintained in Iscove's Modified Dulbecco's Medium (IMDM) with 20% fetal calf serum (FCS, Thermo Fisher Scientific), which is termed complete IMDM. The cells were sub-cultured every 2-3 days to maintain a concentration of 0.2-2 x 10^6 cells/mL.

2.2.1.2 Human myeloma cell lines

Human myeloma cell line (HMCL) RPMI-8226 was purchased from the American Type Culture Collection (ATCC), while the HMCLs LP-1, OPM2 and JJN3 were a kind gift from Prof Andrew Spencer (Monash University, Australia). All HMCLs were maintained in Roswell Park Memorial Institute 1640 (RPMI-1640) medium with 10% FCS (complete RPMI-1640 medium) and sub-cultured every 2-3 days to maintain a concentration of 0.2-1 x 10^6 cells/mL.

2.2.1.3 BM cell lines

The mouse BM stromal cell (BMSC) line OP9 was obtained from the ATCC and was maintained in Dulbecco's Modified Eagle Medium (DMEM) with 10% FCS (complete DMEM). Medium was renewed every 2-3 days and confluent monolayers were split at a sub-cultivation ratio of 1:5. Briefly, cells were harvested by rinsing with sterile PBS and adding 0.05% (v/v) trypsin-EDTA. Cells were incubated at 37°C for 1-5 minutes, depending on the time taken to detach from the culture flask. Trypsin activity was then neutralised by the addition of FCS-containing medium and detached cells were pelleted at 400 x g for 5 minutes. The cell pellet was resuspended in fresh complete DMEM and an appropriate aliquot of the cell suspension was added to a new culture flask.

A transformed human BM endothelial cell (TrHBMEC)[286] line was kindly provided by Prof Babette Walker (Cornell University, USA). TrHBMECs were maintained in gelatin-coated flasks and Medium 199 with 20% FCS and supplements consisting of 0.1% sodium bicarbonate (w/v), 1 mM sodium pyruvate, 20 mM HEPES, 50 U/mL penicillin, 50 µg/mL streptomycin, 1 x non-essential amino acids, 15 mg/mL heparin and 15 mg/mL endothelial cell growth supplement (BD Biosciences). The medium was renewed every 2-3 days and confluent monolayers were harvested by trypsinisation and sub-cultured, as described above. All experiments were performed using cells between passages 17 and 25.

2.2.1.4 Human embryonic kidney (HEK) 293T cell line

HEK293T cells were cultured in complete DMEM and cells were sub-cultured every 2-3 days by trypsinisation, as described in section 2.2.1.3.

2.2.2 Generating primary KaLwRij BMSC-conditioned medium

BMSCs were isolated by plastic adherence from bone chips of healthy adult KaLwRij mice and cryopreserved. Thawed BMSCs were seeded in Minimum Essential Medium Eagle, Alpha Modification (α-MEM) with 10% FCS and 100 mM L-ascorbate-2-phosphate. Medium was refreshed every 2-3 days until the BMSCs reached confluence. The regular medium was then replaced by serum-free α-MEM and the confluent BMSCs were incubated at 37°C with 5% CO_2 for 24 hours. The conditioned medium was then collected and passed through a 0.45 μm filter to remove any cells. Concentration of the conditioned medium was achieved by centrifugation in Centriprep® Centrifugal Filter Units (Merck). Aliquots of concentrated conditioned medium were stored at -20°C.

2.2.3 Generating genetically modified cell lines

2.2.3.1 Generation of Samsn1-HA/Glipr1-overexpressing 5TGM1 cells

HEK293T cells (1.5 x 10^6 cells/transfection) were seeded in 6 cm culture dishes in complete DMEM 24 hours prior to transfection. The cells were then transfected with 5 μg of the gene-encoding or empty pRUFimCH2 plasmid and 5 μg of the murine ecotropic packaging plasmid pEQECO[287] using Lipofectamine 2000 (Invitrogen), according to the manufacturer's instructions. After 48 hours, medium containing retrovirus was collected from the transfected HEK293T cells and added dropwise through a 0.45 μm surfactant-free cellulose acetate membrane filter onto 5TGM1 cells (4×10^5 cells/infection) in complete IMDM containing polybrene (final concentration of 8 μg/mL) in a 6-well plate. The 5TGM1 cell-virus mixture was centrifuged in the 6-well plate at 1,000 x g and room temperature for 1 hour and then incubated at 37°C with 5% CO_2 overnight. The cells were washed with complete IMDM and expanded in culture. Following another wash, the 5TGM1 cells underwent fluorescence activated cell sorting (FACS) for mCherry protein expression, which indicated successful transduction of the pRUFimCH2 plasmid, on a FACSAria™ Fusion (BD Biosciences). Subsequent sorts were conducted, where appropriate, until a pooled cell line consisting of > 90% mCherry$^+$ 5TGM1 cells was obtained. The basal luciferase activity of the modified 5TGM1 cells compared to the paired empty vector (EV) control cells was assessed by seeding an equal number of cells in quadruplicate in a 96-well

plate, adding 0.3 mg/mL D-luciferin (Biosynth) and performing bioluminescence imaging using the IVIS® Spectrum (PerkinElmer). No significant differences in luciferase activity were observed between the modified 5TGM1 cell lines.

2.2.3.2 Generation of SAMSN1-overexpressing HMCLs

HEK293T cells were prepared, as described in section 2.2.3.1, and transfected with 5 µg of the SAMSN1-encoding or empty pRUFiG2 plasmid and 5 µg of the amphotropic packaging plasmid pEQPAM3[287]. HMCLs were infected with the resultant retrovirus, as described in section 2.2.3.1, except the cells were not centrifuged after the addition of virus. Following washing and expansion, virus-exposed HMCLs were sorted for GFP expression, which indicated successful transduction of the pRUFiG2 plasmid, on a FACSAria™ Fusion (BD Biosciences) and pooled cell lines were established, as described in section 2.2.3.1.

2.2.3.3 Generation of SAMSN1 knockdown HMCLs using CRISPR-Cas9

Firstly RPMI-8226 and JJN3 HMCLs constitutively expressing Cas9 were generated by transducing the HMCLs with the FUCas9mCh lentiviral vector[284], which was a kind gift from Assoc Prof Marco Herold (WEHI, Australia). Lentiviral particles were produced using the psPAX2 lentiviral packaging plasmid and the pVSVG envelope protein-expressing plasmid and mCherry$^+$ cell lines were established, as described in section 2.2.3.1. The Cas9-expressing HMCLs were then transduced with an inducible gRNA-containing or empty pFH1tUTG vector, again using psPAX2 and pVSVG to produce lentivirus. Successfully transduced GFP$^+$mCherry$^+$ cells were isolated by FACS and gRNA expression was transiently induced by treating the HMCLs with doxycycline (Sigma-Aldrich) at a final concentration of 1 µg/mL for 72 hours. Following removal of doxycycline from the medium, the pools of treated cells were expanded to create SAMSN1 knockdown HMCLs.

2.2.4 *In vitro* assays

2.2.4.1 Co-culture luciferase proliferation assay

5TGM1 cells were seeded in triplicate at 1×10^5 cells/mL in complete IMDM with, or without, a confluent layer of OP9 cells. After 72 hours of co-culture at 37°C with 5% CO_2, the 5TGM1 cells were enumerated by measuring luciferase activity. Briefly, cells were collected with the aid of trypsin, washed in PBS and lysed in 40 uL of 1x Luciferase Cell Culture Lysis Reagent (Promega). The lysates were vortexed for 10 seconds, centrifuged at 12,000 x g and 4°C for 2 minutes and then 20 µL of supernatant was transferred into an

opaque 96-well plate. Bioluminescence was measured by adding 100 µL of luciferase reaction buffer (5 mM $MgCl_2$, 30 mM HEPES, 150 µg/mL D-luciferin (Biosynth) and 150 µM ATP) per well and reading the signal on a luminometer (Wallac 3000). A standard curve was produced for each cell line to determine the absolute number of cells present, which corrected for any differences in basal luciferase activity.

2.2.4.2 WST-1 proliferation assay

HMCLs were plated at 1 x 10^5 cells/mL in triplicate in 100 µL of complete RPMI-1640 medium in 4 replicate 96-well plates and incubated at 37°C with 5% CO_2. Every 24 hours from day 0 to 3, 10 µL of WST-1 Reagent (Roche) was added to all the relevant wells of one plate, which was then returned to the incubator for 2 hours. During the incubation, the WST-1 tetrazolium salt was cleaved by cellular mitochondrial dehydrogenases to produce a formazan dye (max absorbance at ~440 nm). Following the incubation, the absorbance of each well at 450 nm was measured using the iMark™ Microplate Absorbance Reader (Bio-Rad) and the plate discarded. The background was subtracted from the absorbance values and the fold-change in absorbance was calculated relative to day 0.

2.2.4.3 Colony formation assay

5TGM1 cells were seeded (200 cells per 35 mm dish) in duplicate in MethoCult™ semi-solid methylcellulose medium (StemCell Technologies), according to the manufacturer's instructions. After 12 days of culture at 37 °C and 5% CO_2, colonies were manually counted using a light microscope.

2.2.4.4 Actin remodelling assay

To assess filamentous actin (F-actin) formation, 5TGM1 cells were washed twice in serum-free IMDM media and were stimulated with 200 ng/mL (final concentration) recombinant mouse CXCL12 (R&D Systems) in triplicate for the indicated times. 5TGM1 cells were immediately fixed in 2% paraformaldehyde (pH 8.0) at room temperature for 15 minutes, washed 3 times in wash buffer (0.2% saponin (w/v) and 5% FCS in PBS) and stained with 1:20 Alexa Fluor™ 680 phalloidin (200 U/mL; Life Technologies) on ice and in the dark for 30 minutes. Cells were then washed 3 times with wash buffer and the mean fluorescence intensity (MFI) of phalloidin staining was quantitated on a LSRFortessa™ X-20 flow cytometer using FACSDiva™ software v8.0 (BD Biosciences).

2.2.4.5 Transwell and transendothelial migration assays

Transwell and transendothelial migration assays were performed in 24-well plates with 8 µm pore transwells (Corning). For transwell assays, 5 x 10^5 5TGM1 cells in serum-free IMDM were seeded in transwells in triplicate. The cells were allowed to migrate towards the lower chamber containing serum-free IMDM plus 5% (v/v) concentrated primary KaLwRij BMSC-conditioned medium for 24 hours. For transendothelial assays, 1 x 10^4 TrHBMECs were plated on gelatin-coated transwells and were allowed to adhere for 24 hours. HMCLs (5 x 10^5 cells) in RPMI-1640 medium with 1% FCS were then seeded into the BMEC-coated transwells in triplicate. The cells were allowed to migrate towards the lower chamber containing RPMI-1640 medium with either 20% FCS or 1% FCS and 100 ng/µL CXCL12 for 20 hours. Following the incubation period, the transwells were discarded and the numbers of migrated cells present in the plate were enumerated using an Olympus CKX41 inverted light microscope and ImageJ software (http://imagej.nih.gov/ij/).

2.2.4.6 Adhesion assay

TrHBMECs (1 x 10^4 cells/well) were plated in opaque-walled and clear-bottomed 96-well plates and allowed to adhere overnight. 5TGM1 cells (1 x 10^5 cells/well) in complete IMDM were then overlaid onto the TrHBMECs in quadruplicate and allowed to adhere for 15 minutes at 37°C and 5% CO_2. Following this incubation, the wells were gently washed 3 times with complete IMDM to remove nonadherent cells. The number of adherent 5TGM1 cells in each well was enumerated by the addition of 0.3 mg/mL D-luciferin (Biosynth) followed by bioluminescence imaging using the IVIS® Spectrum (PerkinElmer). The bioluminescent signal from adhered 5TGM1 cells was normalised to the signal from the total cell input.

2.2.4.7 5TGM1 single-colour immunofluorescence staining and flow cytometry

5TGM1 cells were harvested from culture, washed and resuspended in ice-cold PFE buffer (2% FCS and 2 mM EDTA in PBS). 5TGM1 cells at 1 x 10^7 cells/mL were incubated with flow cytometry (FC) blocking buffer (1:100 mouse gamma globulin (Jackson ImmunoResearch) in PFE buffer) on ice for 30 minutes. Aliquots of 1 x 10^6 cells in 0.1 mL of FC blocking buffer were then incubated with 5 µL of primary antibody (Table 2.3) on ice for 1 hour. Cells were washed twice with 2 mL of chilled PFE buffer and then resuspended in 0.1 mL of 1:100 Streptavidin-BV421 secondary antibody (#563259, BD Biosciences) in PFE buffer. Following a 30-minute incubation on ice and in the dark, cells were washed

twice with 2 mL of chilled PFE buffer and resuspended in 0.2 mL of FACS fixation buffer (1% (v/v) formalin, 2% (w/v) D-glucose, and 0.02% (w/v) NaN_3 in PBS). The BV421 MFI was measured for 50,000 cells per sample on a LSRFortessa™ X-20 flow cytometer using FACSDiva™ software v8.0 (BD Biosciences) and the data was analysed using FlowJo v10.0.8 software (FlowJo, LLC).

Table 2.3: Primary antibodies used for MHC immunostaining of 5TGM1 cells.

Target	Source	Conjugate	Concentration	Company	Cat no.
MHC Class I ($H\text{-}2D^b$)	Monoclonal mouse	Biotin	1:20	Thermo Fisher Scientific	13599982
MHC Class I ($H\text{-}2K^b$)	Monoclonal mouse	Biotin	1:20	Thermo Fisher Scientific	13595882
Isotype control	Mouse IgG2a (kappa)	Biotin	1:20	Thermo Fisher Scientific	13472485

2.3 Animal techniques

2.3.1 Generating knockout mice

2.3.1.1 C57BL/*Samsn1*$^{-/-}$ mice

C57BL/*Samsn1*$^{-/-}$ (*Samsn1*$^{-/-}$) mice were generated by first backcrossing the 180 kb *Samsn1* deletion in the KaLwRij genome onto a C57BL/6 background for 10 generations. To genotype the backcrossed mice, genomic DNA samples were generated from ear notches and PCR was performed using AmpliTaq Gold™ DNA Polymerase, as described in section 2.1.1.3. Separate primers were used to detect wildtype (WT) and deletion alleles of *Samsn1* (Table 2.4). The resultant heterozygous (*Samsn1*$^{+/-}$) mice were intercrossed and then the progeny with a homozygous Samsn1 deletion were incrossed to generate a stock *Samsn1*$^{-/-}$ colony.

2.3.1.2 C57BL/*Glipr1*$^{-/-}$ mice

C57BL/*Glipr1*$^{-/-}$ (*Glipr1*$^{-/-}$) mice were generated by the South Australian Genome Editing Facility (University of Adelaide, Australia) using CRISPR-Cas9. Briefly, gRNAs were designed that flanked the first exon of *Glipr1* (gRNA 1: 5'-ATCAGCGGCTCTCGACCCGT-3' and gRNA 2: 5'-ATTGGTTCTTGCCAAATGGGC-3'). These gRNAs and Cas9 mRNA were injected into C57BL/6 zygotes, which were then transferred to pseudopregnant recipients. Founder pups were genotyped by PCR using

Table 2.4: Sequences of primers for genotyping *Samsn1* and *Glipr1* knockout mice.

Allele	Primer	Primer sequence (5' to 3')	Primer position	Primer location (GRCm38)	Product size (bp)	Tm (ºC)
Samsn1 WT*	DEL+55kb.F	GTCAACGCTGCTGTGTTTGT	Intergenic, within KaLwRij deletion (3' end)	75,815,906 - 75,815,925	341	60
	DEL+55kb.R	CCGGAATGACAAGTGAGGCT	Intergenic, within KaLwRij deletion (3' end)	75,816,227 - 75,816,246		
Samsn1 Deletion	SamDEL.F	GGAGGTGATGATCTATTGTC	Intergenic, outside KaLwRij deletion (3’ end)	75,816,109 - 75,816,128	178	60
	SamDEL.R	CCATGATCATACAAGAAGCC	Intergenic, outside KaLwRij deletion (5’ end)	N/A (KaLwRij-specific)		
Glipr1 WT	P1	TTGCATATTAGCCCTCAGAACCCTTAGT	Promoter, outside CRISPR-Cas9 deletion (3’ end)	111,998,442 - 111,998,469	511	60
	P2	TGTGTGCCTTTGTCTGAGGTC	Promoter, within CRISPR-Cas9 deletion	111,997,959 -111,997,979		
Glipr1 Deletion	P1	As above	As above	As above	353[#]	60
	P4	ACACGGTAGCTTTTGTATGAAGGAACAGT	Intron 1, outside CRISPR-Cas9 deletion (5’ end)	111,994,476 - 111,994,504		

*This primer pair was previously described[260].

#The deletion allele produces a 353 bp product and the WT allele produces a 3994 bp product (only when using Phusion® DNA Polymerase).

separate primers to detect WT and deletion alleles of *Glipr1* (Table 2.4). This was performed according to section 2.3.1.1 except Phusion® High-Fidelity DNA Polymerase (New England BioLabs) was used to detect deletion alleles in the founder mice. PCR products from potential deletion alleles were Sanger sequenced, as described in section 2.1.2.6. A male founder that harboured a *Glipr1* exon 1 deletion was crossed with female C57Bl/6 (WT) mice and the resultant *Glipr1* deletion heterozygotes (*Glipr1*$^{+/-}$) were intercrossed. The progeny that were homozygous for the *Glipr1* deletion were then incrossed to generate a stock *Glipr1*$^{-/-}$ colony.

2.3.1.3 C57BL/*Samsn1*$^{-/-}$*Glipr1*$^{-/-}$ mice

C57BL/*Samsn1*$^{-/-}$*Glipr1*$^{-/-}$ (*Samsn1*$^{-/-}$*Glipr1*$^{-/-}$) mice were generated by first crossing *Samsn1*$^{-/-}$ mice with *Glipr1*$^{-/-}$ mice, resulting in double heterozygous deletion mice (*Samsn1*$^{+/-}$*Glipr1*$^{+/-}$). The double heterozygotes were then intercrossed to generate progeny, which were genotyped for both *Samsn1* and *Glipr1* deletions, as described above. The resultant double knockout *Samsn1*$^{-/-}$*Glipr1*$^{-/-}$ mice were incrossed to produce a stock colony. The *Samsn1*$^{-/-}$, *Glipr1*$^{-/-}$, *Samsn1*$^{-/-}$*Glipr1*$^{-/-}$ and C57BL/6 (WT) mice used for experiments were from separate stock colonies and were not littermates.

2.3.2 Peripheral blood counts

Peripheral blood (PB) samples were collected from mice by a tail bleed into EDTA-coated microvette tubes (Sarstedt). Complete blood counts were performed using a HEMAVET950 automated blood analyser (Drew Scientific), according to the manufacturer's instructions.

2.3.3 Multi-colour flow cytometry analyses of primary mouse cells

2.3.3.1 Preparing single cell suspensions from the BM, spleen and PB

BM was collected from cleaned femora and tibiae by repeatedly flushing the bones with 5 mL of chilled PFE buffer using a 10 mL syringe and 21 G needle or crushing the bones in PFE buffer using a mortar and pestle. The BM cell-containing solution was then homogenised and passed through a 70 μm filter. Spleens were excised and cleaned of any connective tissue prior to being pushed through a pre-wet 70 μm filter using the plunger of a 3 mL syringe. To generate a splenic single cell suspension, the filter was then washed with 5 mL of chilled PFE buffer. PB was collected by a terminal cardiac bleed using a 25 G needle and a 1 mL syringe containing 0.05 mL of 50 mM EDTA. The PB was then twice incubated with 9 mL of ACK red blood cell lysis buffer (150 mM NH_4Cl, 10 mM $KHCO_3$ and 0.1 mM

EDTA in milli-Q water) at room temperature for 10 minutes, followed by washing in 10 mL of chilled PFE buffer.

2.3.3.2 Antibody staining and flow cytometry

A defined number of cells (1-2 million depending on the tissue source) was stained with Fixable Viability Stain 700 (BD Biosciences) or hydroxystilbamidine (Invitrogen), according to the manufacturer's instructions. These cells were incubated in FC blocking buffer (section 2.2.4.7) on ice for 30 minutes and then stained with the relevant panel of fluorochrome-conjugated antibodies on ice and in the dark for 30 minutes (Table 2.5). Unstained, single-colour and fluorescence minus one (FMO) controls were also prepared for each panel to assist with gating cell populations. Following staining, the cells were washed twice with 2 mL of PFE buffer and stored in FACS fixation buffer prior to analysis. Typically, at least 100,000 events per sample were run on a LSRFortessa^{TM} X-20 flow cytometer using FACSDiva^{TM} software v8.0 (BD Biosciences) and the data was analysed, including calculating compensation, using FlowJo v10.0.8 software (FlowJo, LLC).

Table 2.5: Primary antibodies used in multi-colour flow cytometry panels for analysing primary mouse cells.

Target	Panel	Source	Conjugate	Conc	Company	Cat no.
B220	BM/spleen B cells and PB	Rat monoclonal (RA3-6B2)	FITC	1:200	Biolegend	103206
IgM	BM/spleen B cells	Rat monoclonal (R6-60.2)	PE-Cy7	1:200	BD Biosciences	552867
CD138	BM/spleen B cells	Rat monoclonal (281-2)	BV421	1:100	BD Biosciences	562610
CD3ε	PB, NK/T cells and CD8 MACS	Hamster monoclonal (145-2C11)	PE/FITC	1:100	Biolegend	100308/ 155604
CD11b	PB	Rat monoclonal (M1/70)	APC-Cy7	1:100	BD Biosciences	561039
Ly-6G	PB	Rat monoclonal (1A8)	PE-Cy7	1:80	Biolegend	127618
CD49b	NK/T cells	Rat monoclonal (DX5)	PE-Cy7	1:100	eBioscience	25597182
CD69	NK/T cells	Hamster monoclonal (H1.2F3)	AF647	1:100	Biolegend	104518
CD8a	CD8 MACS	Rat monoclonal (53-6.7)	PE-Cy5	1:200	Biolegend	100710

BM = bone marrow, PB = peripheral blood, NK = natural killer, MACS = magnetic-activated cell sorting.

2.3.4 Isolation of primary murine PC

BM was collected by flushing the long bones of the hind limbs from C57BL/6 and KaLwRij mice, as described in section 2.3.3.1. PCs were isolated from the BM by staining with a rat anti-CD138 primary antibody (#300506, R&D Systems) and an anti-rat IgG-PE secondary antibody (#3030-09, Southern Biotech), followed by FACS for PE^+ cells using the FACSAria™ Fusion (BD Biosciences).

2.3.5 *In vivo* models of MM tumour growth

KalwRij mice, originally kindly provided by Prof Andrew Spencer (Monash University, Australia) were rederived, bred and housed at the SAHMRI Bioresources Facility. NOD SCID gamma (NSG) and C57BL/6 mice were purchased from the SAHMRI Bioresources Facility. All procedures were performed with the approval of the SAHMRI, or University of Adelaide, Animal Ethics Committee. In all studies, the mice in different experimental groups were age- and sex-matched.

2.3.5.1 5TGM1 cells in KaLwRij/NSG mice intravenous and intratibial models

For i.v. delivery, 5TGM1 cells were washed and resuspended in sterile PBS at a concentration of 5 x 10^6 cells/mL. KaLwRij or NSG mice between 6 and 8 weeks old were injected with 0.1 mL of 5TGM1 cell suspension (5×10^5 cells) via the tail vein. The injected mice underwent *in vivo* bioluminescence imaging (BLI, section 2.3.6) 2, 3 and 4 weeks post-tumour cell injection and were humanely euthanised after 4 weeks. For intratibial (i.t.) delivery, 5TGM1 cells were washed and resuspended in sterile PBS at a concentration of 1 x 10^7 cells/mL. KaLwRij or NSG mice between 5 and 6 weeks old were anaesthetised by isoflurane inhalation for the duration of the procedure. A gas-sterilised 25 µL Hamilton syringe with a 27-gauge needle and containing 10 µL of cell suspension was inserted through the cortex of the anterior tuberosity of the left tibia. Once the bone cortex was traversed, the needle was inserted 3 to 5 mm down the diaphysis of the tibia, and the cell suspension (1 x 10^5 cells per inoculum) was injected into the marrow space. The injected mice underwent weekly *in vivo* BLI beginning on day 9 post-tumour cell injection and were humanely euthanised after 23 days. Mice with extensive extramedullary tumour growth in the injected leg, which indicated that the injection was misdirected, were excluded from the experiment.

2.3.5.2 5TGM1 cells in C57BL/6 mice intravenous model

5TGM1 cells were prepared for injection, as described in section 2.3.5.1, and the same amount was injected i.v. into 6-8-week-old C57BL/6 mice via the tail vein. The injected mice underwent *in vivo* BLI weekly or fortnightly starting 2-weeks post-tumour cell injection and were humanely euthanised after 4 or 7 weeks.

2.3.5.3 HMCLs in NSG mice intratibial model

HMCLs were washed and resuspended in sterile PBS at a concentration of 5 x 10^7 cells/mL. NSG mice between 5 and 6 weeks old received an i.t. injection of 10 µL of cell suspension (5 x 10^5 cells per inoculum), as described in section 2.3.5.1. The endpoint of the experiment was determined based on the first sign of morbidity, which was dependent on the HMCL injected. The experimental endpoint for mice injected with OPM2, JJN3, RPMI-8226 or LP-1 cells was 3, 3, 5 or 8 weeks, respectively. Mice with extensive extramedullary tumour growth in the injected leg, which indicated that the injection was misdirected, were excluded from the experiment.

2.3.6 *In vivo* bioluminescence imaging

Mice injected with luciferase-expressing 5TGM1 cells were shaved under anaesthesia prior to *in vivo* BLI. To measure tumour burden, the mice were administered firefly D-Luciferin substrate (30 mg/mL in PBS, Biosynth) by intraperitoneal injection at a concentration of 150 mg/kg. After 10 minutes, during which time the mice were anaesthetised by isoflurane inhalation, the dorsal, ventral and/or lateral aspects of the mice were scanned using the IVIS® Spectrum In Vivo Imaging System and Living Image® Software v4.5.5 (PerkinElmer), which was also used to quantitate the bioluminescence signal in the mice.

2.3.7 Serum protein electrophoresis

At the experimental endpoint, PB was collected from the 5TGM1-injected mice either by a tail bleed or terminal cardiac bleed. The blood was allowed to clot at room temperature and then centrifuged at 2,000 x g and 4°C for 10 minutes. The serum supernatant was collected and stored at -20°C. Subsequently, the serum samples were thawed and the levels of M protein/paraprotein were assessed by performing serum protein electrophoresis (SPEP) using the Hydragel Protein(E) Kit (Sebia), according to the manufacturer's instructions. The stained SPEP gels were imaged on a Gel Doc™ XR+ Imager (Bio-Rad), and the intensity of

the paraprotein band/M-spike was quantitated and normalised to the albumin band using Image Lab Software v6.0.1 (Bio-Rad).

2.3.8 Detection of GFP$^+$ tumour cells in mouse tissues by flow cytometry

Single cell suspensions of BM, spleen and PB from tumour cell-injected mice were obtained, as described in section 2.3.3.1. Cells from a mouse not injected with tumour cells were also analysed to act as a negative control for gating cell populations. The cells were pelleted, resuspended in PFE buffer and immediately analysed for the presence of GFP$^+$ tumour cells by flow cytometry on the FACSCanto^{TM} II (BD Biosciences) using FACSDiva^{TM} software v8.0 (BD Biosciences).

2.3.9 Immunohistochemistry

Tibiae that were directly injected with 5TGM1 cells were collected from KaLwRij mice at the experimental endpoint (day 23) and fixed in 10% (v/v) buffered formalin. The bones were decalcified by incubation with decalcification solution (0.5 M EDTA and 0.5% (w/v) paraformaldehyde in PBS at pH 8.0) at 4°C and the solution was refreshed twice weekly. The decalcified bones were then paraffin-embedded and 5 µm longitudinal sections were prepared. Sections were deparaffinised and stained with hematoxylin and eosin (H&E) or an anti-GFP antibody. For anti-GFP staining, endogenous peroxidase activity was neutralised by incubation with 0.5% H_2O_2 (v/v) in methanol for 30 minutes and the sections were then incubated with immunohistochemistry (IHC) blocking buffer (3% normal horse serum in PBS) at room temperature for 2 hours. The slides were incubated with a goat anti-GFP monoclonal antibody (#A600-101-215, Rockland) at 1:5,000 in IHC blocking buffer at 4°C overnight. After washing in 1x PBS, the slides were incubated with a biotinylated rabbit anti-goat IgG antibody (#BA5000, Vector Lab) 1:250 in IHC blocking buffer at room temperature for 30 minutes. This was followed by incubation with a streptavidin-peroxidase conjugate at 1:100 in blocking buffer at room temperature for 1 hour. The bound antibody was then visualised by incubating the slides with 3,3'-diaminobenzidine (Sigma-Aldrich) at room temperature and in the dark for 10 minutes. Slides were briefly counterstained with haematoxylin solution and mounted with DePex. Slides were imaged on a BX53 microscope (Olympus).

2.3.10 *In vivo* BM homing assay

5TGM1 cells (5 x 10^6 in 0.2 mL of PBS) were injected i.v. into 6-8-week-old KaLwRij mice via the tail vein. After 1 or 21 days, the mice were culled and both femora and tibiae from each mouse were collected and cleaned. These bones were flushed with PFE buffer and the marrow was collected. While in chilled PFE buffer, the bones were cut longitudinally, scraped and minced with a scalpel blade. All the cells were then filtered through a 70-µm cell strainer, pelleted and resuspended in PFE buffer. The samples were immediately analysed for the presence of GFP^+ tumour cells by flow cytometry on a FACSCanto™ II (BD Biosciences) using FACSDiva™ software v8.0 (BD Biosciences).

2.3.11 *Ex vivo* $CD8^+$ T cell cytotoxicity assay

To prevent proliferation of tumour cells, 5TGM1-Samsn1 and 5TGM1-EV cells were gamma-irradiated (30 Gy) prior to being injected (1 x 10^6 in 0.1 mL of PBS) i.v. into 6-8-week-old KaLwRij mice on days 0 and 14. On day 19, the mice were humanely euthanised and single cell suspensions from the spleen were prepared, as described in section 2.3.3.1. $CD8^+$ splenic T cells were purified by negative selection using the magnetic-activated cell sorting (MACS) $CD8a^+$ T Cell Isolation Kit (Miltenyi Biotec), according to the manufacturer's instructions. The purified T cells were re-stimulated by co-culture with irradiated 5TGM1-Samsn1/5TGM1-EV cells at a 10:1 ratio in T cell medium (complete RPMI-1640 medium supplemented with 0.05 mM β-mercaptoethanol, 1x non-essential amino acids and 2 ng/mL recombinant human IL-2 (R&D Systems)). After 5 days of co-culture, the T cells were harvested and seeded in T cell medium in triplicate with 1 x 10^4 irradiated 5TGM1-Samsn1/5TGM1-EV cells at a ratio of 4:1 or 2:1 in a 96-well plate. Following 24 hours of incubation at 37°C with 5% CO_2, the amount of tumour cell-specific lysis was measured using a lactate dehydrogenase release assay (CytoTox 96® Non-Radioactive Cytotoxicity Assay, Promega), according to the manufacturer's instructions. The maximum LDH release control for each target was determined by adding 10µl of 10X Lysis Solution to target cell-only wells 45 minutes before adding the CytoTox 96® Reagent. The background absorbance was subtracted from the readings and the percentage of specific cytotoxicity was calculated using the equation below.

$$\% \text{ Cytotoxicity} = \frac{\text{Experimental} - \text{Effector spontaneous} - \text{Target spontaneous}}{\text{Target maximum} - \text{Target spontaneous}} \text{ x } 100$$

2.3.12 Detection of anti-Samsn1 antibodies in serum

To potentially generate an anti-Samsn1 humoral immune response, 6-8-week-old KaLwRij, *Samsn1*$^{-/-}$ and C57BL/6 mice were injected i.v. with 5TGM1-Samsn1 cells or control 5TGM1-EV cells (5×10^5 in 0.1 mL of PBS) on days 0 and 14. On day 19, the mice underwent a terminal cardiac bleed and serum was collected, as described in section 2.3.7. To generate blots of size-resolved Samsn1 protein, IPs of Samsn1-HA from 5TGM1-Samsn1 cells were performed, as described in section 2.1.3.3. The only alteration was that 5 x 10^7 cells were lysed in 2 mL of 1% NP-40 IP lysis buffer. Identical IPs were also performed for 5TGM1-EV cells to act as a negative control. The immunoprecipitated eluates were split into 3 fractions (10%, 45% and 45%), which were subjected to SDS-PAGE in separate lanes of a 10% gel. The proteins in the gel were then transferred to a nitrocellulose membrane, which was divided into 3 sections. To confirm the successful IP of Samsn1 and indicate its position, the section of the membrane containing 10% of the IPs was probed with an anti-HA antibody. The remaining sections of membrane were probed with fresh serum from mice inoculated with either 5TGM1-Samsn1 or 5TGM1-EV cells, which was diluted 1:10 in Solution 1 from the SignalBoost™ Immunoreaction Enhancer Kit (Merck), at 4°C overnight. Following removal of unbound antibody, the blots were incubated with goat anti-mouse IgG (H+L) secondary antibody conjugated to DyLight™ 680 (Thermo Fisher Scientific) diluted 1:10,000 in Solution 2 from the enhancer kit at room temperature for 1 hour. The blots were then scanned using the Odyssey® CLx Imager (LI-COR).

2.4 *In silico* analyses and statistics

2.4.1 Publicly available microarray data

For analysis of gene expression differences in CD138$^+$ BM PCs from MM patients with low (< 5 Affymetrix intensity value) vs normal/high levels (> 5 Affymetrix intensity value) of *SAMSN1* mRNA expression, a total of 1,191 patients from 3 independent publicly available microarray datasets were used: GSE19784 (n = 320)[180], GSE24080 (n = 554)[288] and GSE26760 (n = 304)[147]. Gene expression was normalised with the robust multi-array average (RMA) algorithm and differential gene expression was performed using linear models for microarray data (LIMMA) with array weight using R packages. For analysis of mRNA expression levels in CD138$^+$ BM PCs from MGUS patients, MM patients and normal controls, the publicly available microarray dataset GSE6477 was used (normal, n = 15; MGUS, n = 22; MM, n = 133)[289]. GSE19784, GSE24080 and GSE26760 were conducted on Affymetrix GeneChip™ Human Genome U133 plus 2.0 arrays, while GSE6477 was

conducted on Affymetrix GeneChip^{TM} Human Genome U133A arrays. Raw microarray data (CEL files) were downloaded from Gene Expression Omnibus (NCBI) and were normalized by RMA using the Bioconductor package affy and R (version 3.03) and log2 transformed.

2.4.2 Statistics

Unless otherwise described, statistical analysis was performed using GraphPad Prism v8.0.0 (GraphPad Software). The Fisher's exact test was used to determine whether the proportions of one categorical variable were different depending on the value of the other categorical variable. When three or more groups were being compared for a single variable, a parametric one-way ANOVA with Tukey's post-hoc multiple comparisons test or a non-parametric Kruskal-Wallis test with Dunn's multiple comparisons test was used. For time-course experiments, groups were compared using a two-way ANOVA with Sidak's or Tukey's multiple comparisons test. When two groups were being compared for a single variable, a parametric paired t test, a parametric unpaired t test or a non-parametric Mann-Whitney U test was used. Differences were statistically significant when $P < 0.05$.

3 INVESTIGATION OF THE POTENTIAL CO-OPERATIVE TUMOUR SUPPRESSOR EFFECTS OF SAMSN1 AND GLIPR1 IN MULTIPLE MYELOMA

3.1 Introduction

Multiple myeloma (MM) is an incurable haematological malignancy characterised by the uncontrolled proliferation of antibody-producing plasma cells (PCs) within the bone marrow (BM). MM is defined by the presence of 10% or more clonal PCs in the BM and one or more myeloma-defining events[21]. For example, evidence of end-organ damage that can be attributed to the malignant PC expansion, such as hypercalcemia, renal insufficiency, anaemia, and bone lesions. Almost all MM cases are preceded by the premalignant condition monoclonal gammopathy of undetermined significance (MGUS), a benign clonal PC proliferation characterised by less than 10% PCs in the BM and the absence of end-organ damage[19,20]. Approximately 3-4% of people over 50 years of age have MGUS and they have a 1% risk of progressing to MM per year, although the time to progression is variable[24].

The development of MGUS is thought to be initiated in a post-germinal centre B cell by one of two types of primary cytogenetic event; hyperdiploidy or a chromosomal translocation involving the immunoglobulin heavy-chain gene[110]. Malignant transformation and MM disease progression is then thought to occur due to the accumulation of secondary genetic hits, including further chromosomal rearrangements, DNA mutations, as well as transcriptional and epigenetic changes[110]. In terms of the abnormalities present in MM tumours, recent studies have revealed that there is significant interpatient heterogeneity, with low recurrence rates for many mutations[120,147-150]. In addition, there is considerable intrapatient heterogeneity, with most patients displaying a complex subclonal architecture that is dynamic and can evolve over time[148,149,212,214-216,221,231,232]. Notably, many of the chromosomal abnormalities and genetic lesions identified in MM PCs are also found at the MGUS stage[215,227,232], which highlights the possibility that novel epigenetic changes and/or PC-extrinsic factors are involved in driving the progression from asymptomatic MGUS to malignant MM.

In order to identify novel genetic changes that may be involved in promoting MM development, our group, and one other, compared the genetics of the closely related C57BL/6 and C57BL/KaLwRij (KaLwRij) mouse strains[260,261]. Both KaLwRij and C57BL/6 mice develop benign monoclonal gammopathy at a similarly high rate (60-70% by two years old), but the KaLwRij mice are unique in their ability to spontaneously develop an MM-like disease, albeit at a low frequency and with late onset (0.5% in mice over two years old)[263,264]. Whole genome and exome sequencing, as well as genome-wide

transcriptomic analyses, revealed many DNA sequence and gene expression differences between the two strains[260,261]. However, the most striking difference was a 180 kb homozygous genomic deletion on chromosome 16, which specifically encompasses *Samsn1*[260,261]. *Samsn1* encodes a putative adaptor protein, which is most highly expressed in the haematopoietic compartment, including the B cell lineage[240]. Notably, *SAMSN1* expression was found to be lower in $CD138^+$ PCs from MM patients compared to normal controls and MM patients with below median *SAMSN1* expression were found to have reduced overall survival[260,261]. Hence, it was hypothesised that the down-regulation of *SAMSN1* expression in PCs may promote MM development.

In order to test the functional effect of *Samsn1* loss in the context of MM, our group used the 5TGM1/KaLwRij model of MM[264,267]. In this model, the 5TGM1 murine MM cell line, which was established from a spontaneous KaLwRij PC tumour and thus is $Samsn1^{-/-}$, is injected i.v. into syngeneic KaLwRij mice and the tumour cells home to the BM. Once there, the 5TGM1 cells rapidly expand to cause substantial tumour burden throughout the skeleton in just 4 weeks. As the 5TGM1 cells were engineered to express luciferase, tumour burden can be assessed non-invasively by bioluminescence imaging (BLI)[260,290-292]. Notably, the forced expression of Samsn1 in 5TGM1 cells was found to completely inhibit tumour development in KaLwRij mice, suggesting that Samsn1 may have a tumour suppressor role in MM[260].

The development of cancer is a multistep process in which the gradual accumulation of genetic driver events within a cell leads to the deregulation of the normal restrictions on its growth and survival[293]. Next generation sequencing (NGS) studies of large cohorts of MM patients have revealed that specific pairs of genetic lesions recurrently co-occur within PC tumours[120,122,150]. In addition, convergent evolution of genetic lesions has been recurrently found in MM, whereby independent mutations in the same gene were present in different subclones of the same tumour[150,216,232,294]. Furthermore, transgenic mouse studies have demonstrated the importance of co-operation between genetic lesions in promoting the development of MM *in vivo*[158,236,237,239,295]. For example, the over-expression of MYC by the Vk*MYC transgene caused MM tumour development in MGUS-prone C57BL/6 mice but not MGUS-resistant BALB/c mice, suggesting that MYC activation must co-operate with other genetic lesions to drive the malignant transformation of PCs[158,239]. Together, these data suggest that co-operation between specific combinations of genetic driver events plays an

important role in promoting the development and progression of MM. However, the identity of co-operating lesions in MM and the mechanism by which they work together to drive disease development and/or progression is poorly understood.

As discussed above, Samsn1 was found to be a potent tumour suppressor in the 5TGM1/KaLwRij model of MM[260], but the KaLwRij mouse strain only rarely spontaneously develops PC tumours, despite being *Samsn1*$^{-/-}$[264]. This suggests that the loss of Samsn1 is necessary, but not sufficient, for the development of MM in KaLwRij mice. Hence, the down-regulation of SAMSN1 is likely to co-operate with another genetic lesion(s) to promote MM development, which remains to be identified. In this chapter, *in silico* analysis was used to identify reduced expression of *GLIPR1,* which has previously been described as a tumour suppressor gene[296-298], in MM patients who display low *SAMSN1* expression. In addition, *GLIPR1* was found to be expressed at lower levels in the PCs of MM patients compared to normal controls and the 5TGM1/KaLwRij model was used to investigate whether Glipr1 possessed tumour suppressor activity in MM. Furthermore, *Samsn1* and *Glipr1* double knockout mice were generated and the potential co-operative effect of losing both genes on MM disease development *in vivo* was examined.

3.2 Results

3.2.1 Reduced *GLIPR1* expression is associated with reduced *SAMSN1* expression in the PCs of MM patients

In order to identify genetic changes that may co-operate with reduced *SAMSN1* expression levels to drive MM disease development, an *in silico* analysis was performed on 1,178 diagnostic human MM CD138^{+} PC samples from three independent publicly available microarray gene expression datasets (GSE24080, GSE26760 and GSE19784). Only two genes were found to have significantly different expression levels in the PCs of MM patients with low *SAMSN1* expression (probe intensity < 5) compared to normal/high *SAMSN1* expression (probe intensity > 5) across all three datasets. The expression of the histone cluster 3 H2A (*HIST3H2A*) gene was found to be higher, and the expression of the glioma pathogenesis-related protein 1 (*GLIPR1*) gene was found to be lower, in MM PCs with low *SAMSN1* mRNA levels versus normal/high *SAMSN1* mRNA levels (P_{adj} < 0.05, LIMMA; Figure 3.1).

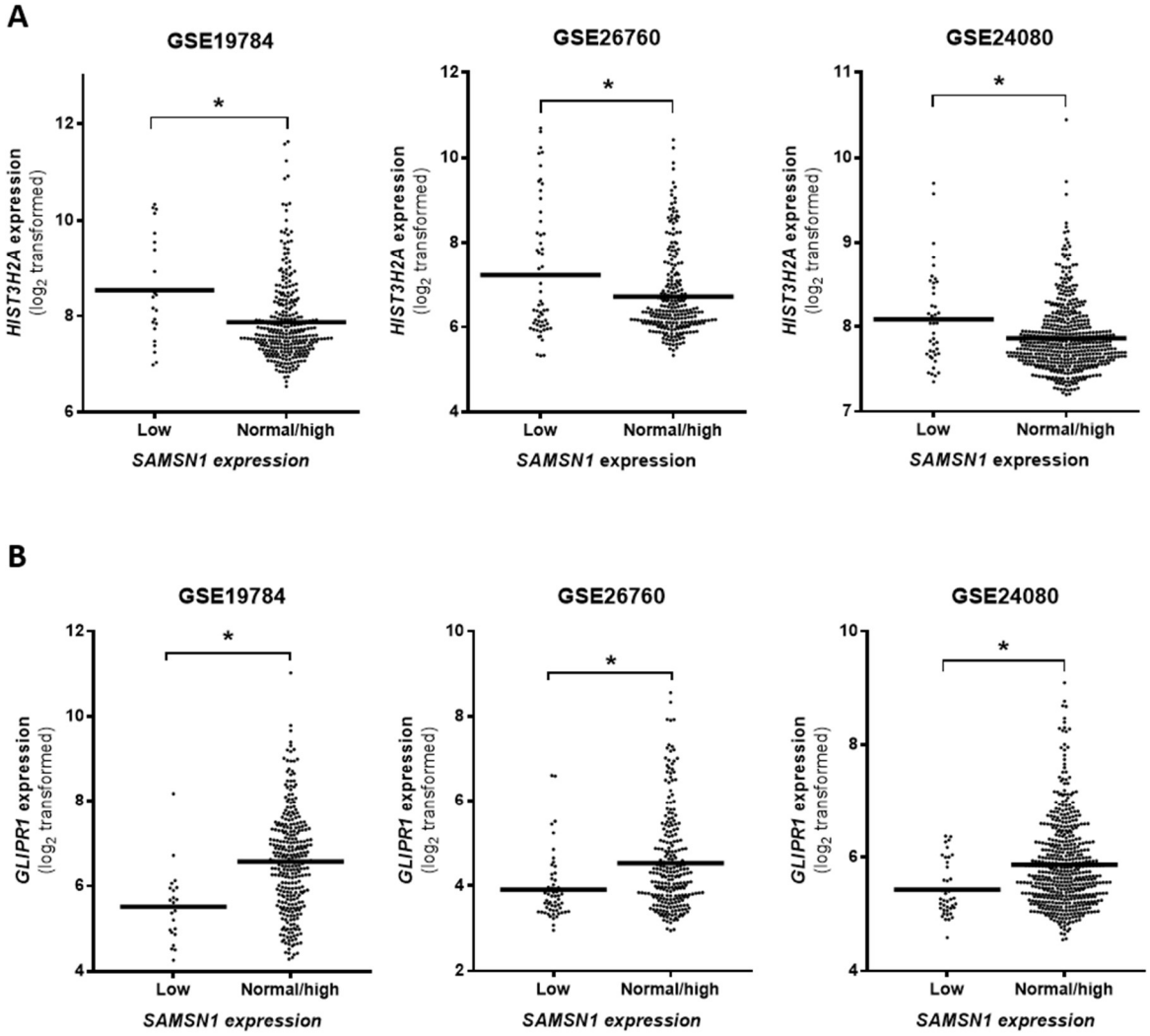

Figure 3.1: The expression levels of *HIST3H2A* and *GLIPR1* are altered in the PCs of MM patients with low *SAMSN1* expression. (**A**&**B**) *In silico* analysis was performed to identify genes with significantly different mRNA expression levels in $CD138^+$ PCs from MM patients with low (probe intensity value < 5) versus normal/high (probe intensity value > 5) *SAMSN1* expression in three microarray datasets: GSE19784 (low n = 22, normal/high n = 206), GSE26760 (low n = 57, normal/high n = 247) and GSE24080 (low n = 41, normal/high n = 518). Across all three datasets, the mRNA expression of *HIST3H2A* was found to be significantly higher (**A**), and the mRNA expression of *GLIPR1* was found to be significantly lower (**B**), in MM tumours with low versus normal/high *SAMSN1* expression. Scatter dot plots show the mean. *$P_{adjusted} < 0.05$, LIMMA.

To determine whether the expression of *HIST3H2A* and/or *GLIPR1* was deregulated in MM, *in silico* analysis of the mRNA levels of both genes in PCs from normal individuals (n = 15), MGUS patients (n = 22) and MM patients (n = 69) was performed using the GSE6477 microarray dataset. *HIST3H2A* expression was found to not be aberrantly expressed in the PCs of MM patients compared to normal controls (P = 0.5911, one-way ANOVA with Tukey's multiple comparisons test; Figure 3.2A), while *GLIPR*1 mRNA expression was significantly reduced in the PCs of MM patients compared to normal controls ($P < 0.0001$, one-way ANOVA with Tukey's multiple comparisons test; Figure 3.2B). In fact, ~70% (n = 48/69) of newly diagnosed MM patients were found to have *GLIPR1* expression levels below the normal range in the PCs of normal individuals. Notably, *GLIPR1* was previously found to have reduced expression in another PC malignancy, light-chain amyloidosis[299], and its absence was shown to promote the development of localised PC tumours in mice[298]. Collectively, these data suggest that *GLIPR1* may be a tumour suppressor gene in MM, the down-regulation of which may co-operate with reduced *SAMSN1* expression to promote disease development.

3.2.2 Re-expression of Glipr1 in 5TGM1 cells reduces MM disease development *in vivo*

To investigate the potential role of Glipr1 in the 5TGM1/KaLwRij murine model of MM, the expression of *Glipr1* in normal and malignant PCs was assessed by reverse transcription (RT)-PCR. *Glipr1* mRNA was found to be undetectable in the 5TGM1 MM PC line, while it was found to be present in normal PCs from KaLwRij mice and C57BL/6 mice (Figure 3.3A). This finding suggests that the loss of Glipr1 may co-operate with the absence of Samsn1 to drive MM development in KaLwRij mice. The next aim was to determine whether restoration of Glipr1 expression in 5TGM1 cells affects their growth *in vitro* and/or *in vivo*. 5TGM1 cells were transduced with a mCherry-labelled Glipr1 expression construct (5TGM1-Glipr1) or empty vector control (5TGM1-EV), and re-expression of Glipr1 in the 5TGM1-Glipr1 cells was confirmed by quantitative reverse transcription PCR (RT-qPCR; data not shown) and Western blot (Figure 3.3B). Glipr1 re-expression was not found to affect the proliferation of 5TGM1 cells following either mono-culture (P = 0.910, paired t test; Figure 3.3C) or co-culture with the OP9 murine BM stromal cell line (P = 0.683, paired t-test; Figure 3.3D). In addition, the number of colonies formed by 5TGM1-Glipr1 cells in semi-solid medium did not differ from that of 5TGM1-EV control cells after 12 days (P = 0.264, paired t test; Figure 3.3E).

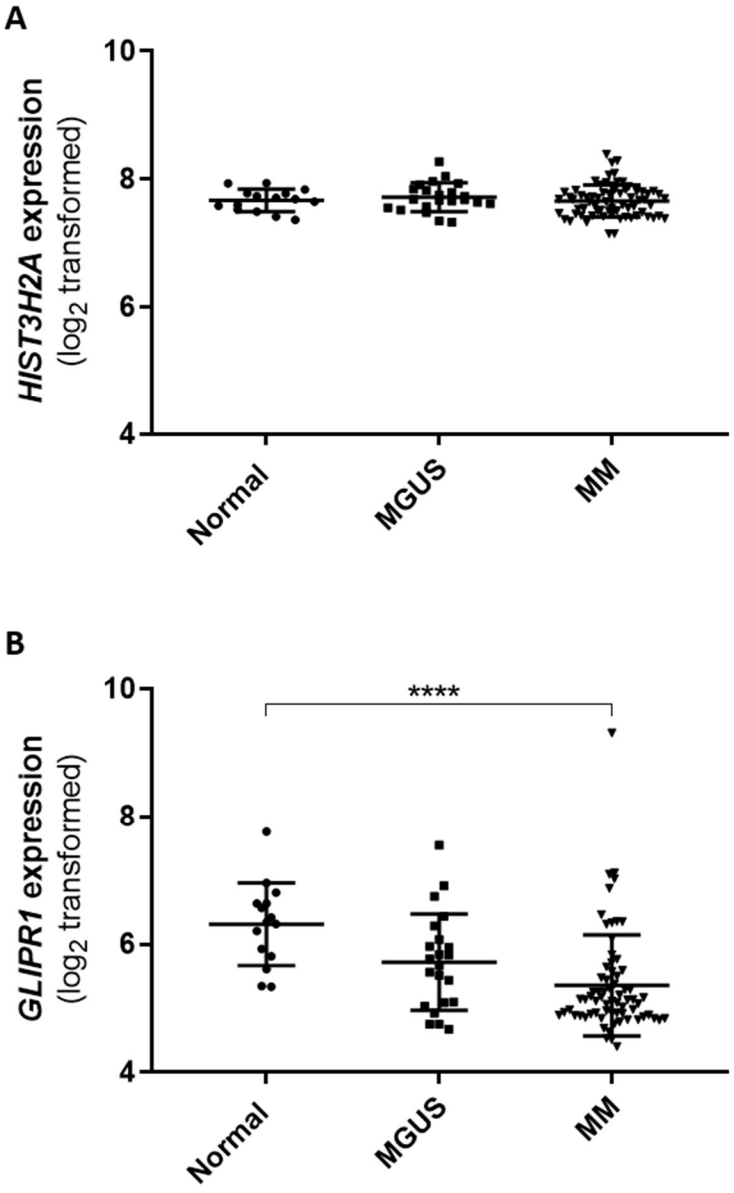

Figure 3.2: *GLIPR1* mRNA expression is down-regulated in PCs from MM patients. (**A**&**B**) *In silico* analysis was performed on publicly available microarray dataset GSE6477 analysing *HIST3H2A* (**A**) and *GLIPR1* (**B**) mRNA expression in $CD138^+$ PCs isolated from normal controls (n = 15), MGUS patients (n = 22) and MM patients (n = 69). Scatter dot plots show the mean ± SD. ****$P < 0.0001$, one-way ANOVA with Tukey's multiple comparisons test.

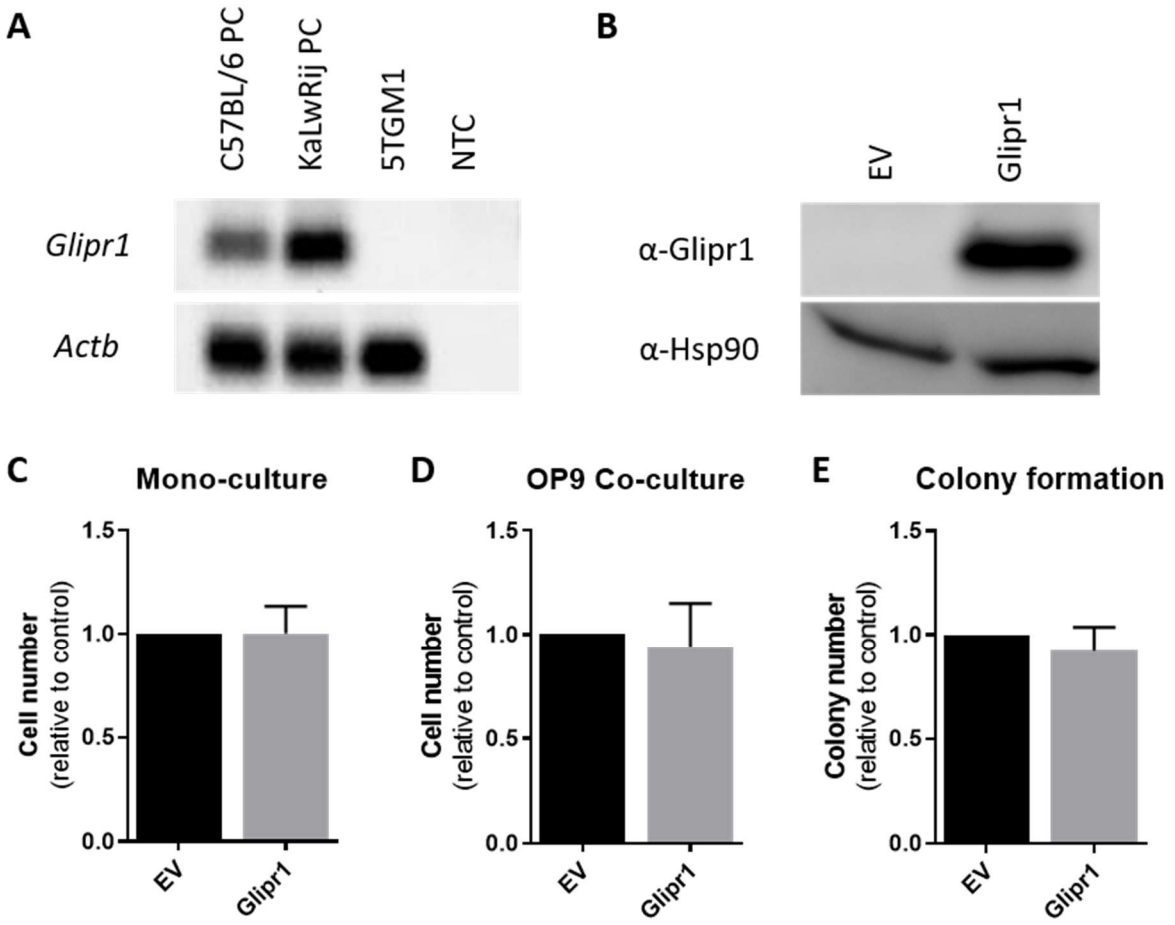

Figure 3.3: *Glipr1* expression is lost in 5TGM1 cells but its re-expression does not affect cell proliferation *in vitro*. (**A**) The expression of *Glipr1* mRNA was assessed in normal CD138^{+} PCs from C57Bl/6 and KaLwRij mice and the KaLwRij-derived 5TGM1 MM PC line by RT-PCR. The products were run on a 2% agarose gel and stained with GelRed®. *Actb* was used as a positive control. NTC = no template control. (**B**) The expression of Glipr1 protein in 5TGM1-Glipr1 (Glipr1) and control 5TGM1-EV (EV) cells was assessed by Western blot. Hsp90 was used as the loading control. The number of 5TGM1-Glipr1 cells in mono-culture (**C**) or co-culture with OP9 bone marrow stromal cells (**D**) was assessed by bioluminescence after 3 days. Cell number is expressed relative to the EV control cells. (**E**) Colony formation by 5TGM1-Glipr1 cells versus 5TGM1-EV cells was assessed in semi-solid methylcellulose-containing medium after 12 days. Colony number is expressed relative to the EV control cells. Graphs depict the mean + SD of three independent experiments. $P > 0.05$, paired t test.

To determine the effect of Glipr1 on MM tumour growth *in vivo*, the 5TGM1-Glipr1 and 5TGM1-EV cell lines were injected i.v. into KaLwRij mice and tumour burden was monitored at weekly intervals by BLI. There was a trend towards reduced tumour burden in the KaLwRij mice inoculated with 5TGM1-Glipr1 cells compared to mice inoculated with 5TGM1-EV cells at 4 weeks, but this decrease did not reach statistical significance (P = 0.2464, two-way ANOVA with Sidak's multiple comparisons test; Figure 3.4A). Tumour burden was also independently assessed at 4 weeks by measuring monoclonal paraprotein (M-spike) levels using serum protein electrophoresis (SPEP). The M-spike intensity showed the same trend toward reduced tumour burden in the 5TGM1-Glipr1 compared to the 5TGM1-EV group, but it did not reach statistical significance (P = 0.4509, Mann-Whitney U test; Figure 3.4B). These data suggest that restoring Glipr1 levels in 5TGM1 cells does not affect murine MM PC proliferation *in vitro* but may have some inhibitory effect on tumour development *in vivo*.

3.2.3 Samsn1 expression in the BM microenvironment does not affect MM tumour growth *in vivo*

Given that *GLIPR1* and *SAMSN1* are concomitantly down-regulated in MM PCs and both genes have a tumour suppressor effect on 5TGM1 tumour growth *in vivo*[260], it was hypothesised that these genes co-operate to inhibit the malignant transformation of PCs. In order to test this, the aim was to generate *Glipr1* and *Samsn1* double knockout mice (*Glipr1*$^{-/-}$*Samsn1*$^{-/-}$) that would be monitored for MM development as they aged. The C57BL/6 mouse strain was selected as the genetic background for these modifications, because it possesses high rates of age-related spontaneous MGUS, and thus is ideal for determining whether genetic alterations drive the malignant transformation of PCs[262]. Firstly, *Samsn1* knockout mice were produced by backcrossing the *Samsn1* deletion present in the genome of KaLwRij mice onto a C57BL/6 background for 10 generations. The absence of *Samsn1* mRNA expression in the BM of the backcrossed C57BL/*Samsn1*$^{-/-}$ (*Samsn1*$^{-/-}$) mice was confirmed by RT-PCR (Figure 3.5A).

A previous study showed that the injection of macrophages from *Samsn1*$^{-/-}$ mice versus wildtype (WT) C57BL/6 mice increased the growth of subcutaneous 5TGM1 tumours, suggesting that the loss of Samsn1 in PC-extrinsic cells of the BM microenvironment may promote the development of MM in KaLwRij mice[261]. To further investigate this hypothesis, the newly generated *Samsn1*$^{-/-}$ mice and WT mice were injected i.v. with 5TGM1 cells and

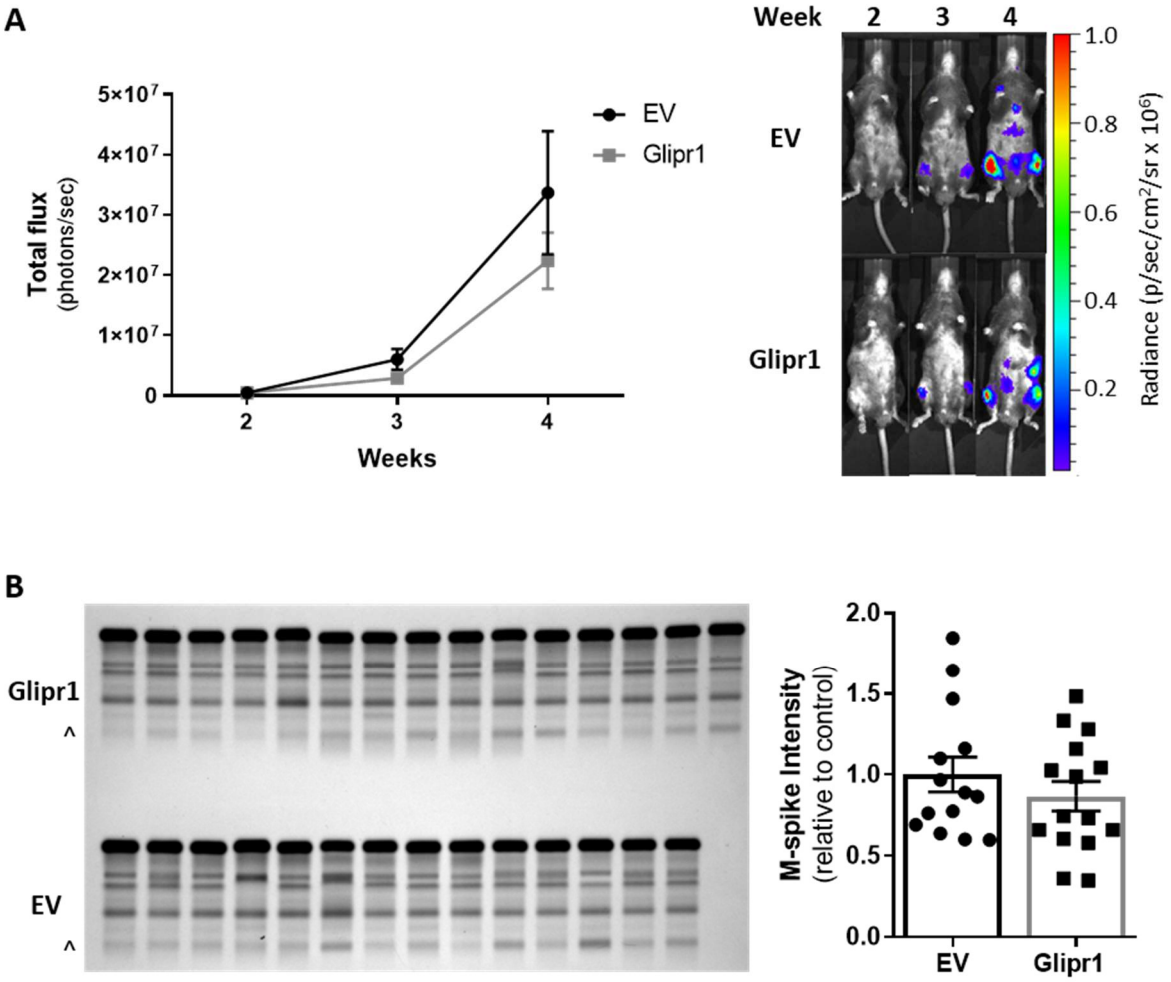

Figure 3.4: *Glipr1* overexpression in 5TGM1 cells reduces tumour growth *in vivo*. (**A**&**B**) KaLwRij mice were injected i.v. with 5 x 10^5 5TGM1-Glipr1 or 5TGM1-EV control cells. (**A**) Tumour burden in the mice was measured weekly from week 2 post-tumour cell inoculation by BLI and the signal from the ventral and dorsal scans were summed for each mouse. A graph of the total flux for the mice injected with 5TGM1-Glipr1 or 5TGM1-EV cells (left) and representative ventral scans of one mouse per cell line over time (right) are shown. (**B**) Serum was collected from the mice after four weeks and the M-spikes were measured by SPEP. M-spikes (^) on the SPEP gel (left) and the quantitated M-spike intensity (right), normalised to albumin and expressed relative to the EV control, are shown. Graphs depict the mean ± SEM of n = 14-15 mice per cell line from three independent experiments. $P > 0.05$, two-way ANOVA with Sidak's multiple comparisons test (**A**) or Mann-Whitney U test (**B**).

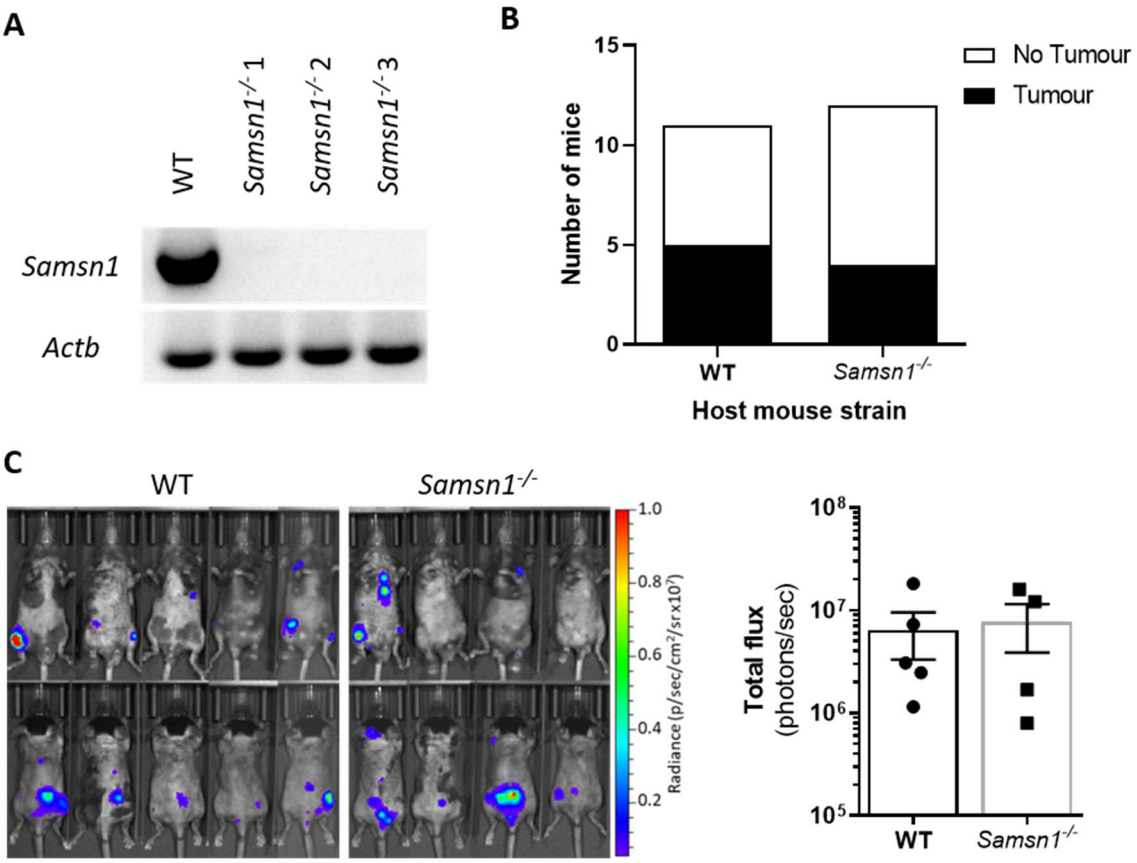

Figure 3.5: Samsn1 levels in the BM microenvironment do not affect 5TGM1 tumour growth *in vivo*. (**A**) The mRNA expression of *Samsn1* was assessed in the BM of *Samsn1*$^{-/-}$ mice and WT control mice by RT-PCR. The products were run on a 2% agarose gel and stained with GelRed®. *Actb* was used as a positive control. *Samsn1*$^{-/-}$ and WT mice were injected i.v. with 5TGM1 cells and tumour burden was measured by BLI (n = 11-12 mice per genotype from two independent experiments). (**B**) The number of *Samsn1*$^{-/-}$ and WT mice with and without tumour development at 4 weeks post-5TGM1 inoculation are shown. (**C**) For the tumour-bearing mice, ventral and dorsal scans (left) and the total flux from the summed ventral and dorsal scans (right) at 4 weeks are shown. The graph depicts the mean ± SEM. P > 0.05, Fisher's exact test (**B**) or Mann-Whitney U test (**C**).

tumour development in the BM was monitored by BLI for 4 weeks. Although the conventional wisdom is that 5TGM1 cells do not grow in mice with a C57BL/6 background[264,300], tumour was detected in 9 of the 23 (39.1%) *Samsn1*$^{-/-}$ and WT mice in this experiment (Figure 3.5B). This may be attributable to the fact that our 5TGM1 cell line was established from BM-resident 5TGM1 cells passaged in mice, which may have greater BM tropism compared to the 5TGM1 cells used by others. Notably, 45.5% (n = 5/11) and 33.3% (n = 4/12) of WT and *Samsn1*$^{-/-}$ mice, respectively, developed 5TGM1 tumours, which does not constitute a significant difference in tumour penetrance between the strains (P = 0.6802, Fisher's exact test; Figure 3.5B). In addition, of those mice that did develop tumour, there was no difference in tumour burden between the WT mice and *Samsn1*$^{-/-}$ mice (P = 0.9048, Mann-Whitney U test; Figure 3.5C). This finding suggests that the loss of Samsn1 in PC-extrinsic cells of the BM microenvironment does not affect the growth of MM tumours in KaLwRij mice.

3.2.4 Generation of *Glipr1* knockout mice using CRIPSR-Cas9 genome editing

In order to produce *Glipr1*$^{-/-}$*Samsn1*$^{-/-}$ double knockout mice, *Glipr1*$^{-/-}$ mice were generated using CRISPR-Cas9 genome editing technology. The strategy was to delete the first exon of the *Glipr1* gene using two guide RNAs (gRNAs), one upstream of the conserved promoter region and the other in the first intron of *Glipr1* (Figure 3.6A). WT mouse zygotes were injected with Cas9 mRNA and both gRNAs before being transferred to pseudopregnant recipients, which resulted in the birth of four founder pups. PCR genotyping coupled with Sanger sequencing revealed that three of the founders had at least one *Glipr1* allele in which the first exon was successfully deleted (Figure 3.6B). The *Glipr1* deletion allele of founder 3, a ~3.6 kb deletion encompassing exon 1 (Figure 3.6B), was selected for breeding to homozygosity because it did not involve any random insertions/deletions and belonged to the only male founder. This *Glipr1* deletion allele was backcrossed onto a C57BL/6 background for one generation and then bred to homozygosity to generate C57BL/*Glipr1*$^{-/-}$ (*Glipr1*$^{-/-}$) mice.

To confirm successful gene knockout in the *Glipr1*$^{-/-}$ mice, RT-PCR for *Glipr1* mRNA was performed on RNA from BM and spleen cells. Two sets of PCR primers were used; one with primers in *Glipr1* exons 1 and 2 (ex1-2) and the other with primers in *Glipr1* exons 3 and 4 (ex3-4). As shown in Figure 73.7A, no PCR products were generated with the ex1-2 primers,

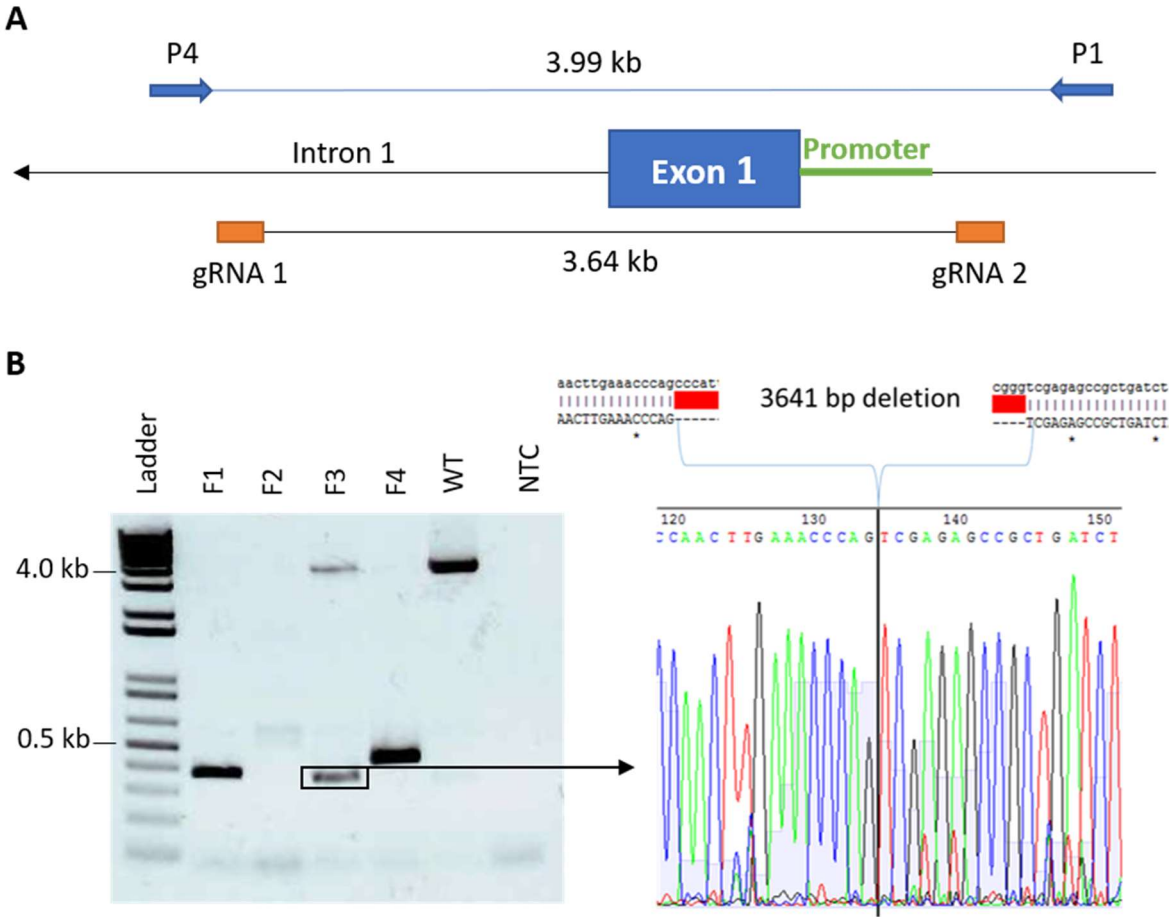

Figure 3.6: Generating *Glipr1* knockout mice using CRISPR-Cas9 genome editing. (**A**) Schematic showing the location of the gRNAs used for CRISPR-Cas9-mediated deletion of *Glipr1* exon 1 and the PCR primers (P1 & P4) used to screen founder mice for deletions. The direction of gene transcription is indicated by the arrow. (**B**) DNA samples from the four founder mice (F1-4) were screened for deletions of *Glipr1* exon 1 by PCR using primers P1 and P4 and the products were run on a 1% agarose gel (left). Sanger sequencing of the highlighted deletion band in F3 showed a 3,641 bp deletion between the two gRNA sites, which removed *Glipr1* exon 1 (right). NTC = no template control.

Figure 3.7: Confirming *Glipr1* knockout in CRISPR-Cas9-generated *Glipr1*$^{-/-}$ mice. (**A**) RT-PCR for *Glipr1* mRNA was performed on RNA from the BM and spleen of *Glipr1*$^{-/-}$ and WT control mice using either primers in exons 1 and 2 (ex1-2) or primers in exons 3 and 4 (ex3-4). PCR products were run on a 2% agarose gel and stained with GelRed®. *Actb* was used as a positive control. (**B**) *Glipr1 p*rimers ex3-4 were used to perform RT-qPCR on RNA from the BM and spleen of *Glipr1*$^{-/-}$ and WT mice. *Glipr1* expression levels were normalised to *Actb* and were expressed relative to WT mice. (**C**) The levels of Glipr1 protein in the BM and spleen of *Glipr1*$^{-/-}$ and WT mice was assessed by Western blot. Hsp90 was used as the loading control. The graph depicts the mean + SD of n = 2 mice per genotype. ****$P <$ 0.0001, unpaired t test.

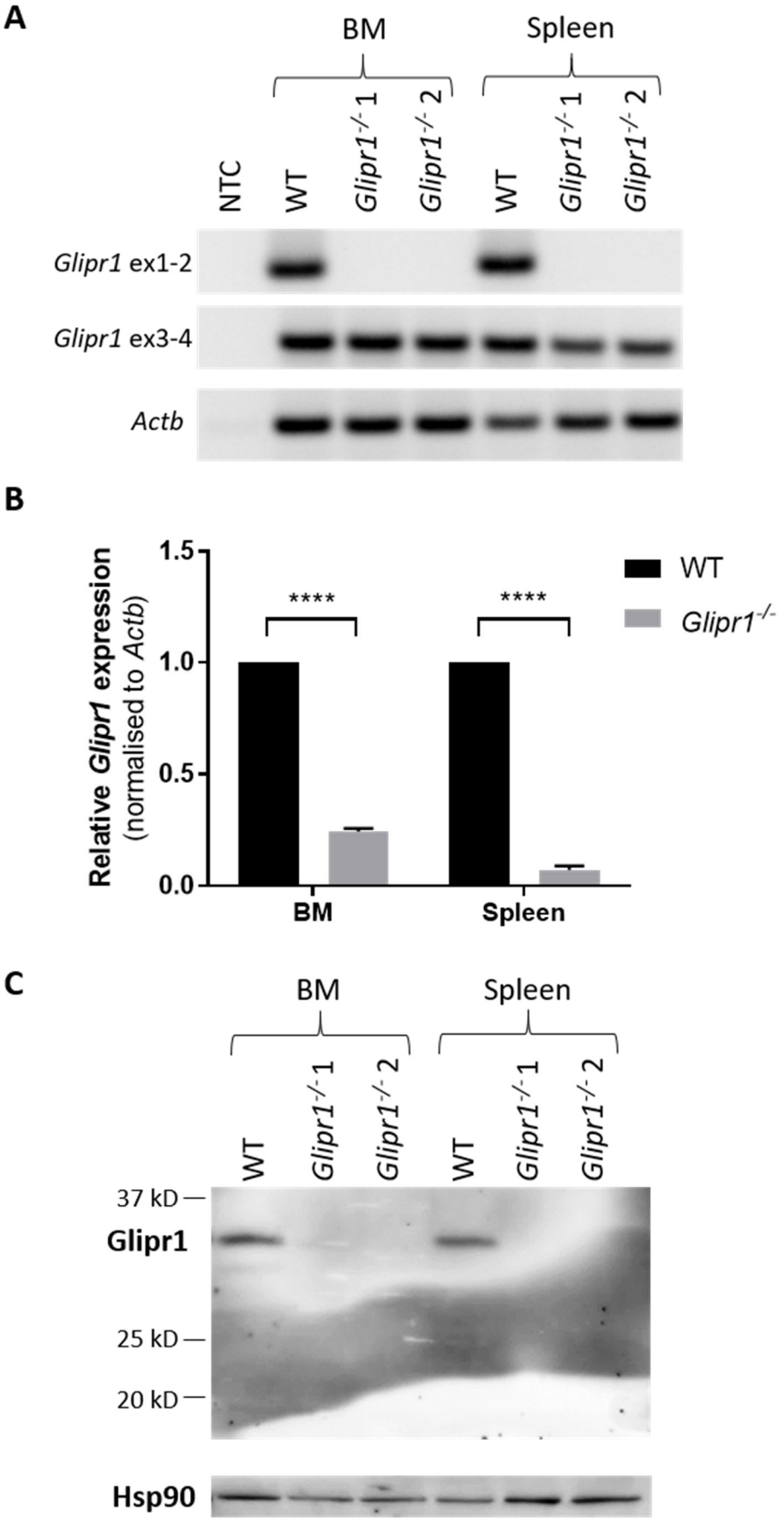
A
BM
Spleen
NTC
WT
Glipr1-/- 1
Glipr1-/- 2
WT
Glipr1-/- 1
Glipr1-/- 2
Glipr1 ex1-2
Glipr1 ex3-4
Actb
B
Relative Glipr1 expression
(normalised to Actb)
1.5
1.0
0.5
0.0
****
****
WT
Glipr1-/-
BM
Spleen
C
BM
Spleen
WT
Glipr1-/- 1
Glipr1-/- 2
WT
Glipr1-/- 1
Glipr1-/- 2
37 kD
Glipr1
25 kD
20 kD
Hsp90

which was expected, given that one of the primers binds within the *Glipr1* deletion region. However, products of the expected size were generated using the ex3-4 primers, suggesting that there was transcription of *Glipr1* downstream of exon 1 (Figure 3.7A). However, RT-qPCR using the ex3-4 primers showed that the expression of *Glipr1* mRNA transcripts in the BM and spleen of *Glipr1*$^{-/-}$ mice was significantly reduced compared to WT mice (Figure 3.7B). In addition, there was no full-length or truncated Glipr1 protein detected in the BM or spleen of the *Glipr1*$^{-/-}$ mice by Western blot using a polyclonal α-Glipr1 antibody (Figure 3.7C). Hence, the truncated *Glipr1* mRNA transcripts generated in the *Glipr1*$^{-/-}$ mice were not translated into protein, which is consistent with the absence of alternative start codons downstream of exon 1. Together, these data indicate that a *Glipr1* knockout mouse was successfully generated using CRISPR-Cas9 genome editing.

3.2.5 Analysis of B cell development in *Glipr1* and/or *Samsn1* knockout mice

In order to generate *Glipr1*$^{-/-}$*Samsn1*$^{-/-}$ double knockout mice, the *Glipr1*$^{-/-}$ mice and *Samsn1*$^{-/-}$ mice were crossed and the resultant heterozygous mice (*Glipr1*$^{+/-}$*Samsn1*$^{+/-}$) were crossed again. From these matings, 3.8% (n = 4/105) of the progeny were found to be *Glipr1*$^{-/-}$*Samsn1*$^{-/-}$ by PCR genotyping, which does not significantly differ from the expected Mendelian frequency of 6.25% ($P = 0.5377$, Fisher's exact test). The *Glipr1*$^{-/-}$*Samsn1*$^{-/-}$ mice were viable, fertile and had no overt phenotypic traits. In order to examine the effect of *Glipr1* and/or *Samsn1* knockout on normal haematopoiesis in adult mice, peripheral blood (PB) from 12-week-old *Glipr1*$^{-/-}$, *Samsn1*$^{-/-}$, *Glipr1*$^{-/-}$*Samsn1*$^{-/-}$ and WT mice was assessed using a HEMAVET analyser. No differences in the number of white blood cells, the number of red blood cells, haemoglobin concentration, or other parameters were observed in the *Glipr1* and/or *Samsn1* knockout mice compared to the WT mice ($P > 0.05$, Kruskal-Wallis test with Dunn's multiple comparisons test; Figure 3.8 and Table 3.1). In addition, flow cytometry analysis of B cells from the BM of 12-week-old *Glipr1*$^{-/-}$, *Samsn1*$^{-/-}$, *Glipr1*$^{-/-}$ *Samsn1*$^{-/-}$ and WT mice was performed. No differences in the populations of pre-pro B cells, immature B cells, mature B cells, total B cells and PCs were observed in the *Glipr1*$^{-/-}$, *Samsn1*$^{-/-}$, and *Glipr1*$^{-/-}$*Samsn1*$^{-/-}$ mice compared to the WT mice ($P > 0.05$, Kruskal-Wallis test with Dunn's multiple comparisons test; Figure 3.9A-F). The knockout mice also demonstrated similar splenic populations of total B cells and PCs compared to WT mice ($P > 0.05$, Kruskal-Wallis test with Dunn's multiple comparisons test;

Figure 3.8: *Glipr1* and/or *Samsn1* knockout does not affect PB counts in adult mice. (**A**-**F**) PB was collected by tail bleed from 12-week-old *Glipr1*$^{-/-}$, *Samsn1*$^{-/-}$, *Glipr1*$^{-/-}$*Samsn1*$^{-/-}$ and WT mice and white blood cell (WBC) number (**A**), lymphocyte number (**B**), monocyte number (**C**), neutrophil number (**D**), red blood cell (RBC) number (**E**) and haemoglobin concentration (**F**) were assessed using a HEMAVET analyser. Graphs depict the mean ± SEM of n = 7 mice per genotype. $P > 0.05$, Kruskal-Wallis test with Dunn's multiple comparisons test.

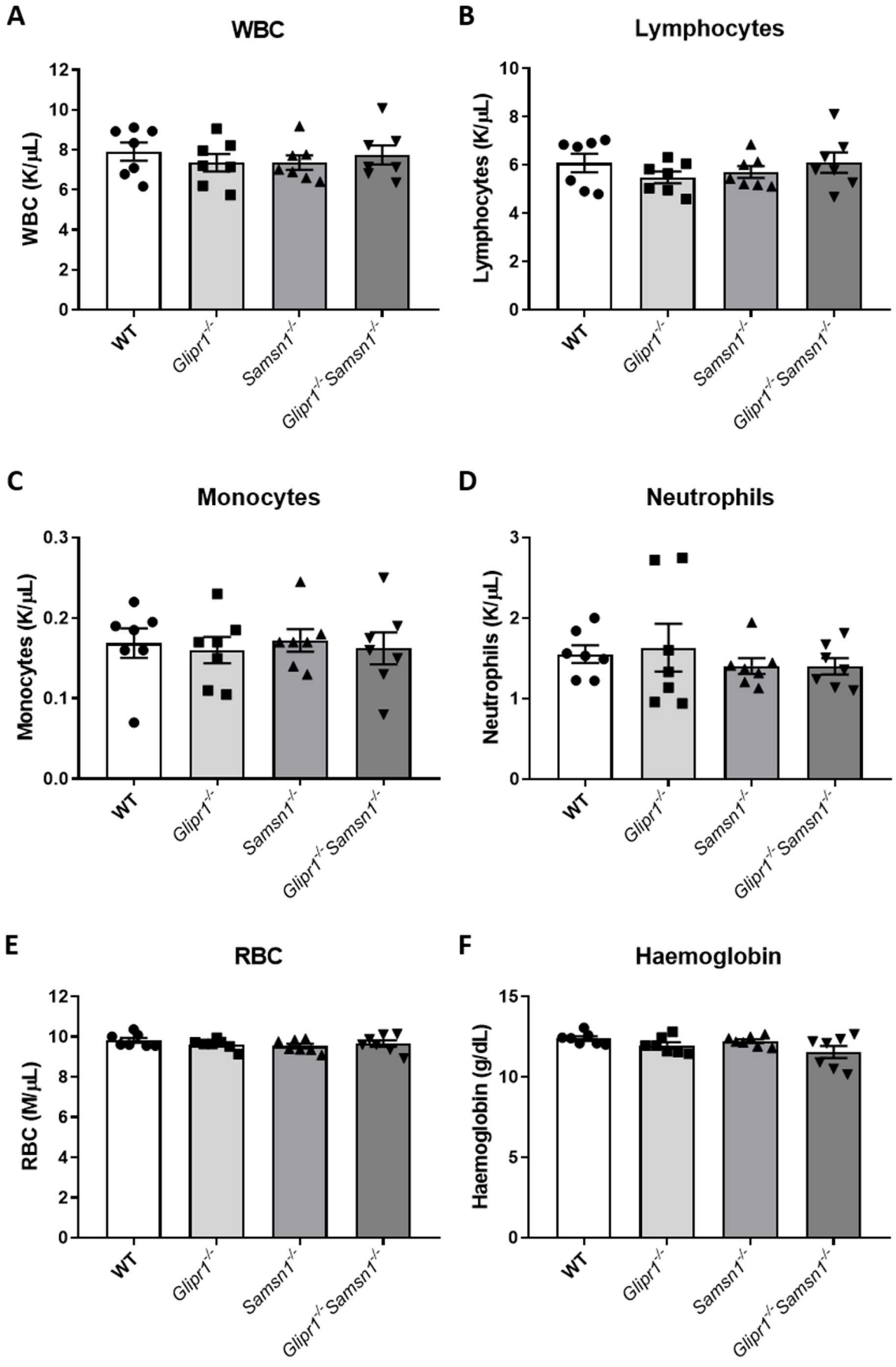
A
WBC
WBC (K/µL)
12
10
8
6
4
2
0
WT
Glipr1-/-
Samsn1-/-
Glipr1-/-Samsn1-/-
B
Lymphocytes
Lymphocytes (K/µL)
10
8
6
4
2
0
WT
Glipr1-/-
Samsn1-/-
Glipr1-/-Samsn1-/-
C
Monocytes
Monocytes (K/µL)
0.3
0.2
0.1
0.0
WT
Glipr1-/-
Samsn1-/-
Glipr1-/-Samsn1-/-
D
Neutrophils
Neutrophils (K/µL)
3
2
1
0
WT
Glipr1-/-
Samsn1-/-
Glipr1-/-Samsn1-/-
E
RBC
RBC (M/µL)
12
10
8
6
4
2
0
WT
Glipr1-/-
Samsn1-/-
Glipr1-/-Samsn1-/-
F
Haemoglobin
Haemoglobin (g/dL)
15
10
5
0
WT
Glipr1-/-
Samsn1-/-
Glipr1-/-Samsn1-/-

Table 3.1: Haematological parameters in the PB of 12-week-old *Glipr1*$^{-/-}$, *Samsn1*$^{-/-}$, *Glipr1*$^{-/-}$*Samsn1*$^{-/-}$ and WT mice. PB was collected by a tail bleed from 12-week-old *Glipr1*$^{-/-}$, *Samsn1*$^{-/-}$, *Glipr1*$^{-/-}$*Samsn1*$^{-/-}$ and WT control mice and was analysed on a HEMAVET analyser (n = 7/genotype). $P > 0.05$, Kruskal-Wallis test with Dunn's multiple comparisons test.

		WT		*Glipr1*$^{-/-}$		*Samsn1*$^{-/-}$		*Glipr1*$^{-/-}$*Samsn1*$^{-/-}$	
		Mean	**SD**	**Mean**	**SD**	**Mean**	**SD**	**Mean**	**SD**
WBC	K/µL	7.909	1.205	7.356	1.153	7.367	0.949	7.740	1.269
NE#	K/µL	1.552	0.290	1.632	0.785	1.403	0.264	1.402	0.271
LY#	K/µL	6.087	1.015	5.490	0.636	5.706	0.652	6.100	1.111
MO#	K/µL	0.169	0.048	0.160	0.043	0.172	0.037	0.162	0.053
EO#	K/µL	0.076	0.039	0.055	0.013	0.063	0.023	0.054	0.031
BA#	K/µL	0.027	0.014	0.019	0.006	0.022	0.006	0.024	0.029
NE%	%	19.727	2.890	21.454	7.610	18.928	1.394	18.089	1.910
LY%	%	76.869	3.337	75.351	7.560	77.617	1.879	78.642	2.873
MO%	%	2.100	0.497	2.164	0.457	2.314	0.252	2.201	0.940
EO%	%	0.953	0.434	0.746	0.182	0.840	0.226	0.729	0.516
BA%	%	0.348	0.208	0.286	0.138	0.301	0.063	0.341	0.446
RBC	M/µL	9.825	0.323	9.617	0.252	9.534	0.304	9.657	0.429
HB	g/dL	12.386	0.366	11.964	0.501	12.229	0.311	11.550	1.005
HCT	%	45.014	1.477	44.071	1.502	43.957	1.203	44.571	2.290
MCV	fL	45.829	0.676	45.814	0.449	46.107	0.641	46.150	1.426
MCH	Pg	12.607	0.516	12.436	0.463	12.829	0.313	11.964	0.673
MCHC	g/dL	27.529	1.171	27.164	1.083	27.836	0.502	25.943	1.502
RDW	%	17.321	0.330	17.393	0.167	17.486	0.325	17.479	0.531
PLT	K/µL	613.43	48.832	662.93	63.304	664.21	81.067	646.29	91.995
MPV	fL	4.586	0.315	4.521	0.202	4.443	0.093	4.543	0.285

SD = standard deviation, # = number, % = percentage, WBC = white blood cell, NE = neutrophil, LY = lymphocytes, MO = monocytes, EO = eosinophils, BA = basophils, RBC = red blood cell, HB = haemoglobin, HCT = haematocrit, MCV = mean corpuscular volume, MCH = mean corpuscular haemoglobin, MCHC = mean corpuscular haemoglobin concentration, RDW = red blood cell distribution width, PLT = platelet, MPV = mean platelet volume.

Figure 3.9: *Glipr1* and/or *Samsn1* knockout does not affect B cell populations in the BM or spleen of 12-week-old mice. Single cell suspensions from the BM (**A**-**F**) and spleen (**G**-**I**) were obtained from 12-week-old *Glipr1*$^{-/-}$, *Samsn1*$^{-/-}$, *Glipr1*$^{-/-}$*Samsn1*$^{-/-}$ and WT control mice. The cells were stained with anti-B220, anti-IgM and anti-CD138 antibodies and analysed by flow cytometry. (**A**-**F**) BM cells were gated, as represented in (**A**), to show the percentage of total B cells (**B**; B220^{+}), mature B cells (**C**; B220^{high}IgM^{low}), immature B cells (**D**; B220^{low}IgM^{+}), pre-pro B cells (**E**; B220^{low}IgM^{-}), and PCs (**F**; B220^{-}IgM^{-}CD138^{+}) among total leukocytes. (**G**-**I**) Spleen cells were gated, as represented in (**G**), to show the percent of total B cells (**H**; B220^{+}) and PCs (**I**; B220^{-}IgM^{-}CD138^{+}) among total leukocytes. Graphs depict the mean ± SEM of n = 9-12 mice per genotype. *P <0.05, **P < 0.01, Kruskal-Wallis test with Dunn's multiple comparisons test.

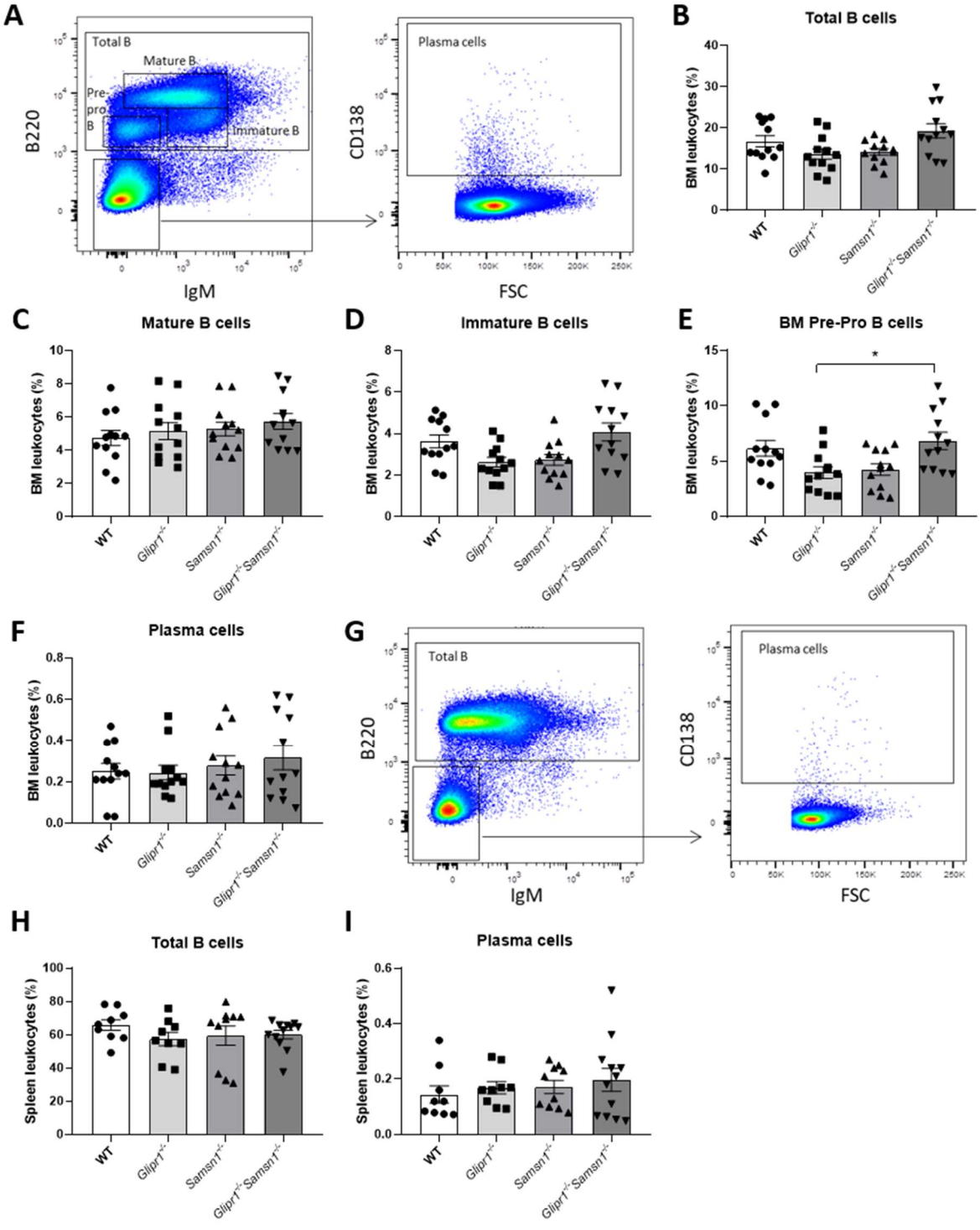
A
Total B
Mature B
Pre-pro B
Immature B
B220
IgM
Plasma cells
CD138
FSC
B
Total B cells
BM leukocytes (%)
C
Mature B cells
D
Immature B cells
E
BM Pre-Pro B cells
*
F
Plasma cells
G
Total B
Plasma cells
H
Total B cells
Spleen leukocytes (%)
I
Plasma cells
WT
Glipr1-/-
Samsn1-/-
Glipr1-/-Samsn1-/-

Figure 3.9G-I). Collectively, these data suggest that the loss of Glipr1 and/or Samsn1 does not significantly affect B cell development, including PC production, *in vivo*.

3.2.6 *Glipr1* and/or *Samsn1* knockout does not result in MM disease development *in vivo*

KaLwRij mice, which are *Samsn1*$^{-/-}$, and *Glipr1*$^{-/-}$ mice are prone to developing PC dyscrasias, albeit with late onset and incomplete penetrance[264,298]. Hence, it was hypothesised that the concomitant loss of Glipr1 and Samsn1 would result in increased penetrance, decreased time to onset and/or increased progression of abnormal PC expansions *in vivo*. To test this, *Glipr1*$^{-/-}$, *Samsn1*$^{-/-}$, *Glipr1*$^{-/-}$*Samsn1*$^{-/-}$ and WT mice were aged for one year and monitored for B cell/PC abnormalities using a HEMAVET analyser, SPEP and flow cytometry analyses (Figure 3.10A). Haematological parameters were measured in serial samples of PB from the *Glipr1*$^{-/-}$, *Samsn1*$^{-/-}$, *Glipr1*$^{-/-}$*Samsn1*$^{-/-}$ and WT mice at 6, 9 and 12 months of age using a HEMAVET analyser (Figure 3.10B-E and Table 3.2). There was a significant increase in the number of lymphocytes at 9 months of age, and monocytes at 6 months of age, in PB from the *Glipr1*$^{-/-}$ mice compared to the WT mice ($P < 0.05$, Kruskal-Wallis test with Dunn's multiple comparisons test; Figure 3.10C&D). In addition, the number of monocytes was significantly higher in the *Glipr1*$^{-/-}$*Samsn1*$^{-/-}$ mice compared to the WT mice at 9 months of age (Figure 3.10D). These data suggested that *Glipr1* knockout may promote progressive expansion of lymphocyte and monocyte populations over time. However, increased lymphocyte and monocyte populations were not observed in the *Glipr1*$^{-/-}$ mice or *Glipr1*$^{-/-}$*Samsn1*$^{-/-}$ mice compared to the WT mice at 12 months of age (Figure 3.10B-E and Table 3.2). This was confirmed by flow cytometry analysis of white blood cell populations in PB from the 12-month-old mice, which showed similar lymphocyte (B and T cell), monocyte and granulocyte populations in the *Glipr1*$^{-/-}$, *Samsn1*$^{-/-}$ and *Glipr1*$^{-/-}$*Samsn1*$^{-/-}$ mice compared to the WT mice ($P > 0.05$, Kruskal-Wallis test with Dunn's multiple comparisons test; Figure 3.11). These data suggest that *Glipr1* and/or *Samsn1* knockout does not cause consistent or progressive changes to PB cell populations in ageing mice.

The ageing *Glipr1* and/or *Samsn1* knockout mice were specifically monitored for expansions of antibody-producing PCs relative to WT control mice by SPEP at 10-week intervals. Across the genotypes, there were more M-spikes in the female mice compared to the male mice, as was seen previously for C57BL/6 mice[262], but the majority were still relatively weak

Figure 3.10: Longitudinal analysis of PB counts in ageing *Glipr1*$^{-/-}$, *Samsn1*$^{-/-}$ and *Glipr1*$^{-/-}$*Samsn1*$^{-/-}$ mice. (**A**) Schematic illustrating the experimental design for monitoring *Glipr1*$^{-/-}$, *Samsn1*$^{-/-}$, *Glipr1*$^{-/-}$*Samsn1*$^{-/-}$ and WT mice for B cell/PC abnormalities. (**B**-**E**) Blood samples were serially collected by a tail bleed from *Glipr1*$^{-/-}$, *Samsn1*$^{-/-}$, *Glipr1*$^{-/-}$*Samsn1*$^{-/-}$ and WT mice at 6 (left), 9 (middle) and 12 (right) months of age. Complete blood counts, including WBC (**B**), lymphocyte (**C**), monocyte (**D**) and neutrophil (**E**) numbers, were measured using a HEMAVET analyser. Graphs depict the mean ± SEM of n = 10 mice per genotype. **P* <0.05, ***P* < 0.01, Kruskal-Wallis test with Dunn's multiple comparisons test.

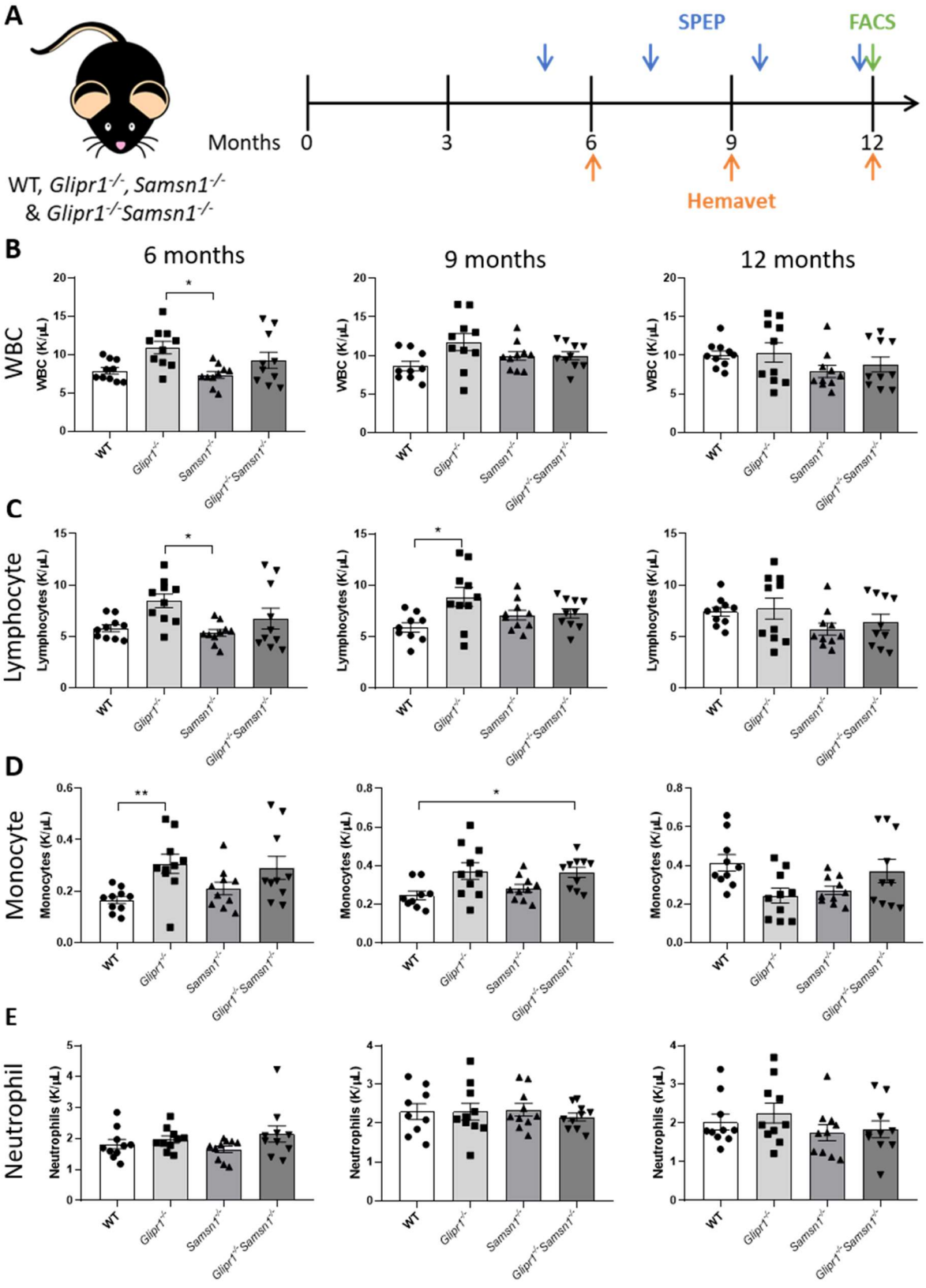
A
SPEP
FACS
Months
0
3
6
9
12
Hemavet
WT, Glipr1-/-, Samsn1-/-
& Glipr1-/-Samsn1-/-
B
6 months
9 months
12 months
WBC
WBC (K/μL)
C
Lymphocyte
Lymphocytes (K/μL)
D
Monocyte
Monocytes (K/μL)
E
Neutrophil
Neutrophils (K/μL)
WT
Glipr1-/-
Samsn1-/-
Glipr1-/-Samsn1-/-

Table 3.2: Haematological parameters in the PB of ageing *Glipr1*$^{-/-}$, *Samsn1*$^{-/-}$ *and Glipr1*$^{-/-}$*Samsn1*$^{-/-}$ mice. PB was collected by a tail bleed from *Glipr1*$^{-/-}$, *Samsn1*$^{-/-}$, *Glipr1*$^{-/-}$*Samsn1*$^{-/-}$ and WT control mice at 6, 9 and 12 months of age and was assessed using a HEMAVET analyser (n = 10/genotype). Data are shown as mean ± SD. **P* < 0.05, ***P* < 0.01 compared to WT, Kruskal-Wallis test with Dunn's multiple comparisons test.

		6 months				9 months				12 months			
		WT	*Glipr1*$^{-/-}$	*Samsn1*$^{-/-}$	*Glipr1*$^{-/-}$ *Samsn1*$^{-/-}$	WT	*Glipr1*$^{-/-}$	*Samsn1*$^{-/-}$	*Glipr1*$^{-/-}$ *Samsn1*$^{-/-}$	WT	*Glipr1*$^{-/-}$	*Samsn1*$^{-/-}$	*Glipr1*$^{-/-}$ *Samsn1*$^{-/-}$
WBC	K/uL	7.89 ± 1.35	10.9 ± 2.55	7.35 ± 1.42	9.27 ± 3.37	8.63 ± 1.86	11.7 ± 3.51	9.94 ± 1.80	9.97 ± 1.68	10.1 ± 1.66	10.4 ± 4.00	7.91 ± 2.47	8.82 ± 3.08
NE#	K/uL	1.82 ± 0.49	1.96 ± 0.37	1.65 ± 0.33	2.14 ± 0.83	2.29 ± 0.61	2.29 ± 0.68	2.34 ± 0.51	2.16 ± 0.32	2.02 ± 0.64	2.25 ± 0.81	1.75 ± 0.65	1.83 ± 0.68
LY#	K/uL	5.8 ± 1.04	8.47 ± 2.11	5.35 ± 1.05	6.75 ± 3.20	5.91 ± 1.37	**8.87 ± 2.89***	7.09 ± 1.48	7.27 ± 1.45	7.42 ± 1.35	7.72 ± 3.22	5.72 ± 1.85	6.4 ± 2.45
MO#	K/uL	0.17 ± 0.05	**0.31 ± 0.12****	0.21 ± 0.08	0.29 ± 0.14	0.25 ± 0.07	0.37 ± 0.14	0.28 ± 0.06	**0.37 ± 0.08***	0.41 ± 0.13	0.24 ± 0.12	0.27 ± 0.07	0.37 ± 0.19
EO#	K/uL	0.08 ± 0.05	0.09 ± 0.05	0.11 ± 0.05	0.07 ± 0.06	0.14 ± 0.10	0.16 ± 0.09	0.16 ± 0.07	0.13 ± 0.10	0.16 ± 0.09	0.13 ± 0.09	0.12 ± 0.05	0.16 ± 0.08
BA#	K/uL	0.03 ± 0.02	0.03 ± 0.01	0.04 ± 0.02	0.02 ± 0.02	0.05 ± 0.04	0.05 ± 0.03	0.06 ± 0.03	0.05 ± 0.04	0.05 ± 0.03	0.04 ± 0.03	0.04 ± 0.03	0.05 ± 0.02
NE%	%	22.9 ± 3.81	18.4 ± 3.30	22.4 ± 2.28	24.8 ± 10.6	26.7 ± 5.35	**20.0 ± 4.29***	23.6 ± 3.45	21.9 ± 3.77	20.1 ± 4.85	22.5 ± 4.92	22.1 ± 4.70	21.5 ± 6.32
LY%	%	73.6 ± 3.78	77.2 ± 3.04	72.7 ± 2.17	70.9 ± 10.5	68.3 ± 6.59	75.1 ± 5.16	71.2 ± 4.89	72.7 ± 4.52	73.8 ± 6.18	73.5 ± 5.49	72.2 ± 4.93	71.7 ± 5.76
MO%	%	2.16 ± 0.68	3.2 ± 1.60	2.82 ± 0.65	3.12 ± 0.78	2.85 ± 0.51	3.19 ± 0.73	2.87 ± 0.60	**3.68 ± 0.52***	4.11 ± 1.09	**2.38 ± 0.86****	3.56 ± 0.85	4.21 ± 1.81
EO%	%	1.08 ± 0.78	0.83 ± 0.27	1.52 ± 0.71	0.89 ± 0.90	1.56 ± 1.00	1.29 ± 0.63	1.69 ± 0.86	1.27 ± 0.83	1.57 ± 0.84	1.27 ± 0.60	1.55 ± 0.33	1.93 ± 0.92
BA%	%	0.34 ± 0.34	0.29 ± 0.13	0.53 ± 0.27	0.28 ± 0.30	0.538 ± 0.27	0.356 ± 0.211	0.643 ± 0.366	0.437 ± 0.313	0.462 ± 0.31	0.342 ± 0.18	0.564 ± 0.34	0.649 ± 0.35
RBC	M/uL	10.1 ± 0.29	10.3 ± 0.51	9.73 ± 0.25	10.1 ± 0.33	9.65 ± 0.38	9.49 ± 1.20	9.66 ± 0.30	9.85 ± 0.51	10.2 ± 0.47	10.2 ± 0.82	10.3 ± 0.31	10.1 ± 1.22
HB	g/dL	11.5 ± 0.32	11.7 ± 0.49	11.4 ± 0.43	11.5 ± 0.68	12.3 ± 0.41	12.1 ± 1.20	12.7 ± 0.40	12.3 ± 0.54	14.4 ± 0.675	14 ± 0.90	14.4 ± 0.49	13.8 ± 1.77
HCT	%	44.5 ± 1.15	45.1 ± 1.75	44 ± 1.05	45.1 ± 1.66	44.1 ± 1.48	44 ± 4.13	45.4 ± 1.23	45.6 ± 2.00	47.2 ± 2.62	46.7 ± 2.22	48.1 ± 1.98	46.0 ± 5.60
MCV	fL	44.1 ± 0.86	43.9 ± 0.94	45.2 ± 0.89	44.8 ± 0.86	45.7 ± 1.29	46.7 ± 2.46	47.0 ± 0.86	46.3 ± 1.21	46.4 ± 1.12	45.8 ± 2.11	46.8 ± 1.14	45.7 ± 1.13
MCH	Pg	11.4 ± 0.33	11.4 ± 0.48	11.7 ± 0.24	11.4 ± 0.64	12.8 ± 0.44	12.8 ± 0.64	13.1 ± 0.21	12.5 ± 0.41	14.1 ± 0.55	13.8 ± 0.58	14.0 ± 0.29	13.7 ± 0.33
MCHC	g/dL	25.9 ± 0.67	26 ± 1.08	26 ± 0.84	25.5 ± 1.51	28.0 ± 0.66	27.4 ± 0.59	27.9 ± 0.53	**26.9 ± 0.60****	30.5 ± 0.91	30.1 ± 0.97	30 ± 1.04	30.1 ± 0.74
RDW	%	18.7 ± 1.23	18.4 ± 0.66	17.9 ± 0.31	17.9 ± 0.53	18.4 ± 0.66	19.7 ± 1.81	18.3 ± 0.45	18.7 ± 0.83	18.2 ± 0.34	18.4 ± 0.66	18.4 ± 0.65	18 ± 0.51
PLT	K/uL	842 ± 85.4	761 ± 203	725 ± 96.7	764 ± 93.2	914 ± 98.3	961 ± 193	852 ± 121	871 ± 92	1263 ± 172	1348 ± 256	1226 ± 117	1181 ± 167
MPV	fL	4.57 ± 0.29	4.49 ± 0.28	4.45 ± 0.13	4.42 ± 0.25	4.67 ± 0.24	4.77 ± 0.27	4.75 ± 0.06	4.66 ± 0.07	5.77 ± 0.21	5.82 ± 0.31	5.72 ± 0.24	5.53 ± 0.16

WBC = white blood cell, NE = neutrophil, LY = lymphocytes, MO = monocytes, EO = eosinophils, BA = basophils, RBC = red blood cell, HB = haemoglobin, HCT = haematocrit, MCV = mean corpuscular volume, MCH = mean corpuscular haemoglobin, MCHC = mean corpuscular haemoglobin concentration, RDW = red blood cell distribution width, PLT = platelet, MPV = mean platelet volume.

Figure 3.11: Flow cytometry analysis of leukocyte populations in the PB of 12-month-old *Glipr1*$^{-/-}$, *Samsn1*$^{-/-}$ *and Glipr1*$^{-/-}$*Samsn1*$^{-/-}$ mice. (**A**-**E**) PB was collected from 12-month-old *Glipr1*$^{-/-}$, *Samsn1*$^{-/-}$, *Glipr1*$^{-/-}$*Samsn1*$^{-/-}$ and WT control mice and single cell leukocyte suspensions were prepared. The cells were stained with anti-B220, anti-CD3, anti-CD11b and anti-Ly6G antibodies and analysed by flow cytometry. (**A**) Representative flow plots showing the gating strategy used to define B cells (B220^{+}), T cells (CD3^{+}), monocytes (CD11b^{+}Ly6G^{-}) and granulocytes (CD11b^{+}Ly6G^{+}). The percentage of B cells (**B**), T cells (**C**), monocytes (**D**) and granulocytes (**E**) among total leukocytes in the PB are shown in the graphs. Graphs depict the mean ± SEM of n = 10 mice per genotype. $P > 0.05$, Kruskal-Wallis test with Dunn's multiple comparisons test.

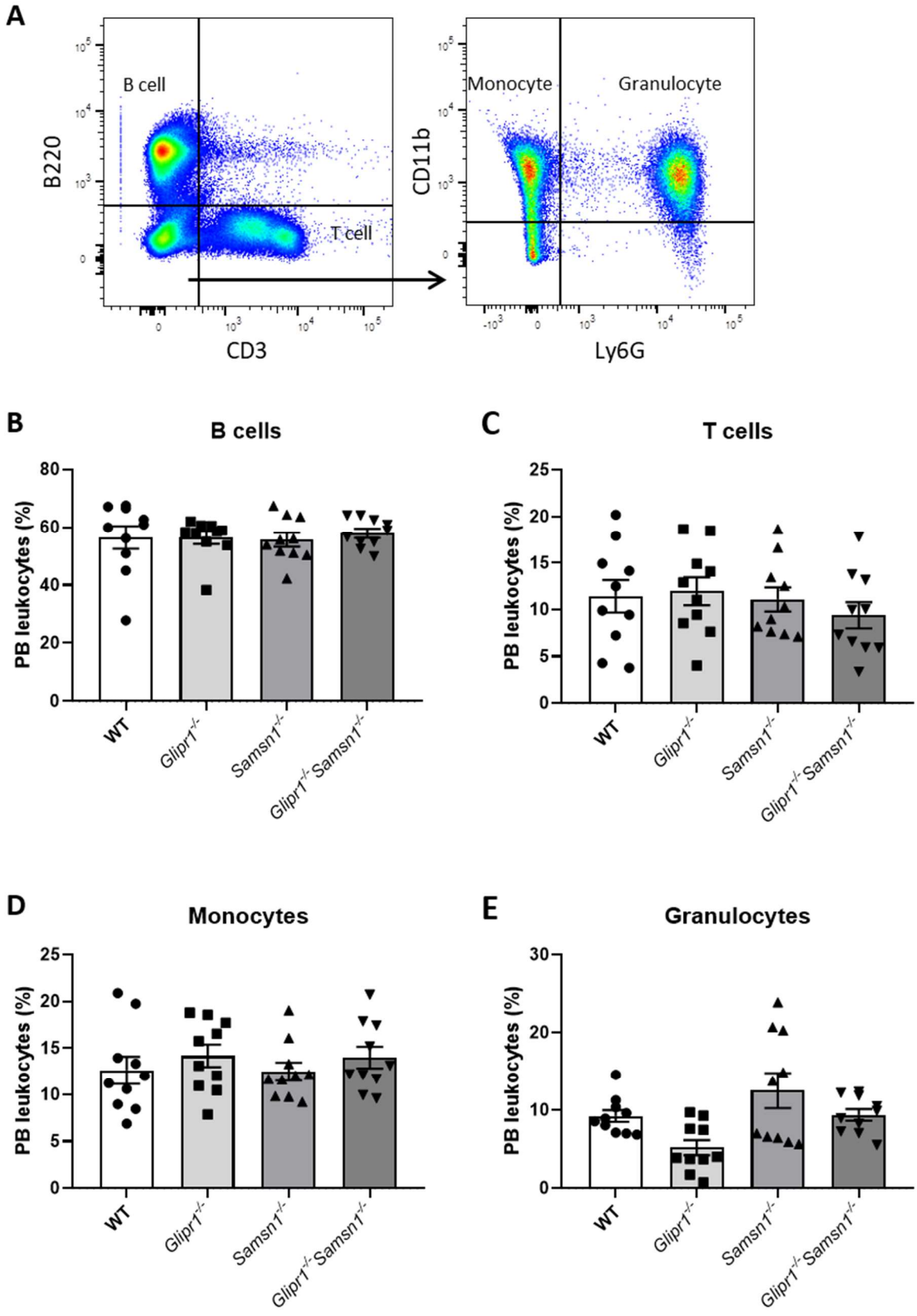
A
B cell
T cell
B220
CD3
Monocyte
Granulocyte
CD11b
Ly6G
B
B cells
PB leukocytes (%)
C
T cells
D
Monocytes
E
Granulocytes
WT
Glipr1-/-
Samsn1-/-
Glipr1-/-Samsn1-/-

compared to the albumin and other globulin bands in the 50-week-old mice (Figure 3.12A). Although the M-spike incidence was higher in the *Glipr1* and/or *Samsn1* knockout mice compared to the WT mice at the earlier time points, this difference was not evident at 50 weeks of age (Figure 3.12B). In addition, flow cytometry analysis revealed that the B cell populations in the BM and spleen of the 12-month-old *Glipr1*$^{-/-}$, *Samsn1*$^{-/-}$ and *Glipr1*$^{-/-}$*Samsn1*$^{-/-}$ mice were similar to those in the WT mice, except for a significant reduction in the BM immature B cell population in the *Samsn1*$^{-/-}$ mice ($P = 0.042$, Kruskal-Wallis test with Dunn's multiple comparisons test; Figure 3.13A-D&F). Notably, no differences were found in the BM and splenic PC populations of the *Glipr1*$^{-/-}$, *Samsn1*$^{-/-}$ and *Glipr1*$^{-/-}$*Samsn1*$^{-/-}$ mice compared to the WT mice ($P > 0.05$, Kruskal-Wallis test with Dunn's multiple comparisons test; Figure 3.13E&G). Together, these data suggest that the loss of Samsn1 and Glipr1 does not promote the development of abnormal clonal PC expansions, or other B cell abnormalities, in mice up to one year of age.

3.3 Discussion

Although Samsn1 was found to be a tumour suppressor in the 5TGM1/KaLwRij murine model of myeloma[260], *Samsn1*$^{-/-}$ KaLwRij mice only spontaneously develop MM with late onset and very low penetrance[264]. This suggests that the loss of Samsn1 is not sufficient to drive malignant transformation and must co-operate with other genetic lesions to promote MM development. In this chapter, it was aimed to identify genetic aberrations that potentially co-operate with reduced *SAMSN1* expression to promote MM. To achieve this, gene expression differences between MM PCs with low versus normal/high *SAMSN1* levels were examined and only two changes in the *SAMSN1*^{low} tumours across multiple microarray datasets were found: up-regulation of *HIST3H2A* and down-regulation of *GLIPR1*. *HIST3H2A* encodes a replication-dependent H2A core histone, which is mainly expressed during S phase of the cell cycle[301]. The expression of this gene was found to not differ in MM PCs compared to normal PCs and HIST3H2A has not previously been described to have a role in cancer. As such, increased *HIST3H2A* expression was deemed unlikely to constitute a co-operative driver of MM development.

GLIPR1 is a ubiquitously expressed gene that encodes a member of the cysteine-rich secretory proteins, antigen 5, and pathogenesis-related 1 proteins (CAP) superfamily with unspecified function[302,303]. *GLIPR1* expression was found to be significantly decreased in the PCs of MM patients compared to normal controls, with most MM patients found to

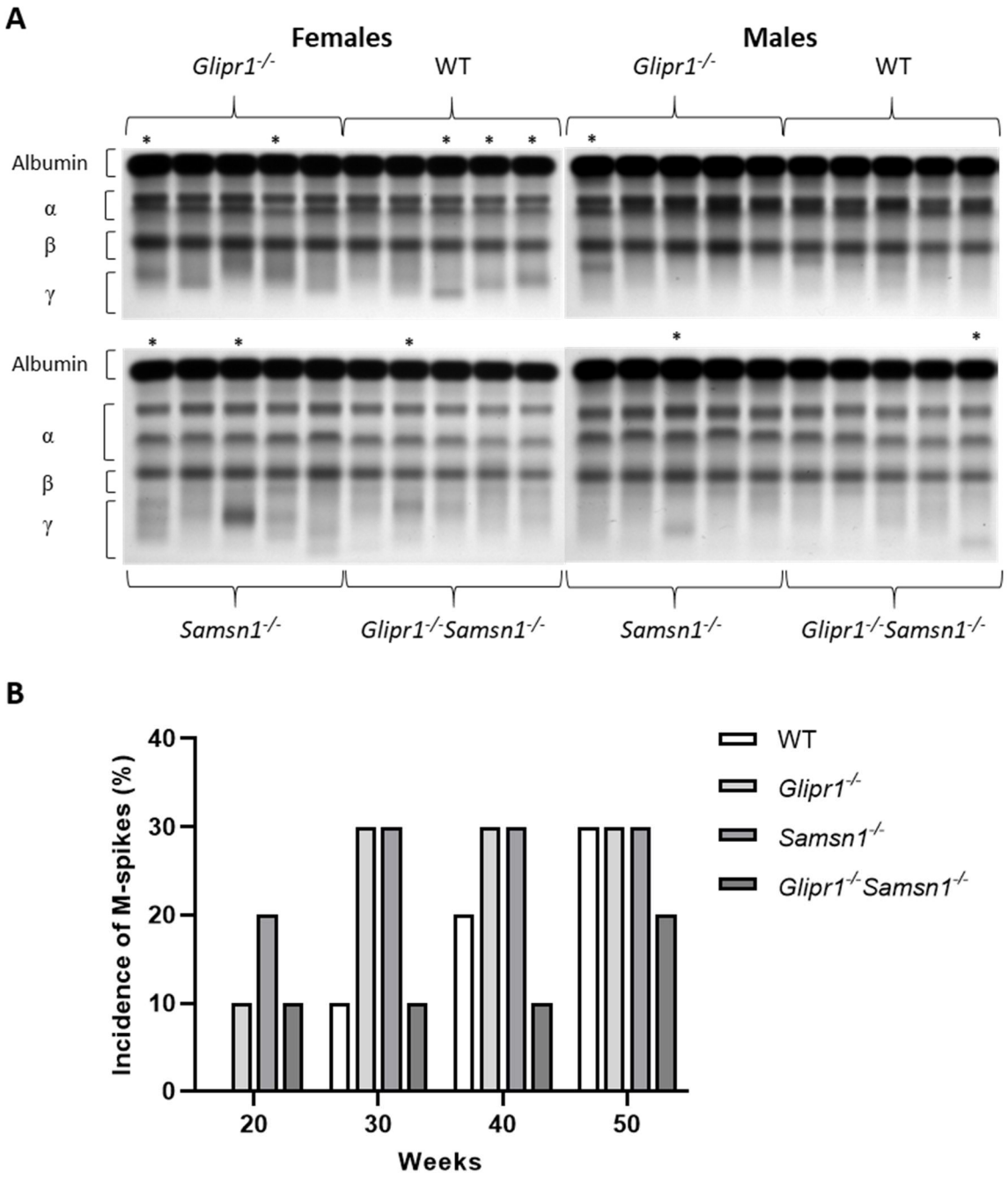

Figure 3.12: *Glipr1* and/or *Samsn1* knockout does not affect M-spike incidence in one-year-old mice. (**A&B**) Serum was serially collected by tail bleed from ageing *Glipr1*$^{-/-}$, *Samsn1*$^{-/-}$, *Glipr1*$^{-/-}$*Samsn1*$^{-/-}$ and WT control mice every 10 weeks and the presence of M-spikes were detected using SPEP (n = 10 mice per genotype). (**A**) SPEP gels for sera collected from 50-week-old mice are shown. The position of the albumin and the different globulin components of the serum are indicated by brackets. * denotes mice with an M-spike. (**B**) The graph depicts the incidence of M-spikes over time for each genotype.

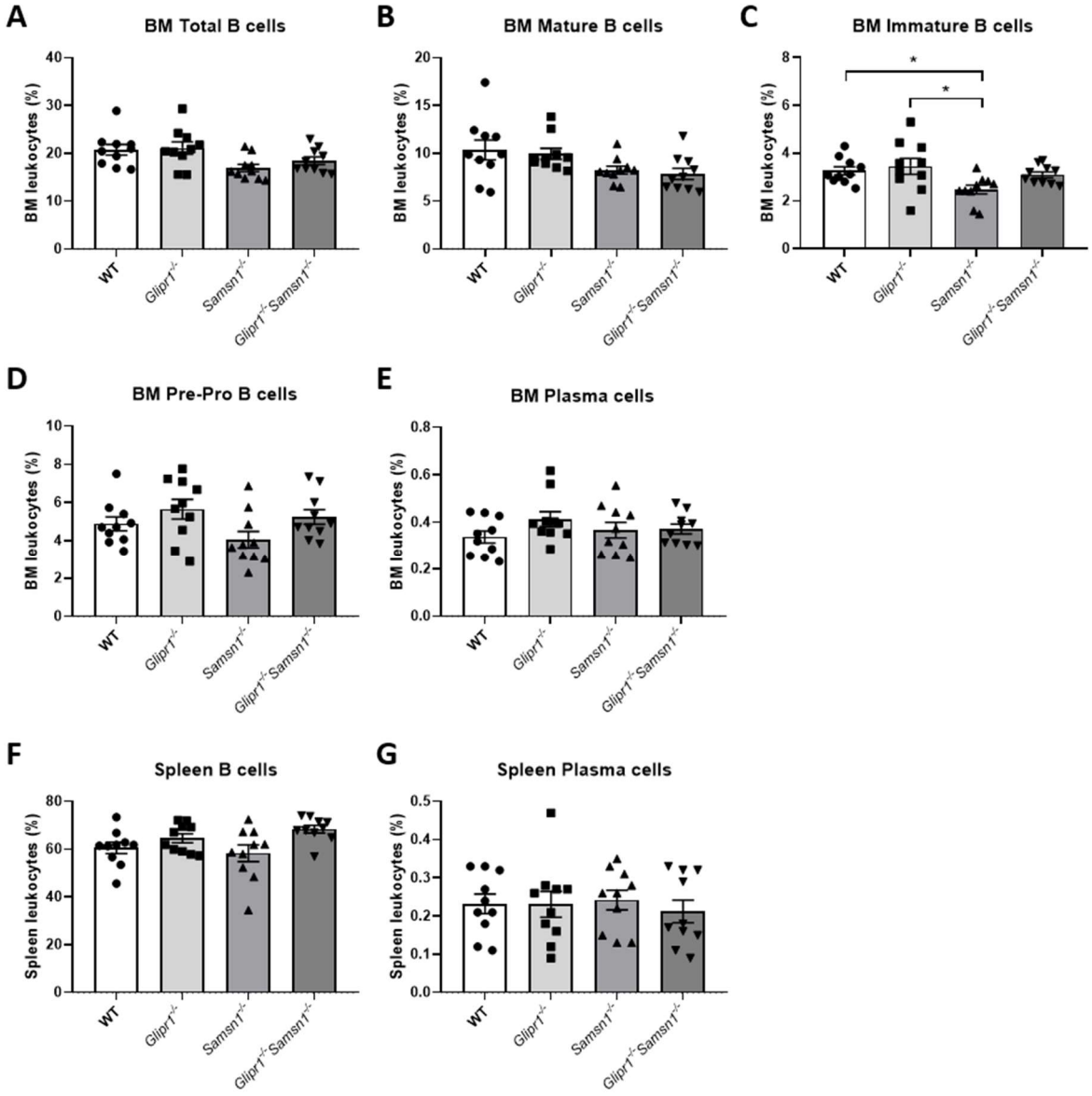

Figure 3.13: *Glipr1* and/or *Samsn1* knockout does not affect PC populations in one-year-old mice. BM and spleen cells were collected from 12-month-old *Glipr1*$^{-/-}$, *Samsn1*$^{-/-}$, *Glipr1*$^{-/-}$*Samsn1*$^{-/-}$ and WT control mice and single cell suspensions were prepared. B cell populations were analysed by flow cytometry through staining cells with anti-B220, anti-IgM and anti-CD138 antibodies. Stained cells were gated to show the percentage of total B cells (**A**&**F**; B220^{+}), mature B cells (**B**; B220^{high}IgM^{low}), immature B cells (**C**; B220^{low}IgM^{+}), pre-pro B cells (**D**; B220^{low}IgM^{-}), and PCs (**E**&**G**; B220^{-}IgM^{-}CD138^{+}) among total leukocytes. Graphs depict the mean ± SEM of n = 10 mice per genotype. *P < 0.05, Kruskal-Wallis test with Dunn's multiple comparisons test.

express *GLIPR1* below the normal range. A reduction in *GLIPR1* expression has also been observed in several solid cancers, including prostate cancer[304], lung cancer[305], sarcoma[306] and bladder cancer [307]. Notably, down-regulation of *GLIPR1* was one of only 38 gene expression changes identified in PCs from patients with the MM-related malignancy light-chain amyloidosis[299]. Together, these findings suggested that *GLIPR1* may be a novel tumour suppressor gene in MM, the down-regulation of which may co-operate with reduced expression of *SAMSN1* to promote MM disease development.

In the context of murine MM, the expression of *Glipr1* was found to be lost in the KaLwRij tumour-derived 5TGM1 MM cell line compared to normal PCs from KaLwRij mice. This is consistent with the loss of Glipr1 being a change that co-operates with the pre-existing absence of Samsn1 in KaLwRij PCs to promote malignant transformation. To investigate whether loss of Glipr1 expression is a common occurrence in the spontaneous MM tumours that arise in KaLwRij mice, other independently-established, KaLwRij PC tumour-derived MM cell lines, such as 5T2[263-266], could be analysed. The mechanism(s) by which *Glipr1*/*GLIPR1* expression is down-regulated in the context of murine/human MM is unknown. Reduced *GLIPR1* expression in prostate cancer was shown to be primarily caused by aberrant DNA hypermethylation[304]. In addition, hemizygous chromosomal deletions encompassing *GLIPR1* have been reported in 9.4% of MM patients[308]. Hence, future studies should investigate DNA methylation and genomic deletion as potential mechanisms that cause down-regulation of *GLIPR1* expression in MM PCs. Notably, the overexpression of Glipr1 in 5TGM1 cells was found to not affect cell proliferation *in vitro* but to reduce tumour burden *in vivo,* suggesting a possible tumour suppressor role for Glipr1 in MM. However, the reduction in 5TGM1-Glipr1 tumour burden did not reach statistical significance, which may have been due to the rapidly progressive nature of the 5TGM1/KaLwRij MM model[267]. Hence, further exploration of the potential tumour suppressor role of *GLIPR1* in MM using less aggressive *in vivo* disease models, such as the human myeloma cell line U266 in immunodeficient mice[309], is warranted.

GLIPR1 has been shown to act as a tumour suppressor in several other malignancies, both *in vitro* and *in vivo*[296-298,304-307]. In addition, previously generated *Glipr1*$^{-/-}$ mice were shown to have reduced survival due to increased rates of spontaneous malignancy[298]. Notably, 40% of the tumours in the *Glipr1*$^{-/-}$ mice were classified as plasmacytomas, which is a localised PC malignancy that frequently progresses to MM[310,311]. Furthermore, like *Samsn1*$^{-/-}$

KaLwRij mice, tumour development in *Glipr1*$^{-/-}$ mice was found to be of late onset (no mortality until 15 months of age) and incomplete penetrance (~17%)[239], which suggests that the loss of *Glipr1* co-operates with additional genetic aberrations to promote malignancy. GLIPR1 has been found to mediate its tumour suppressor effects through several different mechanisms in prostate cancer cells[298,312,313]. For example, it was shown to promote apoptosis by increasing reactive oxygen species production[298] and by modulating HSC70's regulation of apoptosis-related gene expression[312]. In addition, GLIPR1 was found to cause cell cycle arrest by decreasing expression of the oncogenic MYC transcription factor[313]. Whether GLIPR1 performs these tumour suppressor functions in PCs is unknown and warrants future investigation.

Samsn1 knockout mice and *Glipr1* knockout mice on a MGUS-prone C57BL/6 background were generated by backcrossing the KaLwRij-derived *Samsn1* deletion or CRISPR-mediated genetic editing of *Glipr1*, respectively. These single knockout mice were then crossed to generate *Glipr1*$^{-/-}$*Samsn1*$^{-/-}$ double knockout mice, which were used to examine whether the concomitant loss of Samsn1 and Glipr1 induces MM development. After one year, the incidence of M-spikes in the WT mice was 30%, which was in agreement with the previously reported M-spike frequency of ~25-30% in one-year-old C57BL/6 mice[239,262]. Notably, the *Glipr1*$^{-/-}$*, Samsn1*$^{-/-}$ and *Glipr1*$^{-/-}$*Samsn1*$^{-/-}$ mice were found to have an M-spike frequency equal to or less than that of the WT mice. In addition, there was no significant difference in the proportion of PCs in the BM or spleen of the *Glipr1*$^{-/-}$*, Samsn1*$^{-/-}$ or *Glipr1*$^{-/-}$*Samsn1*$^{-/-}$ mice compared to the WT mice at one year of age. Notably, the expression of putative myeloma-promoting transgenes in early B cells was previously shown to cause the development of lymphomas, not MM, in mice [236-238]. Hence, it was considered a possibility that the *Glipr1* and/or *Samsn1* knockout mice may develop B cell malignancies with a less-differentiated cell of origin. However, analyses of B cell populations in the blood, BM and spleen from the *Glipr1*$^{-/-}$*, Samsn1*$^{-/-}$ and *Glipr1*$^{-/-}$*Samsn1*$^{-/-}$ mice showed that there were no expansions of any B cell subsets. Together, these data suggest that the loss of Glipr1 and/or Samsn1 did not promote the development of PC, or other B cell, proliferative disorders in C57BL/6 mice up to one year of age.

The finding that there was no difference in clonal PC expansions between *Samsn1*$^{-/-}$ mice and WT mice was consistent with a previous study that showed no evidence of increased tumorigenesis in *Samsn1*$^{-/-}$ mice up to one year of age.[245]. Whereas, the observation that the

Glipr1$^{-/-}$ mice also did not display increased development of PC dyscrasias compared to WT mice appears to conflict with the previous finding that *Glipr1*$^{-/-}$ mice had a greater propensity to develop plasmacytomas[298]. However, the low penetrance and late onset of the PC tumours observed in the previous *Glipr1*$^{-/-}$ mice suggests that the cohort size (n = 10) and length of monitoring (one year) of the *Glipr1* knockout mice in this study may have been insufficient to observe enhanced tumorigenesis. In addition, previous studies have shown that tumour penetrance and onset is increased in transgenic mice with a 129Sv background compared to a C57BL/6 background[314-317]. Hence, as the previously described *Glipr1* knockout mice were on a C57BL6/129Sv (1:1) hybrid background, they may have been more susceptible to developing PC malignancies compared to the *Glipr1*$^{-/-}$ mice generated in this study, which were on a pure C57BL/6 background. Notably, the *Samsn1*$^{-/-}$*Glipr1*$^{-/-}$ mice did not display evidence of enhanced PC expansions compared to WT mice up to one year of age, suggesting that the loss of both Samsn1 and Glipr1 do not co-operate to drive MM development in MGUS-prone C57BL/6 mice. However, the incidence of MGUS in C57BL/6 mice is known to increase from 25-30% at one year of age to 60-70% by two years of age[239,262]. This suggests that the *Glipr1*$^{-/-}$*Samsn1*$^{-/-}$ mice may need to be aged for longer than one year in order to observe any potential increase in MM development due to the loss of both genes.

A previous study demonstrated that Glipr1 loss and MYC overexpression co-operated to induce invasive prostate carcinomas in mice[313]. Given that MYC activation has been demonstrated to drive MM development and progression[158,160], it is a possibility that *MYC* overexpression and *GLIPR1* down-regulation may co-operate to drive the malignant transformation of PCs. While this remains to be determined, generating *Glipr1*$^{-/-}$*Samsn1*$^{-/-}$ knockout mice that also harbour the Vk*MYC transgene could enable the potential co-operative tumour suppressor effect of these genes in PCs to be assessed over a shorter timeframe *in vivo*. Furthermore, previous studies have shown that *SAMSN1* and *GLIPR1* expression are both down-regulated in other cancers, such as lung cancer[271,305]. *In silico* analysis revealed that *GLIPR1* expression is significantly reduced in lung tumours that have *SAMSN1* expression below the normal range (GSE19804, data not shown), which suggests that these genes may also co-operate to suppress lung cancer and potentially other malignancies. Hence, the effect of *Glipr1* and *Samsn1* knockout on the development of lung cancer should also be examined in future ageing studies of the *Glipr1*$^{-/-}$*Samsn1*$^{-/-}$ mice.

GLIPR1 has been shown to be highly expressed in normal BM and spleen[318], but its function in normal lymphocytes, including B cells remains to be elucidated. *Glipr1* and/or *Samsn1* knockout was found to not affect PB counts or B cell populations, including PC, in the BM or spleen of adult 12-week-old mice. The similarity of B cell populations between the *Samsn1*$^{-/-}$ and WT mice is consistent with the previous finding that there were no defects in B cell development in *Samsn1* knockout[245] or transgenic[249] mice. This suggests that Glipr1 and/or Samsn1 do not play significant roles in haematopoiesis, especially B cell development, in mice. However, it was previously shown that *Samsn1* knockout mice display enhanced B cell function, including increased proliferation in response to antigen stimulation *ex vivo* and increased antigen-specific antibody production *in vivo*[245]. Hence, despite *Glipr1* knockout not affecting the relative size of B cell populations in mice, Glipr1 may have a role in regulating normal B cell function, which is an area for further investigation.

Previous studies have shown that genetic changes in stromal cells, including within the BM, can promote tumour development in surrounding cell types in a process called niche-mediated oncogenesis[319-324]. In the context of MM, the importance of the BM microenvironment in regulating the growth and survival of malignant PCs is well-established[325]. A previous study found that the intratumoral injection of *ex vivo* M2-polarised macrophages from *Samsn1*$^{-/-}$ mice versus WT mice significantly increased the growth of established sub-cutaneous 5TGM1 tumours in immunodeficient mice, suggesting that *Samsn1* expression in PC-extrinsic cells may promote MM development in KaLwRij mice[261]. However, a limitation of the previous study was that the proliferation of 5TGM1 cells *in vivo* was assessed by measuring tumour volume, which included both the 5TGM1 cells and the injected macrophages. Given that the study also showed that *Samsn1*$^{-/-}$ macrophages proliferate faster than WT macrophages, it is possible that at least part of the increased tumour volume observed following injection of *Samsn1*$^{-/-}$ versus WT macrophages was due to differences in the growth of the macrophages, not the tumour cells. Hence, the effect of *Samsn1* loss in PC-extrinsic cells of the BM microenvironment was further investigated in this study by comparing 5TGM1 tumour growth following i.v. inoculation in the newly-generated *Samsn1*$^{-/-}$ mice compared to the WT mice. No significant difference in 5TGM1 tumour development was observed in the *Samsn1*$^{-/-}$ mice compared to the WT mice, suggesting that the absence of Samsn1 in PC-extrinsic cells of the BM microenvironment, including macrophages, is unlikely to influence the development of MM in KaLwRij mice.

In summary, the key genetic abnormalities involved in promoting the transformation from benign MGUS to malignant MM, and how they are interdependent, remain incompletely understood. In this study, *GLIPR1* was identified as a gene that is down-regulated in the clonal PCs of MM patients with low *SAMSN1* expression and the PCs of most MM patients compared to normal controls. Future studies examining the mechanism(s) by which *GLIPR1* expression is reduced and whether this is a cause, consequence or independent of *SAMSN1* down-regulation in MM PCs are warranted. *Glipr1* expression was also found to be lost in the 5TGM1 murine MM cell line and restoration caused a trend towards reduced tumour growth in KaLwRij mice. Further investigation of the potential tumour suppressor role of GLIPR1, and its underlying molecular mechanism of action, in human MM is required. *Glipr1* and *Samsn1* knockout mice were generated and did not show a propensity for enhanced MM disease development up to one year of age. However, further analyses of these mice over a longer timeframe may yet uncover a co-operative tumour suppressor role for Samsn1 and Glipr1 in PCs. Given that *SAMSN1* and *GLIPR1* are concomitantly down-regulated in other malignancies, an improved understanding of the functional relationship between these genes in MM could provide critical insight into the mechanisms of tumourigenesis, and potential treatment strategies, in a range of cancers.

4 INVESTIGATING THE TUMOUR SUPPRESSOR MECHANISM OF SAMSN1 IN MURINE MULTIPLE MYELOMA

4.1 Introduction

The SAM domain, SH3 domain and nuclear localization signals 1 (*SAMSN1*) gene, also known as *SASH2*/*NASH1*/*HACS1*/*SLy2*, encodes a member of the SH3-domain protein expressed in the lymphocyte (SLy) family of evolutionarily conserved proteins, which also includes and SASH1 and SASH3[240,242]. These proteins contain Src homology 3 (SH3) and sterile alpha motif (SAM) domains, both of which mediate protein-protein interactions, and thus have putative adaptor/scaffolding functions[240,242]. SAMSN1 also harbours an N-terminal nuclear localisation signal and a nuclear export signal but is predominantly localised to the cytoplasm[240,241]. The gene is most highly expressed in normal haematopoietic tissues, including BM, spleen, lymph nodes, thymus and PB[240]. *SAMSN1* is also expressed at lower levels in the heart, brain, lung, muscle and placenta[240]. The gene is located on chromosome 21 (21q11.2) and there are three alternative transcripts, with the canonical sequence encoding a polypeptide that is 373 amino acids in length. The orthologous murine *Samsn1* gene is located on chromosome 16 and is highly conserved, sharing 84% homology with human *SAMSN1*.

The molecular functions of SAMSN1 are poorly understood, but SAMSN1/Samsn1 protein was shown to be strongly up-regulated in primary human/mouse B cells following B cell receptor (BCR) engagement[241]. Notably, the overexpression of Samsn1 in primary murine splenic B cells resulted in decreased cellular activation and proliferation in response to BCR stimulation[241]. In addition, primary splenic B cells from *Samsn1*$^{-/-}$ mice were found to have increased proliferation upon BCR stimulation *in vitro*[245]. These *Samsn1*$^{-/-}$ mice also displayed enhanced adaptive immunity *in vivo*, producing significantly higher levels of antigen-specific immunoglobulins following immunisation[245]. Taken together, these data suggest that SAMSN1 is an immunoinhibitory adaptor that has a role in regulating the development and moderating the immune response of B cells. This is consistent with the important role that a range of adaptor/scaffolding proteins, such as kinase suppressor of Ras (KSR) and discs large homolog 1 (DLG1), have been shown to play in regulating immune cell signalling[326].

Investigation of the molecular mechanisms underlying the immunoinhibitory role of Samsn1 in B cells identified the paired Ig-like receptor B (PIR-B) protein, a receptor that negatively regulates BCR signalling, as a potential binding partner of SAMSN1 through a yeast-2-hybrid screen[241]. PIR-B is phosphorylated following BCR stimulation, which results in the

recruitment of SHP-1 phosphatase and the attenuation of BCR signalling[327]. Hence, Samsn1 may inhibit B cell activation/proliferation by binding to PIR-B and amplifying its negative regulation of BCR signalling[245]. However, a physical association between Samsn1 and endogenous PIR-B was not detected in primary murine B cells[241]. The immunoinhibitory effect of Samsn1 has also been attributed to its demonstrated role in actin cytoskeletal remodelling[249]. Notably, the actin reorganisation-mediated spreading of lymphocytes, which is crucial for antigen gathering and subsequent cell activation[257], was found to be drastically reduced for splenic B cells from *Samsn1* transgenic mice compared to WT mice[249]. The lymphocyte-specific homolog of the actin regulator cortactin, Hs1, which is required for T cell spreading[328], was found to interact with Samsn1 in B cells from the transgenic mice[249]. These findings suggest that Samsn1 may inhibit B cell responses by limiting Hs1-mediated B cell spreading. Furthermore, SAMSN1 has been implicated in epigenetic regulation of gene expression, as two members of the Sin3 co-repressor complex, SAP30 and histone deacetylase 1 (HDAC1), co-immunoprecipitated with SAMSN1 when overexpressed in HEK293T cells[251]. While the effect of SAMSN1 on the transcriptome was not assessed, these findings suggest that SAMSN1 may also have an inhibitory effect on B cell function by directly regulating gene expression.

In addition to its role in regulating humoral immune responses, *SAMSN1* has been implicated as a tumour suppressor gene in several cancers, including the plasma cell (PC) malignancy multiple myeloma (MM). A putative tumour suppressor role was first attributed to *SAMSN1* in lung cancer, owing to its location within a region on chromosome 21 that is frequently affected by loss of heterozygosity[271]. Furthermore, *SAMSN1* expression was found to be reduced in lung cancer cell lines compared to normal tissue[271]. *SAMSN1* was subsequently found to have reduced expression in tumour versus normal tissue in the context of other malignancies, including ulcerative colitis-associated colon cancer[272], hepatocellular carcinoma[273], gastric cancer[274] and also MM[260]. Furthermore, low *SAMSN1* expression was associated with negative clinical parameters in MM and other cancers, including increased tumour size and decreased disease-related survival[260,273,274]. In the context of MM, C57BL/KaLwRij (KaLwRij) mice, a small proportion of which spontaneously develop an MM-like disease as they age, were found to be *Samsn1*$^{-/-}$ due to a 180 kb homozygous genomic deletion on chromosome 16[260,261]. Our group assessed the functional effect of *Samsn1* loss in MM PC using the 5TGM1/KaLwRij mouse model of MM, in which the KaLwRij tumour-derived 5TGM1 MM PC line is inoculated i.v. into syngeneic KaLwRij

mice[260]. Once in the circulation, the injected 5TGM1 cells home to and colonise the BM of the mice, resulting in rapid tumour development throughout the skeleton within 4 weeks[268]. Notably, enforced Samsn1 expression in 5TGM1 cells was found to significantly reduce tumour development to undetectable levels *in vivo*, suggesting that *SAMSN1* may be a tumour suppressor gene in MM[260].

The mechanism(s) by which Samsn1 completely inhibits 5TGM1 tumour development in KaLwRij mice, which may also be relevant in human MM, is yet to be fully elucidated. Re-expressing *Samsn1* in 5TGM1 cells has been shown to reduce cellular proliferation *in vitro*, but there are conflicting reports regarding the conditions under which this effect was observed[260,261]. One group found that Samsn1 reduced the proliferation of 5TGM1 cells by ~25% under basal conditions[261], while our group observed a ~15% decrease only when the tumour cells were co-cultured with primary KaLwRij-derived BM stroma[260]. In addition, our group found that Samsn1 increased the adhesion of 5TGM1 cells to BM stroma *in vitro*[260]. Together, these data suggest that Samsn1 may suppress *in vivo* tumour development through a cell adhesion-mediated anti-proliferative effect on 5TGM1 cells in the BM microenvironment[260]. However, given that Samsn1 only modestly reduced 5TGM1 proliferation *in vitro*, it is possible that there may be other mechanisms that contribute to its abrogation of MM tumour growth. For example, as Samsn1 has been implicated in actin cytoskeletal remodelling[249], it could be suppressing MM tumour development through inhibiting 5TGM1 migration/BM homing, but this remains to be determined. In this chapter, the tumour suppressor mechanism of Samsn1 in 5TGM1 cells was investigated through protein binding partner and transcriptome analyses. In addition, the effect of Samsn1 on the tumourigenic behaviour of 5TGM1 cells was further explored through *in vitro* actin remodelling and migration assays and *in vivo* metastasis and BM homing experiments.

4.2 Results

4.2.1 Identifying novel binding partners of Samsn1 in 5TGM1 cells

To gain a better understanding of the mechanism(s) by which Samsn1, a putative adaptor protein, acts as a tumour suppressor in the 5TGM1 murine MM PC line, it was aimed to identify its protein binding partners in these cells by co-immunoprecipitation (co-IP) coupled with mass spectrometry. As an IP-capable antibody for Samsn1 was unavailable, 5TGM1 cells expressing C-terminal HA-tagged Samsn1 were generated, enabling the IP of Samsn1 and associated proteins using an anti-HA antibody. Samsn1-HA protein was detected by

Western blot in 5TGM1-Samsn1-HA cells at the predicted size of 43 kD, confirming successful overexpression of the tagged protein (Figure 4.1A). In addition, 46 kD and 36 kD proteins were also recognised by both anti-Samsn1 and anti-HA antibodies in the 5TGM1-Samsn1-HA cells. The larger molecular species most likely corresponds to the phosphorylated form of Samsn1[251,329], but the identity of the smaller species is unknown. To assess whether the addition of a HA-tag disrupted the tumour suppressor effect of Samsn1 on 5TGM1 cells *in vivo*, the 5TGM1-Samsn1-HA and 5TGM1-EV cell lines were injected i.v. into C57BL/KaLwRij mice and tumour development was monitored for 4 weeks. At the endpoint, there was a significant decrease in tumour burden for the mice inoculated with 5TGM1-Samsn1-HA cells compared to EV control 5TGM1 cells, as measured by BLI (P = 0.0079, Mann-Whitney U test; Figure 4.1B) and SPEP (*P* = 0.0079, Mann-Whitney U test; Figure 4.1C). These data demonstrated that adding a C-terminal HA-tag to Samsn1 in 5TGM1 cells does not interfere with its previously observed ability to completely inhibit MM tumour development *in vivo*.

To identify proteins associated with Samsn1 in 5TGM1 cells, 5TGM1-Samsn1-HA and 5TGM1-EV control cells were lysed with a buffer containing 1% NP-40 and co-IPs were performed using an anti-HA antibody. The isolated proteins were separated into two fractions and resolved separately by SDS- PAGE. The smaller fraction was transferred onto a membrane and the successful IP of HA-tagged Samsn1 was confirmed by Western blot (Figure 4.2A). Gel staining of proteins from the larger co-IP fraction revealed bands corresponding to the size of Samsn1 and several other bands representing co-IPed proteins of different sizes (Figure 4.2B). However, there were no bands that were present in the co-IP from the 5TGM1-Samsn1-HA cells but absent in the negative control co-IP from the 5TGM1-EV cells. This indicated that the co-IPed proteins did not represent genuine binding partners of Samsn1 but rather non-specific background. With the aim of trying to better preserve the interactions between Samsn1 and its binding partners, the co-IP was repeated using a lysis buffer containing 1% CHAPS, which is a detergent with lower stringency than NP-40. However, no co-IPed proteins that were unique to the 5TGM1-Samsn1 cells, and thus potential Samsn1 interactors, were observed on the gel, which negated the use of mass spectrometry to identify them (Figure 4.2C). Overall, proteins representing putative binding partners of Samsn1 in 5TGM1 cells were not identified by co-IP under the conditions tested.

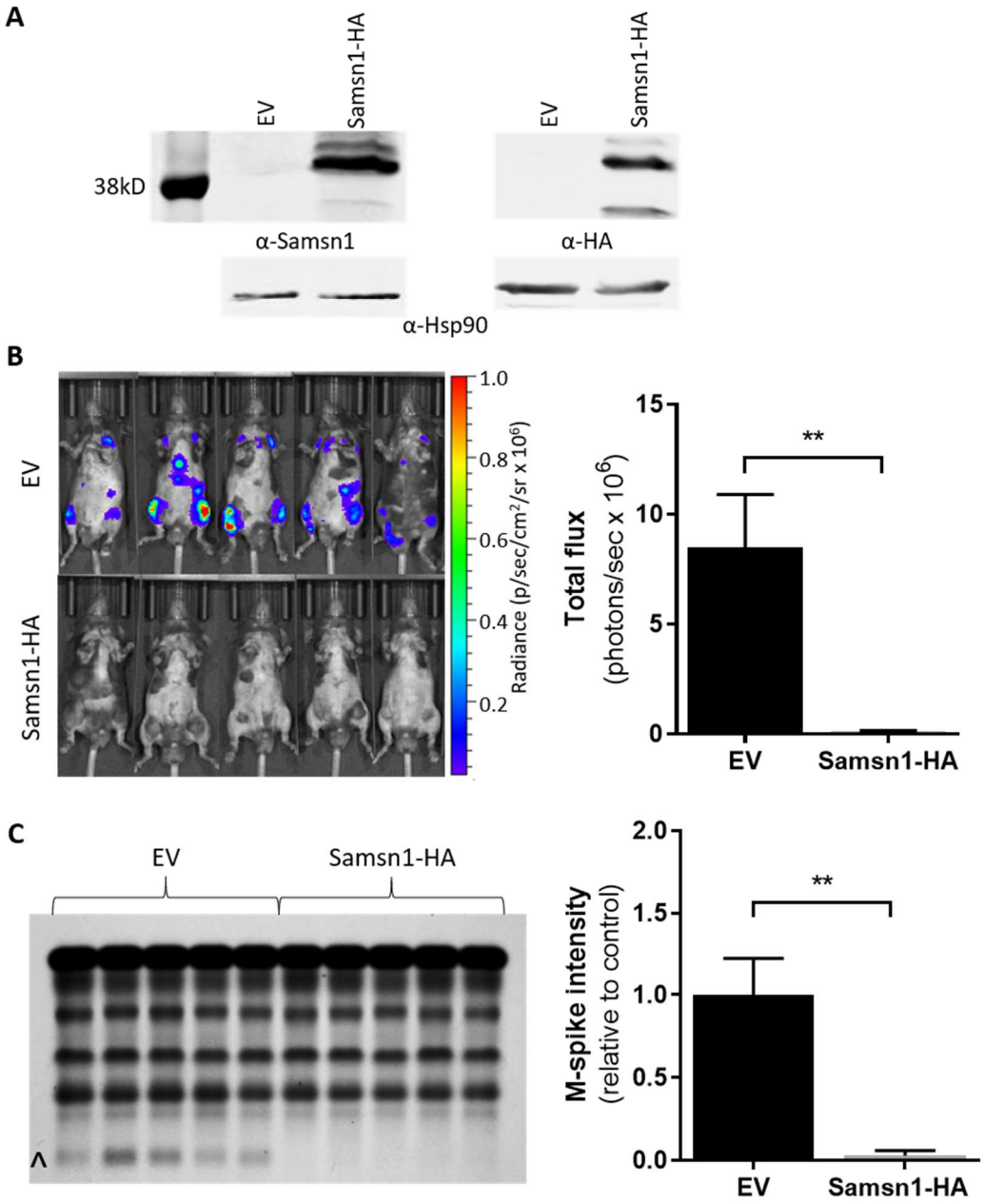

Figure 4.1: HA-tagged Samsn1 significantly inhibits the growth of 5TGM1 cells *in vivo*. (**A**) Protein lysates from 5TGM1-Samsn1-HA and 5TGM1-EV cells were subjected to Western blotting using anti-HA and anti-Samsn1 antibodies. Hsp90 was used as a loading control. (**B**&**C**) KaLwRij mice were injected i.v. with 5×10^5 5TGM1-EV or 5TGM1-Samsn1-HA cells. At 4 weeks, tumour burden was measured by BLI and SPEP. (**B**) Ventral BLI scans of the mice (left) and the total flux (right) are shown. (**C**) M-spikes (^) on the SPEP gel (left) and the M-spike intensity (right), normalised to albumin and expressed relative to the EV control, are shown. The graphs depict the mean + SEM of n = 5 mice per cell line from one experiment. $^{**}P < 0.01$, Mann-Whitney U test.

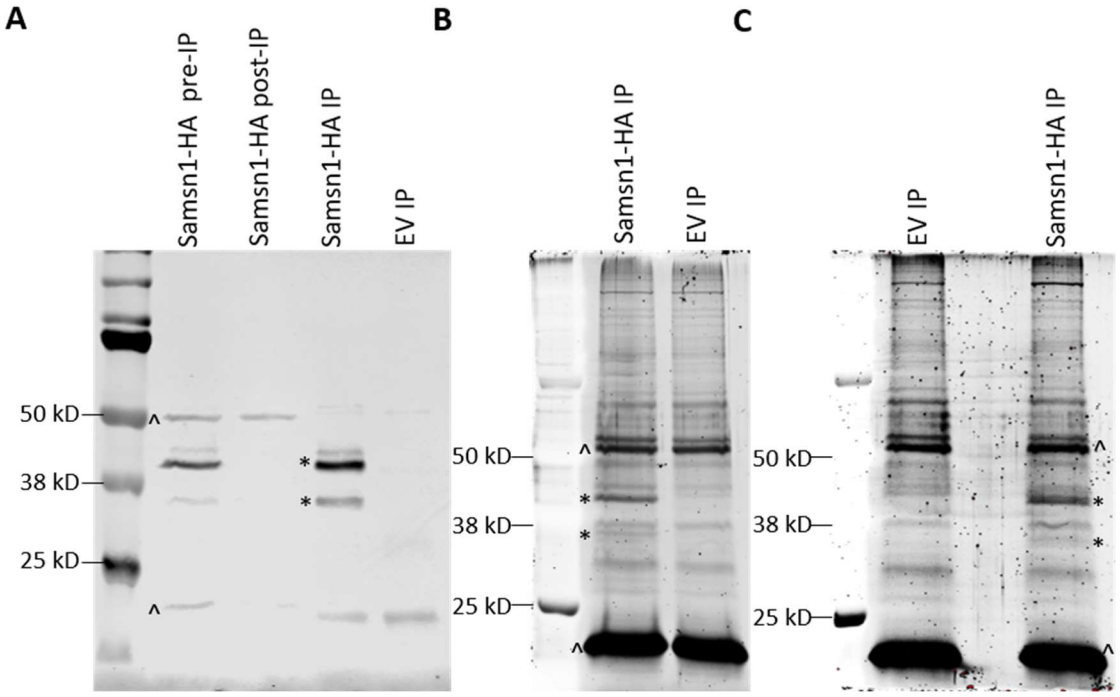

Figure 4.2: Identifying Samsn1 binding partners in 5TGM1 cells by co-IP. 5TGM1-Samsn1-HA or 5TGM1-EV cells were lysed in buffer containing 1% NP-40 (**A**&**B**) or 1% CHAPS detergent (**C**) followed by co-IP using anti-HA antibody-conjugated agarose. (**A**) An equal amount of lysate from the Samsn1-HA cells pre-IP and post-IP, as well as 10% of the co-IPed proteins from the Samsn1-HA and EV 5TGM1 cells were resolved by SDS-PAGE. The proteins were transferred to a membrane, which was probed with an anti-HA antibody. The remaining 90% of co-IPed proteins obtained using lysis buffer containing either NP-40 (**B**) or CHAPS (**C**) were resolved by SDS-PAGE and stained using SYPRO^{TM} Ruby. Images are representative of at least 2 independent experiments. * denotes bands corresponding to HA-tagged Samsn1. ^ denotes bands corresponding to immunoglobulin heavy or light chains.

4.2.2 Samsn1 does not bind to, but reduces the phosphorylation of, Hs1 in 5TGM1 cells

Given that Samsn1 has been shown to interact with endogenous Hs1 in primary mouse B cells[249], the possibility that these proteins are binding partners in 5TGM1 cells was assessed through co-IP coupled with Western blot. Co-IPs were performed on 5TGM1-Samsn1-HA and 5TGM1-EV cell lysates using an anti-HA antibody and the isolated proteins were subjected to Western blot using anti-HA and anti-Hs1 antibodies. Despite Samsn1 being successfully IPed, Hs1 was not detected in the co-IPed proteins from the 5TGM1-Samsn1-HA cell lysates, suggesting that Hs1 is not a binding partner of Samsn1 in 5TGM1 cells under the conditions tested (Figure 4.3A). In addition, the effect of Samsn1 on the activation of Hs1 was assessed by comparing Hs1 phosphorylation in 5TGM1-Samsn1-HA cells and 5TGM1-EV control cells by Western blot. Under basal culture conditions, the amount of Hs1 phosphorylation on the activating tyrosine residue Y397 was found to be significantly reduced in Samsn1-expressing 5TGM1 cells compared to EV control 5TGM1 cells (P = 0.006, paired t test; Figure 4.3B). This finding suggests that Samsn1 may inhibit the activity of the actin cytoskeleton regulatory protein Hs1 in 5TGM1 cells.

4.2.3 Samsn1 does not affect the migration, or adhesion to endothelium, of 5TGM1 cells *in vitro*

Given that Samsn1 may limit the activation of Hs1, it was hypothesised that actin cytoskeletal remodelling may be inhibited in Samsn1-expressing 5TGM1 cells. This was assessed by measuring the induction of polymerised filamentous actin (F-actin) formation in 5TGM1-Samsn1 cells following treatment with CXCL12, which is a potent chemoattractant that drives homing of both normal and malignant PC to the BM[330]. However, neither the positive control 5TGM1-EV cells, nor the 5TGM1-Samsn1 cells, formed F-actin in response to CXCL12 (P > 0.05, two-way ANOVA with Sidak's multiple comparisons test; Figure 4.4A). This is despite the fact that 5TGM1 cells express the receptor for CXCL12, CXCR4, and that CXCL12 has been shown to potently induce actin polymerisation in other MM PC lines[331-333]. Although the results of the actin polymerisation assay were inconclusive, the effect of Samsn1 on cellular processes that require cytoskeletal rearrangement, and are involved in the BM homing of MM PC, were also investigated[334]. The impact of Samsn1 expression on the migration of 5TGM1 cells was assessed by a 24-hour transwell assay using primary murine BM stromal cell-conditioned medium as the chemoattractant. As shown in Figure 4.4B, Samsn1 was found to have no effect on the migration of 5TGM1 cells toward

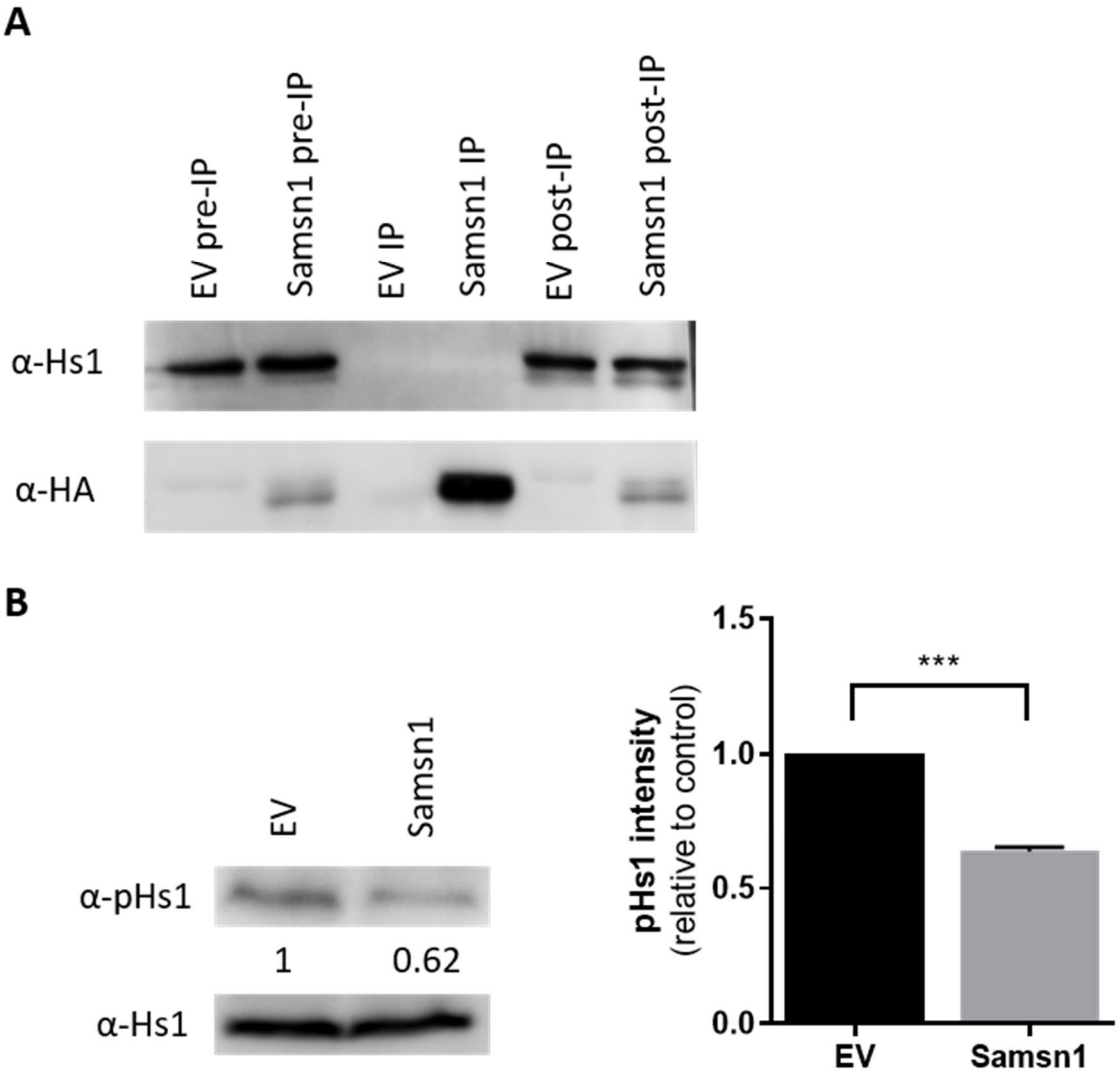

Figure 4.3: Samsn1 does not bind to, but decreases the phosphorylation of, Hs1 in 5TGM1 cells. (**A**) 5TGM1-Samsn1-HA or 5TGM1-EV cells were lysed in buffer containing 1% NP40 and co-IP was performed using anti-HA antibody-conjugated agarose. The proteins isolated by IP, as well as an equal amount of lysate from both cell lines pre-IP and post-IP, were resolved by SDS-PAGE and transferred to a membrane, which was probed with anti-Hs1 and anti-HA antibodies. A representative blot of three independent experiments is shown. (**B**) Western blots were performed on protein lysates from 5TGM1-Samsn1-HA and 5TGM1-EV cells using an anti-pHs1 (Y397) and an anti-Hs1 antibody. A representative blot (left) and the quantitated pHs1 band intensity (right) are shown. The pHs1 intensity was normalised to total Hs1 and was expressed relative to the EV control. The graph depicts the mean + SD of three independent experiments. *** $P = 0.001$, paired t test.

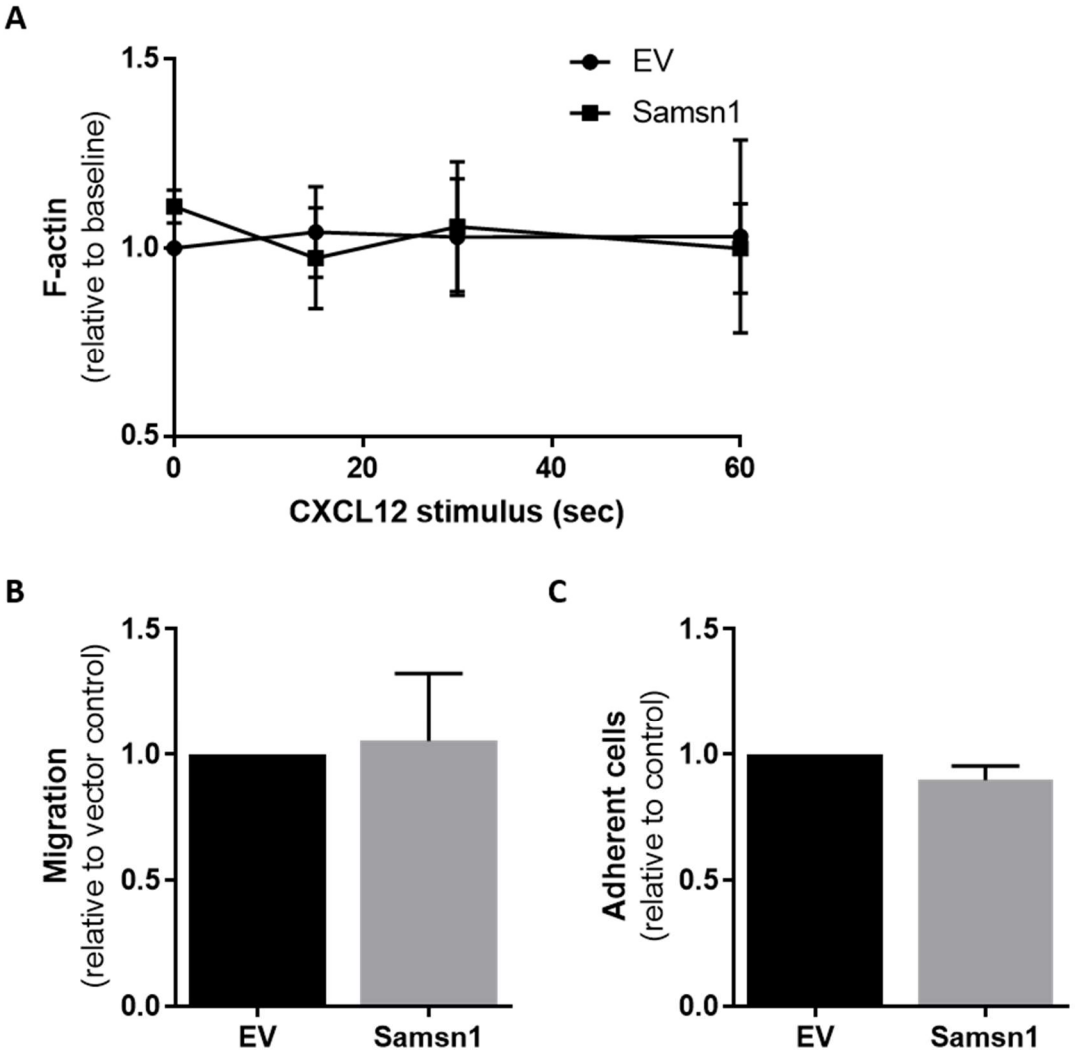

Figure 4.4: Samsn1 does not affect the F-actin polymerisation, migration or adhesion to endothelium of 5TGM1 cells *in vitro*. (**A**) 5TGM1-Samsn1 and 5TGM1-EV cells were stimulated with 200 ng/mL CXCL12 for the indicated times. The cells were immediately fixed and then stained for F-actin using Alexa Fluor^{TM} 680 phalloidin, which was measured by flow cytometry. The MFI was normalised to baseline levels and expressed relative to the EV control. (**B**) Migration of 5TGM1-Samsn1 and 5TGM1-EV cells toward primary mouse BM stromal cell-conditioned medium was assessed in a 24-hour transwell assay. Results are expressed relative to the EV control cells. (**C**) 5TGM1-Samsn1 or 5TGM-EV cells were seeded on a BM endothelial cell monolayer, and percent cell adhesion, relative to total cell input, was assessed by BLI after 15 minutes. Results are expressed relative to the EV control cells. Graphs depict the mean + SEM of three (**A**), or six (**B**&**C**) independent experiments. $P > 0.05$, two-way ANOVA with Sidak's multiple comparisons test (**A**) or paired t test (**B**&**C**).

this stimulus after 24 hours ($P = 0.8565$, paired t test). Furthermore, the adhesion of 5TGM1 cells to BM endothelial cells was shown to not be affected by Samsn1 expression ($P = 0.1267$, paired t test; Figure 4.4C).

4.2.4 Samsn1 expression does not have a significant impact on the transcriptome of 5TGM1 cells

In order to further investigate the potential mechanisms by which Samsn1 inhibits 5TGM1 tumour development *in vivo*, the effect of Samsn1 expression on the transcriptome of 5TGM1 cells was assessed using RNA-seq. Four independent RNA samples from cultured 5TGM1-Samsn1 and 5TGM1-EV cells in the exponential growth phase were analysed. In excess of 44 million reads were obtained for each sample and ~70% were uniquely mapped to the GRCh38/mm10 version of the mouse genome (Table 4.1). Excluding the expression of *Samsn1* itself, principal components analysis revealed that the Samsn1-expressing and EV control 5TGM1 cell samples did not cluster separately, which suggests that Samsn1 had a minimal impact on the transcriptome of 5TGM1 cells (Figure 4.5A). Consistent with this, differential gene expression analysis revealed only 18 genes, including *Samsn1*, that had significantly altered expression (FDR < 0.1) in the Samsn1-expressing compared to control 5TGM1 cells (Table 4.2 and Figure 4.5B). Excluding *Samsn1*, ten of the differentially expressed genes were found to be up-regulated, and seven were found to be down-regulated in the 5TGM1-Samsn1 cells compared to the 5TGM1-EV cells. Notably, only five of the up-regulated and three of the down-regulated genes in the 5TGM1-Samsn1 cells had a fold-change greater than 1.5. Of these genes, increased *Tex101* ($P = 0.0176$, paired t test) and decreased *Negr1* ($P = 0.0109$, paired t test) mRNA expression in the 5TGM1-Samsn1 cells was confirmed by RT-qPCR (Figure 4.5C). To identify the potential biological significance of the *Samsn1*-correlated genes, gene ontology (GO) analysis was performed on the up-regulated or down-regulated genes using the DAVID Bioinformatics Database. However, no GO terms were found to be significantly enriched in the small number of genes that were up-regulated or down-regulated in the 5TGM1-Samsn1 cells compared to the 5TGM1-EV control cells (data not shown).

Table 4.1: Raw, trimmed and uniquely mapped reads for each RNA-seq sample from 5TGM1-EV or 5TGM1-Samsn1 cells.

Sample	Raw reads	Trimmed reads	Uniquely mapped reads	% Uniquely mapped reads
EV 1	48,802,396	48,801,987	34,093,015	69.9%
EV 2	45,391,599	45,390,960	31,947,560	70.4%
EV 3	45,914,933	45,914,394	32,345,450	70.5%
EV 4	44,242,572	44,237,846	31,083,991	70.3%
Samsn1 1	45,443,843	45,441,793	32,199,210	70.9%
Samsn1 2	47,094,205	47,092,431	33,250,348	70.6%
Samsn1 3	46,572,793	46,572,048	33,160,511	71.2%
Samsn1 4	45,883,193	45,876,764	32,618,381	71.1%
EV mean	46,087,875	46,086,297	32,367,504	70.2%
Samsn1 mean	46,248,509	46,245,759	32,807,112	70.9%

Figure 4.5: Differentially expressed genes in Samsn1-overexpressing 5TGM1 cells identified by RNA-Seq. (**A**) Principal components analysis of RNA-seq expression data from four biological replicates of 5TGM1-Samsn1 (S1-4) cells and 5TGM1-EV (E1-4) cells was performed, excluding *Samsn1*, and the multi-dimensional scaling plot is shown. (**B**) Heat map showing two-way hierarchical clustering of the 18 differentially expressed genes (rows) between 5TGM1-Samsn1 and 5TGM1-EV cells (columns). The coloured scale bar represents the log2-transformed copies per million (CPM). (**C**) The expression levels of *Negr1* (left) and *Tex101* (right) were analysed in 5TGM1-Samsn1 cells compared to 5TGM1-EV cells by RT-qPCR. Levels were normalised to the housekeeping gene *Actb* and expressed relative to the EV cells. Graphs depict the mean ± SEM of n = 4 biological replicates. **P* < 0.05, paired t test.

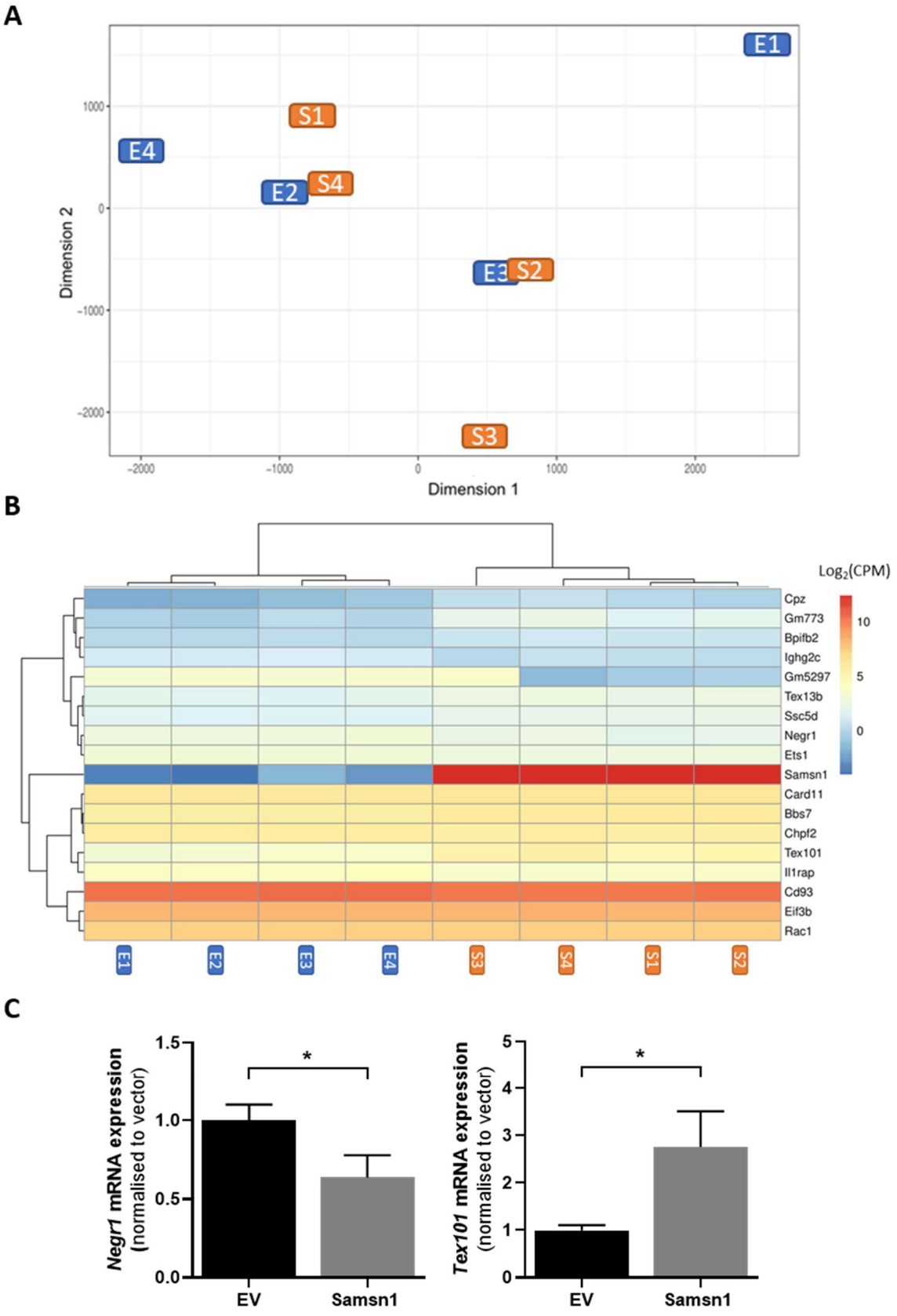
A
E1
S1
E4
S4
E2
E3
S2
S3
Dimension 2
Dimension 1
1000
0
-1000
-2000
-2000
-1000
0
1000
2000
B
Log2(CPM)
10
5
0
Cpz
Gm773
Bpifb2
Ighg2c
Gm5297
Tex13b
Ssc5d
Negr1
Ets1
Samsn1
Card11
Bbs7
Chpf2
Tex101
Il1rap
Cd93
Eif3b
Rac1
E1
E2
E3
E4
S3
S4
S1
S2
C
Negr1 mRNA expression
(normalised to vector)
1.5
1.0
0.5
0.0
*
EV
Samsn1
Tex101 mRNA expression
(normalised to vector)
5
4
3
2
1
0
*
EV
Samsn1

Table 4.2: Differentially expressed genes (FDR < 0.1) in Samsn1-expressing compared to EV control 5TGM1 cells identified by RNA-seq.

Gene name	Entrez gene ID	log_2FC	Average expression (log_2CPM)	FDR
Samsn1	67742	16.15	4.26	1.02E-10
Gm773	331416	2.14	0.92	4.34E-05
Tex101	56746	1.71	4.24	1.64E-04
Cpz	242939	1.70	-0.62	3.60E-02
Bpifb2	66557	0.71	0.47	6.75E-02
Tex13b	83555	0.69	2.14	9.84E-03
Ssc5d	269855	0.52	1.91	7.44E-02
Bbs7	71492	0.31	5.78	2.43E-04
Card11	108723	0.19	6.11	7.97E-03
Rac1	19353	0.12	7.37	7.97E-02
Eif3b	27979	0.12	8.24	3.50E-02
Chpf2	100910	-0.16	5.70	7.55E-02
Cd93	17064	-0.18	10.33	1.77E-03
Il1rap	16180	-0.26	3.86	6.80E-02
Ets1	23871	-0.34	2.93	7.63E-02
Negr1	320840	-0.66	2.49	6.75E-02
Ighg2c	N/A	-0.77	0.74	4.99E-02
Gm5297	N/A	-3.06	1.85	4.99E-02

Positive fold-change (FC) indicates that the gene is up-regulated, and a negative FC indicates that the gene is down-regulated, in 5TGM-Samsn1 cells vs 5TGM1-EV cells. CPM = copies per million, FDR = false discovery rate.

4.2.5 Samsn1 inhibits the metastasis of 5TGM1 cells *in vivo*

Given that the protein interaction and mRNA transcriptome analyses were unable to reveal potential mechanisms by which Samsn1 suppresses 5TGM1 tumour growth, the effect of Samsn1 on the tumourigenic behaviour of 5TGM1 cells was further investigated *in vivo*. To determine the effect of Samsn1 on the growth of 5TGM1 cells in the BM without the prerequisite of tumour cells homing from the circulation, 5TGM1-Samsn1 or 5TGM1-EV cells (1 x 10^5) were injected directly into the left tibia of KaLwRij mice. After 23 days, the primary tumour burden in the injected leg was not found to significantly differ between the mice inoculated with 5TGM1-Samsn1 cells and mice inoculated with 5TGM1-EV cells, as determined by BLI (P = 0.5907, Mann-Whitney U test; Figure 4.6A). In addition, the formation of large primary tumours by both 5TGM1-Samsn1 and 5TGM1-EV cells was confirmed by performing immunohistochemical staining of GFP^+ cells in sections from injected tibiae (Figure 4.6B).

Notably, in some intratibially (i.t.)-inoculated mice, the BLI showed that 5TGM1 cells had metastasised from the injected leg and formed secondary tumours at distal sites. The metastatic tumour burden was significantly lower in the 5TGM1-Samsn1 group of mice compared to 5TGM1-EV group of mice, as measured by BLI (P = 0.0093, Mann-Whitney U test; Figure 4.7A). In addition, the percentage of GFP^+ 5TGM1 tumour cells in the BM of the femur and tibia from the non-injected, contralateral leg was significantly lower in the 5TGM1-Samsn1-inoculated mice compared to the 5TGM1-EV-inoculated mice (P = 0.0140, Mann-Whitney U test; Figure 4.7B). Considering both the BLI and flow cytometry data, the incidence of metastasis was significantly lower in mice inoculated with 5TGM1-Samsn1 cells (n = 1/7, 14.3%) compared to mice inoculated with 5TGM1-EV cells (n = 7/8, 87.5%; P = 0.0101, Fisher's exact test; Figure 4.7C). Together, these data suggest that Samsn1 does not affect the growth of primary tumours following i.t. injection of 5TGM1 cells into KaLwRij mice, but it significantly inhibits the subsequent metastasis of MM PC from these primary tumours.

4.2.6 Samsn1 expression in 5TGM1 cells does not affect homing to, but inhibits expansion within, the BM *in vivo*

Given that Samsn1 was found to inhibit the metastasis of 5TGM1 cells from primary tumours, it was hypothesised that Samsn1 suppresses the homing of MM PC to the BM. To test this *in vivo*, 5TGM1-Samsn1 cells or 5TGM1-EV cells (5 x 10^6) were injected i.v. into

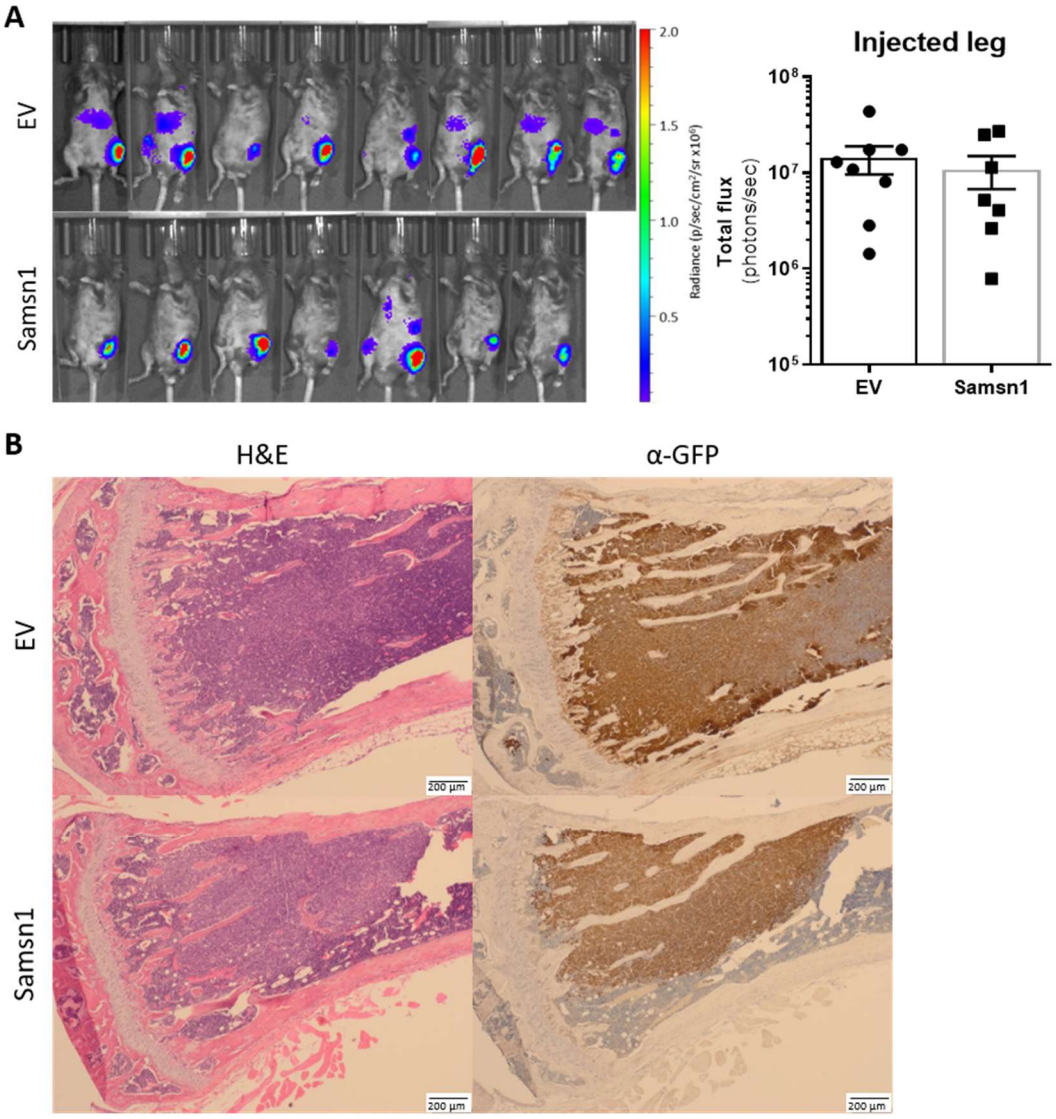

Figure 4.6: Samsn1 does not affect the growth of primary tumours following i.t. injection of 5TGM1 cells *in vivo*. (**A&B**) 5TGM1-Samsn1 (Samsn1) or 5TGM1-EV (EV) cells (1 x 10^5) were injected into the left tibia of KaLwRij mice and tumour burden was measured by BLI. (**A**) Ventral BLI scans of mice injected with 5TGM1-EV (above) or 5TGM1-Samsn1 (below) cells (left) and the quantitated total flux of the injected leg (right) after 23 days are shown. Graph depicts the mean ± SEM of n=7-8 mice per cell line from two independent experiments. $P > 0.05$, Mann-Whitney U test. (**B**) Paraffin-embedded sections of the 5TGM1-injected tibiae were stained with H&E (left) or an anti-GFP antibody (right). Representative images of stained sections from a mouse injected with 5TGM1-EV (above) or 5TGM1-Samsn1 (below) cells (left panel) are shown. Images were taken at the same magnification and the scale bar is shown.

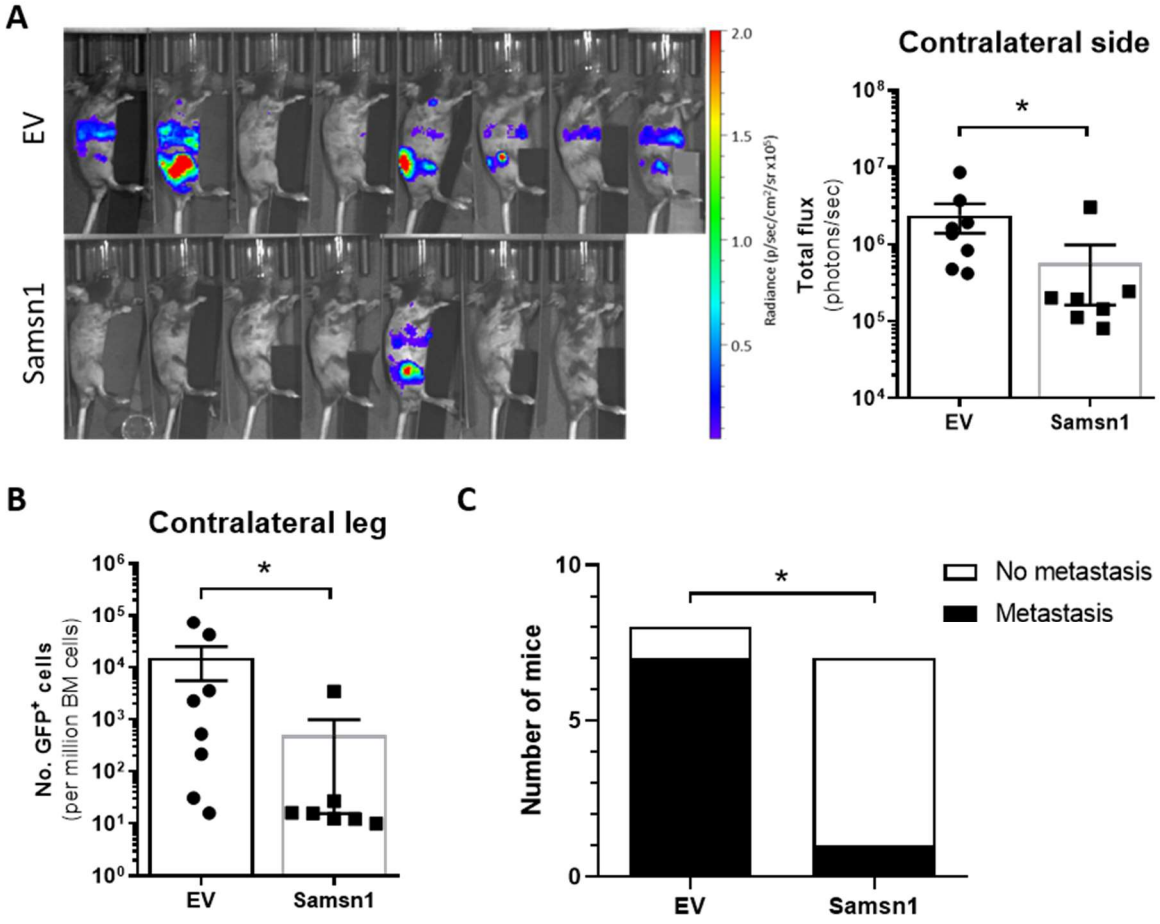

Figure 4.7: Samsn1 inhibits the metastasis of 5TGM1 cells *in vivo*. (**A-C**) 5TGM1-Samsn1 or 5TGM1-EV cells (1 x 10^5) were injected into the left tibia of KaLwRij mice and tumour burden was measured by BLI. (**A**) BLI scans of the contralateral side (injected leg covered) of the mice inoculated with EV (above) or Samsn1-expressing (below) 5TGM1 cells (left) and the quantitated total flux (right) after 23 days are shown. (**B**) The number of GFP^+ tumour cells in the BM from the non-injected, contralateral leg was assessed by flow cytometry after 23 days. (**C**) The number of mice injected i.t. with 5TGM1-EV or 5TGM1-Samsn1 cells with overt metastasis, defined as visible BLI signal outside the injected leg and/or greater than 200 tumour cells per million in the BM of the contralateral leg by flow cytometry. Results were normalised to primary tumour burden and graphs depict the mean ± SEM of n = 7-8 mice per cell line from two independent experiments. *$P < 0.05$, Mann-Whitney U test (**A**&**B**) or Fisher's exact test (**C**).

KaLwRij mice and the number of GFP^+ tumour cells present in the BM after 24 hours was assessed by flow cytometry. Notably, Samsn1 expression was found to not affect the number of 5TGM1 cells present in the long bones of the mice 24 hours post-tumour cell injection ($P = 0.8182$, Mann-Whitney U test; Figure 4.8). To determine the fate of the 5TGM1-Samsn1 cells that successfully homed to the BM, the experiment was repeated, but the number of tumour cells in the long bones of the mice was assessed after 21 days. While the numbers of 5TGM1-EV cells in the BM expanded over time, the numbers of 5TGM1-Samsn1 cells did not significantly differ between day 1 and 21 post-tumour cell injection ($P < 0.0001$, two-way ANOVA with Sidak's multiple comparison test; Figure 4.8). These data suggest that while Samsn1 does not inhibit the homing of 5TGM1 cells to the BM, it does inhibit the outgrowth of disseminated MM PC within the BM microenvironment.

4.3 Discussion

It has previously been shown that *SAMSN1* displays significantly lower expression in PCs from MM patients compared to healthy controls and that low *SAMSN1* expression in the PCs of MM patients confers a poor prognosis[260,261]. In addition, *Samsn1* was found to be deleted in the MM-prone KaLwRij mouse strain and its re-expression in the KaLwRij-derived 5TGM1 MM PC line completely inhibited MM disease development *in vivo*[260]. These findings suggest that SAMSN1 may have a tumour suppressor role in the development and/or progression of MM. Although SAMSN1 has been implicated as a tumour suppressor in other cancers, the mechanism(s) by which it inhibits malignancy remains to be determined[271-274]. In this study, how *SAMSN1* inhibits MM PC tumour development was investigated through unbiased molecular analyses coupled with *in vitro* and *in vivo* assays using Samsn1-expressing 5TGM1 cells.

Given that PC are not circulatory, the fact that most MM patients have multiple tumours throughout their skeleton at diagnosis indicates that there is a continuous spread of tumour cells within the body[335]. This metastasis plays a crucial role in the development of symptomatic MM and disease progression, including the re-population of the BM with treatment-resistant clones during relapse[335]. In this study, the expression of Samsn1 in 5TGM1 cells was found to significantly reduce the metastasis from primary i.t. tumours to distal BM sites *in vivo*. A vital step in the process of metastasis in MM is the active migration/homing of circulating tumour cells to new BM sites[335]. A previous study demonstrated a role for Samsn1 in actin cytoskeleton reorganization, which is a prerequisite

Figure 4.8: Samsn1 does not affect the BM homing, but does inhibit the expansion, of 5TGM1 cells *in vivo.* (**A**&**B**) KaLwRij mice were injected with 5 x 10^6 5TGM1-Samsn1 or 5TGM1-EV cells i.v. and the number of GFP^+ tumour cells in the long bones was determined by flow cytometry after 1 or 21 days. (**A**) Representative flow plots of GFP^+ cells in the BM of mice inoculated with 5TGM1-EV (left) or 5TGM1-Samsn1 (right) cells after 1 day (above) or 21 days (below) are shown. (**B**) Graph shows the number of GFP^+ tumour cells per million BM cells present in the long bones of mice injected with 5TGM1-EV or 5TGM1-Samsn1 cells after 1 and 21 days. Graph depicts the mean ± SEM of n=5-6 mice per cell line at each time point from one (21 days) or two (1 day) independent experiments. ****$P <$ 0.0001, two-way ANOVA with Sidak's multiple comparisons test.

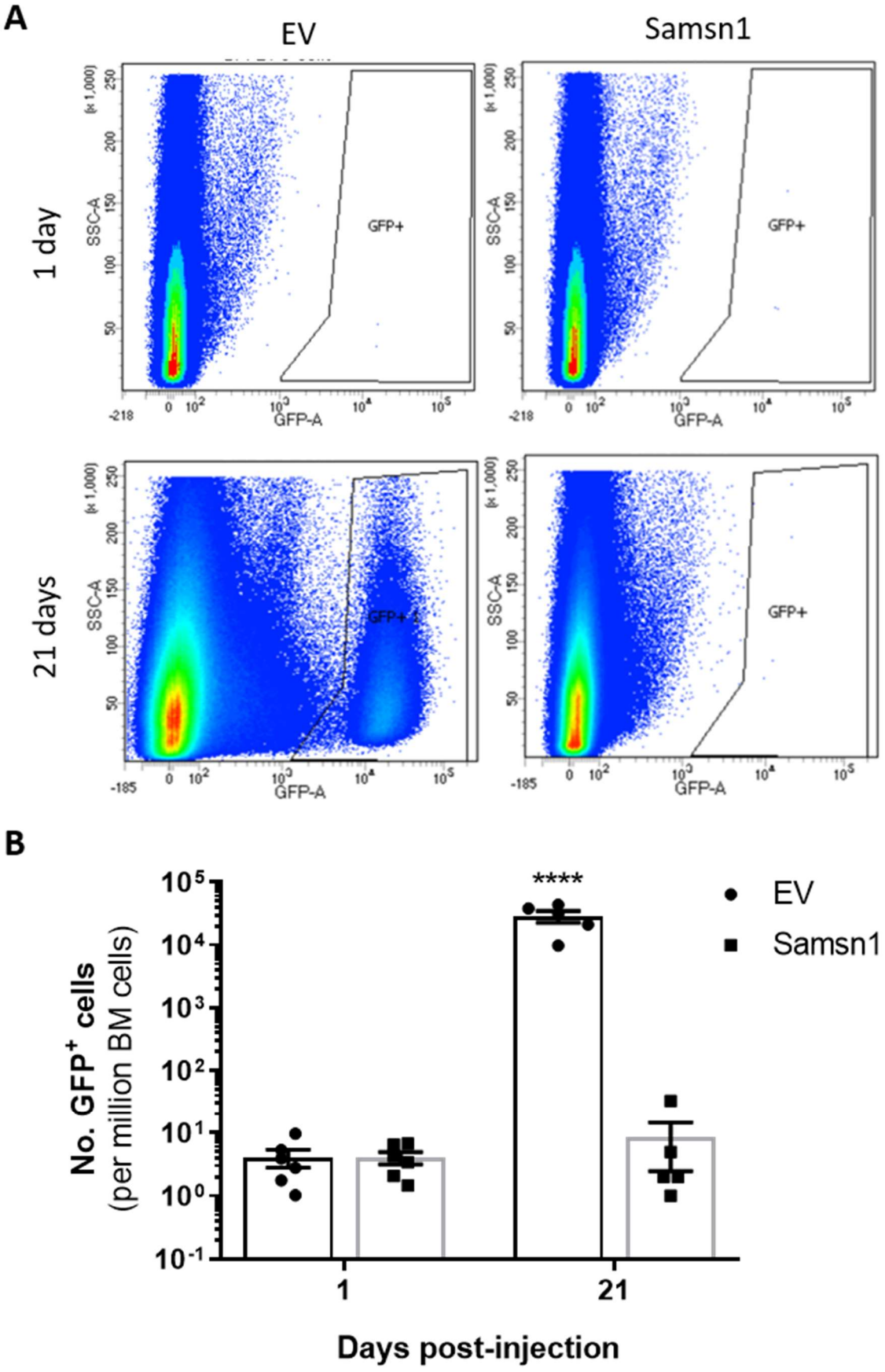
A
EV
Samsn1
1 day
21 days
SSC-A
GFP-A
GFP+
B
No. GFP+ cells
(per million BM cells)
****
EV
Samsn1
Days post-injection
1
21

for cell migration[249]. In addition, the closely related protein SASH1 has been shown to regulate actin cytoskeletal dynamics[258] and inhibit the adhesion, migration and invasion of several epithelial cancer cell types[277,280,281]. The ability of Samsn1 to affect cytoskeletal dynamics was linked to its demonstrated interaction with Hs1[249], which is activated by phosphorylation on key tyrosine residues and mediates actin polymerisation within, and the subsequent migration of, normal lymphocytes[336-340]. Notably, increased Hs1 phosphorylation in malignant chronic lymphocytic leukemia B cells correlated with increased polymerised F-actin and migration of malignant cells *in vitro*[341] and with enhanced BM homing *in vivo*[342]. Although a direct interaction between Hs1 and Samsn1 in 5TGM1 cells was not detected, the levels of Hs1 phosphorylated on the activating Y397 residue were reduced in Samsn1-expressing cells. Hence, it was hypothesised that Samsn1 may suppress the activation of Hs1 within, and thus the migration of, 5TGM1 cells. However, the Samsn1-expressing 5TGM1 cells showed neither decreased migration *in vitro* nor decreased BM homing *in vivo*. Together, these data suggest that the anti-metastatic effect of Samsn1 *in vivo* is unlikely to be attributable to a reduction in the number of MM PC that can migrate to the BM.

Following homing of disseminated tumour cells to the BM, metastasis also involves colonisation, the expansion of solitary or small clusters of cancer cells into macroscopic tumours[335]. In this study, Samsn1 was found to suppress the colonisation of 5TGM1 cells when relatively small numbers were seeding the BM from the circulation, as occurred following i.v. injection or migration from a primary i.t. tumour. However, Samsn1 did not suppress the outgrowth of 5TGM1 cells when much larger numbers were introduced directly into the medullary cavity by i.t. injection. The interaction between 5TGM1 cells and the normal cells/factors within the BM microenvironment was greater when fewer tumour cells were present. Hence, these findings suggest that the ability of Samsn1 to inhibit the expansion of 5TGM1 cells within the BM is dependent on tumour-inhibitory signals derived from the microenvironment. This is consistent with our previous finding that Samsn1 reduced the proliferation of 5TGM1 cells specifically when they were co-cultured with normal primary BM stromal cells[260]

Interactions with the BM microenvironment are known to play an important role in regulating the growth, survival and drug resistance of MM PCs[116]. While interactions between clonal PCs and BM stromal cells typically support tumour growth at the MM

stage[325], there is growing evidence that the normal BM microenvironment can also play an important role in restricting disease progression at the premalignant disease stage[343]. For example, exosomes derived from normal BM mesenchymal stromal cells were found to inhibit myeloma cell growth, whereas exosomes from MM stroma had a tumour-promoting effect[344]. In addition, a recent study demonstrated that PCs taken from MGUS patients with stable disease grow progressively in the BM of humanised mice, suggesting that MM disease progression is constrained by extrinsic signals from the BM microenvironment[233].

The ability of the BM microenvironment to influence the growth of MM PC has previously been demonstrated in the 5TGM1/KaLwRij murine model of MM. Recent studies from our group have shown that the majority of 5TGM1 cells that home to the BM localise to the osteoblast-lined endosteal surface and are maintained in a state of long-term dormancy, with only a few MM PCs undergoing clonal expansion and contributing to tumour burden[345,346]. However, the dormant state was found to be reversible upon re-injection of quiescent 5TGM1 cells into naïve KaLwRij mice, suggesting that PC-extrinsic, not PC intrinsic, factors regulate the proliferative fate of MM PC *in vivo*[345]. Exposure to osteoblast-conditioned medium was shown to reduce 5TGM1 cell proliferation and co-culture with the MC3T3 osteoblast-like cell line increased the rates of 5TGM1 cell dormancy *in vitro*[345]. In addition, the proliferation of primary patient MM PCs was previously found to be reduced when the tumour cells were co-cultured with primary osteoblasts *in vitro*[347]. These data suggest that osteoblastic lineage cells may play a key role in regulating the proliferation of MM PCs in the BM microenvironment through the production of as yet unidentified soluble factors. The fact that these studies were performed with *Samsn1*$^{-/-}$ 5TGM1 cells suggests that Samsn1 is not required *per se* for the establishment of MM PC dormancy. However, Samsn1 may promote the quiescence of disseminated 5TGM1 cells by enhancing their response to osteoblast-derived anti-proliferative signals. Hence, future investigation of the effect of Samsn1 on the proliferation of 5TGM1 cells in the presence of osteoblasts is warranted.

The BM microenvironment-derived signals that promote dormancy in MM PCs are poorly defined, but several factors that regulate haematopoietic stem cell dormancy have been found to induce quiescence in cancer cell types that metastasise to bone[348]. In prostate cancer and head and neck squamous cell carcinoma, osteoblast-derived transforming growth factor-β2 (TGFβ2) was found to promote dormancy of disseminated tumour cells in the BM[349,350]. This effect was shown to be dependent on the stimulation of tumour cell-expressed TGFβ

receptor III (TGFβRIII), which causes cell cycle arrest through the activation of p38 mitogen-activated protein kinase and cyclin dependent kinase inhibitor p27[349,350]. In addition, the related ligand bone morphogenetic protein 7 (BMP7) was found to induce prostate cancer cell dormancy in the BM through a similar mechanism involving p38 activation[351]. Notably, BMP7 has previously been demonstrated to inhibit the proliferation and promote the apoptosis of MM PCs[352]. Given that Samsn1 is a putative adaptor protein, it is hypothesised that Samsn1 may promote MM PC quiescence in the BM through positively regulating the intracellular signalling cascades that occur in response to microenvironment-derived anti-proliferative signals. Hence, examination of TGFβ2 and BMP7 as potential stimulators of MM PC dormancy, and the modulating effect of Samsn1 on their activity, is warranted.

Previous transcriptomic analysis of dormant versus proliferative 5TGM1 cells revealed that the expression of *Axl*, which encodes a receptor of the growth-arrest specific 6 (GAS6) ligand, was increased in dormant MM PCs[345]. Given that Axl has been shown to promote cellular dormancy of prostate cancer cells in the BM, it was hypothesised that it may also have a similar function in 5TGM1 cells[353-356]. *Axl*, or other known dormancy-associated genes, were not among the small number of only 17 genes, excluding *Samsn1*, that were found to be differentially expressed in Samsn1-expressing 5TGM1 cells in culture. The minimal effect of Samsn1 on the transcriptome of 5TGM1 cells suggests that it is more likely to exert its tumour suppressor effect, including potentially promoting MM PC dormancy, at a post-transcriptional level. However, if the tumour suppressor effect of Samsn1 is dependent on the interaction of 5TGM1 cells with the BM microenvironment, performing RNA-seq on 5TGM1-Samsn1 cells either co-cultured with BM stroma or pooled from the BM of KaLwRij mice may reveal additional gene expression changes that contribute to the anti-proliferative effect of Samsn1 *in vivo*.

Further insight into the means by which Samsn1 expression may potentiate anti-colonisation signals from the BM microenvironment could be gained through identifying the interaction partners of this putative cytoplasmic adaptor protein in MM PCs. In the present study, despite the successful IP of HA-tagged Samsn1 from 5TGM1 cells, no proteins were found to co-IP specifically with Samsn1 under the conditions tested. Although several potential Samsn1-interacting proteins have been identified in other cellular contexts, other than Hs1, none of the observed associations were with endogenous proteins[241,249,251]. Notably,

SAMSN1 appeared to bind very few endogenous proteins in a human B lymphoma cell line under basal conditions, but BCR stimulation induced interactions between SAMSN1 and several tyrosine-phosphorylated proteins[241]. This suggests that specific assay conditions and/or stimuli, such as co-culture with BM stroma, may be required to induce binding between Samsn1 and its key partners in 5TGM1 cells. It is also possible that Samsn1-interacting proteins did not co-IP because their interactions in 5TGM1 cells are relatively weak and/or transient. In order to preserve these interactions, chemical cross-linking of proteins within 5TGM1 cells prior to co-IP could be utilised in future studies of the Samsn1 interactome in MM PCs. In addition, given that there is evidence that phosphorylation of one protein (Hs1) is altered by Samsn1, a phosphoproteomic analysis of 5TGM1-Samsn1 versus 5TGM1-EV cells using Stable Isotope Labelling by Amino acids in Cell culture (SILAC)-based mass spectrometry could reveal other proteins, and thus signalling pathways, that are modulated by Samsn1 in MM PCs.

In summary, Samsn1 expression in 5TGM1 cells was shown to not affect the migration/homing of tumour cells to the BM *in vitro* and in mice. Notably, Samsn1 was found to specifically inhibit BM colonisation by small numbers of disseminated, not large numbers of directly injected, 5TGM1 cells *in vivo*. This suggests that Samsn1 may completely inhibit tumour growth in KaLwRij mice by promoting the effect of anti-proliferative signals derived from the BM microenvironment on 5TGM1 cells. Further studies of the possible source and type of BM-derived anti-tumour factors that may be enhanced by Samsn1, and the PC-intrinsic molecular mechanism(s) by which this is achieved, are warranted. Such investigations have the potential to build on our increasing understanding of the important role played by the BM microenvironment in regulating the transition from MGUS to MM. This knowledge may aid in the rational design of therapies that modulate the interaction between clonal PCs and the BM microenvironment, which could not only enhance the effectiveness of the current treatments for MM patients but also delay or prevent disease progression in MGUS patients.

5 INVESTIGATING THE POTENTIAL TUMOUR SUPPRESSOR ROLE OF SAMSN1 IN HUMAN MULTIPLE MYELOMA

5.1 Introduction

Multiple myeloma (MM) is the second most common haematological malignancy in adults and is characterised by the clonal expansion of malignant plasma cells (PCs) within the bone marrow (BM)[1]. Despite recent improvements in the survival of MM patients due to the introduction of novel therapies, relapse is inevitable and MM remains an incurable disease[357]. MM is invariably preceded by an asymptomatic precursor disease, monoclonal gammopathy of undetermined significance (MGUS), which carries a 1% risk of progressing to symptomatic disease per year[22]. The aetiology of MM is complex, with genetic studies revealing an array of different DNA mutations, copy number alterations and epigenetic changes present in the PCs of patients[146]. Despite this variation in PC-intrinsic factors, all MM PCs are, at least initially, dependent on interactions with the BM microenvironment to support their growth and survival[358]. Several studies have found that the transition from MGUS to MM is not accompanied by the acquisition of additional mutations[226,228,230,232] and clonal PCs from MGUS patients have the capacity to grow progressively in humanised mice[233]. These findings suggest that changes to PC-extrinsic factors in the BM microenvironment are likely to play an important role in driving the progression from MGUS to MM. Hence, treatments targeting microenvironmental alterations may be able to promote long-term MM disease control, and even prevent disease progression from the MGUS stage, irrespective of the genetic background of the PCs. However, in order to rationally design such therapies, an improved understanding of the dysregulated neoplastic PC-BM microenvironment interactions that promote MM disease progression is required.

Given the known importance of the BM microenvironment in regulating the growth, survival and drug resistance of MM PCs[325], murine models of MM are crucial for improving our understanding of disease pathogenesis and for pre-clinical testing of novel therapies. Xenograft models of MM are established through the injection of human myeloma cell lines (HMCLs) into immune compromised mice[269]. Previously non-obese diabetic and severe combined immune deficiency (NOD SCID) mice, which lack B and T cells and have reduced natural killer (NK) cell function, were used extensively for this purpose[359]. However, NOD SCID gamma (NSG) mice, which lack B, T and NK cell activity, have since been shown to enable enhanced HMCL engraftment[360,361]. There are various routes by which NSG mice can be inoculated with HMCLs, including sub-cutaneous or intraperitoneal injection. However, these methods of inoculation result in extramedullary tumour growth, which does not recapitulate key aspects of the normal growth site of MM PC, the BM

microenvironment[362]. Alternatively, i.v. administration of HMCLs into NSG mice results in disseminated disease within the BM, but prior irradiation of the mice is required to promote successful MM PC engraftment[359]. In contrast, intratibial (i.t.) injection of HMCLs has been shown to result in efficient primary tumour engraftment and metastatic tumour formation in non-irradiated NSG mice[363]. Furthermore, there is the SCID-hu model in which HMCLs are grown in human fetal bone tissue implanted into irradiated immunodeficient mice[269,364]. While this model enables HMCLs to be grown in a human BM microenvironment, it does not recreate the composition of adult BM, and its use is limited by the availability and ethical concerns associated with the use of human fetal tissue[269].

The *Samsn1* gene was found to be homozygously deleted in the C57BL/KaLwRij (KaLwRij) mouse strain[260,261]. Both KaLwRij and closely-related wildtype (WT) C57BL/6 mice are prone to developing an MGUS-like benign PC expansion, but only KaLwRij mice can develop an MM-like malignancy (0.5% in mice over two years old)[264]. Notably, re-expression of Samsn1 in the KaLwRij-derived 5TGM1 MM PC line completely inhibited tumour development following i.v. inoculation into syngeneic KaLwRij mice[260]. These findings suggest that Samsn1 is a tumour suppressor in the context of murine MM. Our group previously showed that 5TGM1-Samsn1 cells have reduced proliferation compared to control 5TGM1 cells when co-cultured with BM stromal cells *in vitro*[260]. In addition, in the previous chapter, Samsn1 was found to suppress the outgrowth of disseminated 5TGM1 cells in the BM of KaLwRij mice. Collectively, these observations suggest that *Samsn1* acts as a tumour suppressor gene in the 5TGM1/KaLwRij model of murine MM by promoting extrinsic regulation of malignant PC growth by the BM stroma. However, the underlying molecular mechanism by which Samsn1 promotes PC-extrinsic inhibition of BM colonisation by 5TGM1 MM PC remains to be determined.

In relation to human MM, *SAMSN1* expression was found to be significantly reduced in PCs from MM patients compared to MGUS patients and normal controls, with ~25% of MM patients having *SAMSN1* expression below the normal range[260,261]. In addition, reduced *SAMSN1* expression was found to be significantly associated with increased PC burden and reduced overall survival of MM patients[260]. These data are consistent with *SAMSN1* also potentially having a tumour suppressor role in the context of human MM. However, the only previous report of the functional effect of SAMSN1 on human MM PCs was the finding that *SAMSN1* overexpression increased the adhesion of the H929 HMCL to BM stromal cells *in*

vitro[260]. Hence, it remains unclear whether SAMSN1 also promotes tumour suppression in human MM PCs and whether this occurs through a mechanism that is dependent on the BM microenvironment. In this chapter, the aim was to investigate the potential tumour suppressor function of SAMSN1 in HMCLs using *in vitro* assays and an i.t./NSG mouse model of MM.

5.2 Results

5.2.1 Generation of HMCLs with stable knockdown of SAMSN1 using CRISPR-Cas9

To determine if *SAMSN1* has a tumour suppressor role in human MM PCs, the aim was to generate HMCLs with reduced SAMSN1 protein levels using CRISPR-Cas9 genome editing, which would replicate the down-regulation of *SAMSN1* expression observed in the PCs from some MM patients[260]. The RPMI-8226 and JJN3 HMCLs were selected for SAMSN1 knockdown (KD) because they were found to have relatively high *SAMSN1* mRNA expression compared to other HMCLs by examination of a publicly available RNA-seq dataset (http://www.keatslab.org/data-repository). These HMCLs were transduced with lentiviral vectors encoding Cas9 and one of two doxycycline-inducible guide RNAs (gRNAs) targeting exon 4 of *SAMSN1* or an empty vector (EV) control (Figure 5.1A). Exon 4 was selected because it is the first exon that is common to all *SAMSN1* mRNA transcripts and is upstream of the exons that encode the key SAM and SH3 domains of the protein. Following doxycycline treatment of Cas9-expressing HMCLs transduced with either a gRNA-containing or empty vector, the resultant cell populations were analysed for the presence of indels in exon 4 of *SAMSN1* through a heteroduplex mobility assay. Heteroduplex formation by *SAMSN1* exon 4 PCR products was observed in the RPMI-8226 and JJN3 cells expressing gRNA #1 or gRNA #2, but not the EV control, which indicated that indels were successfully generated in at least a proportion of *SAMSN1* alleles in the SAMSN1-KD HMCLs (Figure 5.1B). To determine the effect of CRISPR-Cas9-mediatd DNA editing on the levels of SAMSN1 protein in the HMCLs, a Western blot was performed using lysates prepared from SAMSN1-KD and control RPMI-8226 and JJN3 cells. The expression of gRNA #1 was shown to reduce the levels of SAMSN1 protein by an average of 84% and 78% in the RPMI-8226 and JJN3 cells, respectively, compared to the EV controls (Figure 5.1C). Furthermore, the expression of gRNA #2 produced even greater knockdown of SAMSN1 protein levels, with a reduction of 92% observed for both HMCLs. Hence, SAMSN1-KD HMCLS were successfully generated using CRISPR-Cas9 editing.

Figure 5.1: Generation of HMCLs with SAMSN1 knockdown by CRISPR-Cas9 genome editing. (**A**) Schematic for CRISPR-Cas9 targeting of *SAMSN1* using doxycycline (dox)-inducible guide RNA (gRNA) lentiviral vectors. RPMI-8226 and JJN3 human myeloma cell lines (HMCLs) stably and constitutively expressing Cas9 were generated by lentiviral transduction with a mCherry-tagged expression vector. These cells were then transduced with a lentiviral, dox-inducible gRNA and GFP expression vector encoding one of two gRNAs (#1 and #2) targeting exon 4 of *SAMSN1* or an empty vector (EV) control. The GFP^+ cells were treated with dox for 72 hours to induce transient expression of the gRNAs, which direct Cas9-mediated indel formation in *SAMSN1* exon 4. In turn, this causes knockdown (KD) of SAMSN1 (S) protein levels and thus the resultant HMCLs are denoted as SAMSN1-KD #1 or SAMSN1-KD #2, depending on the gRNA that was expressed. (**B**) DNA was extracted from the SAMSN1-KD #1, SAMSN1-KD #2 and EV RPMI-8226 and JJN3 cells and the *SAMSN1* exon 4 region was amplified by PCR. The products were then analysed for the presence of indels using a heteroduplex mobility assay. Images of GelRed®-stained polyacrylamide gels (6%) showing separation of homoduplex and heteroduplex PCR products for the RPMI-8226 (left) and JJN3 (right) HMCLs are shown. Small and large square brackets indicate homoduplex and heteroduplex bands, respectively. (**C**) Representative Western blots for SAMSN1 in whole cell lysates from CRISPR-Cas9-targeted or control RPMI-8226 (left) and JJN3 (right) HMCLs from two independent experiments are shown. HSP90 was used as the loading control. The quantified densities of the SAMSN1 protein bands, which were normalised to HSP90 and expressed relative to the EV control cell line, are also shown.

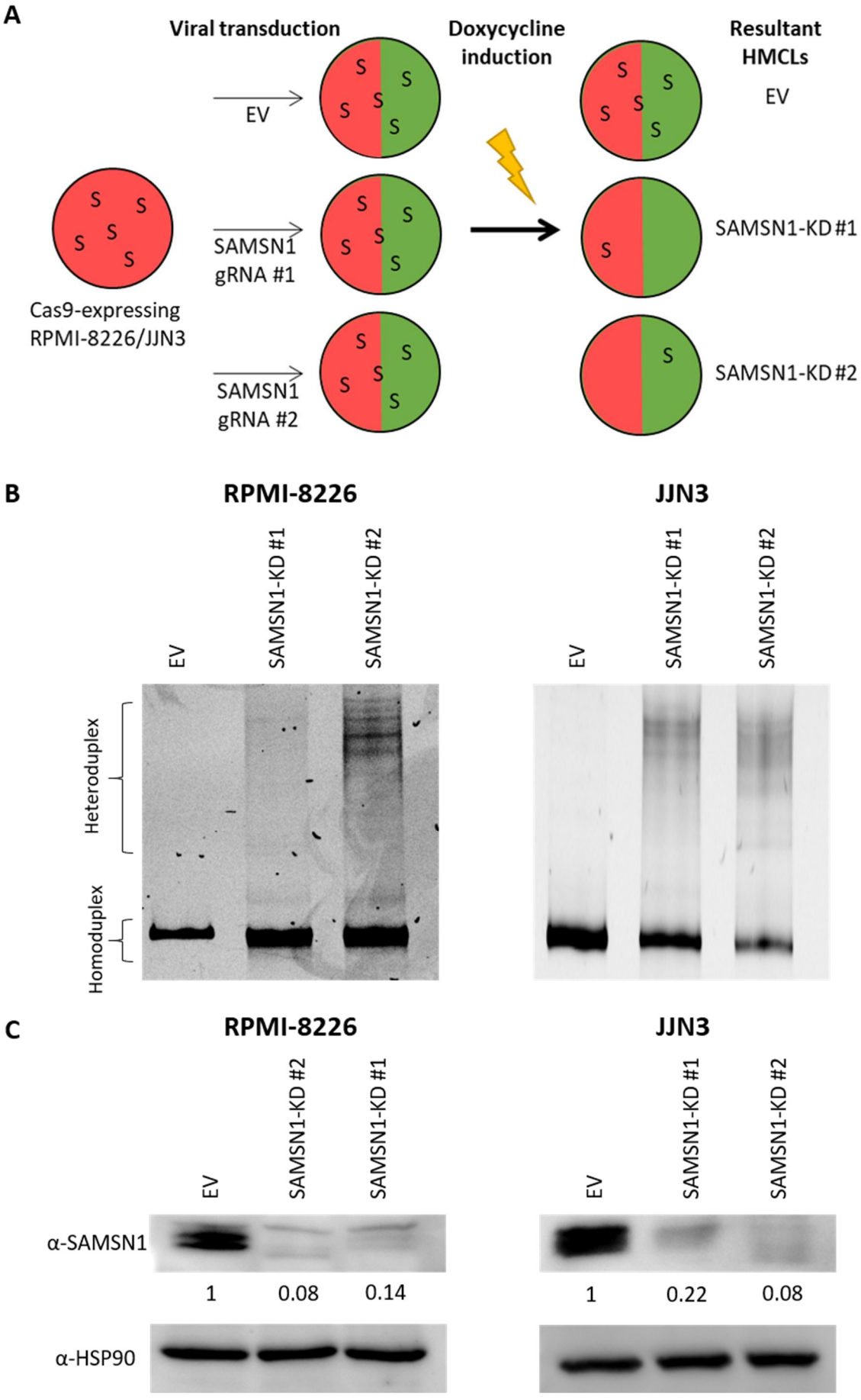
A
Viral transduction
Doxycycline induction
Resultant HMCLs
EV
EV
SAMSN1 gRNA #1
SAMSN1-KD #1
Cas9-expressing RPMI-8226/JJN3
SAMSN1 gRNA #2
SAMSN1-KD #2
B
RPMI-8226
JJN3
EV
SAMSN1-KD #1
SAMSN1-KD #2
Heteroduplex
Homoduplex
C
RPMI-8226
JJN3
EV
SAMSN1-KD #2
SAMSN1-KD #1
α-SAMSN1
1
0.08
0.14
1
0.22
0.08
α-HSP90

5.2.2 Reduced SAMSN1 does not affect the proliferation or migration of HMCLs *in vitro*

To determine whether reduced levels of SAMSN1 affect the growth of HMCLs, the proliferation of RPMI-8226 and JJN3 cells with SAMSN1 KD compared to EV control cells was assessed using a WST-1 assay. Over 3 days, the basal proliferation of both the SAMSN1-KD RPMI-8226 and JJN3 cell lines was not significantly different to that of the EV control cell lines ($P > 0.05$, two-way ANOVA with Sidak's multiple comparisons test; Figure 5.2A). The effect of SAMSN1 KD on the migration of HMCLs was also assessed by a transendothelial assay using 20% FCS or 100 ng/mL CXCL12 as the chemoattractant. The migration of the SAMSN1-KD #1 and SAMSN1-KD #2 RPMI-8226 and JJN3 cell lines did not significantly differ from the EV cell lines in response to either stimulus tested ($P > 0.05$, one-way ANOVA with Tukey's multiple comparisons test; Figure 5.2B). Together, these data suggest that SAMSN1 KD does not affect the proliferation or migration of HMCLs *in vitro*.

5.2.3 Reduced SAMSN1 does not affect the growth or metastasis of HMCLs *in vivo*

To assess the effect of reduced SAMSN1 on the growth of HMCLs *in vivo*, SAMSN1 KD (SAMSN1-KD #2) or EV control RPMI-8226 and JJN3 cells were injected directly into the left tibia of immunodeficient NSG mice. As these HMCLs do not express luciferase, primary and metastatic tumour burden were not able to be assessed non-invasively by BLI. Instead, they were measured by flow cytometric detection of GFP^+ tumour cells in the BM of the injected tibia and the contralateral femur and tibia, respectively, at the experimental endpoint. The endpoint was determined by the first signs of morbidity in the mice, which for the RPMI-8226 and JJN3 xenograft models was 5 and 3 weeks, respectively. There was no difference between the primary tumour burden within the injected tibiae of mice inoculated with SAMSN1-KD cells compared to the EV control cells for either the RPMI-8226 or JJN3 HMCLs ($P > 0.05$, Mann Whitney U test; Figure 5.3A), although the number of animals per group was small and the variation was high in some groups. In addition, reduced SAMSN1 expression did not affect the number of metastatic RPMI-8226 or JJN3 tumour cells in the BM of the non-injected leg of the mice ($P > 0.05$, Mann Whitney U test; Figure 5.3B).These findings suggest that SAMSN1 KD in HMCLs does not affect their ability to form primary i.t. tumours or metastatic BM tumours *in vivo*.

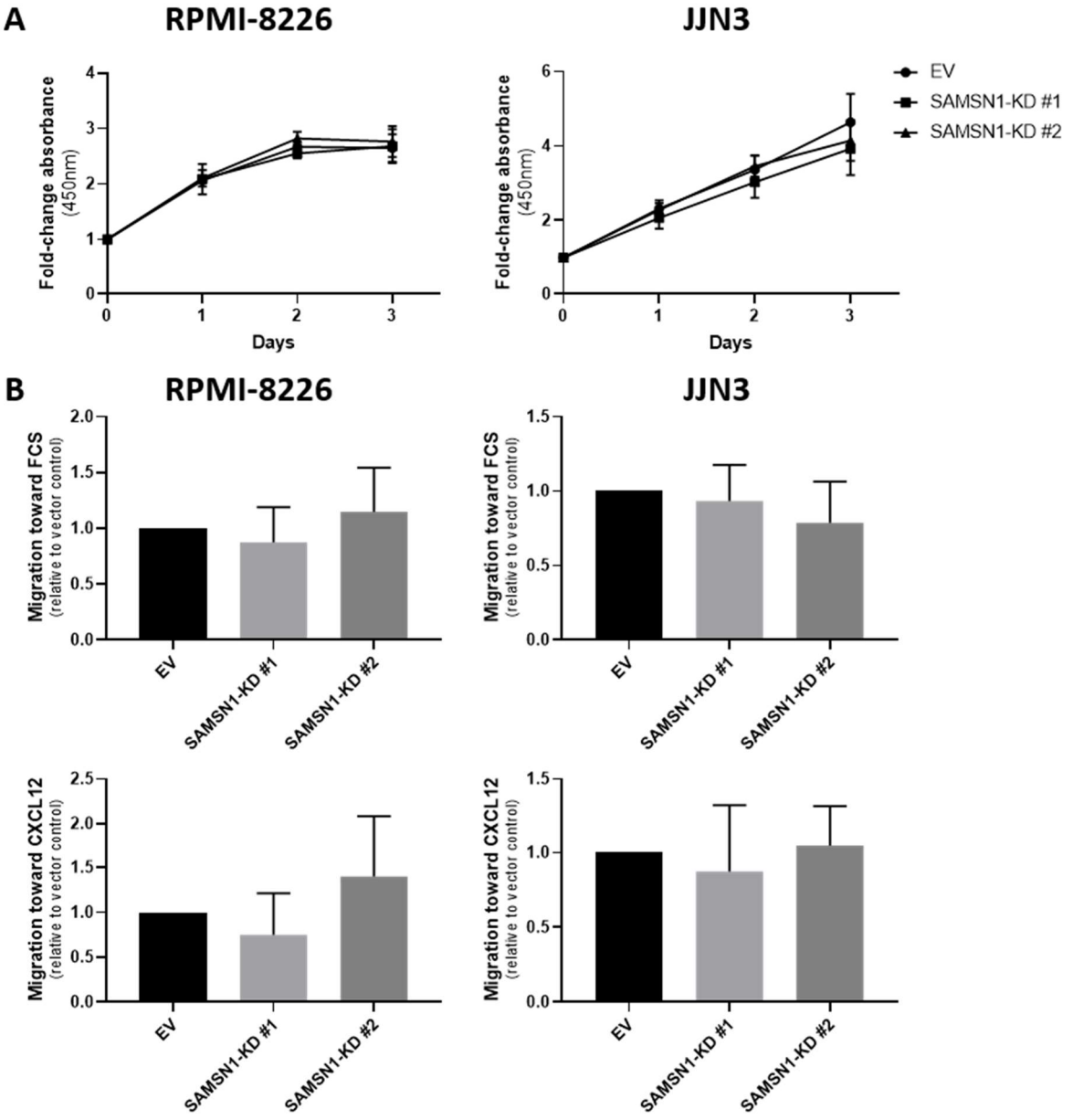

Figure 5.2: Knockdown of SAMSN1 does not affect the proliferation or migration of HMCLs *in vitro*. (**A**) The proliferation of SAMSN1-knockdown (KD) and EV control RPMI-8226 (left) and JJN3 (right) cells was measured over 3 days by a WST-1 assay. Results were expressed as fold-change in absorbance (450nm), normalised to day 0. (**B**) Migration of SAMSN1-KD #1, SAMSN1-KD #2 and control RPMI-8226 (left) and JJN3 (right) cells towards either 20% FCS (above) or 100 ng/mL CXCL12 (below) was assessed by a 20-hour transendothelial assay. Results are expressed relative to the EV control cells. Graphs depict the mean + SD of three or more independent experiments. $P > 0.05$, two-way ANOVA with Sidak's multiple comparisons test (**A**) or one-way ANOVA with Tukey's multiple comparisons test (**B**).

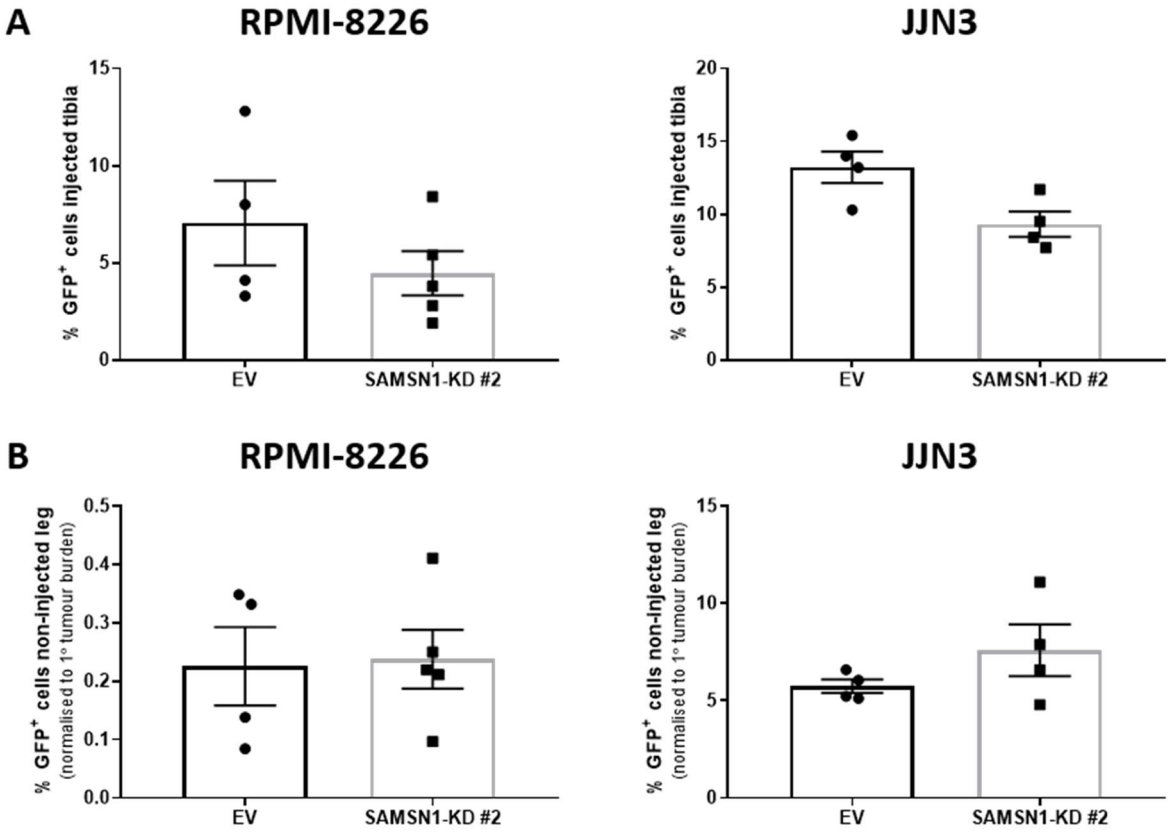

Figure 5.3: SAMSN1 knockdown does not affect the primary or metastatic tumour growth of HMCLs *in vivo*. (**A&B**) SAMSN1-KD #2 or EV control RPM1-8226 and JJN3 HMCLs were injected (5 x 10^5 cells/inoculum) into the left tibia of NSG mice. Tumours were allowed to develop in mice inoculated with RPM1-8226 or JJN3 HMCLs over 5 or 3 weeks, respectively. (**A**) The percentage of GFP^+ SAMSN1-KD and EV RPM1-8226 (left) or JJN3 (right) cells in the BM of the injected tibia was determined by flow cytometry at the experimental endpoint. (**B**) The percentage of GFP^+ SAMSN1-KD and EV RPM1-8226 (left) or JJN3 (right) cells in the BM of the non-injected, contralateral femur and tibia was determined by flow cytometry at the experimental endpoint. Results were normalised to primary tumour burden. Graphs depict the mean ± SEM of n = 4-5 mice per cell line from one experiment. $P > 0.05$, Mann-Whitney U test.

5.2.4 Overexpression of SAMSN1 does not affect the proliferation of HMCLs *in vitro*

In order to closely replicate our previous experiments using a Samsn1-overexpressing murine 5TGM1 MM PC line (Chapter 4), the aim was to generate SAMSN1-overexpressing HMCLs. The LP-1 and OPM2 HMCLs were selected for SAMSN1 overexpression studies, as examination of the aforementioned HMCL RNA-seq dataset revealed that they have relatively low *SAMSN1* mRNA expression compared to other HMCLs. Using retroviral transduction, the LP-1 and OPM2 HMCLs were transduced with a *SAMSN1* expression vector or an empty vector control. Overexpression of *SAMSN1* was confirmed in the LP-1/OPM2-SAMSN1 cells compared to the EV control cells by both RT-qPCR ($P < 0.0001$, two-way ANOVA with Tukey's multiple comparisons test; Figure 5.4A) and Western blot (Figure 5.4B). The effect of SAMSN1 overexpression on the growth of LP-1 and OPM2 HMCLs *in vitro* was determined using a WST-1 assay. Over 3 days, the overexpression of SAMSN1 was not found to affect the proliferation of LP-1 or OPM2 cells ($P > 0.05$, two-way ANOVA with Tukey's multiple comparisons test; Figure 5.4C).

5.2.5 Overexpression of SAMSN1 does not affect the growth of HMCLs *in vivo*

To determine whether SAMSN1 overexpression in HMCLs affects primary and/or metastatic tumour growth *in vivo*, SAMSN1-overexpressing or EV control LP-1 and OPM2 cells were directly injected into the left tibia of NSG mice. The humane endpoint for the LP-1 and OPM2 cell i.t. xenografts was 8 and 3 weeks, respectively. For LP-1 cells, SAMSN1 overexpression did not significantly affect tumour burden either in the injected tibia ($P = 0.0667$, Mann Whitney U test; Figure 5.5A), or the non-injected leg ($P = 0.5273$, Mann Whitney U test; Figure 5.5B). However, the LP-1 cell line was only weakly metastatic, which is consistent with the previous report that LP-1 cells do not migrate *in vitro*[333]. In contrast, OPM2 cells were found to be highly metastatic, but neither the primary ($P = 0.2319$, Mann Whitney U test; Figure 5.5A) nor metastatic ($P = 0.3969$, Mann Whitney U test; Figure 5.5B) tumour burden was found to differ between the mice injected with the OPM2-SAMSN1 cells and those injected with the OPM2-EV control cells. Together, these data suggest that SAMSN1 overexpression in HMCLs does not affect the growth of primary i.t. tumours or metastatic tumours within the BM *in vivo*.

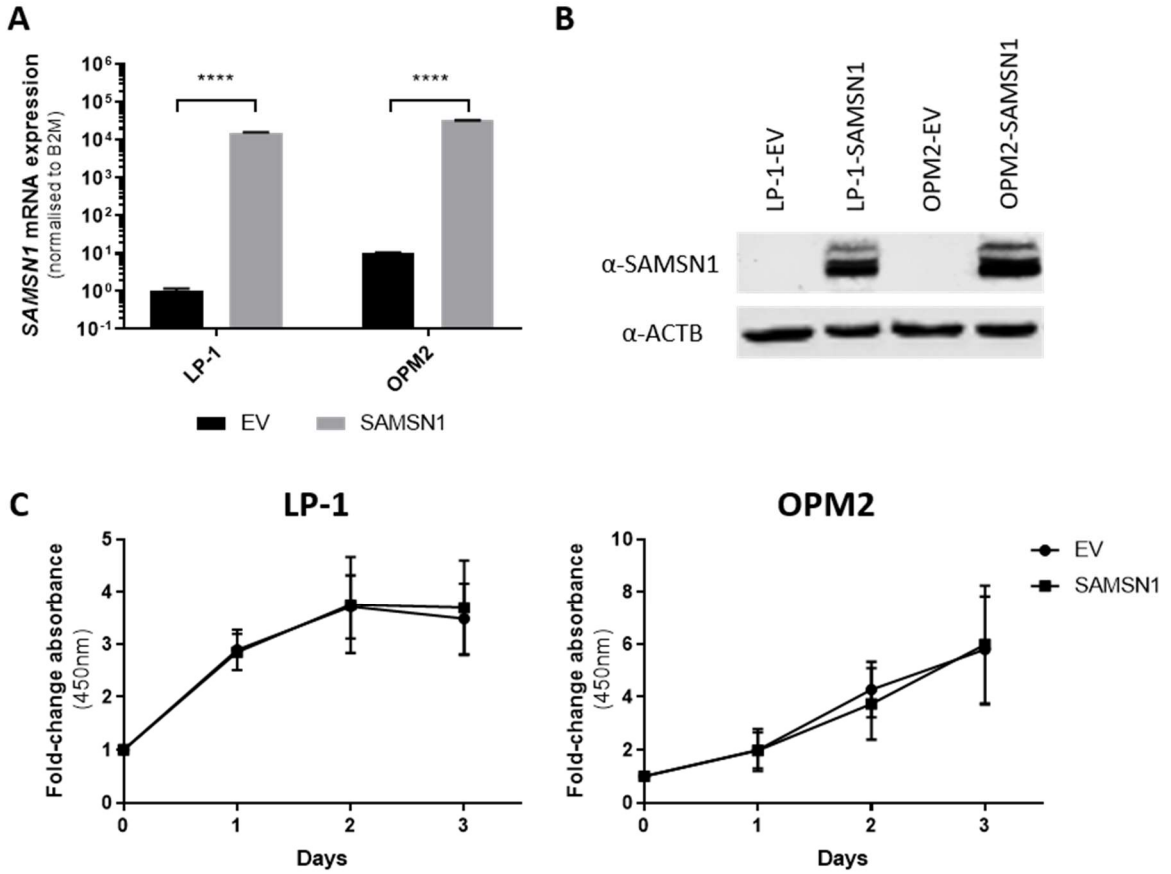

Figure 5.4: SAMSN1 overexpression does not affect the proliferation of HMCLs *in vitro*. (**A**) The expression of *SAMSN1* mRNA was assessed in LP-1 and OPM2 HMCLs transduced with a SAMSN1 expression vector or a control empty vector (EV) by RT-qPCR. Expression values were normalised to *B2M* mRNA levels and expressed relative to the LP-1-EV cells. (**B**) The levels of SAMSN1 protein were assessed in LP-1 and OPM2 HMCLs transduced with a SAMSN1 expression vector or a control EV by Western blot. ACTB was used as the loading control. (**C**) The proliferation of SAMSN1-overexpressing versus EV LP-1 (left) and OPM2 (right) cells was measured over 3 days by a WST-1 assay. Results were expressed as fold-change in absorbance (450nm) normalised to day 0. Graphs depict the mean ± SD of triplicates (**A**) or biological replicates from three independent experiments (**C**). ****$P < 0.0001$, two-way ANOVA with Tukey's multiple comparisons test (**A**&**C**).

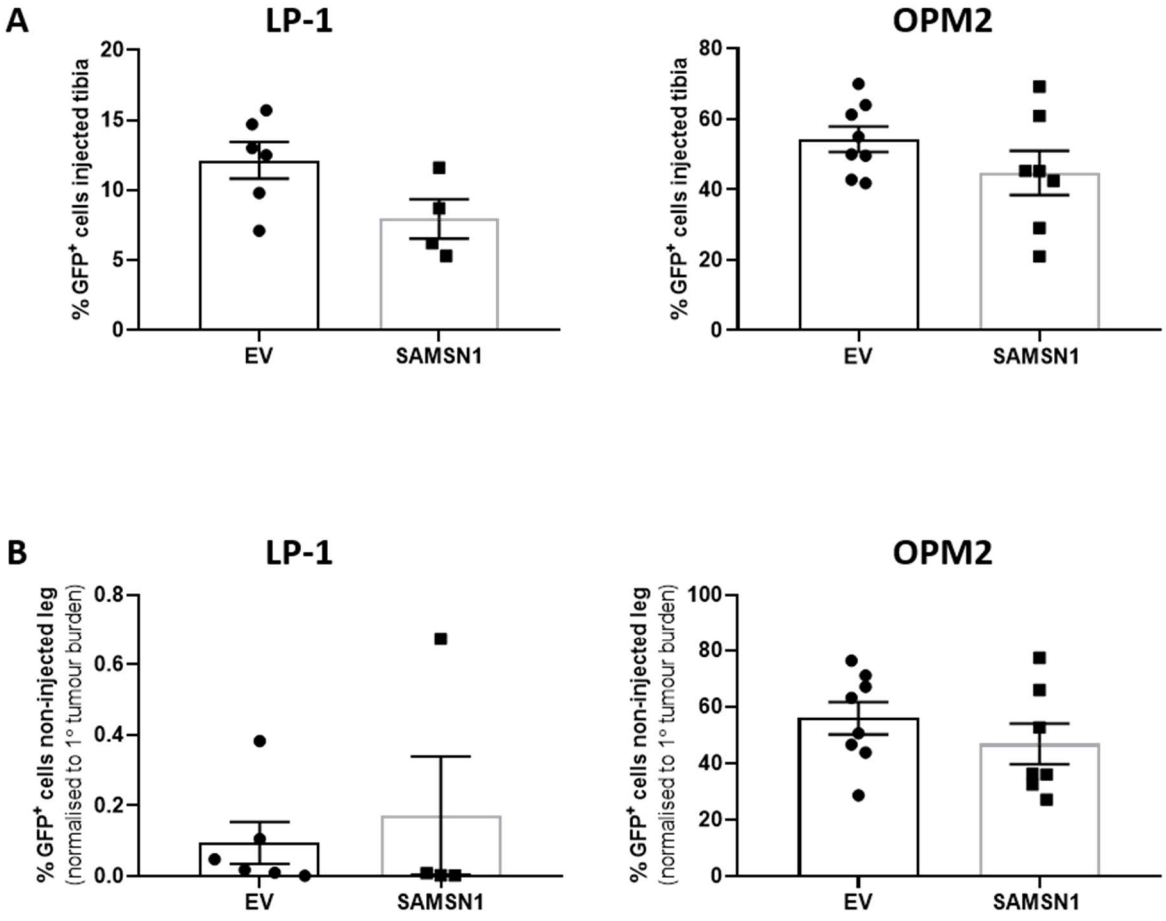

Figure 5.5: SAMSN1 overexpression in HMCLs does not affect primary or metastatic tumour burden *in vivo*. (**A**&**B**) SAMSN1-overexpressing (SAMSN1) or empty vector (EV) control LP-1 and OPM2 cells were injected (5 x 10^5 cells/inoculum) into the left tibia of NSG mice and disease was allowed to develop over 8 or 3 weeks, respectively. (**A**) The percentage of GFP^+ SAMSN1 and EV LP-1 (left) or OPM2 (right) cells in the BM of the injected tibia was determined by flow cytometry at the experimental endpoint. (**B**) The percentage of GFP^+ SAMSN1 and EV LP-1 (left) or OPM2 (right) cells in the BM of the non-injected, contralateral femur and tibia was determined by flow cytometry at the experimental endpoint. Results were normalised to primary tumour burden. Graphs depict the mean ± SEM of n = 4-8 mice per cell line from two independent experiments. $P > 0.05$, Mann-Whitney U test.

5.2.6 Samsn1 expression does not affect 5TGM1 tumour growth in NSG mice

SAMSN1 overexpression in HMCLs did not significantly inhibit metastasis following i.t. injection of tumour cells *in vivo*, which contrasts with the significant suppression of metastasis caused by Samsn1 re-expression in the 5TGM1/KaLwRij i.t. model of MM (Chapter 4). It was hypothesised that these conflicting findings may be attributable to the use of immunodeficient NSG mice in the HMCL xenograft models. To test this, NSG mice were inoculated with Samsn1-expressing or EV control 5TGM1 cells by i.t. injection and primary and metastatic tumour burden were measured by BLI and flow cytometry after 23 days. Similar to the results in KaLwRij mice, Samsn1 did not affect the growth of primary tumours in the injected tibia of NSG mice, as determined by BLI ($P = 0.1649$, Mann Whitney U test; Figure 5.6A&B) and flow cytometry ($P = 0.2319$, Mann Whitney U test; Figure 5.6C). However, the metastatic tumour burden in the non-injected, contralateral hind leg was not reduced in NSG mice inoculated with 5TGM1-Samsn1 cells compared to those inoculated with 5TGM1-EV cells, as determined by flow cytometry ($P = 0.4634$, Mann Whitney U test; Figure 5.6D). In addition, Samsn1 did not inhibit the growth of 5TGM1 cells following i.v. injection into NSG mice, as measured by BLI ($P = 0.9108$, Mann Whitney U test; Figure 5.7A) and SPEP ($P = 0.3095$, Mann Whitney U test; Figure 5.7B). Hence, the previously observed ability of Samsn1 to inhibit the outgrowth of disseminated 5TGM1 cells in immunocompetent KaLwRij mice (Chapter 4) was lost in immunodeficient NSG mice, suggesting that the tumour suppressor effect of Samsn1 in MM PCs is dependent on the presence of a functional immune system.

5.2.7 Samsn1 expression in 5TGM1 cells may enhance cytotoxic T lymphocyte activity

It was hypothesised that Samsn1 suppresses the outgrowth of disseminated MM PC in the BM by promoting immune-mediated control of tumour growth. Both natural killer (NK) cells and T cells have been shown to have important roles in the immune control of cancer, including MM[365]. Hence, to investigate the effect of PC-intrinsic Samsn1 expression on the anti-tumour immune response *in vivo*, the NK, T and NKT cell populations in the peripheral blood (PB), BM and spleen of KaLwRij mice were analysed by flow cytometry following i.v. injection of 5TGM1-Samsn1 cells, 5TGM1-EV cells or PBS. Five days post-injection, no significant differences in the total percentage, or the percentage activated ($CD69^+$), of NK cells ($CD3^-DX5^+$), T cells ($CD3^+DX5^-$) or NKT cells ($CD3^+DX5^+$) were found in the

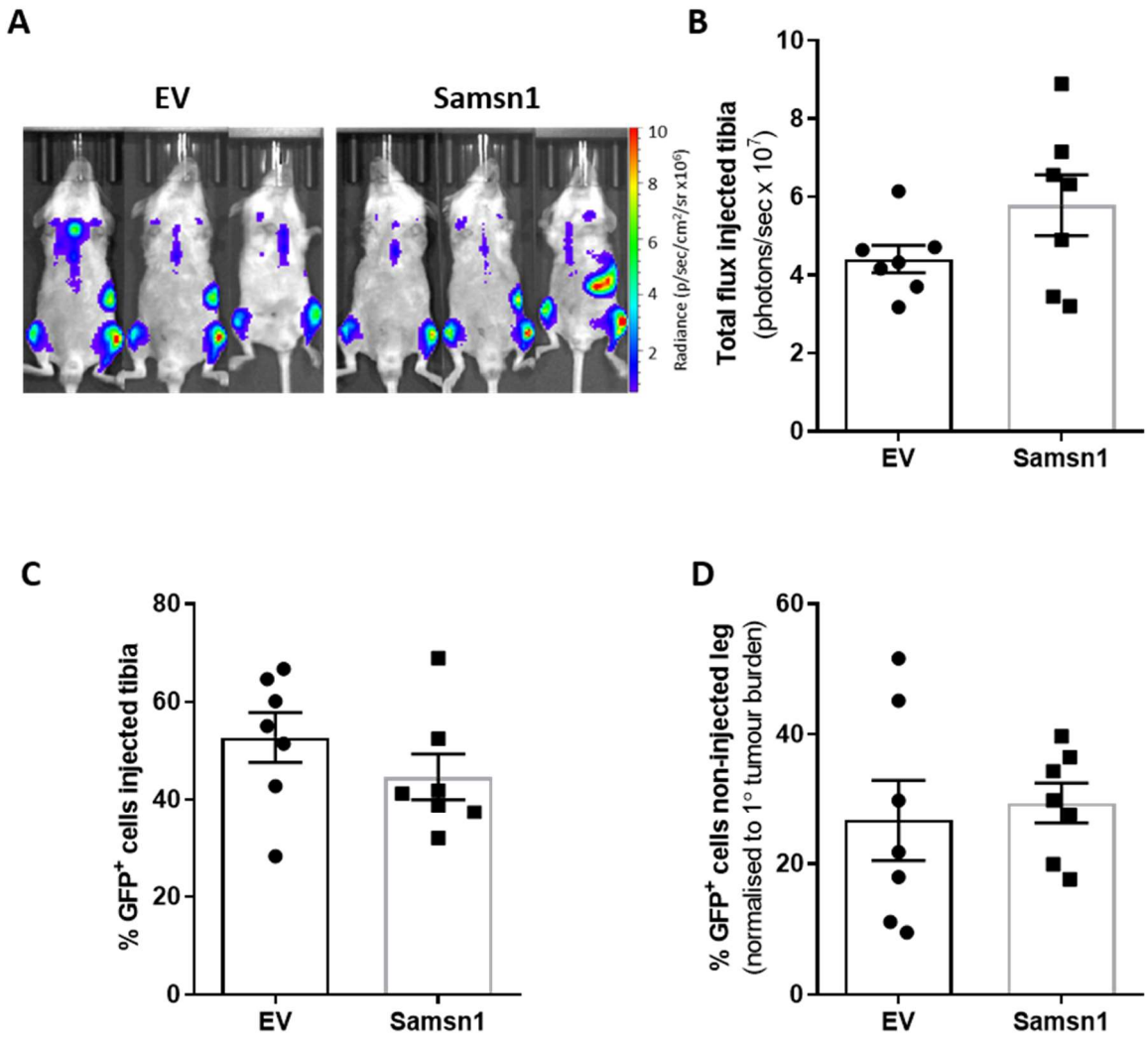

Figure 5.6: Samsn1 expression in 5TGM1 cells does not affect tumour growth following i.t. injection into NSG mice. (**A-D**) Samsn1-expressing or EV control 5TGM1 cells (1 x 10^5) were injected into the left tibia of NSG mice and disease was allowed to develop for 23 days. (**A**) Tumour burden was measured by BLI on day 23 post-tumour cell inoculation and representative ventral scans of the mice are shown. (**B**) The total flux from the injected leg was quantitated from the ventral BLI scans. (**C**) The percentage of GFP^+ Samsn1-overexpressing/EV 5TGM1 cells in the BM of the injected tibia was determined by flow cytometry at the experimental endpoint. (**D**) The percentage of GFP^+ Samsn1-overexpressing/EV 5TGM1 cells in the BM of the non-injected hind leg was determined by flow cytometry at the experimental endpoint. Results were normalised to primary tumour burden. Graphs depict the mean ± SEM of n = 7 mice per cell line from two independent experiments. $P > 0.05$, Mann-Whitney U test.

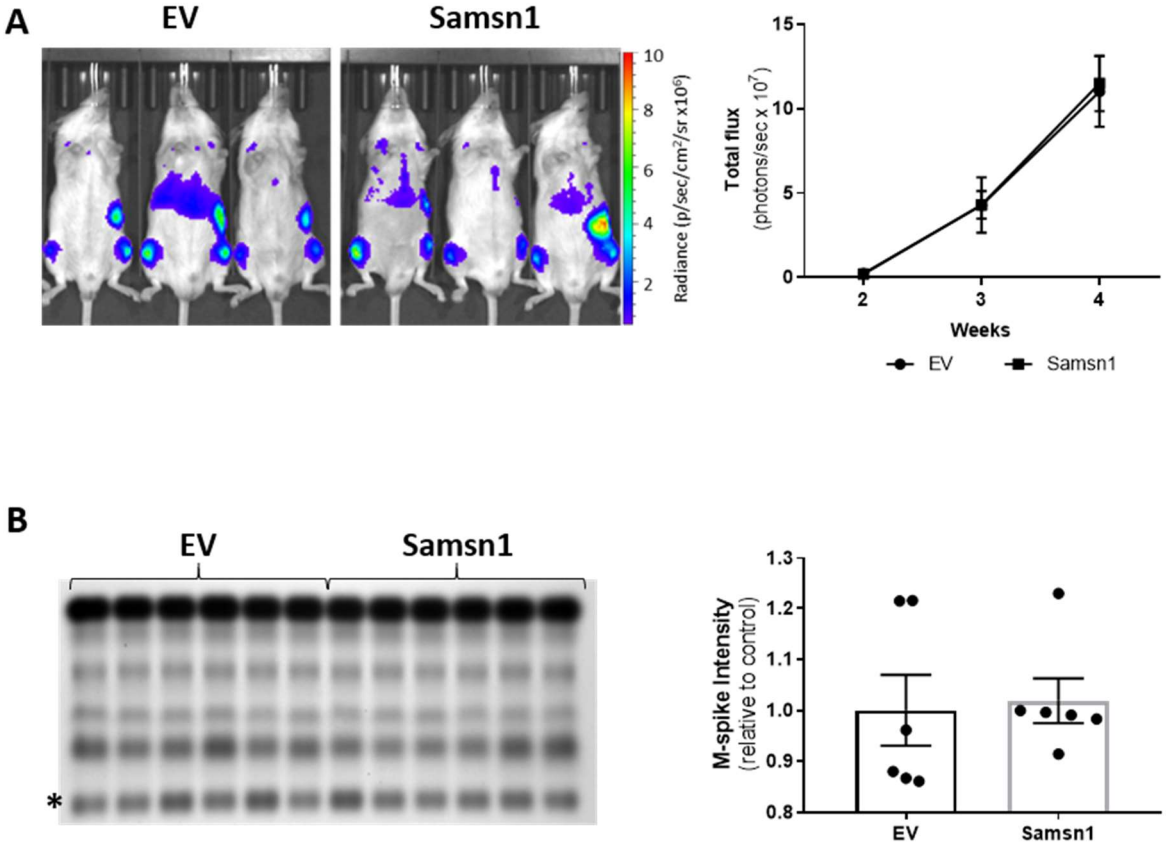

Figure 5.7: Samsn1 expression in 5TGM1 cells does not affect tumour growth following i.v. injection into NSG mice. (**A&B**) Samsn1-expressing or EV control 5TGM1 cells (5 x 10^5) were injected i.v. into NSG mice and disease was allowed to develop for 4 weeks. (**A**) BLI of the mice injected with 5TGM1-Samsn1 or 5TGM1-EV cells was performed weekly from week 2. Representative ventral scans after 4 weeks (left) and the quantitated total flux from the ventral scans over time (right) are shown. (**B**) SPEP was performed on sera collected from the mice after 4 weeks. The SPEP gel (left, * = M-spike) and the M-spike intensity expressed relative to the EV control (right) are shown. Graphs depict the mean ± SEM of n = 6 mice per cell line from one experiment. $P > 0.05$, two-way ANOVA with Sidak's multiple comparisons test (**A**) or Mann-Whitney U test (**B**).

mice inoculated with 5TGM1-Samsn1 cells compared to the mice inoculated with 5TGM1-EV cells (Table 5.1). Moreover, injection of either 5TGM1 cell line did not alter the populations of these immune cells compared to the injection of PBS alone, which suggests that the anti-tumour immune response in KaLwRij mice may not involve the expansion of effector cells.

Despite Samsn1 expression in 5TGM1 cells not influencing immune cell numbers in KaLwRij mice following inoculation, it was hypothesised that Samsn1 expression may enhance the activity of immune effector cells toward 5TGM1 tumour cells. Given that $CD8^+$ cytotoxic T lymphocytes (CTLs) are known to be important mediators of anti-tumour immunity, the effect of Samsn1 on the targeting of 5TGM1 cells by CTLs was assessed *in vitro*. Cytotoxicity assays were performed in which purified splenic $CD8^+$ T cells, which were isolated from KaLwRij mice inoculated with 5TGM1-Samsn1 or 5TGM1-EV cells, were used as effectors (Figure 5.8A&B). Due to a low yield of CTLs, these effectors were co-cultured with 5TGM1-Samsn1 or 5TGM1-EV cells at a ratio of 2:1 or 4:1 for 24 hours, followed by quantitation of tumour cell lysis by a lactate dehydrogenase release assay. A trend towards an increase in CTL-mediated cytotoxicity toward the Samsn1-expressing 5TGM1 cells compared to the EV 5TGM1 cells was observed, which occurred in an effector to target ratio-dependent manner (Figure 5.8C). These data suggest that Samsn1 expression in 5TGM1 cells may promote CTL activity toward MM PCs in KaLwRij mice.

5.2.8 Samsn1 does not affect the expression of MHC class I molecules on the surface of 5TGM1 cells

One of the previously documented mechanisms by which tumour cells mediate escape from immune control is by down-regulating surface expression of major histocompatibility class I (MHC-I) molecules, which inhibits detection and destruction of tumour cells by $CD8^+$ T cells[366]. Hence, it was hypothesised that Samsn1 may promote 5TGM1 tumour cell immunogenicity by up-regulating MHC-I expression. To assess this, the levels of MHC-I molecules on the surface of 5TGM1-Samsn1 compared to 5TGM1-EV control cells were measured by flow cytometry. The levels of both sub-classes of MHC-I molecules expressed by the KaLwRij strain, $H\text{-}2D^b$ and $H\text{-}2K^b$, on 5TGM1-Samsn1 cells were found to not be significantly different compared to the levels on 5TGM1-EV control cells ($P > 0.05$, paired t test; Figure 5.9). This suggests that Samsn1 expression does not enhance immune recognition of 5TGM1 cells through increasing MHC-I-mediated antigen presentation.

Table 5.1: Flow cytometry analysis of NK, T and NKT cells in KaLwRij mice inoculated with Samsn1-expressing 5TGM1 cells. KaLwRij mice were injected with 5TGM1-Samsn1 cells, 5TGM1-EV cells or PBS only. Five days post-injection, cells from the PB, BM and spleen of the mice were stained with anti-CD3 and anti-DX5 antibodies and gated to show the percentages of NK ($CD3^-DX5^+$), T ($CD3^+DX5^-$) and NKT ($CD3^+DX5^+$) cells among total live leukocytes. The cells were also stained with an anti-CD69 antibody and the percentages of NK, T and NKT cells that were positive for this activation marker were assessed. Data are shown as the mean ± SD for n = 3 (PBS) or n = 5 (5TGM1-Samsn1/EV) mice per group from two independent experiments. P > 0.05, Kruskal-Wallis test with Dunn's multiple comparisons test.

Tissue	Cell population	Percentage of cells			*P*-value
		PBS	EV	Samsn1	
Peripheral Blood	**Total NK cells**	5.92 ± 2.86	7.918 ± 2.31	7.86 ± 1.25	0.3955
	$CD69^+$ NK cells	10.10 ± 2.02	8.27 ± 2.68	8.10 ± 2.07	0.5671
	Total T cells	12.57 ± 1.46	11.28 ± 4.87	12.14 ± 3.76	0.8929
	$CD69^+$ T cells	1.19 ± 1.23	1.01 ± 0.95	0.48 ± 0.13	0.4556
	Total NKT cells	0.98 ± 0.35	0.89 ± 0.26	0.89 ± 0.23	0.899
	$CD69^+$ NKT cells	12.02 ± 2.08	12.14 ± 1.67	10.72 ± 1.54	0.4027
Bone Marrow	**Total NK cells**	1.81 ± 0.46	1.56 ± 0.15	1.474 ± 0.22	0.2579
	$CD69^+$ NK cells	21.73 ± 3.89	18.5 ± 4.49	19.6 ± 3.81	0.5775
	Total T cells	3.44 ± 0.75	3.25 ± 0.53	3.73 ± 0.44	0.4083
	$CD69^+$ T cells	12.27 ± 4.98	11.87 ± 5.01	12.36 ± 6.04	0.9892
	Total NKT cells	1.577 ± 0.49	1.59 ± 0.79	1.52 ± 0.38	0.9814
	$CD69^+$ NKT cells	35.00 ± 16.08	35.90 ± 13.9	36.76 ± 12.91	0.985
Spleen	**Total NK cells**	1.693 ± 0.55	1.95 ± 1.09	1.92 ± 0.84	0.9184
	$CD69^+$ NK cells	5.84 ± 1.92	5.76 ± 2.50	5.26 ± 1.91	0.9118
	Total T cells	14.51 ± 7.26	16.88 ± 4.82	16.26 ± 4.40	0.8264
	$CD69^+$ T cells	2.04 ± 0.67	1.62 ± 0.34	2.30 ± 0.78	0.2555
	Total NKT cells	0.65 ± 0.17	0.70 ± 0.31	0.76 ± 0.11	0.7991
	$CD69^+$ NKT cells	13.17 ± 1.85	11.89 ± 1.77	11.02 ± 2.46	0.4047

Figure 5.8: Samsn1 expression may sensitise 5TGM1 cells to KaLwRij-derived CD8$^+$ T cell cytotoxicity *in vitro*. (**A**) Schematic illustrating the experimental design of the cytotoxicity assay. KaLwRij mice were twice i.v. injected with 1 x 10^6 irradiated 5TGM1-Samsn1 or 5TGM1-EV cells. Five days after the last inoculation, splenic cells were isolated from the mice and CD8$^+$ T cells were purified by MACS-mediated negative selection. Following 5 days of re-stimulation with cognate 5TGM1 cells *in vitro*, the CTLs were co-cultured with irradiated 5TGM1-Samsn1 or 5TGM1-EV cells at effector to target ratios of 2:1 and 4:1. After 24 hours, lactate dehydrogenase release was measured and used to calculate the percentage of cell-mediated cytotoxicity. (**B**) Representative flow cytometry plots showing the successful purification of splenic CD8$^+$ T cells by MACS. (**C**) Graph depicting the percentage cytotoxicity of KaLwRij-derived CTLs toward 5TGM1-Samsn1 and 5TGM1-EV cells at the indicated effector to target ratios (n = 3 mice per cell line, which were pooled in one experiment).

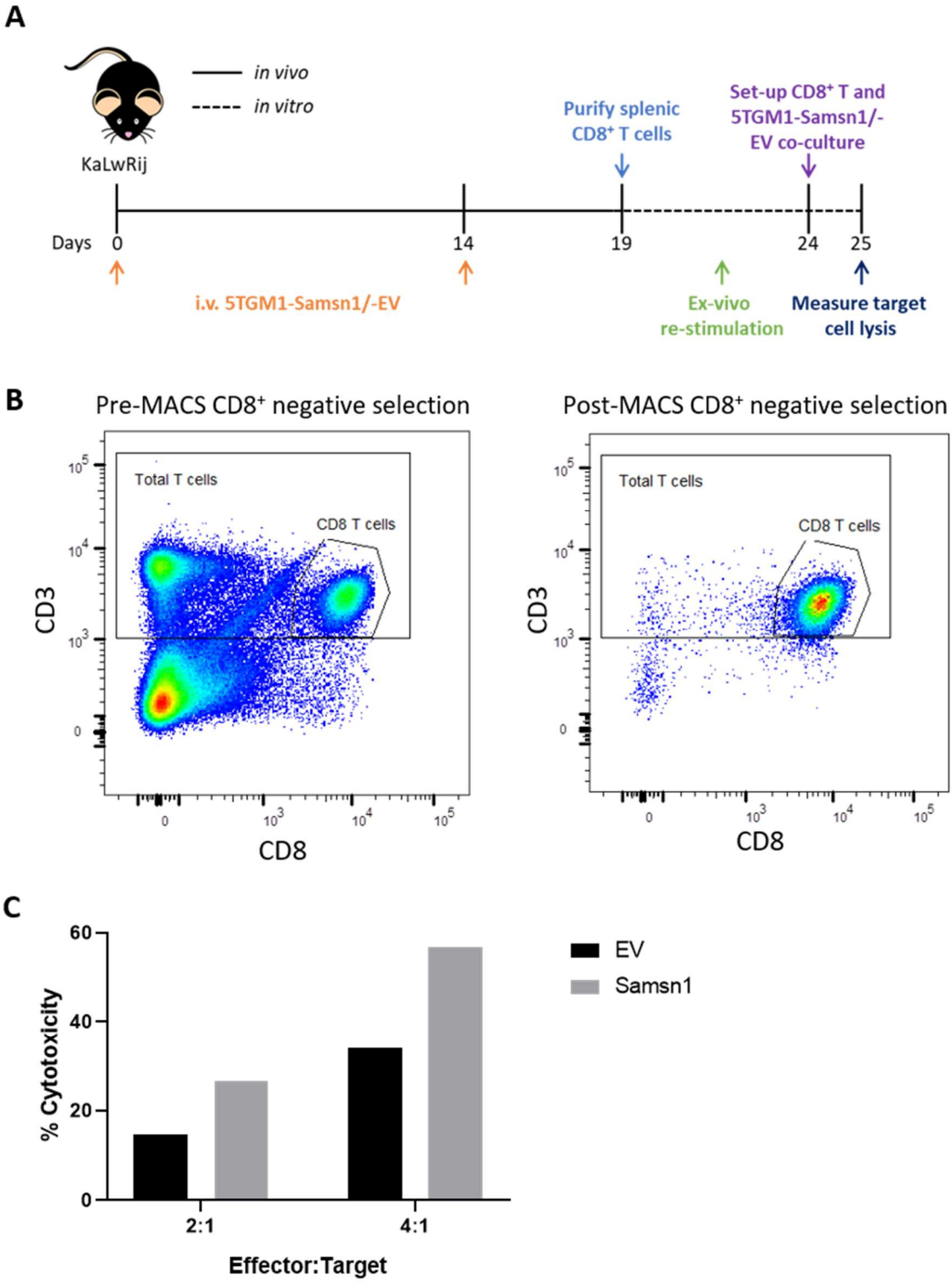
A
in vivo
in vitro
KaLwRij
Purify splenic CD8+ T cells
Set-up CD8+ T and 5TGM1-Samsn1/-EV co-culture
Days 0
14
19
24
25
i.v. 5TGM1-Samsn1/-EV
Ex-vivo re-stimulation
Measure target cell lysis
B
Pre-MACS CD8+ negative selection
Post-MACS CD8+ negative selection
Total T cells
CD8 T cells
CD3
CD8
C
% Cytotoxicity
Effector:Target
2:1
4:1
EV
Samsn1

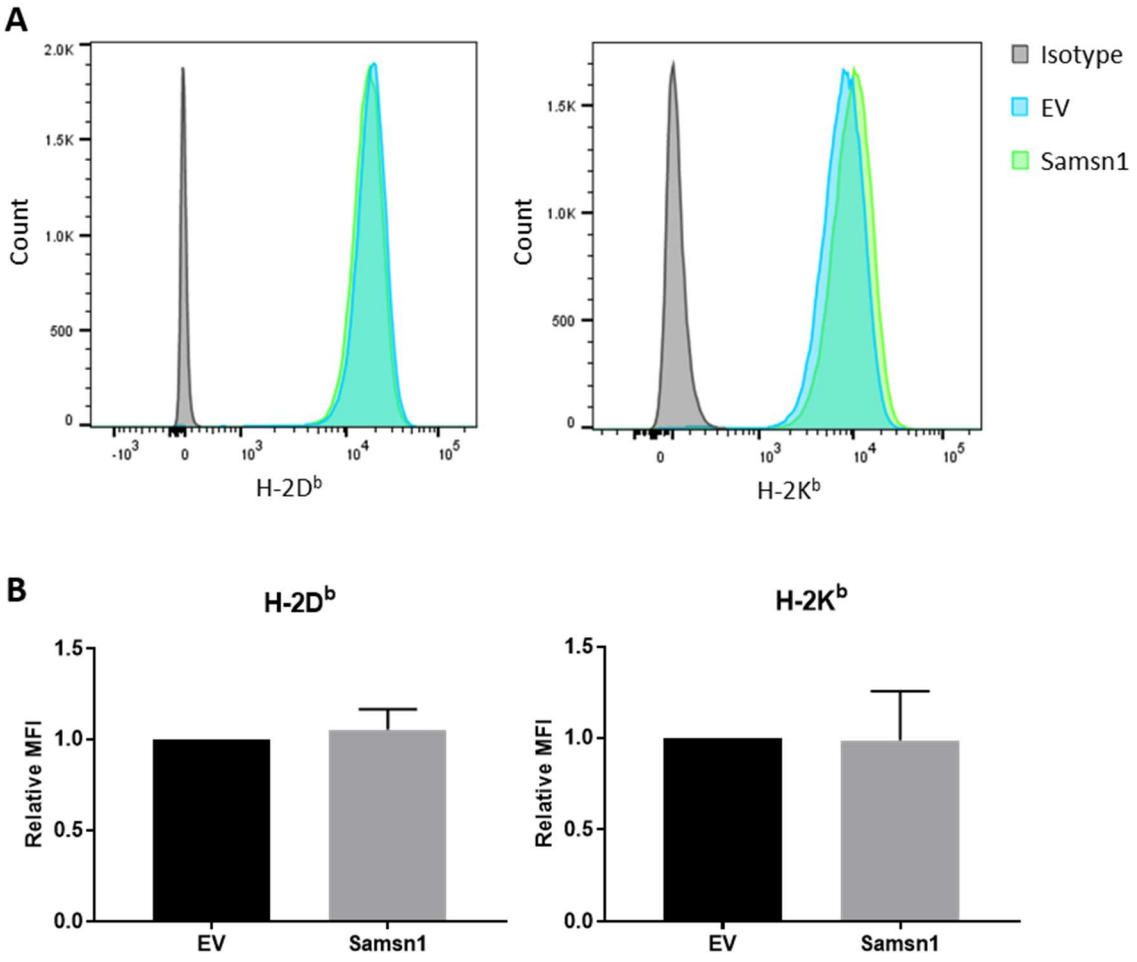

Figure 5.9: Samsn1 expression does not affect MHC-I expression on 5TGM1 cells. (**A**&**B**) 5TGM1-Samsn1 and 5TGM1-EV cells in culture were stained with anti-H-2D^b, anti-H-2K^b or an isotype control antibody and the mean fluorescence intensity (MFI) was determined by flow cytometry. Representative histograms (**A**) and graphs of the MFI (**B**), expressed relative to the EV control cell line, for H-2D^b (left) and H-2K^b (right) on 5TGM1-Samsn1 versus 5TGM1-EV cells are shown. Graphs depict the mean ± SD from three independent experiments. $P > 0.05$, paired t test.

5.2.9 Samsn1 expression in 5TGM1 cells does not affect tumour growth in C57BL/6 mice

Given the tumour suppressor effect of Samsn1 expression in 5TGM1 cells on tumour growth in immunocompetent KaLwRij mice[260], it was hypothesised that Samsn1 would inhibit the growth of 5TGM1 cells in immunocompetent C57BL/6 wildtype (WT) mice. To test this, Samsn1-expressing or EV control 5TGM1 cells were injected i.v. into WT mice, which were then monitored for tumour development over 7 weeks. Contrary to the hypothesis, Samsn1 expression in the 5TGM1 tumour cells was found to not affect tumour penetrance in WT mice, as determined by BLI or SPEP ($P > 0.9999$, Fisher's exact test; Figure 5.10A). In addition, of those WT mice that developed tumour, tumour burden was shown to not differ between the mice injected with 5TGM1-Samsn1 cells and those injected with 5TGM1-EV control cells, as measured by BLI ($P = 0.9722$, two-way ANOVA with Sidak's multiple comparisons test; Figure 5.10B) and SPEP ($P > 0.8357$, Mann Whitney U test; Figure 5.10C). These data suggest that Samsn1 does not suppress MM tumour development in the presence of a competent immune system in WT mice. Hence, there may be unique features of the competent immune system in KalwRij mice that facilitate the suppression of 5TGM1-Samsn1 tumour growth in this mouse strain.

5.2.10 Samsn1 expression in 5TGM1 cells inhibits tumour growth in C57BL/*Samsn1*$^{-/-}$ mice

Given that one of the most striking genetic differences between KaLwRij and WT mice is that KaLwRij mice have lost the *Samsn1* gene[260,261], it was hypothesised that this abnormality may contribute to the unique ability of the KaLwRij immune system to suppress 5TGM1-Samsn1 cell growth *in vivo*. To test this, Samsn1-expressing or EV 5TGM1 cells were injected i.v. into the previously described immunocompetent C57BL/*Samsn1*$^{-/-}$ mice, which were generated by backcrossing the KaLwRij-derived *Samsn1* genomic deletion onto a C57BL/6 background (Chapter 3). At 7 weeks post-tumour cell inoculation, 5 of the 20 (25%) C57BL/*Samsn1*$^{-/-}$ mice injected with EV control 5TGM1 cells had developed tumour, whereas none of the 21 (0%) C57BL/*Samsn1*$^{-/-}$ mice that were injected with 5TGM1-Samsn1 cells had any evidence of disease development, as determined by BLI and SPEP (Figure 5.11). This constituted a significant inhibition of tumour penetrance for 5TGM1-Samsn1 cells compared to 5TGM1-EV control cells in the C57BL/*Samsn1*$^{-/-}$ mice ($P = 0.0207$, Fischer's exact test). These data suggest that the tumour suppressor effect of PC-intrinsic

Figure 5.10: Samsn1 expression in 5TGM1 cells does not affect tumour growth in immunocompetent WT mice. (**A-C**) Samsn1-expressing or EV control 5TGM1 cells (5 x 10^5) were injected i.v. into WT mice and tumour was allowed to develop for 7 weeks (n = 22 mice per cell line). Tumour burden was measured by BLI at weeks 3, 5 and 7 post-tumour cell inoculation and by SPEP at week 7. (**A**) The numbers of WT mice inoculated with 5TGM1-Samsn1 or 5TGM1-EV cells that were tumour-bearing by week 7, as determined by BLI and SPEP. (**B**) For tumour-bearing mice, representative BLI ventral scans at 7 weeks (left) and the quantitated total flux from the ventral scans over time (right) are shown. (**C**) Representative SPEP gel of serum samples from tumour-bearing and non-tumour-bearing WT mice (left, * = M-spike) inoculated with 5TGM1-EV or 5TGM1-Samsn1 cells are shown. For tumour-bearing mice, the quantitated M-spike intensities (right) are shown. Graphs depict the mean ± SEM of n = 6-7 tumour-bearing mice per cell line from two independent experiments (**B**&**C**). $P > 0.05$, Fisher's exact test (**A**), two-way ANOVA with Sidak's multiple comparisons test (**B**) or Mann-Whitney U test (**C**)

.

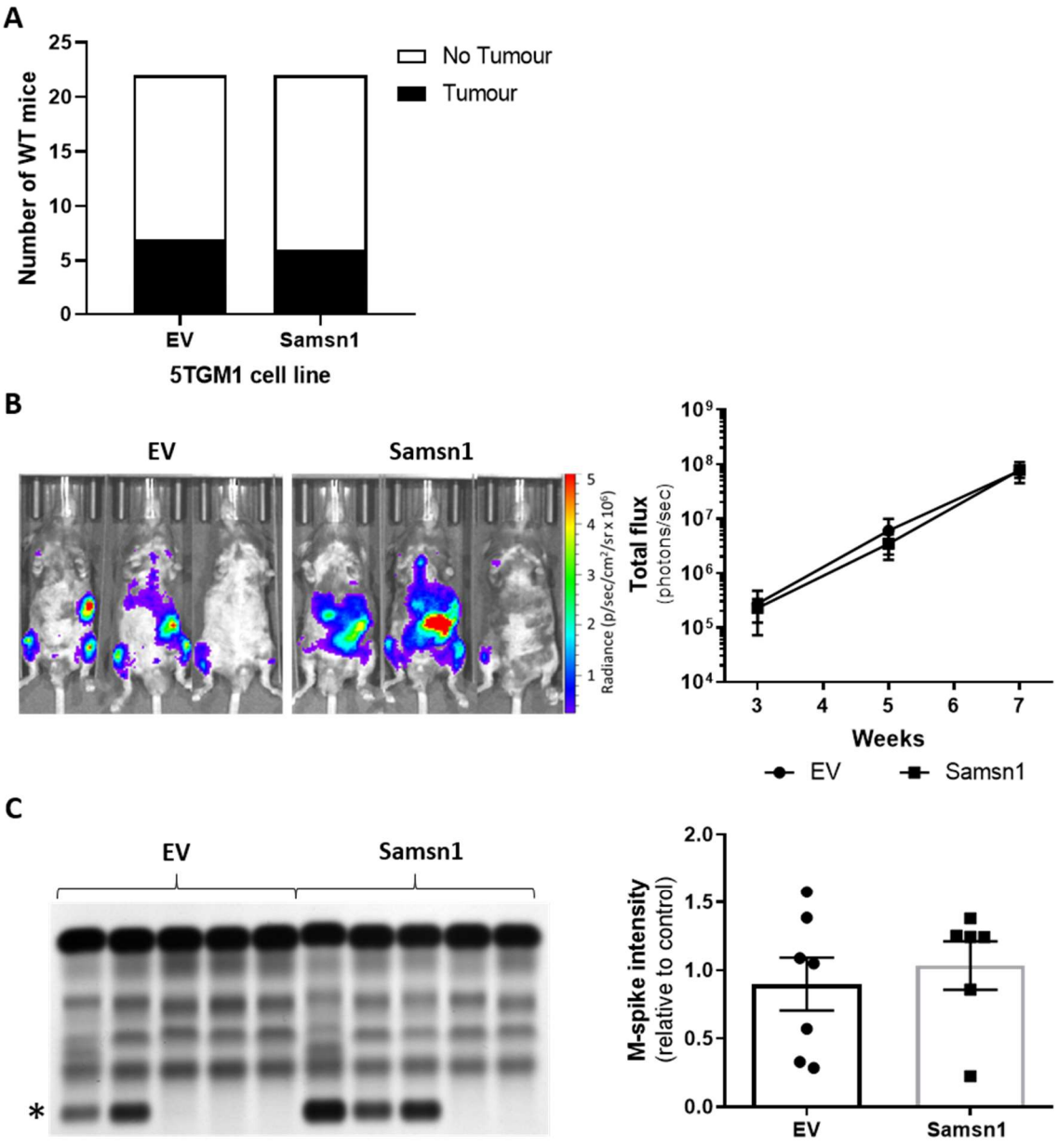
A
No Tumour
Tumour
Number of WT mice
25
20
15
10
5
0
EV
Samsn1
5TGM1 cell line
B
EV
Samsn1
Radiance (p/sec/cm²/sr x 10⁶)
5
4
3
2
1
Total flux
(photons/sec)
10⁹
10⁸
10⁷
10⁶
10⁵
10⁴
3
4
5
6
7
Weeks
EV
Samsn1
C
EV
Samsn1
*
M-spike intensity
(relative to control)
2.0
1.5
1.0
0.5
0.0
EV
Samsn1

Figure 5.11: Samsn1 expression in 5TGM1 cells inhibits MM tumour development in immunocompetent C57BL/*Samsn1*$^{-/-}$ mice. (**A**-**C**) Samsn1-expressing or EV 5TGM1 cells (5 x 10^5) were injected i.v. into C57BL/*Samsn1*$^{-/-}$ mice and tumour was allowed to develop for 7 weeks. Tumour burden was measured by BLI at weeks 3, 5 and 7 post-tumour cell inoculation and by SPEP at week 7. (**A**) Representative ventral BLI scans of mice inoculated with 5TGM1-EV (above) or 5TGM1-Samsn1 (below) cells at week 7 are shown. (**B**) A representative SPEP gel containing serum samples from the mice included in (**A**) is shown (* = M-spike). (**C**) The proportion of tumour-bearing mice inoculated with 5TGM1-Samsn1 or 5TGM1-EV cells by week 7, as determined by BLI and SPEP. Graph depicts n= 20-21 mice per cell line from two independent experiments. *$P < 0.05$, Fisher's exact test.

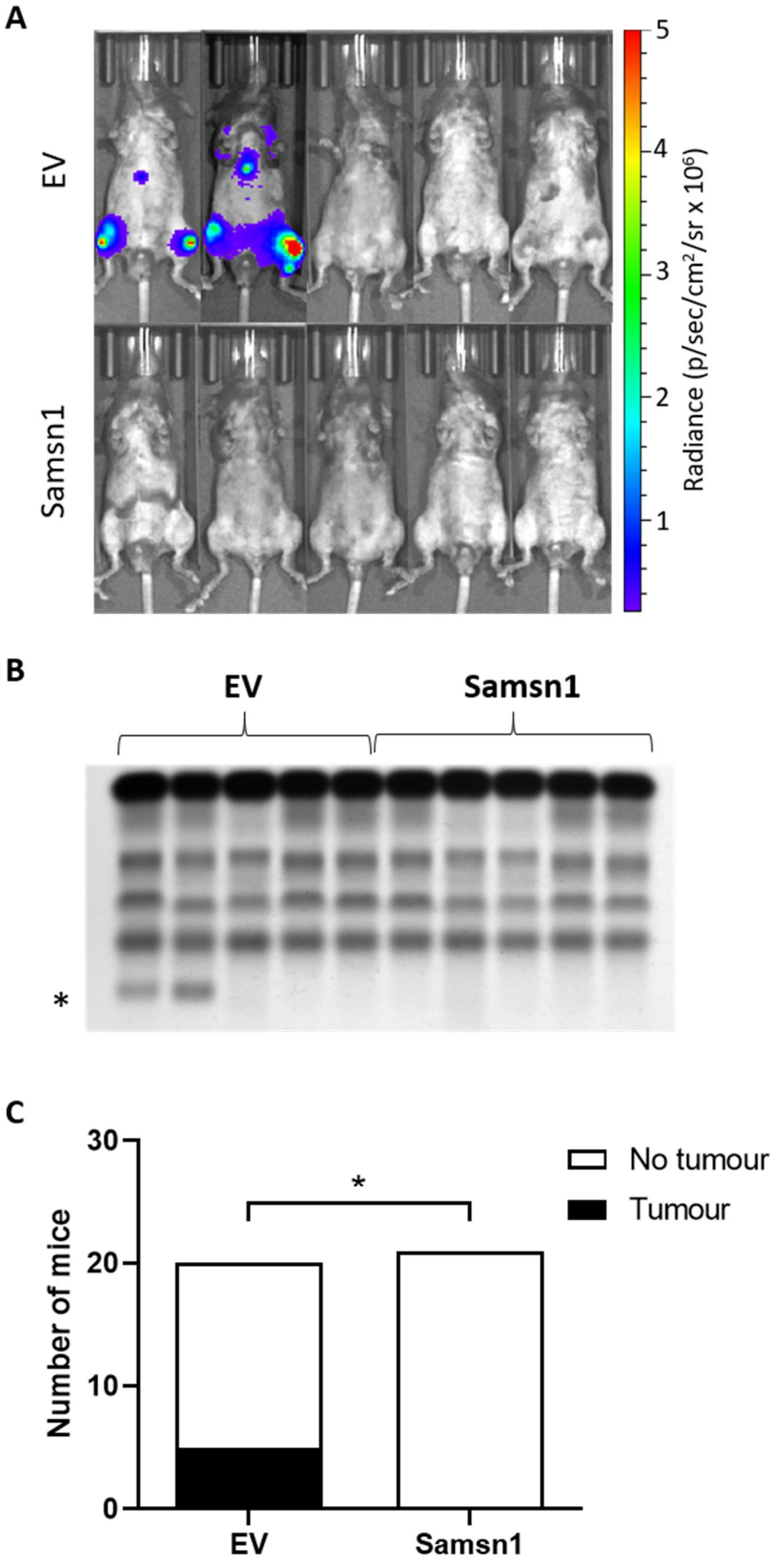
A
EV
Samsn1
5
4
3
2
1
Radiance (p/sec/cm²/sr x 10⁶)
B
EV
Samsn1
*
C
30
20
10
0
Number of mice
*
No tumour
Tumour
EV
Samsn1

Samsn1 expression *in vivo* is dependent on the recipient mouse being both immunocompetent and *Samsn1*$^{-/-}$.

5.2.11 *Samsn1*$^{-/-}$ mice may generate a humoral immune response against 5TGM1-derived Samsn1

It was hypothesised that immune-mediated control of Samsn1-expressing 5TGM1 cells occurs exclusively in immunocompetent *Samsn1*$^{-/-}$ mice because their adaptive immune cells recognise Samsn1 as a foreign antigen. To test this, the production of anti-Samsn1 antibodies following exposure to 5TGM1-Samsn1 cells was assessed *in vivo*. KaLwRij, C57BL/*Samsn1*$^{-/-}$ and WT mice were twice inoculated with either *Samsn1*-expressing or EV control 5TGM1 cells and the presence of anti-Samsn1 antibodies in their serum was then determined by Western blot. Antibodies that bound to Samsn1 were not detected in the serum from any of the negative control WT mice inoculated with 5TGM1-Samsn1 cells or 5TGM1-EV cells (Figure 5.12A). For the C57BL/*Samsn1*$^{-/-}$ mice, anti-Samsn1 antibodies were detected in the serum from one of the five mice inoculated with 5TGM1-Samsn1 cells, whereas anti-Samsn1 antibodies were not detected in the serum from the four mice injected with 5TGM1-EV control cells (Figure 5.12B). However, no anti-Samsn1 antibodies were detected in the serum from any of the three KaLwRij mice inoculated with Samsn1-expressing 5TGM1 cells or EV control 5TGM1 cells (Figure 5.12C). These findings suggest that Samsn1 expression in 5TGM1 cells may cause an antigen-specific humoral immune response specifically in *Samsn1*$^{-/-}$ mice.

5.3 Discussion

Reduced *SAMSN1* expression has been detected in the PCs of MM patients and this was associated with higher tumour burden and poorer overall survival[260]. In addition, *Samsn1* was found to be deleted in the MM-prone KaLwRij mouse strain and restoration of its expression in the syngeneic 5TGM1 MM PC line inhibited tumour growth *in vivo*[260]. This suggested that *SAMSN1* is a tumour suppressor gene in MM PC, but the biological effects of SAMSN1 in the context of human MM remained unknown. Hence, the aim of this chapter was to examine the functions of SAMSN1 in human MM PCs both *in vitro* and *in vivo*. In order to do this, HMCLs with CRISPR-Cas9-mediated knockdown of SAMSN1 levels and HMCLs with overexpression of SAMSN1 were generated. Altered SAMSN1 levels were not found to affect the proliferation or migration of HMCLs *in vitro*, which is consistent with our previous findings that Samsn1 expression does not affect the proliferation[260] or migration

Figure 5.12: *Samsn1*$^{-/-}$ mice may generate an anti-Samsn1 humoral immune response following inoculation of 5TGM1-Samsn1 cells. (**A**-**C**) C57BL/6 (WT), C57BL/*Samsn1*$^{-/-}$ and KaLwRij mice were twice inoculated, 2 weeks apart, with 5TGM1-Samsn1 (S) or 5TGM1-EV (EV) cells and serum was collected five days after the second dose of tumour cells. The serum was incubated with resolved and membrane-bound proteins that were immunoprecipitated from 5TGM1-Samsn1-HA and 5TGM1-EV cell lysates using an anti-HA antibody. The successful immunoprecipitation of Samsn1 from the 5TGM1-Samsn1 cells was confirmed by Western blotting with an anti-HA antibody (**A**-**C** left). Representative blots probed with 5TGM1-Samsn1-inoculated serum (middle) or 5TGM1-EV-inoculated serum (right) from C57BL/6 (**A**), C57BL/*Samsn1*$^{-/-}$ (**B**) and KaLwRij (**C**) mice are shown. In (**B**), the blot probed with serum from a 5TGM1-Samsn1-inoculated C57BL/*Samsn1*$^{-/-}$ mouse was the one out of five that showed evidence of anti-Samsn1 antibodies. The blots for the C57BL/6 (**A**) and KaLwRiJ (**C**) mice are representative of n = 3 per cell line for which there was no evidence of anti-Samsn1 antibodies present in the serum.

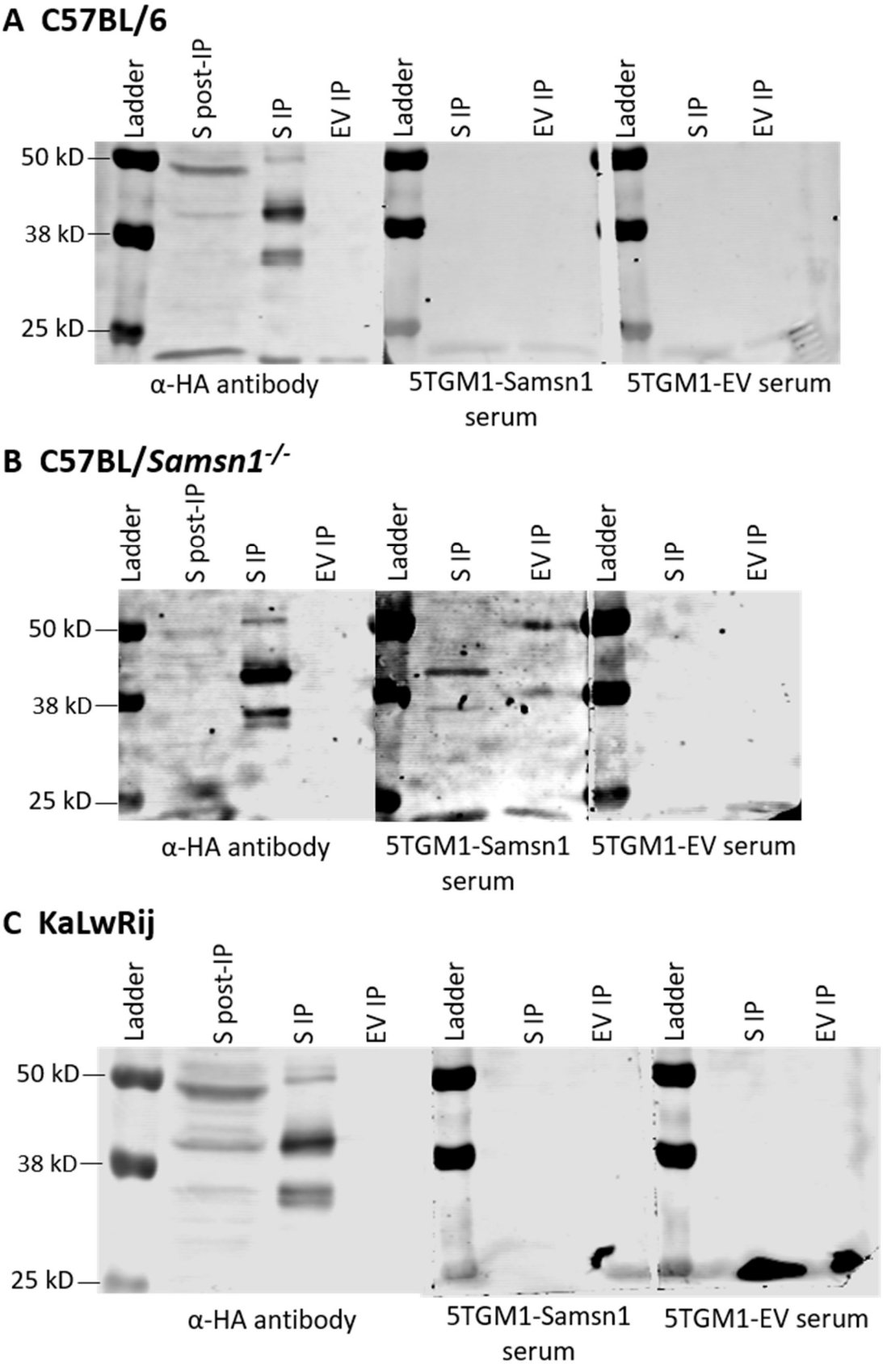
A C57BL/6
Ladder
S post-IP
S IP
EV IP
Ladder
S IP
EV IP
Ladder
S IP
EV IP
50 kD
38 kD
25 kD
α-HA antibody
5TGM1-Samsn1 serum
5TGM1-EV serum
B C57BL/Samsn1-/-
Ladder
S post-IP
S IP
EV IP
Ladder
S IP
EV IP
Ladder
S IP
EV IP
50 kD
38 kD
25 kD
α-HA antibody
5TGM1-Samsn1 serum
5TGM1-EV serum
C KaLwRij
Ladder
S post-IP
S IP
EV IP
Ladder
S IP
EV IP
Ladder
S IP
EV IP
50 kD
38 kD
25 kD
α-HA antibody
5TGM1-Samsn1 serum
5TGM1-EV serum

(Chapter 4) of murine 5TGM1 cells *in vitro*. The growth of primary tumours following i.t. injection of HMCLs into NSG mice was not affected by SAMSN1 levels, as was the case in the 5TGM1/KaLwRij model (Chapter 4). However, SAMSN1 levels were not found to affect the metastasis of HMCLs in NSG mice, which contrasts with the significant reduction in metastasis caused by Samsn1 expression in the 5TGM1/KaLwRij model. These conflicting results suggest that either SAMSN1 does not have a tumour suppressor effect in human MM PCs or, it does, but this effect was not observable in this particular *in vivo* model.

Given that the major difference between the HMCL and 5TGM1 *in vivo* models was the mouse strain used, it was hypothesised that the use of NSG mice may be inhibiting the tumour suppressor effect of SAMSN1 in HMCLs. Consistent with this, the ability of Samsn1 to suppress the outgrowth of disseminated 5TGM1 cells in immunocompetent KaLwRij mice was found to be abolished in severely immunodeficient NSG mice. These data suggest that the tumour suppressor effect of Samsn1 expression on 5TGM1 cells *in vivo* is dependent on the presence of a functional immune system, not stromal cells (Chapter 4), within the BM microenvironment. The immune system is known to play an important role in suppressing the development of tumours, which is evidenced by the fact that immunodeficient mice are more susceptible to carcinogen-induced and spontaneous tumour formation[367-371]. The standard process of cancer immunosurveillance first involves an elimination phase in which effector cells of the innate (NK cells) and adaptive (CTLs) immune systems recognise and eradicate tumour cells[366]. Surviving cancer cells then typically enter the equilibrium phase, in which the adaptive immune system restrains their growth, resulting in a dormant state that can be maintained for extended periods of time[372]. Finally, malignant cells can eventually escape immune-mediated growth suppression through evolving reduced immunogenicity, which leads to the formation of clinically apparent tumours[366]. Hence, it was hypothesised that Samsn1 suppresses the outgrowth of 5TGM1 cells in the BM by promoting their immunogenicity and thus immune-mediated dormancy.

MM disease progression is associated with increasing dysregulation and suppression of the immune system[365]. Depletion studies have shown that NK cells and CTLs have important roles in constraining the growth of MM PCs[373,374], but their effector functions are increasingly inhibited with advancing disease[375-378]. This is at least partly due to an increase in the numbers of immunosuppressive cell types, including regulatory T cells[379-382], tumour-associated macrophages[383,384] and myeloid-derived suppressor cells[385-387]. The finding that

MGUS patient-derived tumour cells grow progressively in a humanised mouse model suggests that PC-extrinsic controls within the BM, such as immunosurveillance, restrain the progression from MGUS to MM[233]. Hence, the reduction in *SAMSN1* expression in the PCs of MM patients compared to healthy controls[260,261] is consistent with the possibility that the down-regulation of *SAMSN1* promotes the escape of abnormal PCs from immune control and thus the development of symptomatic MM. The crucial role of the immune system in controlling MM disease progression is also made evident by the clinical success of immunomodulatory imide drugs (IMiDs), the effectiveness of which is at least partially attributable to increasing the cytotoxic activity of NK cells and CTLs[70,388,389]. Even the efficacy of autologous stem cell transplants has recently been shown to be partly attributable to the promotion of an anti-tumour T cell response[390]. Hence, gaining a better understanding of the potential role of SAMSN1 in regulating MM PC immunogenicity could aid in identifying new immunotherapeutic strategies that may enable long-term MM disease control.

In a previous study in which *IRF7* expression in murine breast cancer cells was found to promote immune-mediated control of metastasis to BM, an increase in the numbers of NK cells and T cells was found in the PB of mice inoculated with IRF7-expressing compared to control tumour cells five days post-injection[391]. Hence, it was hypothesised that if Samsn1 promotes immune-mediated control of 5TGM1 cells in KaLwRij mice, a greater expansion of immune cells would be observed following the inoculation of 5TGM1-Samsn1 cells compared to 5TGM1-EV control cells *in vivo*. However, no differences in the size, or activation status, of NK cell and T cell populations were observed in KaLwRij mice injected with 5TGM1-Samsn1 cells, 5TGM1-EV cells or PBS after five days. This may have been because five days is not the optimal timepoint to observe an expansion of immune cell populations in the 5TGM1/KaLwRij model, or because increased immune cell function, not number, mediates the anti-tumour response in KaLwRij mice. In support of this, KaLwRij-derived CTLs, which are known to be important effectors of tumour immunosurveillance[365], were found to display increased cytotoxicity toward 5TGM1-Samsn1 cells compared to 5TGM1-EV cells *in vitro*. This finding suggests that Samsn1 expression increases the immunogenicity of 5TGM1 cells to CTLs. Further investigation of the importance of CTL activity in maintaining 5TGM1-Samsn1 cells in immune-mediated equilibrium is warranted, for example, by determining the effect of antibody-mediated depletion of CTLs in KaLwRij mice on the growth of 5TGM1-Samsn1 cells compared to 5TGM1-EV cells *in vivo*.

CTLs detect tumour cells through TCR-mediated recognition of tumour-specific antigens, such as peptides from mutated or aberrantly expressed proteins, which are presented on the cell surface by MHC-I molecules[366]. Down-regulating surface expression of MHC-I molecules is a common mechanism by which tumour cells escape from immune-mediated growth suppression[366]. Although there have been conflicting reports as to whether this occurs in MM PCs[392-394], it was hypothesised that Samsn1 expression may promote targeting of 5TGM1 cells by CTLs by increasing surface expression of MHC-I molecules. However, the levels of MHC-I molecules were found to not differ between 5TGM1-Samsn1 and 5TGM1-EV cells, suggesting that Samsn1 does not promote the immunogenicity of MM PCs in this way. Importantly, Samsn1 expression was found to completely inhibit 5TGM1 tumour development in immunocompetent C57BL/*Samsn1*$^{-/-}$ mice but not in immunocompetent WT C57BL/6 mice. These data suggest that the tumour suppressor effect of Samsn1 *in vivo* is dependent on the host being both immunocompetent and *Samsn1*$^{-/-}$. In *Samsn1*$^{-/-}$ mice, developing B and T cells with antigen receptors that recognise Samsn1 peptides are not exposed to Samsn1 during the process of immune tolerance and thus will not undergo clonal deletion, as occurs in WT mice. Hence, it was hypothesised that the observed immune-dependent tumour suppressor effect of Samsn1 on 5TGM1 cells in KaLwRij mice is mediated by Samsn1-specific adaptive immune cells.

The ability to investigate the immunogenicity of Samsn1 in KaLwRij mice was constrained by the fact that there was no commercially available recombinant Samsn1 protein. In addition, antigenic peptides could not be synthesised because the immunodominant CTL epitope of Samsn1 in these mice was unknown. While CTLs are known to be the key mediators of immune responses to transgenes, studies have shown that a humoral immune response can also be generated[395,396]. Hence, the ability of Samsn1 to generate an antigen-specific humoral immune response in *Samsn1*$^{-/-}$ mice inoculated with 5TGM1-Samsn1 cells was assessed by Western blot. Anti-Samsn1-specific antibodies were detected in the serum from a C57BL/*Samsn1*$^{-/-}$ mouse, but not any WT mice inoculated with 5TGM1-Samsn1 cells. However, anti-Samsn1 antibodies were not detected in the serum from the other C57BL/*Samsn1*$^{-/-}$ mice and the KaLwRij mice inoculated with 5TGM1-Samsn1 cells. These data support the hypothesis that there is a Samsn1-specific immune response in *Samsn1*$^{-/-}$ mice exposed to 5TGM1-Samsn1 cells. However, they also suggest that the generation of a humoral response to Samsn1 is rare and, therefore, Samsn1-reactive CTLs are likely to be

the major effectors of the immune response. This is consistent with previous reports of an effective CTL-mediated response to a xenogeneic protein being accompanied by a variable or absent antibody response *in vivo*[395,397]. If the immunodominant CTL epitope of Samsn1 in KaLwRij mice can be determined, Samsn1-reactive CTLs in 5TGM-Samsn1-inoculated mice could be detected using an IFN-γ ELISPOT, as previously described[397].

In summary, the data suggest that the ability of Samsn1 to inhibit MM tumour growth in the 5TGM1/KaLwRij murine model is most likely due to the presence of Samsn1-specific adaptive immune cells in KaLwRij mice. As SAMSN1-reactive lymphocytes would be eliminated during development in humans, the anti-MM effect of Samsn1 in the 5TGM1-KaLwRij model no longer supports a potential tumour suppressor role for *SAMSN1* in the context of human MM. The remaining evidence to suggest a potential role for *SAMSN1* as a tumour suppressor in human MM includes the fact that *Samsn1*$^{-/-}$ KaLwRij mice are prone to developing a MM-like disease as they age[263,264]. However, KaLwRij mice have also been shown to harbour many other genetic abnormalities compared to WT mice[260,261] and the relative contribution of *Samsn1* loss to the development of MM in aged KaLwRij mice remains to be determined. In addition, the expression of *SAMSN1* was found to be significantly reduced in the PCs from MM patients compared to healthy controls[260,261], but this correlation does not demonstrate a causative link between *SAMSN1* down-regulation and MM development. Furthermore, in this study, there was no evidence that SAMSN1 affects the growth of human MM cells *in vitro* or *in vivo*. Collectively, the data no longer support a tumour suppressor role for SAMSN1 in the development of MM in patients. The findings here also highlight the need for caution in interpreting results obtained from immunocompetent tumour models in which the introduced malignant cells express a xenogeneic protein, as this may trigger a protein-specific adaptive immune response *in vivo*.

6 FINAL DISCUSSION

MM is the second most common haematological malignancy and is characterised by the uncontrolled clonal expansion of neoplastic PCs within the BM[1]. All cases of MM are preceded by the premalignant PC proliferative disorder MGUS[19,20], which has a 1% risk of progression to MM per year[24,25]. MM is a genetically heterogeneous disease, even at the MGUS stage, with considerable variation in the adverse genetic events present in clonal PCs both between and within patients[145]. Studies indicate that the transition from MGUS to MM is due to both the accumulation of co-operative PC-intrinsic lesions and tumour-promoting PC-extrinsic factors within the BM microenvironment[343]. Comparisons of paired and unpaired MGUS and MM samples suggest that the malignant transformation of PCs can occur by different pathogenic pathways, but these are incompletely understood[229,232]. This gap in knowledge inhibits accurate identification of MGUS patients who are at high risk of progression, which is crucial for their optimal clinical management. In addition, it means that there are molecules/pathways required for the development of MM, representing potential therapeutic targets, that are yet to be identified.

Our group and others have identified the putative adaptor protein SAMSN1 as a novel tumour suppressor in MM, the down-regulation of which may promote the MGUS to MM transition[260,261]. This assertion was based on the finding that KaLwRij mice, which unlike C57BL/6 mice can progress from MGUS to MM, harbour a spontaneous homozygous deletion of the *Samsn1* gene, suggesting that the loss of *Samsn1* may promote MM development in this strain[260,261]. In support of this, the introduction of Samsn1 into the KaLwRij-derived MM PC 5TGM1 line was shown to abrogate tumour development *in vivo*[260]. In relation to human MM, *SAMSN1* mRNA expression was found to be significantly reduced in the PCs of MM patients compared to healthy individuals, which was also consistent with SAMSN1 having a tumour suppressor role in patients with this disease[260,261]. The fact that *Samsn1*$^{-/-}$ KaLwRij mice only develop MM with late onset and incomplete penetrance (~1 in 200 mice over two years old)[263,264] suggests that the loss of *Samsn1* co-operates with other lesions to promote disease progression from MGUS to MM in these mice, and also potentially in patients.

The development of MM involves the non-random accumulation of genetic hits within PCs[122]. The fact that certain pairs of lesions significantly co-occur in the PCs of MM patients suggests that these genetic events co-operate to drive disease progression[120,122,150]. In Chapter 3, low *SAMSN1* expression in the PCs of MM patients was found to be significantly

associated with reduced *GLIPR1* expression (Figure 3.1), suggesting a putative co-operative relationship between the down-regulation of these genes in promoting the development of MM. The expression of *GLIPR1* was found to be decreased in the PCs from MM patients compared to healthy individuals, with nearly 75% of MM tumours harbouring mRNA levels below the normal range (Figure 3.2). This observation was consistent with studies which showed that *GLIPR1* was down-regulated in other malignancies[296-298,305-307]. Notably, *GLIPR1* was previously found to be deleted in ~9% of MM patients[308], have reduced mRNA expression in HMCLs compared to normal B cells[298] and inhibit the development of spontaneous late-onset plasmacytomas in mice[298]. Collectively, these findings suggested that GLIPR1, like SAMSN1, may have a tumour suppressor role in MM. While previous studies had demonstrated anti-tumour effects of *GLIPR1* in several other malignancies[296-298,305-307], the studies presented in Chapter 3 are the first to assess the functional effects of this gene in MM PCs. While Glipr1 expression was not found to affect the growth of 5TGM1 cells *in vitro* (Figure 3.3), it did result in a reduction in tumour growth in KaLwRij mice, although this did not reach statistical significance (Figure 3.4). While these findings suggest that Glipr1 is not a potent tumour suppressor on its own in MM, further investigation of the functional effects of GLIPR1 in HMCLs is warranted.

To empirically determine if the loss of Samsn1 and the loss of Glipr1 co-operate to promote MM development, *Samsn1*$^{-/-}$*Glipr1*$^{-/-}$ mice on an MGUS-prone C57BL/6 background were generated. This was achieved by using back-crossing or CRISPR-mediated gene editing to generate C57BL/*Samsn1*$^{-/-}$ mice and C57BL/*Glipr1*$^{-/-}$ mice, respectively, which were subsequently crossed (Figure 3.6 and Figure 3.7). The *Glipr1*$^{-/-}$, *Samsn1*$^{-/-}$ and *Samsn1*$^{-/-}$ *Glipr1*$^{-/-}$ mice were then monitored for the emergence of PC proliferative disorders in comparison to WT mice over a period of one year. Based on the frequency of M-spikes in serum and the percentages of PCs in the BM and spleen, the prevalence of clonal PC expansions did not differ between the *Glipr1*$^{-/-}$, *Samsn1*$^{-/-}$ and *Samsn1*$^{-/-}$*Glipr1*$^{-/-}$ mice compared to the WT mice (Figure 3.12 and Figure 3.13). These data suggest that the loss of Samsn1 and/or Glipr1 does not potently drive MM development in MGUS-prone C57BL/6 mice. However, given the increased frequency of monoclonal gammopathy in C57BL/6 mice over one year of age[239,262], a more modest effect of concomitant loss of Glipr1 and Samsn1 on the development of PC disorders cannot be excluded without studying a larger cohort of mice over a longer timeframe. Future studies should also seek to identify other genetic hits that may co-operate with the down-regulation of *SAMSN1* to promote the development of

MM. For example, the Multiple Myeloma Research Foundation (MMRF) CoMMpass dataset, which includes matched cytogenetic, mutational and gene expression profiles from a large cohort of MM patients, could be mined to detect other abnormalities that recurrently co-occur with down-regulated *SAMSN1* expression.

While the abrogation of tumour development by Samsn1 in the 5TGM1/KaLwRij model suggested it was a potent tumour suppressor in MM, the mechanism(s) by which Samsn1 achieved this anti-tumour effect was unclear. Although Samsn1 was shown to have an anti-proliferative effect in normal B cells following BCR stimulation[241,245], Samsn1 expression in 5TGM1 cells was previously found to cause a modest reduction in proliferation only when the tumour cells were co-cultured with BMSCs *in vitro*[260]. This suggested that there may be a mechanism, other than the inhibition of MM PC proliferation, by which Samsn1 inhibits tumour growth *in vivo*. The previous finding that Samsn1 is involved in cytoskeletal remodelling[249] and the discovery in Chapter 4 that the levels of activated Hs1, a regulator of actin dynamics, were reduced in Samsn1-expressing 5TGM1 cells (Figure 4.3), suggested that Samsn1 may limit the migration/homing of MM PCs. However, this was not supported by the findings that Samsn1 did not affect the *in vitro* migration (Figure 4.4) or the *in vivo* BM homing (Figure 4.8) of 5TGM1 cells. Notably, following the intratibial delivery of 5TGM1 cells, Samsn1 was found to inhibit the growth of metastatic, but not primary, tumours in the BM of KaLwRij mice (Figure 4.7). The observation that Samsn1 only limited the outgrowth of 5TGM1 cells when relatively few had seeded the BM suggested that Samsn1 may promote BM microenvironment-mediated control of MM PC outgrowth[343]. Other PC-intrinsic changes have previously been shown to affect tumour growth through altering the interactions of tumour cells with the microenvironment[233,343]. For example, the upregulation of integrin B7 in MM PCs was shown to increase adhesion to BMSCs, thereby promoting tumour growth[398]. However, the identity of the source and type of anti-MM signals from the BM microenvironment that were enhanced by Samsn1 expression, and how Samsn1 mediated this at a molecular level, was yet to be determined.

Other than showing that SAMSN1 increased the adhesion of the H929 HMCL to BMSCs[260], the functional effects of SAMSN1 in HMCLs had not been previously reported. In Chapter 5, it was revealed that neither the up-regulation of SAMSN1 by overexpression, nor the down-regulation of SAMSN1 by CRISPR-mediated genome editing, affected the growth of metastatic tumours within the BM of NSG mice (Figure 5.3 and Figure 5.5). This contrasted

with the significant inhibition of disseminated 5TGM1 cell outgrowth in the BM of immunocompetent KaLwRij mice, which was shown in Chapter 4 (Figure 4.7). Crucially, it was revealed that the ability of Samsn1 to suppress the outgrowth of disseminated 5TGM1 cells in the BM was absent in immunodeficient NSG mice (Figure 5.6), suggesting that functional immune cells are required for the tumour suppressor effect of Samsn1 *in vivo*. This led to the hypothesis that Samsn1 enhances the immunogenicity of MM PC, which was supported by the finding that $CD8^+$ T cells from KaLwRij mice displayed greater cytotoxicity towards Samsn1-expressing 5TGM1 cells compared to control 5TGM1 cells (Figure 5.8). Crucially, given the known contribution of immune dysregulation to the pathogenesis of MM and the success of immunotherapies in treating MM[365], the possibility that Samsn1 promoted an anti-MM immune response was of high clinical relevance. However, Samsn1 was subsequently found to inhibit 5TGM1 cell growth in immunocompetent C57BL/*Samsn1*$^{-/-}$mice (Figure 5.11) but not in immunocompetent WT C57BL/6 mice (Figure 5.10). These findings suggest that Samsn1 only promotes an enhanced anti-5TGM1 immune response from *Samsn1*$^{-/-}$ hosts in which Samsn1-specific adaptive immune cells are not eliminated by immune tolerance (Figure 6.1). This postulate was supported by the detection of anti-Samsn1 antibodies in a *Samsn1*$^{-/-}$ mouse inoculated with 5TGM1-Samsn1 cells (Figure 5.12). Importantly, Samsn1-reactive adaptive immune cells will not be present in patients and, therefore, the previous finding that Samsn1 suppresses tumour development in the 5TGM1/KaLwRij model no longer supports a probable tumour suppressor role for SAMSN1 in the context of human MM.

Immunocompetent murine syngeneic transplantation tumour models are indispensable for the study of the complex interactions between cancer and immune cells and for testing novel immunotherapies. To enable the growth of the tumour to be tracked *in vivo* and *ex vivo*, it is common for the syngeneic tumour cells to be engineered to overexpress reporter proteins, such as GFP and luciferase. Studies have shown that the expression of these xenogeneic proteins can generate reporter-specific CTL responses in some immunocompetent tumour models, which limits tumorigenesis, especially metastasis[397,399-402]. The immunogenicity of the foreign protein is influenced by several factors, including the expression level of the protein, the cell type expressing the protein, and the genetic background of the host[403,404]. This is evidenced by the enhanced immune response to GFP displayed by Balb/c mice compared to C57BL/6 mice[401,405,406]. However, the expression of reporter proteins in syngeneic cancer cells does not prevent tumour growth in many immunocompetent

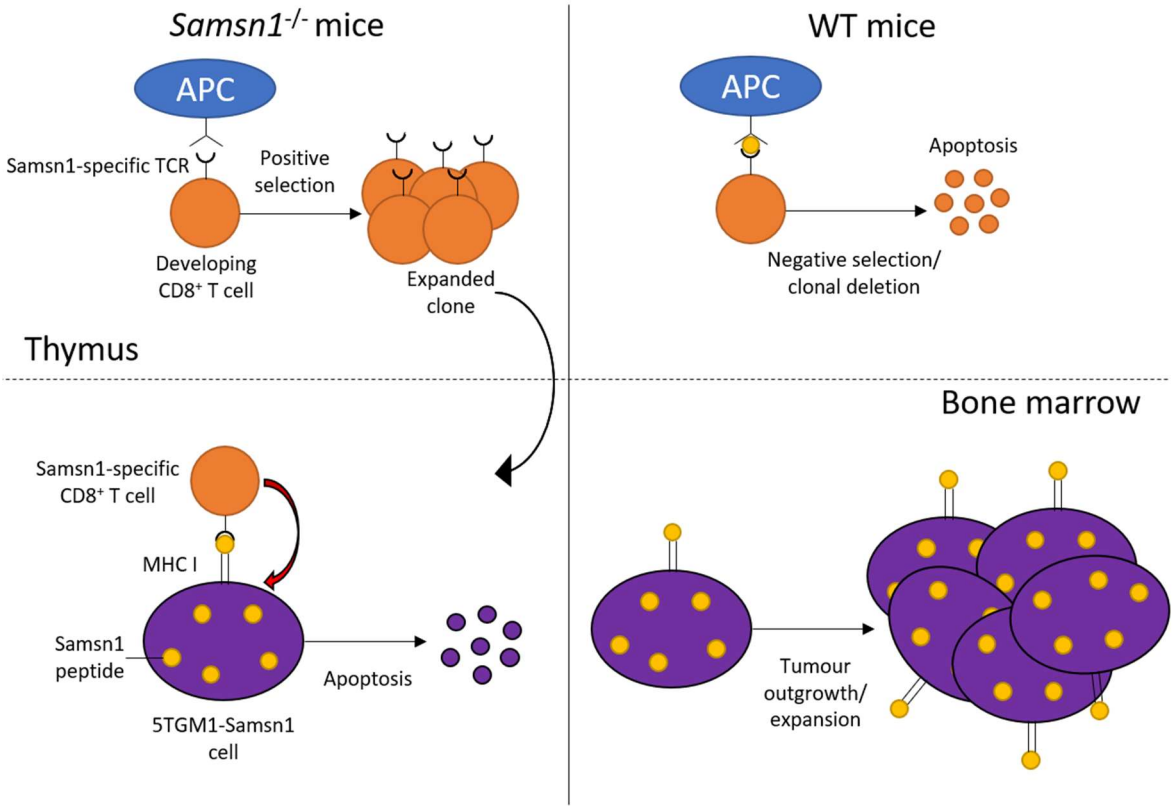

Figure 6.1: Positive selection of Samsn1-specific CD8$^+$ T cells in *Samsn1*$^{-/-}$ mice leads to immune suppression of Samsn1-expressing 5TGM1 tumour development *in vivo*. In *Samsn1*$^{-/-}$ mice (left), developing CD8$^+$ T cells expressing a T cell receptor that recognises a Samsn1-derived peptide are not presented with this in the thymus and thus are positively selected. The expanded Samsn1-specific T cells then migrate to peripheral sites, including the BM, where they recognise the Samsn1 peptides presented in MHC I molecules on the surface of disseminated 5TGM1-Samsn1 cells, causing tumour cell apoptosis and inhibition of tumour formation. Conversely, in WT mice (right), self Samsn1 peptides are presented to developing Samsn1-reactive T cells in the thymus, leading to the negative selection/deletion of the clone by apoptosis. As a result, there are no T cells in the BM that recognise the Samsn1 peptides presented by 5TGM1-Samsn1 cells and, therefore, there is a more limited immune response to these cells in WT mice compared to *Samsn1*$^{-/-}$ mice, enabling MM PC outgrowth and tumour formation. APC = antigen presenting cell, TCR = T cell receptor, WT = wildtype, MHC I = major histocompatibility complex I.

models[407-410], including the 5TGM1/KaLwRij model in which the overexpression of GFP and luciferase does not prevent aggressive tumour development[260,411,412]. This suggests that if there is an immune response to 5TGM1-derived GFP and luciferase in KaLwRij mice, which has yet to be determined, it is not a major impediment to disease progression. Hence, it was unexpected that the expression of Samsn1, which is a foreign protein in *Samsn1*$^{-/-}$ KaLwRij mice, would elicit an immune response that was capable of completely abrogating tumour growth *in vivo*. The fact that Samsn1 is targeted by an effective immune response suggests that its dominant CTL epitope is highly immunogenic in KaLwRij mice. These data highlight the unpredictable nature of immune responses to xenogeneic proteins in immunocompetent *in vivo* tumour models. Hence, to correctly interpret the results from these models, the immunogenicity of each new foreign protein should always be empirically determined.

The remaining lines of evidence suggesting that SAMSN1 may have a tumour suppressor role in human MM are largely circumstantial or inconclusive. Firstly, while the homozygous deletion of *Samsn1* is a striking genomic abnormality in KaLwRij mice, many gene expression differences, single nucleotide variants and copy number alterations have also been discovered in the KaLwRij genome compared to the C57BL/6 genome[260,261]. Hence, it is unknown whether the KaLwRij strain's ability to develop MM is attributable to their *Samsn1*$^{-/-}$ status or another genetic alteration(s). Secondly, the reduced expression of *SAMSN1* in the PCs of MM patients compared to healthy controls[260,261] describes a correlation, not a causative link, between *SAMSN1* down-regulation and the development of MM. Hence, it is possible that *SAMSN1* down-regulation may be a passenger, not a driver, event in the development of MM. Given that the reduced *SAMSN1* expression in HMCLs was shown to be, at least partly, mediated by aberrant promoter hypermethylation[260], *SAMSN1* down-regulation may be a by-product, not a key target, of the known dysregulated epigenetics in MM PCs[193-196].

Thirdly, although below median *SAMSN1* expression was found to be associated with reduced OS, this was based on a univariate survival analysis of one microarray dataset[260]. Hence, it is possible that the negative prognostic impact of low *SAMSN1* expression is attributable to co-occurring independent predictors of inferior MM patient outcomes, as was found to be the case for del(13q)[162]. Finally, while another group has shown that Samsn1 expression decreased the basal proliferation of 5TGM1 cells *in vitro*[261], our laboratory found

that Samsn1 caused a ~15% reduction in 5TGM1 cell proliferation only in the presence of BMSCs *in vitro*[260]. Hence, these conflicting results do not provide consensus support for Samsn1 having an anti-proliferative effect on 5TGM1 cells and thus acting as a tumour suppressor in MM. Notably, only one experiment examining the functional effect of SAMSN1 in another malignancy has been reported[271]. This study found that SAMSN1 overexpression did not affect the growth of a lung cancer cell line *in vitro*[271]. Furthermore, the findings that SAMSN1 did not affect the growth of HMCLs *in vitro* or *in vivo* (Figure 5.2-Figure 5.5) and that Samsn1 did not affect the growth of 5TGM1 cells in WT mice (Figure 5.10) collectively suggest that SAMSN1 is not a tumour suppressor in MM. Hence, the previously promising preliminary evidence suggesting that SAMSN1 was an important tumour suppressor in MM is now outweighed by empirical evidence indicating the contrary.

In conclusion, the findings presented in this thesis show that Samsn1 expression in the 5TGM1 murine MM PC line inhibits tumour growth in *Samsn1*$^{-/-}$ KaLwRij mice because it is targeted by Samsn1-reactive adaptive immune cells. Hence, these data do not support a tumour suppressor role for SAMSN1 in human MM, as SAMSN1-reactive lymphocytes would be deleted by immune tolerance in patients. *In vitro* proliferation/migration assays and *in vivo* tumour models in WT mice did not demonstrate tumour suppressor effects of Samsn1/SAMSN1 in mouse/human MM PCs. Together, these data suggest that the down-regulation of *SAMSN1* expression in MM PCs is not a key driver of malignant transformation. In addition, despite the finding that *GLIPR1* expression is significantly reduced in MM patients, Glipr1 only displayed a non-significant tumour suppressor effect on 5TGM1 cells *in vivo*. Given that the results do not support an important tumour suppressor role for SAMSN1 or GLIPR1 in MM, it is likely that *SAMSN1* and *GLIPR1* down-regulation are passenger events that do not actively co-operate to drive the development of MM. Hence, further research is required to improve the current incomplete understanding of the PC-intrinsic and microenvironmental factors that drive the development of MM. This will enable the rational design of new therapies and combination drug regimens that can prolong, and potentially prevent, the progression from MGUS to MM, thereby improving patient outcomes.

7 REFERENCES

1. Kumar, S. K., Rajkumar, V., Kyle, R. A., van Duin, M., Sonneveld, P., Mateos, M. V., Gay, F. & Anderson, K. C. Multiple myeloma. *Nat Rev Dis Primers*. 2017; 3:17046.

2. Kumar, S. K. & Rajkumar, S. V. The multiple myelomas - current concepts in cytogenetic classification and therapy. *Nat Rev Clin Oncol*. 2018; 15(7):409-421.

3. Kumar, S. K. Targeted Management Strategies in Multiple Myeloma. *Cancer J*. 2019; 25(1):59-64.

4. Rajkumar, S. V. Multiple myeloma: 2018 update on diagnosis, risk-stratification, and management. *Am J Hematol*. 2018; 93(8):981-1114.

5. Australian Institute of Health and Welfare (AIHW). Cancer Data in Australia; Australian Cancer Incidence and Mortality (ACIM) books: multiple myeloma. (AIHW, Canberra, 2018). <https://www.aihw.gov.au/reports/cancer/cancer-data-in-australia/acim-books>.

6. Waxman, A. J., Mink, P. J., Devesa, S. S., Anderson, W. F., Weiss, B. M., Kristinsson, S. Y., McGlynn, K. A. & Landgren, O. Racial disparities in incidence and outcome in multiple myeloma: a population-based study. *Blood*. 2010; 116(25):5501-5506.

7. Durie, B. G., Hoering, A., Abidi, M. H., Rajkumar, S. V., Epstein, J., Kahanic, S. P., Thakuri, M., Reu, F., Reynolds, C. M., Sexton, R., Orlowski, R. Z., Barlogie, B. & Dispenzieri, A. Bortezomib with lenalidomide and dexamethasone versus lenalidomide and dexamethasone alone in patients with newly diagnosed myeloma without intent for immediate autologous stem-cell transplant (SWOG S0777): a randomised, open-label, phase 3 trial. *Lancet*. 2017; 389(10068):519-527.

8. Roodman, G. D. Pathogenesis of myeloma bone disease. *Leukemia*. 2009; 23(3):435-441.

9. Farrugia, A. N., Atkins, G. J., To, L. B., Pan, B., Horvath, N., Kostakis, P., Findlay, D. M., Bardy, P. & Zannettino, A. C. Receptor activator of nuclear factor-kappaB ligand expression by human myeloma cells mediates osteoclast formation in vitro and correlates with bone destruction in vivo. *Cancer Res*. 2003; 63(17):5438-5445.

10. Giuliani, N., Bataille, R., Mancini, C., Lazzaretti, M. & Barille, S. Myeloma cells induce imbalance in the osteoprotegerin/osteoprotegerin ligand system in the human bone marrow environment. *Blood*. 2001; 98(13):3527-3533.

11. Pearse, R. N., Sordillo, E. M., Yaccoby, S., Wong, B. R., Liau, D. F., Colman, N., Michaeli, J., Epstein, J. & Choi, Y. Multiple myeloma disrupts the TRANCE/osteoprotegerin cytokine axis to trigger bone destruction and promote tumor progression. *Proc Natl Acad Sci U S A*. 2001; 98(20):11581-11586.

12. Zannettino, A. C., Farrugia, A. N., Kortesidis, A., Manavis, J., To, L. B., Martin, S. K., Diamond, P., Tamamura, H., Lapidot, T., Fujii, N. & Gronthos, S. Elevated serum levels of stromal-derived factor-1alpha are associated with increased osteoclast activity and osteolytic bone disease in multiple myeloma patients. *Cancer Res*. 2005; 65(5):1700-1709.

13. Tian, E., Zhan, F., Walker, R., Rasmussen, E., Ma, Y., Barlogie, B. & Shaughnessy, J. D., Jr. The role of the Wnt-signaling antagonist DKK1 in the development of osteolytic lesions in multiple myeloma. *N Engl J Med*. 2003; 349(26):2483-2494.

14. Oyajobi, B. O. Multiple myeloma/hypercalcemia. *Arthritis Res Ther*. 2007; 9 Suppl 1:S4.

15. Dimopoulos, M. A., Kastritis, E., Rosinol, L., Blade, J. & Ludwig, H. Pathogenesis and treatment of renal failure in multiple myeloma. *Leukemia*. 2008; 22(8):1485-1493.

16. Kyle, R. A., Gertz, M. A., Witzig, T. E., Lust, J. A., Lacy, M. Q., Dispenzieri, A., Fonseca, R., Rajkumar, S. V., Offord, J. R., Larson, D. R., Plevak, M. E., Therneau, T. M. & Greipp, P. R. Review of 1027 patients with newly diagnosed multiple myeloma. *Mayo Clin Proc*. 2003; 78(1):21-33.

17. International Myeloma Working Group. Criteria for the classification of monoclonal gammopathies, multiple myeloma and related disorders: a report of the International Myeloma Working Group. *Br J Haematol*. 2003; 121(5):749-757.

18. Blimark, C., Holmberg, E., Mellqvist, U. H., Landgren, O., Bjorkholm, M., Hultcrantz, M., Kjellander, C., Turesson, I. & Kristinsson, S. Y. Multiple myeloma and infections: a population-based study on 9253 multiple myeloma patients. *Haematologica*. 2015; 100(1):107-113.

19. Landgren, O., Kyle, R. A., Pfeiffer, R. M., Katzmann, J. A., Caporaso, N. E., Hayes, R. B., Dispenzieri, A., Kumar, S., Clark, R. J., Baris, D., Hoover, R. & Rajkumar, S. V. Monoclonal gammopathy of undetermined significance (MGUS) consistently precedes multiple myeloma: a prospective study. *Blood*. 2009; 113(22):5412-5417.

20. Weiss, B. M., Abadie, J., Verma, P., Howard, R. S. & Kuehl, W. M. A monoclonal gammopathy precedes multiple myeloma in most patients. *Blood*. 2009; 113(22):5418-5422.

21. Rajkumar, S. V., Dimopoulos, M. A., Palumbo, A., Blade, J., Merlini, G., Mateos, M. V., Kumar, S., Hillengass, J., Kastritis, E., Richardson, P., Landgren, O., Paiva, B., Dispenzieri, A., Weiss, B., LeLeu, X., Zweegman, S., Lonial, S., Rosinol, L., Zamagni, E., Jagannath, S., Sezer, O., Kristinsson, S. Y., Caers, J., Usmani, S. Z., Lahuerta, J. J., Johnsen, H. E., Beksac, M., Cavo, M., Goldschmidt, H., Terpos, E., Kyle, R. A., Anderson, K. C., Durie, B. G. & Miguel, J. F. International Myeloma Working Group updated criteria for the diagnosis of multiple myeloma. *Lancet Oncol*. 2014; 15(12):e538-548.

22. Kyle, R. A., Therneau, T. M., Rajkumar, S. V., Larson, D. R., Plevak, M. F., Offord, J. R., Dispenzieri, A., Katzmann, J. A. & Melton, L. J., 3rd. Prevalence of monoclonal gammopathy of undetermined significance. *N Engl J Med*. 2006; 354(13):1362-1369.

23. Dispenzieri, A., Katzmann, J. A., Kyle, R. A., Larson, D. R., Melton, L. J., 3rd, Colby, C. L., Therneau, T. M., Clark, R., Kumar, S. K., Bradwell, A., Fonseca, R., Jelinek, D. F. & Rajkumar, S. V. Prevalence and risk of progression of light-chain monoclonal gammopathy of undetermined significance: a retrospective population-based cohort study. *Lancet*. 2010; 375(9727):1721-1728.

24. Kyle, R. A., Therneau, T. M., Rajkumar, S. V., Offord, J. R., Larson, D. R., Plevak, M. F. & Melton, L. J., 3rd. A long-term study of prognosis in monoclonal gammopathy of undetermined significance. *N Engl J Med*. 2002; 346(8):564-569.

25. Kyle, R. A., Larson, D. R., Therneau, T. M., Dispenzieri, A., Kumar, S., Cerhan, J. R. & Rajkumar, S. V. Long-Term Follow-up of Monoclonal Gammopathy of Undetermined Significance. *N Engl J Med*. 2018; 378(3):241-249.

26. Rajkumar, S. V., Kyle, R. A., Therneau, T. M., Melton, L. J., 3rd, Bradwell, A. R., Clark, R. J., Larson, D. R., Plevak, M. F., Dispenzieri, A. & Katzmann, J. A. Serum free light chain ratio is an independent risk factor for progression in monoclonal gammopathy of undetermined significance. *Blood*. 2005; 106(3):812-817.

27. Fernandez de Larrea, C., Kyle, R. A., Durie, B. G., Ludwig, H., Usmani, S., Vesole, D. H., Hajek, R., San Miguel, J. F., Sezer, O., Sonneveld, P., Kumar, S. K., Mahindra, A., Comenzo, R., Palumbo, A., Mazumber, A., Anderson, K. C., Richardson, P. G., Badros, A. Z., Caers, J., Cavo, M., LeLeu, X., Dimopoulos, M. A., Chim, C. S., Schots, R., Noeul, A., Fantl, D., Mellqvist, U. H., Landgren, O., Chanan-Khan, A., Moreau, P., Fonseca, R., Merlini, G., Lahuerta, J. J., Blade, J., Orlowski, R. Z. *et al.* Plasma cell leukemia: consensus statement on diagnostic requirements, response criteria and treatment recommendations by the International Myeloma Working Group. *Leukemia*. 2013; 27(4):780-791.

28. Go, R. S. & Rajkumar, S. V. How I manage monoclonal gammopathy of undetermined significance. *Blood*. 2018; 131(2):163-173.

29. Kyle, R. A., Durie, B. G., Rajkumar, S. V., Landgren, O., Blade, J., Merlini, G., Kroger, N., Einsele, H., Vesole, D. H., Dimopoulos, M., San Miguel, J., Avet-Loiseau, H., Hajek, R., Chen, W. M., Anderson, K. C., Ludwig, H., Sonneveld, P., Pavlovsky, S., Palumbo, A., Richardson, P. G., Barlogie, B., Greipp, P., Vescio, R., Turesson, I., Westin, J. & Boccadoro, M. Monoclonal gammopathy of undetermined significance (MGUS) and smoldering (asymptomatic) multiple myeloma: IMWG consensus perspectives risk factors for progression and guidelines for monitoring and management. *Leukemia*. 2010; 24(6):1121-1127.

30. Kyle, R. A., Remstein, E. D., Therneau, T. M., Dispenzieri, A., Kurtin, P. J., Hodnefield, J. M., Larson, D. R., Plevak, M. F., Jelinek, D. F., Fonseca, R., Melton, L. J., 3rd & Rajkumar, S. V. Clinical course and prognosis of smoldering (asymptomatic) multiple myeloma. *N Engl J Med*. 2007; 356(25):2582-2590.

31. Rajkumar, S. V., Landgren, O. & Mateos, M. V. Smoldering multiple myeloma. *Blood*. 2015; 125(20):3069-3075.

32. Ravi, P., Kumar, S., Larsen, J. T., Gonsalves, W., Buadi, F., Lacy, M. Q., Go, R., Dispenzieri, A., Kapoor, P., Lust, J. A., Dingli, D., Lin, Y., Russell, S. J., Leung, N., Gertz, M. A., Kyle, R. A., Bergsagel, P. L. & Rajkumar, S. V. Evolving changes in disease biomarkers and risk of early progression in smoldering multiple myeloma. *Blood Cancer J*. 2016; 6(7):e454.

33. Fernandez de Larrea, C., Isola, I., Pereira, A., Cibeira, M. T., Magnano, L., Tovar, N., Rodriguez-Lobato, L. G., Calvo, X., Arostegui, J. I., Diaz, T., Lozano, E., Rozman, M., Yague, J., Blade, J. & Rosinol, L. Evolving M-protein pattern in patients with smoldering multiple myeloma: impact on early progression. *Leukemia*. 2018; 32(6):1427-1434.

34. Perez-Persona, E., Vidriales, M. B., Mateo, G., Garcia-Sanz, R., Mateos, M. V., de Coca, A. G., Galende, J., Martin-Nunez, G., Alonso, J. M., de Las Heras, N., Hernandez, J. M., Martin, A., Lopez-Berges, C., Orfao, A. & San Miguel, J. F. New criteria to identify risk of progression in monoclonal gammopathy of uncertain significance and smoldering multiple myeloma based on multiparameter flow cytometry analysis of bone marrow plasma cells. *Blood*. 2007; 110(7):2586-2592.

35. Dispenzieri, A., Kyle, R. A., Katzmann, J. A., Therneau, T. M., Larson, D., Benson, J., Clark, R. J., Melton, L. J., 3rd, Gertz, M. A., Kumar, S. K., Fonseca, R., Jelinek, D. F. &

Rajkumar, S. V. Immunoglobulin free light chain ratio is an independent risk factor for progression of smoldering (asymptomatic) multiple myeloma. *Blood*. 2008; 111(2):785-789.

36. Rajkumar, S. V., Larson, D. & Kyle, R. A. Diagnosis of smoldering multiple myeloma. *N Engl J Med*. 2011; 365(5):474-475.

37. Kastritis, E., Terpos, E., Moulopoulos, L., Spyropoulou-Vlachou, M., Kanellias, N., Eleftherakis-Papaiakovou, E., Gkotzamanidou, M., Migkou, M., Gavriatopoulou, M., Roussou, M., Tasidou, A. & Dimopoulos, M. A. Extensive bone marrow infiltration and abnormal free light chain ratio identifies patients with asymptomatic myeloma at high risk for progression to symptomatic disease. *Leukemia*. 2013; 27(4):947-953.

38. Larsen, J. T., Kumar, S. K., Dispenzieri, A., Kyle, R. A., Katzmann, J. A. & Rajkumar, S. V. Serum free light chain ratio as a biomarker for high-risk smoldering multiple myeloma. *Leukemia*. 2013; 27(4):941-946.

39. Hillengass, J., Fechtner, K., Weber, M. A., Bauerle, T., Ayyaz, S., Heiss, C., Hielscher, T., Moehler, T. M., Egerer, G., Neben, K., Ho, A. D., Kauczor, H. U., Delorme, S. & Goldschmidt, H. Prognostic significance of focal lesions in whole-body magnetic resonance imaging in patients with asymptomatic multiple myeloma. *J Clin Oncol*. 2010; 28(9):1606-1610.

40. Kastritis, E., Moulopoulos, L. A., Terpos, E., Koutoulidis, V. & Dimopoulos, M. A. The prognostic importance of the presence of more than one focal lesion in spine MRI of patients with asymptomatic (smoldering) multiple myeloma. *Leukemia*. 2014; 28(12):2402-2403.

41. Mateos, M. V., Hernandez, M. T., Giraldo, P., de la Rubia, J., de Arriba, F., Lopez Corral, L., Rosinol, L., Paiva, B., Palomera, L., Bargay, J., Oriol, A., Prosper, F., Lopez, J., Olavarria, E., Quintana, N., Garcia, J. L., Blade, J., Lahuerta, J. J. & San Miguel, J. F. Lenalidomide plus dexamethasone for high-risk smoldering multiple myeloma. *N Engl J Med*. 2013; 369(5):438-447.

42. Mateos, M. V., Hernandez, M. T., Giraldo, P., de la Rubia, J., de Arriba, F., Corral, L. L., Rosinol, L., Paiva, B., Palomera, L., Bargay, J., Oriol, A., Prosper, F., Lopez, J., Arguinano, J. M., Quintana, N., Garcia, J. L., Blade, J., Lahuerta, J. J. & Miguel, J. S. Lenalidomide plus dexamethasone versus observation in patients with high-risk smouldering multiple myeloma (QuiRedex): long-term follow-up of a randomised, controlled, phase 3 trial. *Lancet Oncol*. 2016; 17(8):1127-1136.

43. Lakshman, A., Rajkumar, S. V., Buadi, F. K., Binder, M., Gertz, M. A., Lacy, M. Q., Dispenzieri, A., Dingli, D., Fonder, A. L., Hayman, S. R., Hobbs, M. A., Gonsalves, W. I., Hwa, Y. L., Kapoor, P., Leung, N., Go, R. S., Lin, Y., Kourelis, T. V., Warsame, R., Lust, J. A., Russell, S. J., Zeldenrust, S. R., Kyle, R. A. & Kumar, S. K. Risk stratification of smoldering multiple myeloma incorporating revised IMWG diagnostic criteria. *Blood Cancer J*. 2018; 8(6):59.

44. Goyal, G., Rajkumar, S. V., Lacy, M. Q., Gertz, M. A., Buadi, F. K., Dispenzieri, A., Hwa, Y. L., Fonder, A. L., Hobbs, M. A., Hayman, S. R., Zeldenrust, S. R., Lust, J. A., Russell, S. J., Leung, N., Kapoor, P., Go, R. S., Gonsalves, W. I., Kourelis, T. V., Warsame, R., Kyle, R. A. & Kumar, S. K. Impact of prior diagnosis of monoclonal gammopathy on outcomes in newly diagnosed multiple myeloma. *Leukemia*. 2019; [Epub ahead of print] doi: 10.1038/s41375-019-0419-7.

45. Kumar, S., Perez, W. S., Zhang, M. J., Ballen, K., Bashey, A., To, L. B., Bredeson, C. N., Cairo, M. S., Elfenbein, G. J., Freytes, C. O., Gale, R. P., Gibson, J., Kyle, R. A., Lacy, M. Q., Lazarus, H. M., McCarthy, P. L., Milone, G. A., Moreb, J. S., Pavlovsky, S., Reece, D. E., Vesole, D. H., Wiernik, P. H. & Hari, P. Comparable outcomes in nonsecretory and secretory multiple myeloma after autologous stem cell transplantation. *Biol Blood Marrow Transplant*. 2008; 14(10):1134-1140.

46. Greipp, P. R., San Miguel, J., Durie, B. G., Crowley, J. J., Barlogie, B., Blade, J., Boccadoro, M., Child, J. A., Avet-Loiseau, H., Kyle, R. A., Lahuerta, J. J., Ludwig, H., Morgan, G., Powles, R., Shimizu, K., Shustik, C., Sonneveld, P., Tosi, P., Turesson, I. & Westin, J. International staging system for multiple myeloma. *J Clin Oncol*. 2005; 23(15):3412-3420.

47. Palumbo, A., Avet-Loiseau, H., Oliva, S., Lokhorst, H. M., Goldschmidt, H., Rosinol, L., Richardson, P., Caltagirone, S., Lahuerta, J. J., Facon, T., Bringhen, S., Gay, F., Attal, M., Passera, R., Spencer, A., Offidani, M., Kumar, S., Musto, P., Lonial, S., Petrucci, M. T., Orlowski, R. Z., Zamagni, E., Morgan, G., Dimopoulos, M. A., Durie, B. G., Anderson, K. C., Sonneveld, P., San Miguel, J., Cavo, M., Rajkumar, S. V. & Moreau, P. Revised International Staging System for Multiple Myeloma: A Report From International Myeloma Working Group. *J Clin Oncol*. 2015; 33(26):2863-2869.

48. Mikhael, J. R., Dingli, D., Roy, V., Reeder, C. B., Buadi, F. K., Hayman, S. R., Dispenzieri, A., Fonseca, R., Sher, T., Kyle, R. A., Lin, Y., Russell, S. J., Kumar, S., Bergsagel, P. L., Zeldenrust, S. R., Leung, N., Drake, M. T., Kapoor, P., Ansell, S. M., Witzig, T. E., Lust, J. A., Dalton, R. J., Gertz, M. A., Stewart, A. K., Rajkumar, S. V., Chanan-Khan, A. & Lacy, M. Q. Management of newly diagnosed symptomatic multiple myeloma: updated Mayo Stratification of Myeloma and Risk-Adapted Therapy (mSMART) consensus guidelines 2013. *Mayo Clin Proc*. 2013; 88(4):360-376.

49. Mayo Clinic Myeloma Physicians. *mSMART 3.0: Classification of Active MM*, <https://www.msmart.org/multiple-myeloma> (2018).

50. Pawlyn, C. & Morgan, G. J. Evolutionary biology of high-risk multiple myeloma. *Nat Rev Cancer*. 2017; 17(9):543-556.

51. Kyle, R. A., Maldonado, J. E. & Bayrd, E. D. Plasma cell leukemia. Report on 17 cases. *Arch Intern Med*. 1974; 133(5):813-818.

52. Noel, P. & Kyle, R. A. Plasma cell leukemia: an evaluation of response to therapy. *Am J Med*. 1987; 83(6):1062-1068.

53. Jurczyszyn, A., Castillo, J. J., Avivi, I., Czepiel, J., Davila, J., Vij, R., Fiala, M. A., Gozzetti, A., Grzasko, N., Milunovic, V., Hus, I., Madry, K., Waszczuk-Gajda, A., Usnarska-Zubkiewicz, L., Debski, J., Atilla, E., Beksac, M., Mele, G., Sawicki, W., Jayabalan, D., Charlinski, G., Gyula Szabo, A., Hajek, R., Delforge, M., Kopacz, A., Fantl, D., Waage, A., Crusoe, E., Hungria, V., Richardson, P., Laubach, J., Guerrero-Garcia, T., Liu, J. & Vesole, D. H. Secondary plasma cell leukemia: a multicenter retrospective study of 101 patients. *Leuk Lymphoma*. 2019; 60(1):118-123.

54. Tiedemann, R. E., Gonzalez-Paz, N., Kyle, R. A., Santana-Davila, R., Price-Troska, T., Van Wier, S. A., Chng, W. J., Ketterling, R. P., Gertz, M. A., Henderson, K., Greipp, P. R., Dispenzieri, A., Lacy, M. Q., Rajkumar, S. V., Bergsagel, P. L., Stewart, A. K. & Fonseca, R. Genetic aberrations and survival in plasma cell leukemia. *Leukemia*. 2008; 22(5):1044-1052.

55. Ravi, P., Kumar, S. K., Roeker, L., Gonsalves, W., Buadi, F., Lacy, M. Q., Go, R. S., Dispenzieri, A., Kapoor, P., Lust, J. A., Dingli, D., Lin, Y., Russell, S. J., Leung, N., Gertz, M. A., Kyle, R. A., Bergsagel, P. L. & Rajkumar, S. V. Revised diagnostic criteria for plasma cell leukemia: results of a Mayo Clinic study with comparison of outcomes to multiple myeloma. *Blood Cancer J*. 2018; 8(12):116.

56. An, G., Qin, X., Acharya, C., Xu, Y., Deng, S., Shi, L., Zang, M., Sui, W., Yi, S., Li, Z., Hao, M., Feng, X., Jin, F., Zou, D., Qi, J., Zhao, Y., Tai, Y. T., Wang, J. & Qiu, L. Multiple myeloma patients with low proportion of circulating plasma cells had similar survival with primary plasma cell leukemia patients. *Ann Hematol*. 2015; 94(2):257-264.

57. Granell, M., Calvo, X., Garcia-Guinon, A., Escoda, L., Abella, E., Martinez, C. M., Teixido, M., Gimenez, M. T., Senin, A., Sanz, P., Campoy, D., Vicent, A., Arenillas, L., Rosinol, L., Sierra, J., Blade, J. & de Larrea, C. F. Prognostic impact of circulating plasma cells in patients with multiple myeloma: implications for plasma cell leukemia definition. *Haematologica*. 2017; 102(6):1099-1104.

58. Touzeau, C. & Moreau, P. How I treat extramedullary myeloma. *Blood*. 2016; 127(8):971-976.

59. Bartel, T. B., Haessler, J., Brown, T. L., Shaughnessy, J. D., Jr., van Rhee, F., Anaissie, E., Alpe, T., Angtuaco, E., Walker, R., Epstein, J., Crowley, J. & Barlogie, B. F18-fluorodeoxyglucose positron emission tomography in the context of other imaging techniques and prognostic factors in multiple myeloma. *Blood*. 2009; 114(10):2068-2076.

60. Varga, C., Xie, W., Laubach, J., Ghobrial, I. M., O'Donnell, E. K., Weinstock, M., Paba-Prada, C., Warren, D., Maglio, M. E., Schlossman, R., Munshi, N. C., Raje, N., Weller, E., Anderson, K. C., Mitsiades, C. S. & Richardson, P. G. Development of extramedullary myeloma in the era of novel agents: no evidence of increased risk with lenalidomide-bortezomib combinations. *Br J Haematol*. 2015; 169(6):843-850.

61. Short, K. D., Rajkumar, S. V., Larson, D., Buadi, F., Hayman, S., Dispenzieri, A., Gertz, M., Kumar, S., Mikhael, J., Roy, V., Kyle, R. A. & Lacy, M. Q. Incidence of extramedullary disease in patients with multiple myeloma in the era of novel therapy, and the activity of pomalidomide on extramedullary myeloma. *Leukemia*. 2011; 25(6):906-908.

62. Pour, L., Sevcikova, S., Greslikova, H., Kupska, R., Majkova, P., Zahradova, L., Sandecka, V., Adam, Z., Krejci, M., Kuglik, P. & Hajek, R. Soft-tissue extramedullary multiple myeloma prognosis is significantly worse in comparison to bone-related extramedullary relapse. *Haematologica*. 2014; 99(2):360-364.

63. Weinstock, M., Aljawai, Y., Morgan, E. A., Laubach, J., Gannon, M., Roccaro, A. M., Varga, C., Mitsiades, C. S., Paba-Prada, C., Schlossman, R., Munshi, N., Anderson, K. C., Richardson, P. P., Weller, E. & Ghobrial, I. M. Incidence and clinical features of extramedullary multiple myeloma in patients who underwent stem cell transplantation. *Br J Haematol*. 2015; 169(6):851-858.

64. Drexler, H. G. & Matsuo, Y. Malignant hematopoietic cell lines: in vitro models for the study of multiple myeloma and plasma cell leukemia. *Leuk Res*. 2000; 24(8):681-703.

65. Kumar, S. K., Dispenzieri, A., Lacy, M. Q., Gertz, M. A., Buadi, F. K., Pandey, S., Kapoor, P., Dingli, D., Hayman, S. R., Leung, N., Lust, J., McCurdy, A., Russell, S. J., Zeldenrust, S. R., Kyle, R. A. & Rajkumar, S. V. Continued improvement in survival in

multiple myeloma: changes in early mortality and outcomes in older patients. *Leukemia*. 2014; 28(5):1122-1128.

66. Costa, L. J., Brill, I. K., Omel, J., Godby, K., Kumar, S. K. & Brown, E. E. Recent trends in multiple myeloma incidence and survival by age, race, and ethnicity in the United States. *Blood Adv*. 2017; 1(4):282-287.

67. Obeng, E. A., Carlson, L. M., Gutman, D. M., Harrington, W. J., Jr., Lee, K. P. & Boise, L. H. Proteasome inhibitors induce a terminal unfolded protein response in multiple myeloma cells. *Blood*. 2006; 107(12):4907-4916.

68. Quach, H., Ritchie, D., Stewart, A. K., Neeson, P., Harrison, S., Smyth, M. J. & Prince, H. M. Mechanism of action of immunomodulatory drugs (IMiDS) in multiple myeloma. *Leukemia*. 2010; 24(1):22-32.

69. Ocio, E. M., Richardson, P. G., Rajkumar, S. V., Palumbo, A., Mateos, M. V., Orlowski, R., Kumar, S., Usmani, S., Roodman, D., Niesvizky, R., Einsele, H., Anderson, K. C., Dimopoulos, M. A., Avet-Loiseau, H., Mellqvist, U. H., Turesson, I., Merlini, G., Schots, R., McCarthy, P., Bergsagel, L., Chim, C. S., Lahuerta, J. J., Shah, J., Reiman, A., Mikhael, J., Zweegman, S., Lonial, S., Comenzo, R., Chng, W. J., Moreau, P., Sonneveld, P., Ludwig, H., Durie, B. G. & Miguel, J. F. New drugs and novel mechanisms of action in multiple myeloma in 2013: a report from the International Myeloma Working Group (IMWG). *Leukemia*. 2014; 28(3):525-542.

70. Kronke, J., Udeshi, N. D., Narla, A., Grauman, P., Hurst, S. N., McConkey, M., Svinkina, T., Heckl, D., Comer, E., Li, X., Ciarlo, C., Hartman, E., Munshi, N., Schenone, M., Schreiber, S. L., Carr, S. A. & Ebert, B. L. Lenalidomide causes selective degradation of IKZF1 and IKZF3 in multiple myeloma cells. *Science*. 2014; 343(6168):301-305.

71. Lu, G., Middleton, R. E., Sun, H., Naniong, M., Ott, C. J., Mitsiades, C. S., Wong, K. K., Bradner, J. E. & Kaelin, W. G., Jr. The myeloma drug lenalidomide promotes the cereblon-dependent destruction of Ikaros proteins. *Science*. 2014; 343(6168):305-309.

72. Quach, H. & Prince, H. M. Clinical Practice Guideline Multiple Myeloma V.4. (Myeloma Foundation of Australia, Victoria, Australia, 2017). <http://myeloma.org.au/wp-content/uploads/2017/10/MSAG-Clinical-Practice-Guideline-Myeloma-V4-March-2017.pdf>.

73. Attal, M., Harousseau, J. L., Stoppa, A. M., Sotto, J. J., Fuzibet, J. G., Rossi, J. F., Casassus, P., Maisonneuve, H., Facon, T., Ifrah, N., Payen, C. & Bataille, R. A prospective, randomized trial of autologous bone marrow transplantation and chemotherapy in multiple myeloma. Intergroupe Francais du Myelome. *N Engl J Med*. 1996; 335(2):91-97.

74. Child, J. A., Morgan, G. J., Davies, F. E., Owen, R. G., Bell, S. E., Hawkins, K., Brown, J., Drayson, M. T. & Selby, P. J. High-dose chemotherapy with hematopoietic stem-cell rescue for multiple myeloma. *N Engl J Med*. 2003; 348(19):1875-1883.

75. Palumbo, A., Cavallo, F., Gay, F., Di Raimondo, F., Ben Yehuda, D., Petrucci, M. T., Pezzatti, S., Caravita, T., Cerrato, C., Ribakovsky, E., Genuardi, M., Cafro, A., Marcatti, M., Catalano, L., Offidani, M., Carella, A. M., Zamagni, E., Patriarca, F., Musto, P., Evangelista, A., Ciccone, G., Omede, P., Crippa, C., Corradini, P., Nagler, A., Boccadoro, M. & Cavo, M. Autologous transplantation and maintenance therapy in multiple myeloma. *N Engl J Med*. 2014; 371(10):895-905.

76. Morgan, G. J., Gregory, W. M., Davies, F. E., Bell, S. E., Szubert, A. J., Brown, J. M., Coy, N. N., Cook, G., Russell, N. H., Rudin, C., Roddie, H., Drayson, M. T., Owen, R. G., Ross, F. M., Jackson, G. H. & Child, J. A. The role of maintenance thalidomide therapy in multiple myeloma: MRC Myeloma IX results and meta-analysis. *Blood*. 2012; 119(1):7-15.

77. McCarthy, P. L., Holstein, S. A., Petrucci, M. T., Richardson, P. G., Hulin, C., Tosi, P., Bringhen, S., Musto, P., Anderson, K. C., Caillot, D., Gay, F., Moreau, P., Marit, G., Jung, S. H., Yu, Z., Winograd, B., Knight, R. D., Palumbo, A. & Attal, M. Lenalidomide Maintenance After Autologous Stem-Cell Transplantation in Newly Diagnosed Multiple Myeloma: A Meta-Analysis. *J Clin Oncol*. 2017; 35(29):3279-3289.

78. Dingli, D., Ailawadhi, S., Bergsagel, P. L., Buadi, F. K., Dispenzieri, A., Fonseca, R., Gertz, M. A., Gonsalves, W. I., Hayman, S. R., Kapoor, P., Kourelis, T., Kumar, S. K., Kyle, R. A., Lacy, M. Q., Leung, N., Lin, Y., Lust, J. A., Mikhael, J. R., Reeder, C. B., Roy, V., Russell, S. J., Sher, T., Stewart, A. K., Warsame, R., Zeldenrust, S. R., Rajkumar, S. V. & Chanan Khan, A. A. Therapy for Relapsed Multiple Myeloma: Guidelines From the Mayo Stratification for Myeloma and Risk-Adapted Therapy. *Mayo Clin Proc*. 2017; 92(4):578-598.

79. Dimopoulos, M. A., Goldschmidt, H., Niesvizky, R., Joshua, D., Chng, W. J., Oriol, A., Orlowski, R. Z., Ludwig, H., Facon, T., Hajek, R., Weisel, K., Hungria, V., Minuk, L., Feng, S., Zahlten-Kumeli, A., Kimball, A. S. & Moreau, P. Carfilzomib or bortezomib in relapsed or refractory multiple myeloma (ENDEAVOR): an interim overall survival analysis of an open-label, randomised, phase 3 trial. *Lancet Oncol*. 2017; 18(10):1327-1337.

80. Stewart, A. K., Rajkumar, S. V., Dimopoulos, M. A., Masszi, T., Spicka, I., Oriol, A., Hajek, R., Rosinol, L., Siegel, D. S., Mihaylov, G. G., Goranova-Marinova, V., Rajnics, P., Suvorov, A., Niesvizky, R., Jakubowiak, A. J., San-Miguel, J. F., Ludwig, H., Wang, M., Maisnar, V., Minarik, J., Bensinger, W. I., Mateos, M. V., Ben-Yehuda, D., Kukreti, V., Zojwalla, N., Tonda, M. E., Yang, X., Xing, B., Moreau, P. & Palumbo, A. Carfilzomib, lenalidomide, and dexamethasone for relapsed multiple myeloma. *N Engl J Med*. 2015; 372(2):142-152.

81. Moreau, P., Masszi, T., Grzasko, N., Bahlis, N. J., Hansson, M., Pour, L., Sandhu, I., Ganly, P., Baker, B. W., Jackson, S. R., Stoppa, A. M., Simpson, D. R., Gimsing, P., Palumbo, A., Garderet, L., Cavo, M., Kumar, S., Touzeau, C., Buadi, F. K., Laubach, J. P., Berg, D. T., Lin, J., Di Bacco, A., Hui, A. M., van de Velde, H. & Richardson, P. G. Oral Ixazomib, Lenalidomide, and Dexamethasone for Multiple Myeloma. *N Engl J Med*. 2016; 374(17):1621-1634.

82. Kumar, S. K., Berdeja, J. G., Niesvizky, R., Lonial, S., Laubach, J. P., Hamadani, M., Stewart, A. K., Hari, P., Roy, V., Vescio, R., Kaufman, J. L., Berg, D., Liao, E., Di Bacco, A., Estevam, J., Gupta, N., Hui, A. M., Rajkumar, V. & Richardson, P. G. Safety and tolerability of ixazomib, an oral proteasome inhibitor, in combination with lenalidomide and dexamethasone in patients with previously untreated multiple myeloma: an open-label phase 1/2 study. *Lancet Oncol*. 2014; 15(13):1503-1512.

83. Lacy, M. Q., Hayman, S. R., Gertz, M. A., Dispenzieri, A., Buadi, F., Kumar, S., Greipp, P. R., Lust, J. A., Russell, S. J., Dingli, D., Kyle, R. A., Fonseca, R., Bergsagel, P. L., Roy, V., Mikhael, J. R., Stewart, A. K., Laumann, K., Allred, J. B., Mandrekar, S. J. & Rajkumar, S. V. Pomalidomide (CC4047) plus low-dose dexamethasone as therapy for relapsed multiple myeloma. *J Clin Oncol*. 2009; 27(30):5008-5014.

84. Miguel, J. S., Weisel, K., Moreau, P., Lacy, M., Song, K., Delforge, M., Karlin, L., Goldschmidt, H., Banos, A., Oriol, A., Alegre, A., Chen, C., Cavo, M., Garderet, L., Ivanova, V., Martinez-Lopez, J., Belch, A., Palumbo, A., Schey, S., Sonneveld, P., Yu, X., Sternas, L., Jacques, C., Zaki, M. & Dimopoulos, M. Pomalidomide plus low-dose dexamethasone versus high-dose dexamethasone alone for patients with relapsed and refractory multiple myeloma (MM-003): a randomised, open-label, phase 3 trial. *Lancet Oncol*. 2013; 14(11):1055-1066.

85. San-Miguel, J. F., Richardson, P. G., Gunther, A., Sezer, O., Siegel, D., Blade, J., LeBlanc, R., Sutherland, H., Sopala, M., Mishra, K. K., Mu, S., Bourquelot, P. M., Victoria Mateos, M. & Anderson, K. C. Phase Ib study of panobinostat and bortezomib in relapsed or relapsed and refractory multiple myeloma. *J Clin Oncol*. 2013; 31(29):3696-3703.

86. Richardson, P. G., Schlossman, R. L., Alsina, M., Weber, D. M., Coutre, S. E., Gasparetto, C., Mukhopadhyay, S., Ondovik, M. S., Khan, M., Paley, C. S. & Lonial, S. PANORAMA 2: panobinostat in combination with bortezomib and dexamethasone in patients with relapsed and bortezomib-refractory myeloma. *Blood*. 2013; 122(14):2331-2337.

87. Lokhorst, H. M., Plesner, T., Laubach, J. P., Nahi, H., Gimsing, P., Hansson, M., Minnema, M. C., Lassen, U., Krejcik, J., Palumbo, A., van de Donk, N. W., Ahmadi, T., Khan, I., Uhlar, C. M., Wang, J., Sasser, A. K., Losic, N., Lisby, S., Basse, L., Brun, N. & Richardson, P. G. Targeting CD38 with Daratumumab Monotherapy in Multiple Myeloma. *N Engl J Med*. 2015; 373(13):1207-1219.

88. Palumbo, A., Chanan-Khan, A., Weisel, K., Nooka, A. K., Masszi, T., Beksac, M., Spicka, I., Hungria, V., Munder, M., Mateos, M. V., Mark, T. M., Qi, M., Schecter, J., Amin, H., Qin, X., Deraedt, W., Ahmadi, T., Spencer, A. & Sonneveld, P. Daratumumab, Bortezomib, and Dexamethasone for Multiple Myeloma. *N Engl J Med*. 2016; 375(8):754-766.

89. Lonial, S., Dimopoulos, M., Palumbo, A., White, D., Grosicki, S., Spicka, I., Walter-Croneck, A., Moreau, P., Mateos, M. V., Magen, H., Belch, A., Reece, D., Beksac, M., Spencer, A., Oakervee, H., Orlowski, R. Z., Taniwaki, M., Rollig, C., Einsele, H., Wu, K. L., Singhal, A., San-Miguel, J., Matsumoto, M., Katz, J., Bleickardt, E., Poulart, V., Anderson, K. C. & Richardson, P. Elotuzumab Therapy for Relapsed or Refractory Multiple Myeloma. *N Engl J Med*. 2015; 373(7):621-631.

90. Brudno, J. N., Maric, I., Hartman, S. D., Rose, J. J., Wang, M., Lam, N., Stetler-Stevenson, M., Salem, D., Yuan, C., Pavletic, S., Kanakry, J. A., Ali, S. A., Mikkilineni, L., Feldman, S. A., Stroncek, D. F., Hansen, B. G., Lawrence, J., Patel, R., Hakim, F., Gress, R. E. & Kochenderfer, J. N. T Cells Genetically Modified to Express an Anti-B-Cell Maturation Antigen Chimeric Antigen Receptor Cause Remissions of Poor-Prognosis Relapsed Multiple Myeloma. *J Clin Oncol*. 2018; 36(22):2267-2280.

91. Kumar, S., Kaufman, J. L., Gasparetto, C., Mikhael, J., Vij, R., Pegourie, B., Benboubker, L., Facon, T., Amiot, M., Moreau, P., Punnoose, E. A., Alzate, S., Dunbar, M., Xu, T., Agarwal, S. K., Enschede, S. H., Leverson, J. D., Ross, J. A., Maciag, P. C., Verdugo, M. & Touzeau, C. Efficacy of venetoclax as targeted therapy for relapsed/refractory t(11;14) multiple myeloma. *Blood*. 2017; 130(22):2401-2409.

92. Moreau, P., Chanan-Khan, A., Roberts, A. W., Agarwal, A. B., Facon, T., Kumar, S., Touzeau, C., Punnoose, E. A., Cordero, J., Munasinghe, W., Jia, J., Salem, A. H., Freise,

K. J., Leverson, J. D., Enschede, S. H., Ross, J. A., Maciag, P. C., Verdugo, M. & Harrison, S. J. Promising efficacy and acceptable safety of venetoclax plus bortezomib and dexamethasone in relapsed/refractory MM. *Blood*. 2017; 130(22):2392-2400.

93. Gonzalez, D., van der Burg, M., Garcia-Sanz, R., Fenton, J. A., Langerak, A. W., Gonzalez, M., van Dongen, J. J., San Miguel, J. F. & Morgan, G. J. Immunoglobulin gene rearrangements and the pathogenesis of multiple myeloma. *Blood*. 2007; 110(9):3112-3121.

94. Shapiro-Shelef, M. & Calame, K. Regulation of plasma-cell development. *Nat Rev Immunol*. 2005; 5(3):230-242.

95. Victora, G. D. & Nussenzweig, M. C. Germinal centers. *Annu Rev Immunol*. 2012; 30:429-457.

96. Corcoran, L. M. & Tarlinton, D. M. Regulation of germinal center responses, memory B cells and plasma cell formation-an update. *Curr Opin Immunol*. 2016; 39:59-67.

97. Nutt, S. L., Hodgkin, P. D., Tarlinton, D. M. & Corcoran, L. M. The generation of antibody-secreting plasma cells. *Nat Rev Immunol*. 2015; 15(3):160-171.

98. Lynch, H. T., Sanger, W. G., Pirruccello, S., Quinn-Laquer, B. & Weisenburger, D. D. Familial multiple myeloma: a family study and review of the literature. *J Natl Cancer Inst*. 2001; 93(19):1479-1483.

99. Bizzaro, N. & Pasini, P. Familial occurrence of multiple myeloma and monoclonal gammopathy of undetermined significance in 5 siblings. *Haematologica*. 1990; 75(1):58-63.

100. Lynch, H. T., Ferrara, K., Barlogie, B., Coleman, E. A., Lynch, J. F., Weisenburger, D., Sanger, W., Watson, P., Nipper, H., Witt, V. & Thome, S. Familial myeloma. *N Engl J Med*. 2008; 359(2):152-157.

101. Vachon, C. M., Kyle, R. A., Therneau, T. M., Foreman, B. J., Larson, D. R., Colby, C. L., Phelps, T. K., Dispenzieri, A., Kumar, S. K., Katzmann, J. A. & Rajkumar, S. V. Increased risk of monoclonal gammopathy in first-degree relatives of patients with multiple myeloma or monoclonal gammopathy of undetermined significance. *Blood*. 2009; 114(4):785-790.

102. Landgren, O., Kristinsson, S. Y., Goldin, L. R., Caporaso, N. E., Blimark, C., Mellqvist, U. H., Wahlin, A., Bjorkholm, M. & Turesson, I. Risk of plasma cell and lymphoproliferative disorders among 14621 first-degree relatives of 4458 patients with monoclonal gammopathy of undetermined significance in Sweden. *Blood*. 2009; 114(4):791-795.

103. Clay-Gilmour, A. I., Kumar, S., Rajkumar, S. V., Rishi, A., Kyle, R. A., Katzmann, J. A., Murray, D. L., Norman, A. D., Greenberg, A. J., Larson, D. R., O'Byrne, M. M., Slager, S. L. & Vachon, C. M. Risk of MGUS in relatives of multiple myeloma cases by clinical and tumor characteristics. *Leukemia*. 2019; 33(2):499-507.

104. Broderick, P., Chubb, D., Johnson, D. C., Weinhold, N., Forsti, A., Lloyd, A., Olver, B., Ma, Y. P., Dobbins, S. E., Walker, B. A., Davies, F. E., Gregory, W. A., Child, J. A., Ross, F. M., Jackson, G. H., Neben, K., Jauch, A., Hoffmann, P., Muhleisen, T. W., Nothen, M. M., Moebus, S., Tomlinson, I. P., Goldschmidt, H., Hemminki, K., Morgan, G. J. & Houlston, R. S. Common variation at 3p22.1 and 7p15.3 influences multiple myeloma risk. *Nat Genet*. 2012; 44(1):58-61.

105. Chubb, D., Weinhold, N., Broderick, P., Chen, B., Johnson, D. C., Forsti, A., Vijayakrishnan, J., Migliorini, G., Dobbins, S. E., Holroyd, A., Hose, D., Walker, B. A., Davies, F. E., Gregory, W. A., Jackson, G. H., Irving, J. A., Pratt, G., Fegan, C., Fenton, J. A., Neben, K., Hoffmann, P., Nothen, M. M., Muhleisen, T. W., Eisele, L., Ross, F. M., Straka, C., Einsele, H., Langer, C., Dorner, E., Allan, J. M., Jauch, A., Morgan, G. J., Hemminki, K., Houlston, R. S. & Goldschmidt, H. Common variation at 3q26.2, 6p21.33, 17p11.2 and 22q13.1 influences multiple myeloma risk. *Nat Genet*. 2013; 45(10):1221-1225.

106. Mitchell, J. S., Li, N., Weinhold, N., Forsti, A., Ali, M., van Duin, M., Thorleifsson, G., Johnson, D. C., Chen, B., Halvarsson, B. M., Gudbjartsson, D. F., Kuiper, R., Stephens, O. W., Bertsch, U., Broderick, P., Campo, C., Einsele, H., Gregory, W. A., Gullberg, U., Henrion, M., Hillengass, J., Hoffmann, P., Jackson, G. H., Johnsson, E., Joud, M., Kristinsson, S. Y., Lenhoff, S., Lenive, O., Mellqvist, U. H., Migliorini, G., Nahi, H., Nelander, S., Nickel, J., Nothen, M. M., Rafnar, T. *et al.* Genome-wide association study identifies multiple susceptibility loci for multiple myeloma. *Nat Commun*. 2016; 7:12050.

107. Went, M., Sud, A., Forsti, A., Halvarsson, B. M., Weinhold, N., Kimber, S., van Duin, M., Thorleifsson, G., Holroyd, A., Johnson, D. C., Li, N., Orlando, G., Law, P. J., Ali, M., Chen, B., Mitchell, J. S., Gudbjartsson, D. F., Kuiper, R., Stephens, O. W., Bertsch, U., Broderick, P., Campo, C., Bandapalli, O. R., Einsele, H., Gregory, W. A., Gullberg, U., Hillengass, J., Hoffmann, P., Jackson, G. H., Jockel, K. H., Johnsson, E., Kristinsson, S. Y., Mellqvist, U. H., Nahi, H., Easton, D. *et al.* Identification of multiple risk loci and regulatory mechanisms influencing susceptibility to multiple myeloma. *Nat Commun*. 2018; 9(1):3707.

108. Swaminathan, B., Thorleifsson, G., Joud, M., Ali, M., Johnsson, E., Ajore, R., Sulem, P., Halvarsson, B. M., Eyjolfsson, G., Haraldsdottir, V., Hultman, C., Ingelsson, E., Kristinsson, S. Y., Kahler, A. K., Lenhoff, S., Masson, G., Mellqvist, U. H., Mansson, R., Nelander, S., Olafsson, I., Sigurethardottir, O., Steingrimsdottir, H., Vangsted, A., Vogel, U., Waage, A., Nahi, H., Gudbjartsson, D. F., Rafnar, T., Turesson, I., Gullberg, U., Stefansson, K., Hansson, M., Thorsteinsdottir, U. & Nilsson, B. Variants in ELL2 influencing immunoglobulin levels associate with multiple myeloma. *Nat Commun*. 2015; 6:7213.

109. Wei, X., Calvo-Vidal, M. N., Chen, S., Wu, G., Revuelta, M. V., Sun, J., Zhang, J., Walsh, M. F., Nichols, K. E., Joseph, V., Snyder, C., Vachon, C. M., McKay, J. D., Wang, S. P., Jayabalan, D. S., Jacobs, L. M., Becirovic, D., Waller, R. G., Artomov, M., Viale, A., Patel, J., Phillip, J., Chen-Kiang, S., Curtin, K., Salama, M., Atanackovic, D., Niesvizky, R., Landgren, O., Slager, S. L., Godley, L. A., Churpek, J., Garber, J. E., Anderson, K. C., Daly, M. J., Roeder, R. G. *et al.* Germline Lysine-Specific Demethylase 1 (LSD1/KDM1A) Mutations Confer Susceptibility to Multiple Myeloma. *Cancer Res*. 2018; 78(10):2747-2759.

110. Morgan, G. J., Walker, B. A. & Davies, F. E. The genetic architecture of multiple myeloma. *Nat Rev Cancer*. 2012; 12(5):335-348.

111. Fonseca, R., Debes-Marun, C. S., Picken, E. B., Dewald, G. W., Bryant, S. C., Winkler, J. M., Blood, E., Oken, M. M., Santana-Davila, R., Gonzalez-Paz, N., Kyle, R. A., Gertz, M. A., Dispenzieri, A., Lacy, M. Q. & Greipp, P. R. The recurrent IgH translocations are highly associated with nonhyperdiploid variant multiple myeloma. *Blood*. 2003; 102(7):2562-2567.

112. Smadja, N. V., Leroux, D., Soulier, J., Dumont, S., Arnould, C., Taviaux, S., Taillemite, J. L. & Bastard, C. Further cytogenetic characterization of multiple myeloma confirms that 14q32 translocations are a very rare event in hyperdiploid cases. *Genes Chromosomes Cancer*. 2003; 38(3):234-239.

113. Avet-Loiseau, H., Facon, T., Daviet, A., Godon, C., Rapp, M. J., Harousseau, J. L., Grosbois, B. & Bataille, R. 14q32 translocations and monosomy 13 observed in monoclonal gammopathy of undetermined significance delineate a multistep process for the oncogenesis of multiple myeloma. Intergroupe Francophone du Myelome. *Cancer Res*. 1999; 59(18):4546-4550.

114. Fonseca, R., Bailey, R. J., Ahmann, G. J., Rajkumar, S. V., Hoyer, J. D., Lust, J. A., Kyle, R. A., Gertz, M. A., Greipp, P. R. & Dewald, G. W. Genomic abnormalities in monoclonal gammopathy of undetermined significance. *Blood*. 2002; 100(4):1417-1424.

115. Chng, W. J., Van Wier, S. A., Ahmann, G. J., Winkler, J. M., Jalal, S. M., Bergsagel, P. L., Chesi, M., Trendle, M. C., Oken, M. M., Blood, E., Henderson, K., Santana-Davila, R., Kyle, R. A., Gertz, M. A., Lacy, M. Q., Dispenzieri, A., Greipp, P. R. & Fonseca, R. A validated FISH trisomy index demonstrates the hyperdiploid and nonhyperdiploid dichotomy in MGUS. *Blood*. 2005; 106(6):2156-2161.

116. Bianchi, G. & Munshi, N. C. Pathogenesis beyond the cancer clone(s) in multiple myeloma. *Blood*. 2015; 125(20):3049-3058.

117. Fonseca, R., Blood, E., Rue, M., Harrington, D., Oken, M. M., Kyle, R. A., Dewald, G. W., Van Ness, B., Van Wier, S. A., Henderson, K. J., Bailey, R. J. & Greipp, P. R. Clinical and biologic implications of recurrent genomic aberrations in myeloma. *Blood*. 2003; 101(11):4569-4575.

118. Keats, J. J., Reiman, T., Maxwell, C. A., Taylor, B. J., Larratt, L. M., Mant, M. J., Belch, A. R. & Pilarski, L. M. In multiple myeloma, t(4;14)(p16;q32) is an adverse prognostic factor irrespective of FGFR3 expression. *Blood*. 2003; 101(4):1520-1529.

119. Avet-Loiseau, H., Attal, M., Moreau, P., Charbonnel, C., Garban, F., Hulin, C., Leyvraz, S., Michallet, M., Yakoub-Agha, I., Garderet, L., Marit, G., Michaux, L., Voillat, L., Renaud, M., Grosbois, B., Guillerm, G., Benboubker, L., Monconduit, M., Thieblemont, C., Casassus, P., Caillot, D., Stoppa, A. M., Sotto, J. J., Wetterwald, M., Dumontet, C., Fuzibet, J. G., Azais, I., Dorvaux, V., Zandecki, M., Bataille, R., Minvielle, S., Harousseau, J. L., Facon, T. & Mathiot, C. Genetic abnormalities and survival in multiple myeloma: the experience of the Intergroupe Francophone du Myelome. *Blood*. 2007; 109(8):3489-3495.

120. Walker, B. A., Boyle, E. M., Wardell, C. P., Murison, A., Begum, D. B., Dahir, N. M., Proszek, P. Z., Johnson, D. C., Kaiser, M. F., Melchor, L., Aronson, L. I., Scales, M., Pawlyn, C., Mirabella, F., Jones, J. R., Brioli, A., Mikulasova, A., Cairns, D. A., Gregory, W. M., Quartilho, A., Drayson, M. T., Russell, N., Cook, G., Jackson, G. H., Leleu, X., Davies, F. E. & Morgan, G. J. Mutational Spectrum, Copy Number Changes, and Outcome: Results of a Sequencing Study of Patients With Newly Diagnosed Myeloma. *J Clin Oncol*. 2015; 33(33):3911-3920.

121. Shah, V., Sherborne, A. L., Walker, B. A., Johnson, D. C., Boyle, E. M., Ellis, S., Begum, D. B., Proszek, P. Z., Jones, J. R., Pawlyn, C., Savola, S., Jenner, M. W., Drayson, M. T., Owen, R. G., Houlston, R. S., Cairns, D. A., Gregory, W. M., Cook, G., Davies, F. E., Jackson, G. H., Morgan, G. J. & Kaiser, M. F. Prediction of outcome in newly diagnosed

myeloma: a meta-analysis of the molecular profiles of 1905 trial patients. *Leukemia*. 2018; 32(1):102-110.

122. Walker, B. A., Mavrommatis, K., Wardell, C. P., Ashby, T. C., Bauer, M., Davies, F. E., Rosenthal, A., Wang, H., Qu, P., Hoering, A., Samur, M., Towfic, F., Ortiz, M., Flynt, E., Yu, Z., Yang, Z., Rozelle, D., Obenauer, J., Trotter, M., Auclair, D., Keats, J., Bolli, N., Fulciniti, M., Szalat, R., Moreau, P., Durie, B., Stewart, A. K., Goldschmidt, H., Raab, M. S., Einsele, H., Sonneveld, P., San Miguel, J., Lonial, S., Jackson, G. H., Anderson, K. C. *et al.* Identification of novel mutational drivers reveals oncogene dependencies in multiple myeloma. *Blood*. 2018; 132(6):587-597.

123. Bergsagel, P. L., Chesi, M., Nardini, E., Brents, L. A., Kirby, S. L. & Kuehl, W. M. Promiscuous translocations into immunoglobulin heavy chain switch regions in multiple myeloma. *Proc Natl Acad Sci U S A*. 1996; 93(24):13931-13936.

124. Chesi, M., Bergsagel, P. L., Brents, L. A., Smith, C. M., Gerhard, D. S. & Kuehl, W. M. Dysregulation of cyclin D1 by translocation into an IgH gamma switch region in two multiple myeloma cell lines. *Blood*. 1996; 88(2):674-681.

125. Walker, B. A., Wardell, C. P., Murison, A., Boyle, E. M., Begum, D. B., Dahir, N. M., Proszek, P. Z., Melchor, L., Pawlyn, C., Kaiser, M. F. & Johnson, D. C. APOBEC family mutational signatures are associated with poor prognosis translocations in multiple myeloma. *Nat Commun*. 2015; 6:6997.

126. Lagana, A., Perumal, D., Melnekoff, D., Readhead, B., Kidd, B. A., Leshchenko, V., Kuo, P. Y., Keats, J., DeRome, M., Yesil, J., Auclair, D., Lonial, S., Chari, A., Cho, H. J., Barlogie, B., Jagannath, S., Dudley, J. T. & Parekh, S. Integrative network analysis identifies novel drivers of pathogenesis and progression in newly diagnosed multiple myeloma. *Leukemia*. 2018; 32(1):120-130.

127. Walker, B. A., Mavrommatis, K., Wardell, C. P., Ashby, T. C., Bauer, M., Davies, F., Rosenthal, A., Wang, H., Qu, P., Hoering, A., Samur, M., Towfic, F., Ortiz, M., Flynt, E., Yu, Z., Yang, Z., Rozelle, D., Obenauer, J., Trotter, M., Auclair, D., Keats, J., Bolli, N., Fulciniti, M., Szalat, R., Moreau, P., Durie, B., Stewart, A. K., Goldschmidt, H., Raab, M. S., Einsele, H., Sonneveld, P., San Miguel, J., Lonial, S., Jackson, G. H., Anderson, K. C. *et al.* A high-risk, Double-Hit, group of newly diagnosed myeloma identified by genomic analysis. *Leukemia*. 2019; 33(1):159-170.

128. Chesi, M., Nardini, E., Lim, R. S., Smith, K. D., Kuehl, W. M. & Bergsagel, P. L. The t(4;14) translocation in myeloma dysregulates both FGFR3 and a novel gene, MMSET, resulting in IgH/MMSET hybrid transcripts. *Blood*. 1998; 92(9):3025-3034.

129. Bergsagel, P. L., Kuehl, W. M., Zhan, F., Sawyer, J., Barlogie, B. & Shaughnessy, J., Jr. Cyclin D dysregulation: an early and unifying pathogenic event in multiple myeloma. *Blood*. 2005; 106(1):296-303.

130. Martinez-Garcia, E., Popovic, R., Min, D. J., Sweet, S. M., Thomas, P. M., Zamdborg, L., Heffner, A., Will, C., Lamy, L., Staudt, L. M., Levens, D. L., Kelleher, N. L. & Licht, J. D. The MMSET histone methyl transferase switches global histone methylation and alters gene expression in t(4;14) multiple myeloma cells. *Blood*. 2011; 117(1):211-220.

131. San Miguel, J. F., Schlag, R., Khuageva, N. K., Dimopoulos, M. A., Shpilberg, O., Kropff, M., Spicka, I., Petrucci, M. T., Palumbo, A., Samoilova, O. S., Dmoszynska, A., Abdulkadyrov, K. M., Schots, R., Jiang, B., Mateos, M. V., Anderson, K. C., Esseltine, D.

L., Liu, K., Cakana, A., van de Velde, H. & Richardson, P. G. Bortezomib plus melphalan and prednisone for initial treatment of multiple myeloma. *N Engl J Med*. 2008; 359(9):906-917.

132. Cavo, M., Tacchetti, P., Patriarca, F., Petrucci, M. T., Pantani, L., Galli, M., Di Raimondo, F., Crippa, C., Zamagni, E., Palumbo, A., Offidani, M., Corradini, P., Narni, F., Spadano, A., Pescosta, N., Deliliers, G. L., Ledda, A., Cellini, C., Caravita, T., Tosi, P. & Baccarani, M. Bortezomib with thalidomide plus dexamethasone compared with thalidomide plus dexamethasone as induction therapy before, and consolidation therapy after, double autologous stem-cell transplantation in newly diagnosed multiple myeloma: a randomised phase 3 study. *Lancet*. 2010; 376(9758):2075-2085.

133. Avet-Loiseau, H., Leleu, X., Roussel, M., Moreau, P., Guerin-Charbonnel, C., Caillot, D., Marit, G., Benboubker, L., Voillat, L., Mathiot, C., Kolb, B., Macro, M., Campion, L., Wetterwald, M., Stoppa, A. M., Hulin, C., Facon, T., Attal, M., Minvielle, S. & Harousseau, J. L. Bortezomib plus dexamethasone induction improves outcome of patients with t(4;14) myeloma but not outcome of patients with del(17p). *J Clin Oncol*. 2010; 28(30):4630-4634.

134. Sonneveld, P., Schmidt-Wolf, I. G., van der Holt, B., El Jarari, L., Bertsch, U., Salwender, H., Zweegman, S., Vellenga, E., Broyl, A., Blau, I. W., Weisel, K. C., Wittebol, S., Bos, G. M., Stevens-Kroef, M., Scheid, C., Pfreundschuh, M., Hose, D., Jauch, A., van der Velde, H., Raymakers, R., Schaafsma, M. R., Kersten, M. J., van Marwijk-Kooy, M., Duehrsen, U., Lindemann, W., Wijermans, P. W., Lokhorst, H. M. & Goldschmidt, H. M. Bortezomib induction and maintenance treatment in patients with newly diagnosed multiple myeloma: results of the randomized phase III HOVON-65/ GMMG-HD4 trial. *J Clin Oncol*. 2012; 30(24):2946-2955.

135. Chng, W. J., Dispenzieri, A., Chim, C. S., Fonseca, R., Goldschmidt, H., Lentzsch, S., Munshi, N., Palumbo, A., Miguel, J. S., Sonneveld, P., Cavo, M., Usmani, S., Durie, B. G. & Avet-Loiseau, H. IMWG consensus on risk stratification in multiple myeloma. *Leukemia*. 2014; 28(2):269-277.

136. Chesi, M., Bergsagel, P. L., Shonukan, O. O., Martelli, M. L., Brents, L. A., Chen, T., Schrock, E., Ried, T. & Kuehl, W. M. Frequent dysregulation of the c-maf proto-oncogene at 16q23 by translocation to an Ig locus in multiple myeloma. *Blood*. 1998; 91(12):4457-4463.

137. Hanamura, I., Iida, S., Akano, Y., Hayami, Y., Kato, M., Miura, K., Harada, S., Banno, S., Wakita, A., Kiyoi, H., Naoe, T., Shimizu, S., Sonta, S. I., Nitta, M., Taniwaki, M. & Ueda, R. Ectopic expression of MAFB gene in human myeloma cells carrying (14;20)(q32;q11) chromosomal translocations. *Jpn J Cancer Res*. 2001; 92(6):638-644.

138. Hurt, E. M., Wiestner, A., Rosenwald, A., Shaffer, A. L., Campo, E., Grogan, T., Bergsagel, P. L., Kuehl, W. M. & Staudt, L. M. Overexpression of c-maf is a frequent oncogenic event in multiple myeloma that promotes proliferation and pathological interactions with bone marrow stroma. *Cancer Cell*. 2004; 5(2):191-199.

139. Boersma-Vreugdenhil, G. R., Kuipers, J., Van Stralen, E., Peeters, T., Michaux, L., Hagemeijer, A., Pearson, P. L., Clevers, H. C. & Bast, B. J. The recurrent translocation t(14;20)(q32;q12) in multiple myeloma results in aberrant expression of MAFB: a molecular and genetic analysis of the chromosomal breakpoint. *Br J Haematol*. 2004; 126(3):355-363.

140. Shaughnessy, J., Jr., Gabrea, A., Qi, Y., Brents, L., Zhan, F., Tian, E., Sawyer, J., Barlogie, B., Bergsagel, P. L. & Kuehl, M. Cyclin D3 at 6p21 is dysregulated by recurrent chromosomal translocations to immunoglobulin loci in multiple myeloma. *Blood*. 2001; 98(1):217-223.

141. Smadja, N. V., Fruchart, C., Isnard, F., Louvet, C., Dutel, J. L., Cheron, N., Grange, M. J., Monconduit, M. & Bastard, C. Chromosomal analysis in multiple myeloma: cytogenetic evidence of two different diseases. *Leukemia*. 1998; 12(6):960-969.

142. Debes-Marun, C. S., Dewald, G. W., Bryant, S., Picken, E., Santana-Davila, R., Gonzalez-Paz, N., Winkler, J. M., Kyle, R. A., Gertz, M. A., Witzig, T. E., Dispenzieri, A., Lacy, M. Q., Rajkumar, S. V., Lust, J. A., Greipp, P. R. & Fonseca, R. Chromosome abnormalities clustering and its implications for pathogenesis and prognosis in myeloma. *Leukemia*. 2003; 17(2):427-436.

143. Brousseau, M., Leleu, X., Gerard, J., Gastinne, T., Godon, A., Genevieve, F., Dib, M., Lai, J. L., Facon, T. & Zandecki, M. Hyperdiploidy is a common finding in monoclonal gammopathy of undetermined significance and monosomy 13 is restricted to these hyperdiploid patients. *Clin Cancer Res*. 2007; 13(20):6026-6031.

144. Chng, W. J., Winkler, J. M., Greipp, P. R., Jalal, S. M., Bergsagel, P. L., Chesi, M., Trendle, M. C., Ahmann, G. J., Henderson, K., Blood, E., Oken, M. M., Hulbert, A., Van Wier, S. A., Santana-Davila, R., Kyle, R. A., Gertz, M. A., Lacy, M. Q., Dispenzieri, A. & Fonseca, R. Ploidy status rarely changes in myeloma patients at disease progression. *Leuk Res*. 2006; 30(3):266-271.

145. Manier, S., Salem, K. Z., Park, J., Landau, D. A., Getz, G. & Ghobrial, I. M. Genomic complexity of multiple myeloma and its clinical implications. *Nat Rev Clin Oncol*. 2017; 14(2):100-113.

146. Dutta, A. K., Hewett, D. R., Fink, J. L., Grady, J. P. & Zannettino, A. C. W. Cutting edge genomics reveal new insights into tumour development, disease progression and therapeutic impacts in multiple myeloma. *Br J Haematol*. 2017; 178(2):196-208.

147. Chapman, M. A., Lawrence, M. S., Keats, J. J., Cibulskis, K., Sougnez, C., Schinzel, A. C., Harview, C. L., Brunet, J. P., Ahmann, G. J., Adli, M., Anderson, K. C., Ardlie, K. G., Auclair, D., Baker, A., Bergsagel, P. L., Bernstein, B. E., Drier, Y., Fonseca, R., Gabriel, S. B., Hofmeister, C. C., Jagannath, S., Jakubowiak, A. J., Krishnan, A., Levy, J., Liefeld, T., Lonial, S., Mahan, S., Mfuko, B., Monti, S., Perkins, L. M., Onofrio, R., Pugh, T. J., Rajkumar, S. V., Ramos, A. H., Siegel, D. S. *et al.* Initial genome sequencing and analysis of multiple myeloma. *Nature*. 2011; 471(7339):467-472.

148. Lohr, J. G., Stojanov, P., Carter, S. L., Cruz-Gordillo, P., Lawrence, M. S., Auclair, D., Sougnez, C., Knoechel, B., Gould, J., Saksena, G., Cibulskis, K., McKenna, A., Chapman, M. A., Straussman, R., Levy, J., Perkins, L. M., Keats, J. J., Schumacher, S. E., Rosenberg, M., Getz, G. & Golub, T. R. Widespread genetic heterogeneity in multiple myeloma: implications for targeted therapy. *Cancer Cell*. 2014; 25(1):91-101.

149. Bolli, N., Avet-Loiseau, H., Wedge, D. C., Van Loo, P., Alexandrov, L. B., Martincorena, I., Dawson, K. J., Iorio, F., Nik-Zainal, S., Bignell, G. R., Hinton, J. W., Li, Y., Tubio, J. M., McLaren, S., S, O. M., Butler, A. P., Teague, J. W., Mudie, L., Anderson, E., Rashid, N., Tai, Y. T., Shammas, M. A., Sperling, A. S., Fulciniti, M., Richardson, P. G., Parmigiani, G., Magrangeas, F., Minvielle, S., Moreau, P., Attal, M., Facon, T., Futreal, P.

A., Anderson, K. C., Campbell, P. J. & Munshi, N. C. Heterogeneity of genomic evolution and mutational profiles in multiple myeloma. *Nat Commun*. 2014; 5:2997.

150. Bolli, N., Biancon, G., Moarii, M., Gimondi, S., Li, Y., de Philippis, C., Maura, F., Sathiaseelan, V., Tai, Y. T., Mudie, L., O'Meara, S., Raine, K., Teague, J. W., Butler, A. P., Carniti, C., Gerstung, M., Bagratuni, T., Kastritis, E., Dimopoulos, M., Corradini, P., Anderson, K. C., Moreau, P., Minvielle, S., Campbell, P. J., Papaemmanuil, E., Avet-Loiseau, H. & Munshi, N. C. Analysis of the genomic landscape of multiple myeloma highlights novel prognostic markers and disease subgroups. *Leukemia*. 2018; 32(12):2604-2616.

151. Zhu, Y. X., Shi, C. X., Bruins, L. A., Jedlowski, P., Wang, X., Kortum, K. M., Luo, M., Ahmann, J. M., Braggio, E. & Stewart, A. K. Loss of FAM46C Promotes Cell Survival in Myeloma. *Cancer Res*. 2017; 77(16):4317-4327.

152. Mroczek, S., Chlebowska, J., Kulinski, T. M., Gewartowska, O., Gruchota, J., Cysewski, D., Liudkovska, V., Borsuk, E., Nowis, D. & Dziembowski, A. The non-canonical poly(A) polymerase FAM46C acts as an onco-suppressor in multiple myeloma. *Nat Commun*. 2017; 8(1):619.

153. Keats, J. J., Fonseca, R., Chesi, M., Schop, R., Baker, A., Chng, W. J., Van Wier, S., Tiedemann, R., Shi, C. X., Sebag, M., Braggio, E., Henry, T., Zhu, Y. X., Fogle, H., Price-Troska, T., Ahmann, G., Mancini, C., Brents, L. A., Kumar, S., Greipp, P., Dispenzieri, A., Bryant, B., Mulligan, G., Bruhn, L., Barrett, M., Valdez, R., Trent, J., Stewart, A. K., Carpten, J. & Bergsagel, P. L. Promiscuous mutations activate the noncanonical NF-kappaB pathway in multiple myeloma. *Cancer Cell*. 2007; 12(2):131-144.

154. Annunziata, C. M., Davis, R. E., Demchenko, Y., Bellamy, W., Gabrea, A., Zhan, F., Lenz, G., Hanamura, I., Wright, G., Xiao, W., Dave, S., Hurt, E. M., Tan, B., Zhao, H., Stephens, O., Santra, M., Williams, D. R., Dang, L., Barlogie, B., Shaughnessy, J. D., Jr., Kuehl, W. M. & Staudt, L. M. Frequent engagement of the classical and alternative NF-kappaB pathways by diverse genetic abnormalities in multiple myeloma. *Cancer Cell*. 2007; 12(2):115-130.

155. Chng, W. J., Price-Troska, T., Gonzalez-Paz, N., Van Wier, S., Jacobus, S., Blood, E., Henderson, K., Oken, M., Van Ness, B., Greipp, P., Rajkumar, S. V. & Fonseca, R. Clinical significance of TP53 mutation in myeloma. *Leukemia*. 2007; 21(3):582-584.

156. Avet-Loiseau, H., Gerson, F., Magrangeas, F., Minvielle, S., Harousseau, J. L. & Bataille, R. Rearrangements of the c-myc oncogene are present in 15% of primary human multiple myeloma tumors. *Blood*. 2001; 98(10):3082-3086.

157. Walker, B. A., Wardell, C. P., Brioli, A., Boyle, E., Kaiser, M. F., Begum, D. B., Dahir, N. B., Johnson, D. C., Ross, F. M., Davies, F. E. & Morgan, G. J. Translocations at 8q24 juxtapose MYC with genes that harbor superenhancers resulting in overexpression and poor prognosis in myeloma patients. *Blood Cancer J*. 2014; 4:e191.

158. Affer, M., Chesi, M., Chen, W. D., Keats, J. J., Demchenko, Y. N., Tamizhmani, K., Garbitt, V. M., Riggs, D. L., Brents, L. A., Roschke, A. V., Van Wier, S., Fonseca, R., Bergsagel, P. L. & Kuehl, W. M. Promiscuous MYC locus rearrangements hijack enhancers but mostly super-enhancers to dysregulate MYC expression in multiple myeloma. *Leukemia*. 2014; 28(8):1725-1735.

159. Weinhold, N., Kirn, D., Seckinger, A., Hielscher, T., Granzow, M., Bertsch, U., Egerer, G., Salwender, H., Blau, I. W., Weisel, K., Hillengass, J., Raab, M. S., Hose, D., Goldschmidt, H. & Jauch, A. Concomitant gain of 1q21 and MYC translocation define a poor prognostic subgroup of hyperdiploid multiple myeloma. *Haematologica*. 2016; 101(3):e116-119.

160. Chng, W. J., Huang, G. F., Chung, T. H., Ng, S. B., Gonzalez-Paz, N., Troska-Price, T., Mulligan, G., Chesi, M., Bergsagel, P. L. & Fonseca, R. Clinical and biological implications of MYC activation: a common difference between MGUS and newly diagnosed multiple myeloma. *Leukemia*. 2011; 25(6):1026-1035.

161. Morgan, G. J., He, J., Tytarenko, R., Patel, P., Stephens, O. W., Zhong, S., Deshpande, S., Bauer, M., Weinhold, N., Schinke, C., Rasche, L., Bailey, M., Ali, S., Ross, J., Miller, V. A., Stephens, P., Thanendrarajan, S., Zangari, M., van Rhee, F., Mughal, T., Davies, F. E. & Walker, B. A. Kinase domain activation through gene rearrangement in multiple myeloma. *Leukemia*. 2018; 32(11):2435-2444.

162. Walker, B. A., Leone, P. E., Chiecchio, L., Dickens, N. J., Jenner, M. W., Boyd, K. D., Johnson, D. C., Gonzalez, D., Dagrada, G. P., Protheroe, R. K., Konn, Z. J., Stockley, D. M., Gregory, W. M., Davies, F. E., Ross, F. M. & Morgan, G. J. A compendium of myeloma-associated chromosomal copy number abnormalities and their prognostic value. *Blood*. 2010; 116(15):e56-65.

163. Fonseca, R., Oken, M. M., Harrington, D., Bailey, R. J., Van Wier, S. A., Henderson, K. J., Kay, N. E., Van Ness, B., Greipp, P. R. & Dewald, G. W. Deletions of chromosome 13 in multiple myeloma identified by interphase FISH usually denote large deletions of the q arm or monosomy. *Leukemia*. 2001; 15(6):981-986.

164. Boyd, K. D., Ross, F. M., Walker, B. A., Wardell, C. P., Tapper, W. J., Chiecchio, L., Dagrada, G., Konn, Z. J., Gregory, W. M., Jackson, G. H., Child, J. A., Davies, F. E. & Morgan, G. J. Mapping of chromosome 1p deletions in myeloma identifies FAM46C at 1p12 and CDKN2C at 1p32.3 as being genes in regions associated with adverse survival. *Clin Cancer Res*. 2011; 17(24):7776-7784.

165. Leone, P. E., Walker, B. A., Jenner, M. W., Chiecchio, L., Dagrada, G., Protheroe, R. K., Johnson, D. C., Dickens, N. J., Brito, J. L., Else, M., Gonzalez, D., Ross, F. M., Chen-Kiang, S., Davies, F. E. & Morgan, G. J. Deletions of CDKN2C in multiple myeloma: biological and clinical implications. *Clin Cancer Res*. 2008; 14(19):6033-6041.

166. Shaughnessy, J. Amplification and overexpression of CKS1B at chromosome band 1q21 is associated with reduced levels of p27Kip1 and an aggressive clinical course in multiple myeloma. *Hematology*. 2005; 10 Suppl 1:117-126.

167. Zhan, F., Colla, S., Wu, X., Chen, B., Stewart, J. P., Kuehl, W. M., Barlogie, B. & Shaughnessy, J. D., Jr. CKS1B, overexpressed in aggressive disease, regulates multiple myeloma growth and survival through SKP2- and p27Kip1-dependent and -independent mechanisms. *Blood*. 2007; 109(11):4995-5001.

168. Shi, L., Wang, S., Zangari, M., Xu, H., Cao, T. M., Xu, C., Wu, Y., Xiao, F., Liu, Y., Yang, Y., Salama, M., Li, G., Tricot, G. & Zhan, F. Over-expression of CKS1B activates both MEK/ERK and JAK/STAT3 signaling pathways and promotes myeloma cell drug-resistance. *Oncotarget*. 2010; 1(1):22-33.

169. Marchesini, M., Ogoti, Y., Fiorini, E., Aktas Samur, A., Nezi, L., D'Anca, M., Storti, P., Samur, M. K., Ganan-Gomez, I., Fulciniti, M. T., Mistry, N., Jiang, S., Bao, N., Marchica, V., Neri, A., Bueso-Ramos, C., Wu, C. J., Zhang, L., Liang, H., Peng, X., Giuliani, N., Draetta, G., Clise-Dwyer, K., Kantarjian, H., Munshi, N., Orlowski, R., Garcia-Manero, G., DePinho, R. A. & Colla, S. ILF2 Is a Regulator of RNA Splicing and DNA Damage Response in 1q21-Amplified Multiple Myeloma. *Cancer Cell*. 2017; 32(1):88-100.e106.

170. Thanendrarajan, S., Tian, E., Qu, P., Mathur, P., Schinke, C., van Rhee, F., Zangari, M., Rasche, L., Weinhold, N., Alapat, D., Bellamy, W., Ashby, C., Mattox, S., Epstein, J., Yaccoby, S., Barlogie, B., Hoering, A., Bauer, M., Walker, B. A., Davies, F. E. & Morgan, G. J. The level of deletion 17p and bi-allelic inactivation of TP53 has a significant impact on clinical outcome in multiple myeloma. *Haematologica*. 2017; 102(9):e364-e367.

171. Shah, V., Johnson, D. C., Sherborne, A. L., Ellis, S., Aldridge, F. M., Howard-Reeves, J., Begum, F., Price, A., Kendall, J., Chiecchio, L., Savola, S., Jenner, M. W., Drayson, M. T., Owen, R. G., Gregory, W. M., Morgan, G. J., Davies, F. E., Houlston, R. S., Cook, G., Cairns, D. A., Jackson, G. & Kaiser, M. F. Subclonal TP53 copy number is associated with prognosis in multiple myeloma. *Blood*. 2018; 132(23):2465-2469.

172. Thakurta, A., Ortiz, M., Blecua, P., Towfic, F., Corre, J., Serbina, N. V., Flynt, E., Yu, Z., Yang, Z., Palumbo, A., Dimopoulos, M. A., Guttierez, N., Goldschmidt, H., Sonneveld, P. & Avet-Loiseau, H. High sub-clonal fraction of 17p deletion is associated with poor prognosis in Multiple Myeloma. *Blood*. 2019; 133(11):1217-1221.

173. An, G., Li, Z., Tai, Y. T., Acharya, C., Li, Q., Qin, X., Yi, S., Xu, Y., Feng, X., Li, C., Zhao, J., Shi, L., Zang, M., Deng, S., Sui, W., Hao, M., Zou, D., Zhao, Y., Qi, J., Cheng, T., Ru, K., Wang, J., Anderson, K. C. & Qiu, L. The impact of clone size on the prognostic value of chromosome aberrations by fluorescence in situ hybridization in multiple myeloma. *Clin Cancer Res*. 2015; 21(9):2148-2156.

174. Zhan, F., Hardin, J., Kordsmeier, B., Bumm, K., Zheng, M., Tian, E., Sanderson, R., Yang, Y., Wilson, C., Zangari, M., Anaissie, E., Morris, C., Muwalla, F., van Rhee, F., Fassas, A., Crowley, J., Tricot, G., Barlogie, B. & Shaughnessy, J., Jr. Global gene expression profiling of multiple myeloma, monoclonal gammopathy of undetermined significance, and normal bone marrow plasma cells. *Blood*. 2002; 99(5):1745-1757.

175. Davies, F. E., Dring, A. M., Li, C., Rawstron, A. C., Shammas, M. A., O'Connor, S. M., Fenton, J. A., Hideshima, T., Chauhan, D., Tai, I. T., Robinson, E., Auclair, D., Rees, K., Gonzalez, D., Ashcroft, A. J., Dasgupta, R., Mitsiades, C., Mitsiades, N., Chen, L. B., Wong, W. H., Munshi, N. C., Morgan, G. J. & Anderson, K. C. Insights into the multistep transformation of MGUS to myeloma using microarray expression analysis. *Blood*. 2003; 102(13):4504-4511.

176. Zhan, F., Barlogie, B., Arzoumanian, V., Huang, Y., Williams, D. R., Hollmig, K., Pineda-Roman, M., Tricot, G., van Rhee, F., Zangari, M., Dhodapkar, M. & Shaughnessy, J. D., Jr. Gene-expression signature of benign monoclonal gammopathy evident in multiple myeloma is linked to good prognosis. *Blood*. 2007; 109(4):1692-1700.

177. Lopez-Corral, L., Corchete, L. A., Sarasquete, M. E., Mateos, M. V., Garcia-Sanz, R., Ferminan, E., Lahuerta, J. J., Blade, J., Oriol, A., Teruel, A. I., Martino, M. L., Hernandez, J., Hernandez-Rivas, J. M., Burguillo, F. J., San Miguel, J. F. & Gutierrez, N. C. Transcriptome analysis reveals molecular profiles associated with evolving steps of monoclonal gammopathies. *Haematologica*. 2014; 99(8):1365-1372.

178. Anguiano, A., Tuchman, S. A., Acharya, C., Salter, K., Gasparetto, C., Zhan, F., Dhodapkar, M., Nevins, J., Barlogie, B., Shaughnessy, J. D., Jr. & Potti, A. Gene expression profiles of tumor biology provide a novel approach to prognosis and may guide the selection of therapeutic targets in multiple myeloma. *J Clin Oncol*. 2009; 27(25):4197-4203.

179. Zhan, F., Huang, Y., Colla, S., Stewart, J. P., Hanamura, I., Gupta, S., Epstein, J., Yaccoby, S., Sawyer, J., Burington, B., Anaissie, E., Hollmig, K., Pineda-Roman, M., Tricot, G., van Rhee, F., Walker, R., Zangari, M., Crowley, J., Barlogie, B. & Shaughnessy, J. D., Jr. The molecular classification of multiple myeloma. *Blood*. 2006; 108(6):2020-2028.

180. Broyl, A., Hose, D., Lokhorst, H., de Knegt, Y., Peeters, J., Jauch, A., Bertsch, U., Buijs, A., Stevens-Kroef, M., Beverloo, H. B., Vellenga, E., Zweegman, S., Kersten, M. J., van der Holt, B., el Jarari, L., Mulligan, G., Goldschmidt, H., van Duin, M. & Sonneveld, P. Gene expression profiling for molecular classification of multiple myeloma in newly diagnosed patients. *Blood*. 2010; 116(14):2543-2553.

181. Weinhold, N., Heuck, C. J., Rosenthal, A., Thanendrarajan, S., Stein, C. K., Van Rhee, F., Zangari, M., Hoering, A., Tian, E., Davies, F. E., Barlogie, B. & Morgan, G. J. Clinical value of molecular subtyping multiple myeloma using gene expression profiling. *Leukemia*. 2016; 30(2):423-430.

182. Decaux, O., Lode, L., Magrangeas, F., Charbonnel, C., Gouraud, W., Jezequel, P., Attal, M., Harousseau, J. L., Moreau, P., Bataille, R., Campion, L., Avet-Loiseau, H. & Minvielle, S. Prediction of survival in multiple myeloma based on gene expression profiles reveals cell cycle and chromosomal instability signatures in high-risk patients and hyperdiploid signatures in low-risk patients: a study of the Intergroupe Francophone du Myelome. *J Clin Oncol*. 2008; 26(29):4798-4805.

183. Chung, T. H., Mulligan, G., Fonseca, R. & Chng, W. J. A novel measure of chromosome instability can account for prognostic difference in multiple myeloma. *PLoS One*. 2013; 8(6):e66361.

184. Chng, W. J., Braggio, E., Mulligan, G., Bryant, B., Remstein, E., Valdez, R., Dogan, A. & Fonseca, R. The centrosome index is a powerful prognostic marker in myeloma and identifies a cohort of patients that might benefit from aurora kinase inhibition. *Blood*. 2008; 111(3):1603-1609.

185. Moreaux, J., Klein, B., Bataille, R., Descamps, G., Maiga, S., Hose, D., Goldschmidt, H., Jauch, A., Reme, T., Jourdan, M., Amiot, M. & Pellat-Deceunynck, C. A high-risk signature for patients with multiple myeloma established from the molecular classification of human myeloma cell lines. *Haematologica*. 2011; 96(4):574-582.

186. Dickens, N. J., Walker, B. A., Leone, P. E., Johnson, D. C., Brito, J. L., Zeisig, A., Jenner, M. W., Boyd, K. D., Gonzalez, D., Gregory, W. M., Ross, F. M., Davies, F. E. & Morgan, G. J. Homozygous deletion mapping in myeloma samples identifies genes and an expression signature relevant to pathogenesis and outcome. *Clin Cancer Res*. 2010; 16(6):1856-1864.

187. Hose, D., Reme, T., Hielscher, T., Moreaux, J., Messner, T., Seckinger, A., Benner, A., Shaughnessy, J. D., Jr., Barlogie, B., Zhou, Y., Hillengass, J., Bertsch, U., Neben, K., Mohler, T., Rossi, J. F., Jauch, A., Klein, B. & Goldschmidt, H. Proliferation is a central independent prognostic factor and target for personalized and risk-adapted treatment in multiple myeloma. *Haematologica*. 2011; 96(1):87-95.

188. Kuiper, R., Broyl, A., de Knegt, Y., van Vliet, M. H., van Beers, E. H., van der Holt, B., el Jarari, L., Mulligan, G., Gregory, W., Morgan, G., Goldschmidt, H., Lokhorst, H. M., van Duin, M. & Sonneveld, P. A gene expression signature for high-risk multiple myeloma. *Leukemia*. 2012; 26(11):2406-2413.

189. Shaughnessy, J. D., Jr., Zhan, F., Burington, B. E., Huang, Y., Colla, S., Hanamura, I., Stewart, J. P., Kordsmeier, B., Randolph, C., Williams, D. R., Xiao, Y., Xu, H., Epstein, J., Anaissie, E., Krishna, S. G., Cottler-Fox, M., Hollmig, K., Mohiuddin, A., Pineda-Roman, M., Tricot, G., van Rhee, F., Sawyer, J., Alsayed, Y., Walker, R., Zangari, M., Crowley, J. & Barlogie, B. A validated gene expression model of high-risk multiple myeloma is defined by deregulated expression of genes mapping to chromosome 1. *Blood*. 2007; 109(6):2276-2284.

190. Chng, W. J., Chung, T. H., Kumar, S., Usmani, S., Munshi, N., Avet-Loiseau, H., Goldschmidt, H., Durie, B. & Sonneveld, P. Gene signature combinations improve prognostic stratification of multiple myeloma patients. *Leukemia*. 2016; 30(5):1071-1078.

191. Szalat, R., Avet-Loiseau, H. & Munshi, N. C. Gene Expression Profiles in Myeloma: Ready for the Real World? *Clin Cancer Res*. 2016; 22(22):5434-5442.

192. Pawlyn, C., Kaiser, M. F., Heuck, C., Melchor, L., Wardell, C. P., Murison, A., Chavan, S. S., Johnson, D. C., Begum, D. B., Dahir, N. M., Proszek, P. Z., Cairns, D. A., Boyle, E. M., Jones, J. R., Cook, G., Drayson, M. T., Owen, R. G., Gregory, W. M., Jackson, G. H., Barlogie, B., Davies, F. E., Walker, B. A. & Morgan, G. J. The Spectrum and Clinical Impact of Epigenetic Modifier Mutations in Myeloma. *Clin Cancer Res*. 2016; 22(23):5783-5794.

193. Salhia, B., Baker, A., Ahmann, G., Auclair, D., Fonseca, R. & Carpten, J. DNA methylation analysis determines the high frequency of genic hypomethylation and low frequency of hypermethylation events in plasma cell tumors. *Cancer Res*. 2010; 70(17):6934-6944.

194. Walker, B. A., Wardell, C. P., Chiecchio, L., Smith, E. M., Boyd, K. D., Neri, A., Davies, F. E., Ross, F. M. & Morgan, G. J. Aberrant global methylation patterns affect the molecular pathogenesis and prognosis of multiple myeloma. *Blood*. 2011; 117(2):553-562.

195. Heuck, C. J., Mehta, J., Bhagat, T., Gundabolu, K., Yu, Y., Khan, S., Chrysofakis, G., Schinke, C., Tariman, J., Vickrey, E., Pulliam, N., Nischal, S., Zhou, L., Bhattacharyya, S., Meagher, R., Hu, C., Maqbool, S., Suzuki, M., Parekh, S., Reu, F., Steidl, U., Greally, J., Verma, A. & Singhal, S. B. Myeloma is characterized by stage-specific alterations in DNA methylation that occur early during myelomagenesis. *J Immunol*. 2013; 190(6):2966-2975.

196. Agirre, X., Castellano, G., Pascual, M., Heath, S., Kulis, M., Segura, V., Bergmann, A., Esteve, A., Merkel, A., Raineri, E., Agueda, L., Blanc, J., Richardson, D., Clarke, L., Datta, A., Russinol, N., Queiros, A. C., Beekman, R., Rodriguez-Madoz, J. R., Jose-Eneriz, E. S., Fang, F., Gutierrez, N. C., Garcia-Verdugo, J. M., Robson, M. I., Schirmer, E. C., Guruceaga, E., Martens, J. H., Gut, M., Calasanz, M. J., Flicek, P., Siebert, R., Campo, E., Miguel, J. F., Melnick, A., Stunnenberg, H. G. *et al.* Whole-epigenome analysis in multiple myeloma reveals DNA hypermethylation of B cell-specific enhancers. *Genome Res*. 2015; 25(4):478-487.

197. Eden, A., Gaudet, F., Waghmare, A. & Jaenisch, R. Chromosomal instability and tumors promoted by DNA hypomethylation. *Science*. 2003; 300(5618):455.

198. Kaiser, M. F., Johnson, D. C., Wu, P., Walker, B. A., Brioli, A., Mirabella, F., Wardell, C. P., Melchor, L., Davies, F. E. & Morgan, G. J. Global methylation analysis identifies prognostically important epigenetically inactivated tumor suppressor genes in multiple myeloma. *Blood*. 2013; 122(2):219-226.

199. Agarwal, P., Alzrigat, M., Parraga, A. A., Enroth, S., Singh, U., Ungerstedt, J., Osterborg, A., Brown, P. J., Ma, A., Jin, J., Nilsson, K., Oberg, F., Kalushkova, A. & Jernberg-Wiklund, H. Genome-wide profiling of histone H3 lysine 27 and lysine 4 trimethylation in multiple myeloma reveals the importance of Polycomb gene targeting and highlights EZH2 as a potential therapeutic target. *Oncotarget*. 2016; 7(6):6809-6823.

200. Pawlyn, C., Bright, M. D., Buros, A. F., Stein, C. K., Walters, Z., Aronson, L. I., Mirabella, F., Jones, J. R., Kaiser, M. F., Walker, B. A., Jackson, G. H., Clarke, P. A., Bergsagel, P. L., Workman, P., Chesi, M., Morgan, G. J. & Davies, F. E. Overexpression of EZH2 in multiple myeloma is associated with poor prognosis and dysregulation of cell cycle control. *Blood Cancer J*. 2017; 7(3):e549.

201. Mithraprabhu, S., Kalff, A., Chow, A., Khong, T. & Spencer, A. Dysregulated Class I histone deacetylases are indicators of poor prognosis in multiple myeloma. *Epigenetics*. 2014; 9(11):1511-1520.

202. Maiso, P., Carvajal-Vergara, X., Ocio, E. M., Lopez-Perez, R., Mateo, G., Gutierrez, N., Atadja, P., Pandiella, A. & San Miguel, J. F. The histone deacetylase inhibitor LBH589 is a potent antimyeloma agent that overcomes drug resistance. *Cancer Res*. 2006; 66(11):5781-5789.

203. San-Miguel, J. F., Hungria, V. T., Yoon, S. S., Beksac, M., Dimopoulos, M. A., Elghandour, A., Jedrzejczak, W. W., Gunther, A., Nakorn, T. N., Siritanaratkul, N., Corradini, P., Chuncharunee, S., Lee, J. J., Schlossman, R. L., Shelekhova, T., Yong, K., Tan, D., Numbenjapon, T., Cavenagh, J. D., Hou, J., LeBlanc, R., Nahi, H., Qiu, L., Salwender, H., Pulini, S., Moreau, P., Warzocha, K., White, D., Blade, J., Chen, W., de la Rubia, J., Gimsing, P., Lonial, S., Kaufman, J. L., Ocio, E. M. *et al.* Panobinostat plus bortezomib and dexamethasone versus placebo plus bortezomib and dexamethasone in patients with relapsed or relapsed and refractory multiple myeloma: a multicentre, randomised, double-blind phase 3 trial. *Lancet Oncol*. 2014; 15(11):1195-1206.

204. Jin, Y., Chen, K., De Paepe, A., Hellqvist, E., Krstic, A. D., Metang, L., Gustafsson, C., Davis, R. E., Levy, Y. M., Surapaneni, R., Wallblom, A., Nahi, H., Mansson, R. & Lin, Y. C. Active enhancer and chromatin accessibility landscapes chart the regulatory network of primary multiple myeloma. *Blood*. 2018; 131(19):2138-2150.

205. Pichiorri, F., Suh, S. S., Ladetto, M., Kuehl, M., Palumbo, T., Drandi, D., Taccioli, C., Zanesi, N., Alder, H., Hagan, J. P., Munker, R., Volinia, S., Boccadoro, M., Garzon, R., Palumbo, A., Aqeilan, R. I. & Croce, C. M. MicroRNAs regulate critical genes associated with multiple myeloma pathogenesis. *Proc Natl Acad Sci U S A*. 2008; 105(35):12885-12890.

206. Roccaro, A. M., Sacco, A., Thompson, B., Leleu, X., Azab, A. K., Azab, F., Runnels, J., Jia, X., Ngo, H. T., Melhem, M. R., Lin, C. P., Ribatti, D., Rollins, B. J., Witzig, T. E., Anderson, K. C. & Ghobrial, I. M. MicroRNAs 15a and 16 regulate tumor proliferation in multiple myeloma. *Blood*. 2009; 113(26):6669-6680.

207. Corthals, S. L., Sun, S. M., Kuiper, R., de Knegt, Y., Broyl, A., van der Holt, B., Beverloo, H. B., Peeters, J. K., el Jarari, L., Lokhorst, H. M., Zweegman, S., Jongen-

Lavrencic, M. & Sonneveld, P. MicroRNA signatures characterize multiple myeloma patients. *Leukemia*. 2011; 25(11):1784-1789.

208. Chi, J., Ballabio, E., Chen, X. H., Kusec, R., Taylor, S., Hay, D., Tramonti, D., Saunders, N. J., Littlewood, T., Pezzella, F., Boultwood, J., Wainscoat, J. S., Hatton, C. S. & Lawrie, C. H. MicroRNA expression in multiple myeloma is associated with genetic subtype, isotype and survival. *Biol Direct*. 2011; 6:23.

209. Manier, S., Powers, J. T., Sacco, A., Glavey, S. V., Huynh, D., Reagan, M. R., Salem, K. Z., Moschetta, M., Shi, J., Mishima, Y., Roche-Lestienne, C., Leleu, X., Roccaro, A. M., Daley, G. Q. & Ghobrial, I. M. The LIN28B/let-7 axis is a novel therapeutic pathway in multiple myeloma. *Leukemia*. 2017; 31(4):853-860.

210. Pichiorri, F., Suh, S. S., Rocci, A., De Luca, L., Taccioli, C., Santhanam, R., Zhou, W., Benson, D. M., Jr., Hofmainster, C., Alder, H., Garofalo, M., Di Leva, G., Volinia, S., Lin, H. J., Perrotti, D., Kuehl, M., Aqeilan, R. I., Palumbo, A. & Croce, C. M. Downregulation of p53-inducible microRNAs 192, 194, and 215 impairs the p53/MDM2 autoregulatory loop in multiple myeloma development. *Cancer Cell*. 2010; 18(4):367-381.

211. Manier, S., Liu, C. J., Avet-Loiseau, H., Park, J., Shi, J., Campigotto, F., Salem, K. Z., Huynh, D., Glavey, S. V., Rivotto, B., Sacco, A., Roccaro, A. M., Bouyssou, J., Minvielle, S., Moreau, P., Facon, T., Leleu, X., Weller, E., Trippa, L. & Ghobrial, I. M. Prognostic role of circulating exosomal miRNAs in multiple myeloma. *Blood*. 2017; 129(17):2429-2436.

212. Walker, B. A., Wardell, C. P., Melchor, L., Hulkki, S., Potter, N. E., Johnson, D. C., Fenwick, K., Kozarewa, I., Gonzalez, D., Lord, C. J., Ashworth, A., Davies, F. E. & Morgan, G. J. Intraclonal heterogeneity and distinct molecular mechanisms characterize the development of t(4;14) and t(11;14) myeloma. *Blood*. 2012; 120(5):1077-1086.

213. Egan, J. B., Shi, C. X., Tembe, W., Christoforides, A., Kurdoglu, A., Sinari, S., Middha, S., Asmann, Y., Schmidt, J., Braggio, E., Keats, J. J., Fonseca, R., Bergsagel, P. L., Craig, D. W., Carpten, J. D. & Stewart, A. K. Whole-genome sequencing of multiple myeloma from diagnosis to plasma cell leukemia reveals genomic initiating events, evolution, and clonal tides. *Blood*. 2012; 120(5):1060-1066.

214. Keats, J. J., Chesi, M., Egan, J. B., Garbitt, V. M., Palmer, S. E., Braggio, E., Van Wier, S., Blackburn, P. R., Baker, A. S., Dispenzieri, A., Kumar, S., Rajkumar, S. V., Carpten, J. D., Barrett, M., Fonseca, R., Stewart, A. K. & Bergsagel, P. L. Clonal competition with alternating dominance in multiple myeloma. *Blood*. 2012; 120(5):1067-1076.

215. Walker, B. A., Wardell, C. P., Melchor, L., Brioli, A., Johnson, D. C., Kaiser, M. F., Mirabella, F., Lopez-Corral, L., Humphray, S., Murray, L., Ross, M., Bentley, D., Gutierrez, N. C., Garcia-Sanz, R., San Miguel, J., Davies, F. E., Gonzalez, D. & Morgan, G. J. Intraclonal heterogeneity is a critical early event in the development of myeloma and precedes the development of clinical symptoms. *Leukemia*. 2014; 28(2):384-390.

216. Melchor, L., Brioli, A., Wardell, C. P., Murison, A., Potter, N. E., Kaiser, M. F., Fryer, R. A., Johnson, D. C., Begum, D. B., Hulkki Wilson, S., Vijayaraghavan, G., Titley, I., Cavo, M., Davies, F. E., Walker, B. A. & Morgan, G. J. Single-cell genetic analysis reveals the composition of initiating clones and phylogenetic patterns of branching and parallel evolution in myeloma. *Leukemia*. 2014; 28(8):1705-1715.

217. Jones, J. R., Weinhold, N., Ashby, C., Walker, B. A., Wardell, C., Pawlyn, C., Rasche, L., Melchor, L., Cairns, D. A., Gregory, W. M., Johnson, D., Begum, D. B., Ellis, S., Sherborne, A. L., Cook, G., Kaiser, M. F., Drayson, M. T., Owen, R. G., Jackson, G. H., Davies, F. E., Greaves, M. & Morgan, G. J. Clonal evolution in myeloma: the impact of maintenance lenalidomide and depth of response on the genetics and sub-clonal structure of relapsed disease in uniformly treated newly diagnosed patients. *Haematologica*. 2019; [Epub ahead of print] doi: 10.3324/haematol.2018.202200.

218. Rasche, L., Chavan, S. S., Stephens, O. W., Patel, P. H., Tytarenko, R., Ashby, C., Bauer, M., Stein, C., Deshpande, S., Wardell, C., Buzder, T., Molnar, G., Zangari, M., van Rhee, F., Thanendrarajan, S., Schinke, C., Epstein, J., Davies, F. E., Walker, B. A., Meissner, T., Barlogie, B., Morgan, G. J. & Weinhold, N. Spatial genomic heterogeneity in multiple myeloma revealed by multi-region sequencing. *Nat Commun*. 2017; 8(1):268.

219. Landau, D. A., Carter, S. L., Getz, G. & Wu, C. J. Clonal evolution in hematological malignancies and therapeutic implications. *Leukemia*. 2014; 28(1):34-43.

220. Corre, J., Munshi, N. & Avet-Loiseau, H. Genetics of multiple myeloma: another heterogeneity level? *Blood*. 2015; 125(12):1870-1876.

221. Weinhold, N., Ashby, C., Rasche, L., Chavan, S. S., Stein, C., Stephens, O. W., Tytarenko, R., Bauer, M. A., Meissner, T., Deshpande, S., Patel, P. H., Buzder, T., Molnar, G., Peterson, E. A., van Rhee, F., Zangari, M., Thanendrarajan, S., Schinke, C., Tian, E., Epstein, J., Barlogie, B., Davies, F. E., Heuck, C. J., Walker, B. A. & Morgan, G. J. Clonal selection and double-hit events involving tumor suppressor genes underlie relapse in myeloma. *Blood*. 2016; 128(13):1735-1744.

222. Rajkumar, S. V., Gupta, V., Fonseca, R., Dispenzieri, A., Gonsalves, W. I., Larson, D., Ketterling, R. P., Lust, J. A., Kyle, R. A. & Kumar, S. K. Impact of primary molecular cytogenetic abnormalities and risk of progression in smoldering multiple myeloma. *Leukemia*. 2013; 27(8):1738-1744.

223. Neben, K., Jauch, A., Hielscher, T., Hillengass, J., Lehners, N., Seckinger, A., Granzow, M., Raab, M. S., Ho, A. D., Goldschmidt, H. & Hose, D. Progression in smoldering myeloma is independently determined by the chromosomal abnormalities del(17p), t(4;14), gain 1q, hyperdiploidy, and tumor load. *J Clin Oncol*. 2013; 31(34):4325-4332.

224. Lakshman, A., Paul, S., Rajkumar, S. V., Ketterling, R. P., Greipp, P. T., Dispenzieri, A., Gertz, M. A., Buadi, F. K., Lacy, M. Q., Dingli, D., Fonder, A. L., Hayman, S. R., Hobbs, M. A., Gonsalves, W. I., Hwa, Y. L., Kapoor, P., Leung, N., Go, R. S., Lin, Y., Kourelis, T. V., Warsame, R., Lust, J. A., Russell, S. J., Zeldenrust, S. R., Kyle, R. A. & Kumar, S. K. Prognostic significance of interphase FISH in monoclonal gammopathy of undetermined significance. *Leukemia*. 2018; 32(8):1811-1815.

225. Kaufmann, H., Ackermann, J., Baldia, C., Nosslinger, T., Wieser, R., Seidl, S., Sagaster, V., Gisslinger, H., Jager, U., Pfeilstocker, M., Zielinski, C. & Drach, J. Both IGH translocations and chromosome 13q deletions are early events in monoclonal gammopathy of undetermined significance and do not evolve during transition to multiple myeloma. *Leukemia*. 2004; 18(11):1879-1882.

226. Lopez-Corral, L., Gutierrez, N. C., Vidriales, M. B., Mateos, M. V., Rasillo, A., Garcia-Sanz, R., Paiva, B. & San Miguel, J. F. The progression from MGUS to smoldering

myeloma and eventually to multiple myeloma involves a clonal expansion of genetically abnormal plasma cells. *Clin Cancer Res*. 2011; 17(7):1692-1700.

227. Lopez-Corral, L., Sarasquete, M. E., Bea, S., Garcia-Sanz, R., Mateos, M. V., Corchete, L. A., Sayagues, J. M., Garcia, E. M., Blade, J., Oriol, A., Hernandez-Garcia, M. T., Giraldo, P., Hernandez, J., Gonzalez, M., Hernandez-Rivas, J. M., San Miguel, J. F. & Gutierrez, N. C. SNP-based mapping arrays reveal high genomic complexity in monoclonal gammopathies, from MGUS to myeloma status. *Leukemia*. 2012; 26(12):2521-2529.

228. Mikulasova, A., Wardell, C. P., Murison, A., Boyle, E. M., Jackson, G. H., Smetana, J., Kufova, Z., Pour, L., Sandecka, V., Almasi, M., Vsianska, P., Gregora, E., Kuglik, P., Hajek, R., Davies, F. E., Morgan, G. J. & Walker, B. A. The spectrum of somatic mutations in monoclonal gammopathy of undetermined significance indicates a less complex genomic landscape than that in multiple myeloma. *Haematologica*. 2017; 102(9):1617-1625.

229. Dhodapkar, M. V. MGUS to myeloma: a mysterious gammopathy of underexplored significance. *Blood*. 2016; 128(23):2599-2606.

230. Zhao, S., Choi, M., Heuck, C., Mane, S., Barlogie, B., Lifton, R. P. & Dhodapkar, M. V. Serial exome analysis of disease progression in premalignant gammopathies. *Leukemia*. 2014; 28(7):1548-1552.

231. Bolli, N., Maura, F., Minvielle, S., Gloznik, D., Szalat, R., Fullam, A., Martincorena, I., Dawson, K. J., Samur, M. K., Zamora, J., Tarpey, P., Davies, H., Fulciniti, M., Shammas, M. A., Tai, Y. T., Magrangeas, F., Moreau, P., Corradini, P., Anderson, K., Alexandrov, L., Wedge, D. C., Avet-Loiseau, H., Campbell, P. & Munshi, N. Genomic patterns of progression in smoldering multiple myeloma. *Nat Commun*. 2018; 9(1):3363.

232. Dutta, A. K., Fink, J. L., Grady, J. P., Morgan, G. J., Mullighan, C. G., To, L. B., Hewett, D. R. & Zannettino, A. C. W. Subclonal evolution in disease progression from MGUS/SMM to multiple myeloma is characterised by clonal stability. *Leukemia*. 2018; 33(2):457-468.

233. Das, R., Strowig, T., Verma, R., Koduru, S., Hafemann, A., Hopf, S., Kocoglu, M. H., Borsotti, C., Zhang, L., Branagan, A., Eynon, E., Manz, M. G., Flavell, R. A. & Dhodapkar, M. V. Microenvironment-dependent growth of preneoplastic and malignant plasma cells in humanized mice. *Nat Med*. 2016; 22(11):1351-1357.

234. Vandenberg, C. J., Waring, P., Strasser, A. & Cory, S. Plasmacytomagenesis in Emu-v-abl transgenic mice is accelerated when apoptosis is restrained. *Blood*. 2014; 124(7):1099-1109.

235. Cheung, W. C., Kim, J. S., Linden, M., Peng, L., Van Ness, B., Polakiewicz, R. D. & Janz, S. Novel targeted deregulation of c-Myc cooperates with Bcl-X(L) to cause plasma cell neoplasms in mice. *J Clin Invest*. 2004; 113(12):1763-1773.

236. Zingone, A., Cultraro, C. M., Shin, D. M., Bean, C. M., Morse, H. C., 3rd, Janz, S. & Kuehl, W. M. Ectopic expression of wild-type FGFR3 cooperates with MYC to accelerate development of B-cell lineage neoplasms. *Leukemia*. 2010; 24(6):1171-1178.

237. Linden, M. A., Kirchhof, N., Carlson, C. S. & Van Ness, B. G. Targeted overexpression of an activated N-ras gene results in B-cell and plasma cell lymphoproliferation and cooperates with c-myc to induce fatal B-cell neoplasia. *Exp Hematol*. 2012; 40(3):216-227.

238. Morito, N., Yoh, K., Maeda, A., Nakano, T., Fujita, A., Kusakabe, M., Hamada, M., Kudo, T., Yamagata, K. & Takahashi, S. A novel transgenic mouse model of the human multiple myeloma chromosomal translocation t(14;16)(q32;q23). *Cancer Res*. 2011; 71(2):339-348.

239. Chesi, M., Robbiani, D. F., Sebag, M., Chng, W. J., Affer, M., Tiedemann, R., Valdez, R., Palmer, S. E., Haas, S. S., Stewart, A. K., Fonseca, R., Kremer, R., Cattoretti, G. & Bergsagel, P. L. AID-dependent activation of a MYC transgene induces multiple myeloma in a conditional mouse model of post-germinal center malignancies. *Cancer Cell*. 2008; 13(2):167-180.

240. Claudio, J. O., Zhu, Y. X., Benn, S. J., Shukla, A. H., McGlade, C. J., Falcioni, N. & Stewart, A. K. HACS1 encodes a novel SH3-SAM adaptor protein differentially expressed in normal and malignant hematopoietic cells. *Oncogene*. 2001; 20(38):5373-5377.

241. Zhu, Y. X., Benn, S., Li, Z. H., Wei, E., Masih-Khan, E., Trieu, Y., Bali, M., McGlade, C. J., Claudio, J. O. & Stewart, A. K. The SH3-SAM adaptor HACS1 is up-regulated in B cell activation signaling cascades. *J Exp Med*. 2004; 200(6):737-747.

242. Uchida, T., Nakao, A., Nakano, N., Kuramasu, A., Saito, H., Okumura, K., Ra, C. & Ogawa, H. Identification of Nash1, a novel protein containing a nuclear localization signal, a sterile alpha motif, and an SH3 domain preferentially expressed in mast cells. *Biochem Biophys Res Commun*. 2001; 288(1):137-141.

243. Beer, S., Simins, A. B., Schuster, A. & Holzmann, B. Molecular cloning and characterization of a novel SH3 protein (SLY) preferentially expressed in lymphoid cells. *Biochim Biophys Acta*. 2001; 1520(1):89-93.

244. Zeller, C., Hinzmann, B., Seitz, S., Prokoph, H., Burkhard-Goettges, E., Fischer, J., Jandrig, B., Schwarz, L. E., Rosenthal, A. & Scherneck, S. SASH1: a candidate tumor suppressor gene on chromosome 6q24.3 is downregulated in breast cancer. *Oncogene*. 2003; 22(19):2972-2983.

245. Wang, D., Stewart, A. K., Zhuang, L., Zhu, Y., Wang, Y., Shi, C., Keating, A., Slutsky, A., Zhang, H. & Wen, X. Y. Enhanced adaptive immunity in mice lacking the immunoinhibitory adaptor Hacs1. *Faseb j*. 2010; 24(3):947-956.

246. Weidmann, H. 'SASH1, a new potential link between smoking and atherosclerosis'. PhD thesis, Université Pierre et Marie Curie, Paris, 2015.

247. Shi, W., Liao, Y., Willis, S. N., Taubenheim, N., Inouye, M., Tarlinton, D. M., Smyth, G. K., Hodgkin, P. D., Nutt, S. L. & Corcoran, L. M. Transcriptional profiling of mouse B cell terminal differentiation defines a signature for antibody-secreting plasma cells. *Nat Immunol*. 2015; 16(6):663-673.

248. Schmitt, F., Schall, D., Bucher, K., Schindler, T. I., Hector, A., Biedermann, T., Zemlin, M., Hartl, D. & Beer-Hammer, S. SLy2 controls the antibody response to pneumococcal vaccine through an IL-5Ralpha-dependent mechanism in B-1 cells. *Eur J Immunol*. 2015; 45(1):60-70.

249. von Holleben, M., Gohla, A., Janssen, K. P., Iritani, B. M. & Beer-Hammer, S. Immunoinhibitory adapter protein Src homology domain 3 lymphocyte protein 2 (SLy2) regulates actin dynamics and B cell spreading. *J Biol Chem*. 2011; 286(15):13489-13501.

250. Blery, M., Kubagawa, H., Chen, C. C., Vely, F., Cooper, M. D. & Vivier, E. The paired Ig-like receptor PIR-B is an inhibitory receptor that recruits the protein-tyrosine phosphatase SHP-1. *Proc Natl Acad Sci U S A*. 1998; 95(5):2446-2451.

251. Brandt, S., Ellwanger, K., Beuter-Gunia, C., Schuster, M., Hausser, A., Schmitz, I. & Beer-Hammer, S. SLy2 targets the nuclear SAP30/HDAC1 complex. *Int J Biochem Cell Biol*. 2010; 42(9):1472-1481.

252. Zhang, Y., Iratni, R., Erdjument-Bromage, H., Tempst, P. & Reinberg, D. Histone deacetylases and SAP18, a novel polypeptide, are components of a human Sin3 complex. *Cell*. 1997; 89(3):357-364.

253. Ridley, A. J., Paterson, H. F., Johnston, C. L., Diekmann, D. & Hall, A. The small GTP-binding protein rac regulates growth factor-induced membrane ruffling. *Cell*. 1992; 70(3):401-410.

254. Allen, W. E., Jones, G. E., Pollard, J. W. & Ridley, A. J. Rho, Rac and Cdc42 regulate actin organization and cell adhesion in macrophages. *J Cell Sci*. 1997; 110(Pt 6):707-720.

255. Uruno, T., Liu, J., Zhang, P., Fan, Y., Egile, C., Li, R., Mueller, S. C. & Zhan, X. Activation of Arp2/3 complex-mediated actin polymerization by cortactin. *Nat Cell Biol*. 2001; 3(3):259-266.

256. Uruno, T., Zhang, P., Liu, J., Hao, J. J. & Zhan, X. Haematopoietic lineage cell-specific protein 1 (HS1) promotes actin-related protein (Arp) 2/3 complex-mediated actin polymerization. *Biochem J*. 2003; 371(Pt 2):485-493.

257. Fleire, S. J., Goldman, J. P., Carrasco, Y. R., Weber, M., Bray, D. & Batista, F. D. B cell ligand discrimination through a spreading and contraction response. *Science*. 2006; 312(5774):738-741.

258. Martini, M., Gnann, A., Scheikl, D., Holzmann, B. & Janssen, K. P. The candidate tumor suppressor SASH1 interacts with the actin cytoskeleton and stimulates cell-matrix adhesion. *Int J Biochem Cell Biol*. 2011; 43(11):1630-1640.

259. Zhou, D., Wei, Z., Deng, S., Wang, T., Zai, M., Wang, H., Guo, L., Zhang, J., Zhong, H., He, L. & Xing, Q. SASH1 regulates melanocyte transepithelial migration through a novel Galphas-SASH1-IQGAP1-E-Cadherin dependent pathway. *Cell Signal*. 2013; 25(6):1526-1538.

260. Noll, J. E., Hewett, D. R., Williams, S. A., Vandyke, K., Kok, C., To, L. B. & Zannettino, A. C. SAMSN1 is a tumor suppressor gene in multiple myeloma. *Neoplasia*. 2014; 16(7):572-585.

261. Amend, S. R., Wilson, W. C., Chu, L., Lu, L., Liu, P., Serie, D., Su, X., Xu, Y., Wang, D., Gramolini, A., Wen, X. Y., O'Neal, J., Hurchla, M., Vachon, C. M., Colditz, G., Vij, R., Weilbaecher, K. N. & Tomasson, M. H. Whole Genome Sequence of Multiple Myeloma-Prone C57BL/KaLwRij Mouse Strain Suggests the Origin of Disease Involves Multiple Cell Types. *PLoS One*. 2015; 10(5):e0127828.

262. Radl, J., Hollander, C. F., van den Berg, P. & de Glopper, E. Idiopathic paraproteinaemia. I. Studies in an animal model--the ageing C57BL/KaLwRij mouse. *Clin Exp Immunol*. 1978; 33(3):395-402.

263. Radl, J., De Glopper, E. D., Schuit, H. R. & Zurcher, C. Idiopathic paraproteinemia. II. Transplantation of the paraprotein-producing clone from old to young C57BL/KaLwRij mice. *J Immunol*. 1979; 122(2):609-613.

264. Radl, J., Croese, J. W., Zurcher, C., Van den Enden-Vieveen, M. H. & de Leeuw, A. M. Animal model of human disease. Multiple myeloma. *Am J Pathol*. 1988; 132(3):593-597.

265. Radl, J., Croese, J. W., Zurcher, C., van den Enden-Vieveen, M. H., Brondijk, R. J., Kazil, M., Haaijman, J. J., Reitsma, P. H. & Bijvoet, O. L. Influence of treatment with APD-bisphosphonate on the bone lesions in the mouse 5T2 multiple myeloma. *Cancer*. 1985; 55(5):1030-1040.

266. Croese, J. W., Vas Nunes, C. M., Radl, J., van den Enden-Vieveen, M. H., Brondijk, R. J. & Boersma, W. J. The 5T2 mouse multiple myeloma model: characterization of 5T2 cells within the bone marrow. *Br J Cancer*. 1987; 56(5):555-560.

267. Garrett, I. R., Dallas, S., Radl, J. & Mundy, G. R. A murine model of human myeloma bone disease. *Bone*. 1997; 20(6):515-520.

268. Dallas, S. L., Garrett, I. R., Oyajobi, B. O., Dallas, M. R., Boyce, B. F., Bauss, F., Radl, J. & Mundy, G. R. Ibandronate reduces osteolytic lesions but not tumor burden in a murine model of myeloma bone disease. *Blood*. 1999; 93(5):1697-1706.

269. Lwin, S. T., Edwards, C. M. & Silbermann, R. Preclinical animal models of multiple myeloma. *Bonekey Rep*. 2016; 5:772.

270. Maes, K., Boeckx, B., Vlummens, P., De Veirman, K., Menu, E., Vanderkerken, K., Lambrechts, D. & De Bruyne, E. The genetic landscape of 5T models for multiple myeloma. *Sci Rep*. 2018; 8(1):15030.

271. Yamada, H., Yanagisawa, K., Tokumaru, S., Taguchi, A., Nimura, Y., Osada, H., Nagino, M. & Takahashi, T. Detailed characterization of a homozygously deleted region corresponding to a candidate tumor suppressor locus at 21q11-21 in human lung cancer. *Genes Chromosomes Cancer*. 2008; 47(9):810-818.

272. Watanabe, T., Kobunai, T., Yamamoto, Y., Ikeuchi, H., Matsuda, K., Ishihara, S., Nozawa, K., Iinuma, H., Kanazawa, T., Tanaka, T., Yokoyama, T., Konishi, T., Eshima, K., Ajioka, Y., Hibi, T., Watanabe, M., Muto, T. & Nagawa, H. Predicting ulcerative colitis-associated colorectal cancer using reverse-transcription polymerase chain reaction analysis. *Clin Colorectal Cancer*. 2011; 10(2):134-141.

273. Sueoka, S., Kanda, M., Sugimoto, H., Shimizu, D., Nomoto, S., Oya, H., Takami, H., Ezaka, K., Hashimoto, R., Tanaka, Y., Okamura, Y., Yamada, S., Fujii, T., Nakayama, G., Koike, M., Fujiwara, M. & Kodera, Y. Suppression of SAMSN1 Expression is Associated with the Malignant Phenotype of Hepatocellular Carcinoma. *Ann Surg Oncol*. 2015.

274. Kanda, M., Shimizu, D., Sueoka, S., Nomoto, S., Oya, H., Takami, H., Ezaka, K., Hashimoto, R., Tanaka, Y., Kobayashi, D., Tanaka, C., Yamada, S., Fujii, T., Nakayama, G., Sugimoto, H., Koike, M., Fujiwara, M. & Kodera, Y. Prognostic relevance of SAMSN1 expression in gastric cancer. *Oncol Lett*. 2016; 12(6):4708-4716.

275. Yan, Y., Zhang, L., Xu, T., Zhou, J., Qin, R., Chen, C., Zou, Y., Fu, D., Hu, G., Chen, J. & Lu, Y. SAMSN1 is highly expressed and associated with a poor survival in glioblastoma multiforme. *PLoS One*. 2013; 8(11):e81905.

276. Rimkus, C., Martini, M., Friederichs, J., Rosenberg, R., Doll, D., Siewert, J. R., Holzmann, B. & Janssen, K. P. Prognostic significance of downregulated expression of the candidate tumour suppressor gene SASH1 in colon cancer. *Br J Cancer*. 2006; 95(10):1419-1423.

277. Meng, Q., Zheng, M., Liu, H., Song, C., Zhang, W., Yan, J., Qin, L. & Liu, X. SASH1 regulates proliferation, apoptosis, and invasion of osteosarcoma cell. *Mol Cell Biochem*. 2013; 373(1-2):201-210.

278. Staaf, J., Isaksson, S., Karlsson, A., Jonsson, M., Johansson, L., Jonsson, P., Botling, J., Micke, P., Baldetorp, B. & Planck, M. Landscape of somatic allelic imbalances and copy number alterations in human lung carcinoma. *Int J Cancer*. 2013; 132(9):2020-2031.

279. Wang, M., Zhang, S., Chuang, S. S., Ashton-Key, M., Ochoa, E., Bolli, N., Vassiliou, G., Gao, Z. & Du, M. Q. Angioimmunoblastic T cell lymphoma: novel molecular insights by mutation profiling. *Oncotarget*. 2017; 8(11):17763-17770.

280. Chen, E. G., Chen, Y., Dong, L. L. & Zhang, J. S. Effects of SASH1 on lung cancer cell proliferation, apoptosis, and invasion in vitro. *Tumour Biol*. 2012; 33(5):1393-1401.

281. Sun, D., Zhou, R., Liu, H., Sun, W., Dong, A. & Zhang, H. SASH1 inhibits proliferation and invasion of thyroid cancer cells through PI3K/Akt signaling pathway. *Int J Clin Exp Pathol*. 2015; 8(10):12276-12283.

282. Huang da, W., Sherman, B. T. & Lempicki, R. A. Systematic and integrative analysis of large gene lists using DAVID bioinformatics resources. *Nat Protoc*. 2009; 4(1):44-57.

283. Simon, P. Q-Gene: processing quantitative real-time RT-PCR data. *Bioinformatics*. 2003; 19(11):1439-1440.

284. Aubrey, B. J., Kelly, G. L., Kueh, A. J., Brennan, M. S., O'Connor, L., Milla, L., Wilcox, S., Tai, L., Strasser, A. & Herold, M. J. An inducible lentiviral guide RNA platform enables the identification of tumor-essential genes and tumor-promoting mutations in vivo. *Cell Rep*. 2015; 10(8):1422-1432.

285. Diamond, P., Labrinidis, A., Martin, S. K., Farrugia, A. N., Gronthos, S., To, L. B., Fujii, N., O'Loughlin, P. D., Evdokiou, A. & Zannettino, A. C. Targeted disruption of the CXCL12/CXCR4 axis inhibits osteolysis in a murine model of myeloma-associated bone loss. *J Bone Miner Res*. 2009; 24(7):1150-1161.

286. Schweitzer, K. M., Vicart, P., Delouis, C., Paulin, D., Drager, A. M., Langenhuijsen, M. M. & Weksler, B. B. Characterization of a newly established human bone marrow endothelial cell line: distinct adhesive properties for hematopoietic progenitors compared with human umbilical vein endothelial cells. *Lab Invest*. 1997; 76(1):25-36.

287. Persons, D. A., Mehaffey, M. G., Kaleko, M., Nienhuis, A. W. & Vanin, E. F. An improved method for generating retroviral producer clones for vectors lacking a selectable marker gene. *Blood Cells Mol Dis*. 1998; 24(2):167-182.

288. Shi, L., Campbell, G., Jones, W. D., Campagne, F., Wen, Z., Walker, S. J., Su, Z., Chu, T. M., Goodsaid, F. M., Pusztai, L., Shaughnessy, J. D., Jr., Oberthuer, A., Thomas, R. S., Paules, R. S., Fielden, M., Barlogie, B., Chen, W., Du, P., Fischer, M., Furlanello, C., Gallas, B. D., Ge, X., Megherbi, D. B., Symmans, W. F., Wang, M. D., Zhang, J., Bitter, H., Brors, B., Bushel, P. R., Bylesjo, M., Chen, M., Cheng, J., Cheng, J., Chou, J., Davison, T. S. *et al.* The MicroArray Quality Control (MAQC)-II study of common practices for the development and validation of microarray-based predictive models. *Nat Biotechnol*. 2010; 28(8):827-838.

289. Chng, W. J., Kumar, S., Vanwier, S., Ahmann, G., Price-Troska, T., Henderson, K., Chung, T. H., Kim, S., Mulligan, G., Bryant, B., Carpten, J., Gertz, M., Rajkumar, S. V., Lacy, M., Dispenzieri, A., Kyle, R., Greipp, P., Bergsagel, P. L. & Fonseca, R. Molecular dissection of hyperdiploid multiple myeloma by gene expression profiling. *Cancer Res*. 2007; 67(7):2982-2989.

290. Cheong, C. M., Chow, A. W., Fitter, S., Hewett, D. R., Martin, S. K., Williams, S. A., To, L. B., Zannettino, A. C. & Vandyke, K. Tetraspanin 7 (TSPAN7) expression is upregulated in multiple myeloma patients and inhibits myeloma tumour development in vivo. *Exp Cell Res*. 2015; 332(1):24-38.

291. Mrozik, K. M., Cheong, C. M., Hewett, D., Chow, A. W., Blaschuk, O. W., Zannettino, A. C. & Vandyke, K. Therapeutic targeting of N-cadherin is an effective treatment for multiple myeloma. *Br J Haematol*. 2015; 171(3):387-399.

292. Noll, J. E., Vandyke, K., Hewett, D. R., Mrozik, K. M., Bala, R. J., Williams, S. A., Kok, C. H. & Zannettino, A. C. PTTG1 expression is associated with hyperproliferative disease and poor prognosis in multiple myeloma. *J Hematol Oncol*. 2015; 8:106.

293. Hanahan, D. & Weinberg, R. A. Hallmarks of cancer: the next generation. *Cell*. 2011; 144(5):646-674.

294. Ruiz-Heredia, Y., Sanchez-Vega, B., Onecha, E., Barrio, S., Alonso, R., Martinez-Avila, J. C., Cuenca, I., Agirre, X., Braggio, E., Hernandez, M. T., Martinez, R., Rosinol, L., Gutierrez, N., Martin-Ramos, M., Ocio, E. M., Echeveste, M. A., de Oteyza, J. P., Oriol, A., Bargay, J., Gironella, M., Ayala, R., Blade, J., Mateos, M. V., Kortum, K. M., Stewart, K., Garcia-Sanz, R., Miguel, J. S., Lahuerta, J. J. & Martinez-Lopez, J. Mutational screening of newly diagnosed multiple myeloma patients by deep targeted sequencing. *Haematologica*. 2018; 103(11):e544-e548.

295. Hu, Y., Zheng, M., Gali, R., Tian, Z., Topal Gorgun, G., Munshi, N. C., Mitsiades, C. S. & Anderson, K. C. A novel rapid-onset high-penetrance plasmacytoma mouse model driven by deregulation of cMYC cooperating with KRAS12V in BALB/c mice. *Blood Cancer J*. 2013; 3:e156.

296. Ren, C., Li, L., Goltsov, A. A., Timme, T. L., Tahir, S. A., Wang, J., Garza, L., Chinault, A. C. & Thompson, T. C. mRTVP-1, a novel p53 target gene with proapoptotic activities. *Mol Cell Biol*. 2002; 22(10):3345-3357.

297. Satoh, T., Timme, T. L., Saika, T., Ebara, S., Yang, G., Wang, J., Ren, C., Kusaka, N., Mouraviev, V. & Thompson, T. C. Adenoviral vector-mediated mRTVP-1 gene therapy for prostate cancer. *Hum Gene Ther*. 2003; 14(2):91-101.

298. Li, L., Abdel Fattah, E., Cao, G., Ren, C., Yang, G., Goltsov, A. A., Chinault, A. C., Cai, W. W., Timme, T. L. & Thompson, T. C. Glioma pathogenesis-related protein 1 exerts

tumor suppressor activities through proapoptotic reactive oxygen species-c-Jun-NH2 kinase signaling. *Cancer Res*. 2008; 68(2):434-443.

299. Paiva, B., Martinez-Lopez, J., Corchete, L. A., Sanchez-Vega, B., Rapado, I., Puig, N., Barrio, S., Sanchez, M. L., Alignani, D., Lasa, M., Garcia de Coca, A., Pardal, E., Oriol, A., Garcia, M. E., Escalante, F., Gonzalez-Lopez, T. J., Palomera, L., Alonso, J., Prosper, F., Orfao, A., Vidriales, M. B., Mateos, M. V., Lahuerta, J. J., Gutierrez, N. C. & San Miguel, J. F. Phenotypic, transcriptomic, and genomic features of clonal plasma cells in light-chain amyloidosis. *Blood*. 2016; 127(24):3035-3039.

300. Fowler, J. A., Mundy, G. R., Lwin, S. T., Lynch, C. C. & Edwards, C. M. A murine model of myeloma that allows genetic manipulation of the host microenvironment. *Dis Model Mech*. 2009; 2(11-12):604-611.

301. Marzluff, W. F., Gongidi, P., Woods, K. R., Jin, J. & Maltais, L. J. The human and mouse replication-dependent histone genes. *Genomics*. 2002; 80(5):487-498.

302. Ren, C., Ren, C. H., Li, L., Goltsov, A. A. & Thompson, T. C. Identification and characterization of RTVP1/GLIPR1-like genes, a novel p53 target gene cluster. *Genomics*. 2006; 88(2):163-172.

303. Gibbs, G. M., Roelants, K. & O'Bryan, M. K. The CAP superfamily: cysteine-rich secretory proteins, antigen 5, and pathogenesis-related 1 proteins--roles in reproduction, cancer, and immune defense. *Endocr Rev*. 2008; 29(7):865-897.

304. Ren, C., Li, L., Yang, G., Timme, T. L., Goltsov, A., Ren, C., Ji, X., Addai, J., Luo, H., Ittmann, M. M. & Thompson, T. C. RTVP-1, a tumor suppressor inactivated by methylation in prostate cancer. *Cancer Res*. 2004; 64(3):969-976.

305. Sheng, X., Bowen, N. & Wang, Z. GLI pathogenesis-related 1 functions as a tumor-suppressor in lung cancer. *Mol Cancer*. 2016; 15:25.

306. Dong, J., Bi, B., Zhang, L. & Gao, K. GLIPR1 inhibits the proliferation and induces the differentiation of cancer-initiating cells by regulating miR-16 in osteosarcoma. *Oncol Rep*. 2016; 36(3):1585-1591.

307. Yan, L., Li, Q., Yang, J. & Qiao, B. TPX2-p53-GLIPR1 regulatory circuitry in cell proliferation, invasion, and tumor growth of bladder cancer. *J Cell Biochem*. 2018; 119(2):1791-1803.

308. Tam, M., Lin, P., Hu, P. & Lennon, P. A. Examining Hedgehog pathway genes GLI3, SHH, and PTCH1 and the p53 target GLIPR1/GLIPR1L1/GLIPR1L2 gene cluster using fluorescence in situ hybridization uncovers GLIPR1/GLIPR1L1/GLIPR1L2 deletion in 9% of patients with multiple myeloma. *J Assoc Genet Technol*. 2010; 36(3):111-114.

309. Shay, G., Tauro, M., Loiodice, F., Tortorella, P., Sullivan, D. M., Hazlehurst, L. A. & Lynch, C. C. Selective inhibition of matrix metalloproteinase-2 in the multiple myeloma-bone microenvironment. *Oncotarget*. 2017; 8(26):41827-41840.

310. Paiva, B., Chandia, M., Vidriales, M. B., Colado, E., Caballero-Velazquez, T., Escalante, F., Garcia de Coca, A., Montes, M. C., Garcia-Sanz, R., Ocio, E. M., Mateos, M. V. & San Miguel, J. F. Multiparameter flow cytometry for staging of solitary bone plasmacytoma: new criteria for risk of progression to myeloma. *Blood*. 2014; 124(8):1300-1303.

311. Hill, Q. A., Rawstron, A. C., de Tute, R. M. & Owen, R. G. Outcome prediction in plasmacytoma of bone: a risk model utilizing bone marrow flow cytometry and light-chain analysis. *Blood*. 2014; 124(8):1296-1299.

312. Li, L., Yang, G., Ren, C., Tanimoto, R., Hirayama, T., Wang, J., Hawke, D., Kim, S. M., Lee, J. S., Goltsov, A. A., Park, S., Ittmann, M. M., Troncoso, P. & Thompson, T. C. Glioma pathogenesis-related protein 1 induces prostate cancer cell death through Hsc70-mediated suppression of AURKA and TPX2. *Mol Oncol*. 2013; 7(3):484-496.

313. Li, L., Ren, C., Yang, G., Fattah, E. A., Goltsov, A. A., Kim, S. M., Lee, J. S., Park, S., Demayo, F. J., Ittmann, M. M., Troncoso, P. & Thompson, T. C. GLIPR1 suppresses prostate cancer development through targeted oncoprotein destruction. *Cancer Res*. 2011; 71(24):7694-7704.

314. Donehower, L. A., Harvey, M., Vogel, H., McArthur, M. J., Montgomery, C. A., Jr., Park, S. H., Thompson, T., Ford, R. J. & Bradley, A. Effects of genetic background on tumorigenesis in p53-deficient mice. *Mol Carcinog*. 1995; 14(1):16-22.

315. Petiniot, L. K., Weaver, Z., Vacchio, M., Shen, R., Wangsa, D., Barlow, C., Eckhaus, M., Steinberg, S. M., Wynshaw-Boris, A., Ried, T. & Hodes, R. J. RAG-mediated V(D)J recombination is not essential for tumorigenesis in Atm-deficient mice. *Mol Cell Biol*. 2002; 22(9):3174-3177.

316. Weiss, W. A., Aldape, K., Mohapatra, G., Feuerstein, B. G. & Bishop, J. M. Targeted expression of MYCN causes neuroblastoma in transgenic mice. *EMBO J*. 1997; 16(11):2985-2995.

317. Puccini, J., Dorstyn, L. & Kumar, S. Genetic background and tumour susceptibility in mouse models. *Cell Death Differ*. 2013; 20(7):964.

318. Rosenzweig, T., Ziv-Av, A., Xiang, C., Lu, W., Cazacu, S., Taler, D., Miller, C. G., Reich, R., Shoshan, Y., Anikster, Y., Kazimirsky, G., Sarid, R. & Brodie, C. Related to testes-specific, vespid, and pathogenesis protein-1 (RTVP-1) is overexpressed in gliomas and regulates the growth, survival, and invasion of glioma cells. *Cancer Res*. 2006; 66(8):4139-4148.

319. Bhowmick, N. A., Chytil, A., Plieth, D., Gorska, A. E., Dumont, N., Shappell, S., Washington, M. K., Neilson, E. G. & Moses, H. L. TGF-beta signaling in fibroblasts modulates the oncogenic potential of adjacent epithelia. *Science*. 2004; 303(5659):848-851.

320. Yang, F. C., Ingram, D. A., Chen, S., Zhu, Y., Yuan, J., Li, X., Yang, X., Knowles, S., Horn, W., Li, Y., Zhang, S., Yang, Y., Vakili, S. T., Yu, M., Burns, D., Robertson, K., Hutchins, G., Parada, L. F. & Clapp, D. W. Nf1-dependent tumors require a microenvironment containing Nf1+/-- and c-kit-dependent bone marrow. *Cell*. 2008; 135(3):437-448.

321. Raaijmakers, M. H., Mukherjee, S., Guo, S., Zhang, S., Kobayashi, T., Schoonmaker, J. A., Ebert, B. L., Al-Shahrour, F., Hasserjian, R. P., Scadden, E. O., Aung, Z., Matza, M., Merkenschlager, M., Lin, C., Rommens, J. M. & Scadden, D. T. Bone progenitor dysfunction induces myelodysplasia and secondary leukaemia. *Nature*. 2010; 464(7290):852-857.

322. Walkley, C. R., Shea, J. M., Sims, N. A., Purton, L. E. & Orkin, S. H. Rb regulates interactions between hematopoietic stem cells and their bone marrow microenvironment. *Cell*. 2007; 129(6):1081-1095.

323. Kode, A., Manavalan, J. S., Mosialou, I., Bhagat, G., Rathinam, C. V., Luo, N., Khiabanian, H., Lee, A., Murty, V. V., Friedman, R., Brum, A., Park, D., Galili, N., Mukherjee, S., Teruya-Feldstein, J., Raza, A., Rabadan, R., Berman, E. & Kousteni, S. Leukaemogenesis induced by an activating beta-catenin mutation in osteoblasts. *Nature*. 2014; 506(7487):240-244.

324. Kode, A., Mosialou, I., Manavalan, S. J., Rathinam, C. V., Friedman, R. A., Teruya-Feldstein, J., Bhagat, G., Berman, E. & Kousteni, S. FoxO1-dependent induction of acute myeloid leukemia by osteoblasts in mice. *Leukemia*. 2016; 30(1):1-13.

325. Kawano, Y., Moschetta, M., Manier, S., Glavey, S., Gorgun, G. T., Roccaro, A. M., Anderson, K. C. & Ghobrial, I. M. Targeting the bone marrow microenvironment in multiple myeloma. *Immunol Rev*. 2015; 263(1):160-172.

326. Shaw, A. S. & Filbert, E. L. Scaffold proteins and immune-cell signalling. *Nat Rev Immunol*. 2009; 9(1):47-56.

327. Kurosaki, T. Regulation of B-cell signal transduction by adaptor proteins. *Nat Rev Immunol*. 2002; 2(5):354-363.

328. Gomez, T. S., McCarney, S. D., Carrizosa, E., Labno, C. M., Comiskey, E. O., Nolz, J. C., Zhu, P., Freedman, B. D., Clark, M. R., Rawlings, D. J., Billadeau, D. D. & Burkhardt, J. K. HS1 functions as an essential actin-regulatory adaptor protein at the immune synapse. *Immunity*. 2006; 24(6):741-752.

329. Raijmakers, R., Kraiczek, K., de Jong, A. P., Mohammed, S. & Heck, A. J. Exploring the human leukocyte phosphoproteome using a microfluidic reversed-phase-TiO2-reversed-phase high-performance liquid chromatography phosphochip coupled to a quadrupole time-of-flight mass spectrometer. *Anal Chem*. 2010; 82(3):824-832.

330. Alsayed, Y., Ngo, H., Runnels, J., Leleu, X., Singha, U. K., Pitsillides, C. M., Spencer, J. A., Kimlinger, T., Ghobrial, J. M., Jia, X., Lu, G., Timm, M., Kumar, A., Cote, D., Veilleux, I., Hedin, K. E., Roodman, G. D., Witzig, T. E., Kung, A. L., Hideshima, T., Anderson, K. C., Lin, C. P. & Ghobrial, I. M. Mechanisms of regulation of CXCR4/SDF-1 (CXCL12)-dependent migration and homing in multiple myeloma. *Blood*. 2007; 109(7):2708-2717.

331. Sanz-Rodriguez, F., Hidalgo, A. & Teixido, J. Chemokine stromal cell-derived factor-1alpha modulates VLA-4 integrin-mediated multiple myeloma cell adhesion to CS-1/fibronectin and VCAM-1. *Blood*. 2001; 97(2):346-351.

332. Azab, A. K., Azab, F., Blotta, S., Pitsillides, C. M., Thompson, B., Runnels, J. M., Roccaro, A. M., Ngo, H. T., Melhem, M. R., Sacco, A., Jia, X., Anderson, K. C., Lin, C. P., Rollins, B. J. & Ghobrial, I. M. RhoA and Rac1 GTPases play major and differential roles in stromal cell-derived factor-1-induced cell adhesion and chemotaxis in multiple myeloma. *Blood*. 2009; 114(3):619-629.

333. Vandyke, K., Zeissig, M. N., Hewett, D. R., Martin, S. K., Mrozik, K. M., Cheong, C. M., Diamond, P., To, L. B., Gronthos, S., Peet, D. J., Croucher, P. I. & Zannettino, A. C.

W. HIF-2alpha Promotes Dissemination of Plasma Cells in Multiple Myeloma by Regulating CXCL12/CXCR4 and CCR1. *Cancer Res*. 2017; 77(20):5452-5463.

334. Vande Broek, I., Vanderkerken, K., Van Camp, B. & Van Riet, I. Extravasation and homing mechanisms in multiple myeloma. *Clin Exp Metastasis*. 2008; 25(4):325-334.

335. Ghobrial, I. M. Myeloma as a model for the process of metastasis: implications for therapy. *Blood*. 2012; 120(1):20-30.

336. Butler, B., Kastendieck, D. H. & Cooper, J. A. Differently phosphorylated forms of the cortactin homolog HS1 mediate distinct functions in natural killer cells. *Nat Immunol*. 2008; 9(8):887-897.

337. Mukherjee, S., Kim, J., Mooren, O. L., Shahan, S. T., Cohan, M. & Cooper, J. A. Role of cortactin homolog HS1 in transendothelial migration of natural killer cells. *PLoS One*. 2015; 10(2):e0118153.

338. Lettau, M., Kabelitz, D. & Janssen, O. SDF1alpha-induced interaction of the adapter proteins Nck and HS1 facilitates actin polymerization and migration in T cells. *Eur J Immunol*. 2015; 45(2):551-561.

339. Bendell, A. C., Williamson, E. K., Chen, C. S., Burkhardt, J. K. & Hammer, D. A. The Arp2/3 complex binding protein HS1 is required for efficient dendritic cell random migration and force generation. *Integr Biol (Camb)*. 2017; 9(8):695-708.

340. Cavnar, P. J., Mogen, K., Berthier, E., Beebe, D. J. & Huttenlocher, A. The actin regulatory protein HS1 interacts with Arp2/3 and mediates efficient neutrophil chemotaxis. *J Biol Chem*. 2012; 287(30):25466-25477.

341. ten Hacken, E., Scielzo, C., Bertilaccio, M. T., Scarfo, L., Apollonio, B., Barbaglio, F., Stamatopoulos, K., Ponzoni, M., Ghia, P. & Caligaris-Cappio, F. Targeting the LYN/HS1 signaling axis in chronic lymphocytic leukemia. *Blood*. 2013; 121(12):2264-2273.

342. Scielzo, C., Bertilaccio, M. T., Simonetti, G., Dagklis, A., ten Hacken, E., Fazi, C., Muzio, M., Caiolfa, V., Kitamura, D., Restuccia, U., Bachi, A., Rocchi, M., Ponzoni, M., Ghia, P. & Caligaris-Cappio, F. HS1 has a central role in the trafficking and homing of leukemic B cells. *Blood*. 2010; 116(18):3537-3546.

343. Ghobrial, I. M., Detappe, A., Anderson, K. C. & Steensma, D. P. The bone-marrow niche in MDS and MGUS: implications for AML and MM. *Nat Rev Clin Oncol*. 2018; 15(4):219-233.

344. Roccaro, A. M., Sacco, A., Maiso, P., Azab, A. K., Tai, Y. T., Reagan, M., Azab, F., Flores, L. M., Campigotto, F., Weller, E., Anderson, K. C., Scadden, D. T. & Ghobrial, I. M. BM mesenchymal stromal cell-derived exosomes facilitate multiple myeloma progression. *J Clin Invest*. 2013; 123(4):1542-1555.

345. Lawson, M. A., McDonald, M. M., Kovacic, N., Hua Khoo, W., Terry, R. L., Down, J., Kaplan, W., Paton-Hough, J., Fellows, C., Pettitt, J. A., Neil Dear, T., Van Valckenborgh, E., Baldock, P. A., Rogers, M. J., Eaton, C. L., Vanderkerken, K., Pettit, A. R., Quinn, J. M., Zannettino, A. C., Phan, T. G. & Croucher, P. I. Osteoclasts control reactivation of dormant myeloma cells by remodelling the endosteal niche. *Nat Commun*. 2015; 6:8983.

346. Hewett, D. R., Vandyke, K., Lawrence, D. M., Friend, N., Noll, J. E., Geoghegan, J. M., Croucher, P. I. & Zannettino, A. C. W. DNA Barcoding Reveals Habitual Clonal Dominance of Myeloma Plasma Cells in the Bone Marrow Microenvironment. *Neoplasia*. 2017; 19(12):972-981.

347. Yaccoby, S., Wezeman, M. J., Zangari, M., Walker, R., Cottler-Fox, M., Gaddy, D., Ling, W., Saha, R., Barlogie, B., Tricot, G. & Epstein, J. Inhibitory effects of osteoblasts and increased bone formation on myeloma in novel culture systems and a myelomatous mouse model. *Haematologica*. 2006; 91(2):192-199.

348. Lambert, A. W., Pattabiraman, D. R. & Weinberg, R. A. Emerging Biological Principles of Metastasis. *Cell*. 2017; 168(4):670-691.

349. Bragado, P., Estrada, Y., Parikh, F., Krause, S., Capobianco, C., Farina, H. G., Schewe, D. M. & Aguirre-Ghiso, J. A. TGF-beta2 dictates disseminated tumour cell fate in target organs through TGF-beta-RIII and p38alpha/beta signalling. *Nat Cell Biol*. 2013; 15(11):1351-1361.

350. Yu-Lee, L. Y., Yu, G., Lee, Y. C., Lin, S. C., Pan, J., Pan, T., Yu, K. J., Liu, B., Creighton, C. J., Rodriguez-Canales, J., Villalobos, P. A., Wistuba, II, de Nadal, E., Posas, F., Gallick, G. E. & Lin, S. H. Osteoblast-Secreted Factors Mediate Dormancy of Metastatic Prostate Cancer in the Bone via Activation of the TGFbetaRIII-p38MAPK-pS249/T252RB Pathway. *Cancer Res*. 2018; 78(11):2911-2924.

351. Kobayashi, A., Okuda, H., Xing, F., Pandey, P. R., Watabe, M., Hirota, S., Pai, S. K., Liu, W., Fukuda, K., Chambers, C., Wilber, A. & Watabe, K. Bone morphogenetic protein 7 in dormancy and metastasis of prostate cancer stem-like cells in bone. *J Exp Med*. 2011; 208(13):2641-2655.

352. Ro, T. B., Holt, R. U., Brenne, A. T., Hjorth-Hansen, H., Waage, A., Hjertner, O., Sundan, A. & Borset, M. Bone morphogenetic protein-5, -6 and -7 inhibit growth and induce apoptosis in human myeloma cells. *Oncogene*. 2004; 23(17):3024-3032.

353. Axelrod, H. D., Valkenburg, K. C., Amend, S. R., Hicks, J. L., Parsana, P., Torga, G., DeMarzo, A. M. & Pienta, K. J. AXL Is a Putative Tumor Suppressor and Dormancy Regulator in Prostate Cancer. *Mol Cancer Res*. 2018.

354. Shiozawa, Y., Pedersen, E. A., Patel, L. R., Ziegler, A. M., Havens, A. M., Jung, Y., Wang, J., Zalucha, S., Loberg, R. D., Pienta, K. J. & Taichman, R. S. GAS6/AXL axis regulates prostate cancer invasion, proliferation, and survival in the bone marrow niche. *Neoplasia*. 2010; 12(2):116-127.

355. Taichman, R. S., Patel, L. R., Bedenis, R., Wang, J., Weidner, S., Schumann, T., Yumoto, K., Berry, J. E., Shiozawa, Y. & Pienta, K. J. GAS6 receptor status is associated with dormancy and bone metastatic tumor formation. *PLoS One*. 2013; 8(4):e61873.

356. Yumoto, K., Eber, M. R., Wang, J., Cackowski, F. C., Decker, A. M., Lee, E., Nobre, A. R., Aguirre-Ghiso, J. A., Jung, Y. & Taichman, R. S. Axl is required for TGF-beta2-induced dormancy of prostate cancer cells in the bone marrow. *Sci Rep*. 2016; 6:36520.

357. Ravi, P., Kumar, S. K., Cerhan, J. R., Maurer, M. J., Dingli, D., Ansell, S. M. & Rajkumar, S. V. Defining cure in multiple myeloma: a comparative study of outcomes of young individuals with myeloma and curable hematologic malignancies. *Blood Cancer J*. 2018; 8(3):26.

358. Noll, J. E., Williams, S. A., Purton, L. E. & Zannettino, A. C. Tug of war in the haematopoietic stem cell niche: do myeloma plasma cells compete for the HSC niche? *Blood Cancer J*. 2012; 2:e91.

359. Paton-Hough, J., Chantry, A. D. & Lawson, M. A. A review of current murine models of multiple myeloma used to assess the efficacy of therapeutic agents on tumour growth and bone disease. *Bone*. 2015; 77:57-68.

360. Miyakawa, Y., Ohnishi, Y., Tomisawa, M., Monnai, M., Kohmura, K., Ueyama, Y., Ito, M., Ikeda, Y., Kizaki, M. & Nakamura, M. Establishment of a new model of human multiple myeloma using NOD/SCID/gammac(null) (NOG) mice. *Biochem Biophys Res Commun*. 2004; 313(2):258-262.

361. Lawson, M. A., Paton-Hough, J. M., Evans, H. R., Walker, R. E., Harris, W., Ratnabalan, D., Snowden, J. A. & Chantry, A. D. NOD/SCID-GAMMA mice are an ideal strain to assess the efficacy of therapeutic agents used in the treatment of myeloma bone disease. *PLoS One*. 2015; 10(3):e0119546.

362. Rossi, M., Botta, C., Arbitrio, M., Grembiale, R. D., Tagliaferri, P. & Tassone, P. Mouse models of multiple myeloma: technologic platforms and perspectives. *Oncotarget*. 2018; 9(28):20119-20133.

363. Schueler, J., Wider, D., Klingner, K., Siegers, G. M., May, A. M., Wasch, R., Fiebig, H. H. & Engelhardt, M. Intratibial injection of human multiple myeloma cells in NOD/SCID IL-2Rgamma(null) mice mimics human myeloma and serves as a valuable tool for the development of anticancer strategies. *PLoS One*. 2013; 8(11):e79939.

364. Urashima, M., Chen, B. P., Chen, S., Pinkus, G. S., Bronson, R. T., Dedera, D. A., Hoshi, Y., Teoh, G., Ogata, A., Treon, S. P., Chauhan, D. & Anderson, K. C. The development of a model for the homing of multiple myeloma cells to human bone marrow. *Blood*. 1997; 90(2):754-765.

365. Guillerey, C., Nakamura, K., Vuckovic, S., Hill, G. R. & Smyth, M. J. Immune responses in multiple myeloma: role of the natural immune surveillance and potential of immunotherapies. *Cell Mol Life Sci*. 2016; 73(8):1569-1589.

366. Vesely, M. D., Kershaw, M. H., Schreiber, R. D. & Smyth, M. J. Natural innate and adaptive immunity to cancer. *Annu Rev Immunol*. 2011; 29:235-271.

367. Kaplan, D. H., Shankaran, V., Dighe, A. S., Stockert, E., Aguet, M., Old, L. J. & Schreiber, R. D. Demonstration of an interferon gamma-dependent tumor surveillance system in immunocompetent mice. *Proc Natl Acad Sci U S A*. 1998; 95(13):7556-7561.

368. Shankaran, V., Ikeda, H., Bruce, A. T., White, J. M., Swanson, P. E., Old, L. J. & Schreiber, R. D. IFNgamma and lymphocytes prevent primary tumour development and shape tumour immunogenicity. *Nature*. 2001; 410(6832):1107-1111.

369. Smyth, M. J., Thia, K. Y., Street, S. E., MacGregor, D., Godfrey, D. I. & Trapani, J. A. Perforin-mediated cytotoxicity is critical for surveillance of spontaneous lymphoma. *J Exp Med*. 2000; 192(5):755-760.

370. Smyth, M. J., Thia, K. Y., Street, S. E., Cretney, E., Trapani, J. A., Taniguchi, M., Kawano, T., Pelikan, S. B., Crowe, N. Y. & Godfrey, D. I. Differential tumor surveillance by natural killer (NK) and NKT cells. *J Exp Med*. 2000; 191(4):661-668.

371. Girardi, M., Oppenheim, D. E., Steele, C. R., Lewis, J. M., Glusac, E., Filler, R., Hobby, P., Sutton, B., Tigelaar, R. E. & Hayday, A. C. Regulation of cutaneous malignancy by gammadelta T cells. *Science*. 2001; 294(5542):605-609.

372. Koebel, C. M., Vermi, W., Swann, J. B., Zerafa, N., Rodig, S. J., Old, L. J., Smyth, M. J. & Schreiber, R. D. Adaptive immunity maintains occult cancer in an equilibrium state. *Nature*. 2007; 450(7171):903-907.

373. Guillerey, C., Ferrari de Andrade, L., Vuckovic, S., Miles, K., Ngiow, S. F., Yong, M. C., Teng, M. W., Colonna, M., Ritchie, D. S., Chesi, M., Bergsagel, P. L., Hill, G. R., Smyth, M. J. & Martinet, L. Immunosurveillance and therapy of multiple myeloma are CD226 dependent. *J Clin Invest*. 2015; 125(7):2904.

374. Ponzetta, A., Benigni, G., Antonangeli, F., Sciume, G., Sanseviero, E., Zingoni, A., Ricciardi, M. R., Petrucci, M. T., Santoni, A. & Bernardini, G. Multiple Myeloma Impairs Bone Marrow Localization of Effector Natural Killer Cells by Altering the Chemokine Microenvironment. *Cancer Res*. 2015; 75(22):4766-4777.

375. Jinushi, M., Vanneman, M., Munshi, N. C., Tai, Y. T., Prabhala, R. H., Ritz, J., Neuberg, D., Anderson, K. C., Carrasco, D. R. & Dranoff, G. MHC class I chain-related protein A antibodies and shedding are associated with the progression of multiple myeloma. *Proc Natl Acad Sci U S A*. 2008; 105(4):1285-1290.

376. Dhodapkar, M. V., Krasovsky, J., Osman, K. & Geller, M. D. Vigorous premalignancy-specific effector T cell response in the bone marrow of patients with monoclonal gammopathy. *J Exp Med*. 2003; 198(11):1753-1757.

377. Dhodapkar, M. V., Geller, M. D., Chang, D. H., Shimizu, K., Fujii, S., Dhodapkar, K. M. & Krasovsky, J. A reversible defect in natural killer T cell function characterizes the progression of premalignant to malignant multiple myeloma. *J Exp Med*. 2003; 197(12):1667-1676.

378. Dhodapkar, M. V., Krasovsky, J. & Olson, K. T cells from the tumor microenvironment of patients with progressive myeloma can generate strong, tumor-specific cytolytic responses to autologous, tumor-loaded dendritic cells. *Proc Natl Acad Sci U S A*. 2002; 99(20):13009-13013.

379. Kawano, Y., Zavidij, O., Park, J., Moschetta, M., Kokubun, K., Mouhieddine, T. H., Manier, S., Mishima, Y., Murakami, N., Bustoros, M., Pistofidis, R. S., Reidy, M., Shen, Y. J., Rahmat, M., Lukyanchykov, P., Karreci, E. S., Tsukamoto, S., Shi, J., Takagi, S., Huynh, D., Sacco, A., Tai, Y. T., Chesi, M., Bergsagel, P. L., Roccaro, A. M., Azzi, J. & Ghobrial, I. M. Blocking IFNAR1 inhibits multiple myeloma-driven Treg expansion and immunosuppression. *J Clin Invest*. 2018; 128(6):2487-2499.

380. Feyler, S., von Lilienfeld-Toal, M., Jarmin, S., Marles, L., Rawstron, A., Ashcroft, A. J., Owen, R. G., Selby, P. J. & Cook, G. CD4(+)CD25(+)FoxP3(+) regulatory T cells are increased whilst CD3(+)CD4(-)CD8(-)alphabetaTCR(+) Double Negative T cells are decreased in the peripheral blood of patients with multiple myeloma which correlates with disease burden. *Br J Haematol*. 2009; 144(5):686-695.

381. Muthu Raja, K. R., Rihova, L., Zahradova, L., Klincova, M., Penka, M. & Hajek, R. Increased T regulatory cells are associated with adverse clinical features and predict progression in multiple myeloma. *PLoS One*. 2012; 7(10):e47077.

382. Feng, X., Zhang, L., Acharya, C., An, G., Wen, K., Qiu, L., Munshi, N. C., Tai, Y. T. & Anderson, K. C. Targeting CD38 Suppresses Induction and Function of T Regulatory Cells to Mitigate Immunosuppression in Multiple Myeloma. *Clin Cancer Res*. 2017; 23(15):4290-4300.

383. Roussou, M., Tasidou, A., Dimopoulos, M. A., Kastritis, E., Migkou, M., Christoulas, D., Gavriatopoulou, M., Zagouri, F., Matsouka, C., Anagnostou, D. & Terpos, E. Increased expression of macrophage inflammatory protein-1alpha on trephine biopsies correlates with extensive bone disease, increased angiogenesis and advanced stage in newly diagnosed patients with multiple myeloma. *Leukemia*. 2009; 23(11):2177-2181.

384. Gutierrez-Gonzalez, A., Martinez-Moreno, M., Samaniego, R., Arellano-Sanchez, N., Salinas-Munoz, L., Relloso, M., Valeri, A., Martinez-Lopez, J., Corbi, A. L., Hidalgo, A., Garcia-Pardo, A., Teixido, J. & Sanchez-Mateos, P. Evaluation of the potential therapeutic benefits of macrophage reprogramming in multiple myeloma. *Blood*. 2016; 128(18):2241-2252.

385. Ramachandran, I. R., Martner, A., Pisklakova, A., Condamine, T., Chase, T., Vogl, T., Roth, J., Gabrilovich, D. & Nefedova, Y. Myeloid-derived suppressor cells regulate growth of multiple myeloma by inhibiting T cells in bone marrow. *J Immunol*. 2013; 190(7):3815-3823.

386. Gorgun, G. T., Whitehill, G., Anderson, J. L., Hideshima, T., Maguire, C., Laubach, J., Raje, N., Munshi, N. C., Richardson, P. G. & Anderson, K. C. Tumor-promoting immune-suppressive myeloid-derived suppressor cells in the multiple myeloma microenvironment in humans. *Blood*. 2013; 121(15):2975-2987.

387. Nakamura, K., Kassem, S., Cleynen, A., Chretien, M. L., Guillerey, C., Putz, E. M., Bald, T., Forster, I., Vuckovic, S., Hill, G. R., Masters, S. L., Chesi, M., Bergsagel, P. L., Avet-Loiseau, H., Martinet, L. & Smyth, M. J. Dysregulated IL-18 Is a Key Driver of Immunosuppression and a Possible Therapeutic Target in the Multiple Myeloma Microenvironment. *Cancer Cell*. 2018; 33(4):634-648 e635.

388. Davies, F. E., Raje, N., Hideshima, T., Lentzsch, S., Young, G., Tai, Y. T., Lin, B., Podar, K., Gupta, D., Chauhan, D., Treon, S. P., Richardson, P. G., Schlossman, R. L., Morgan, G. J., Muller, G. W., Stirling, D. I. & Anderson, K. C. Thalidomide and immunomodulatory derivatives augment natural killer cell cytotoxicity in multiple myeloma. *Blood*. 2001; 98(1):210-216.

389. Luptakova, K., Rosenblatt, J., Glotzbecker, B., Mills, H., Stroopinsky, D., Kufe, T., Vasir, B., Arnason, J., Tzachanis, D., Zwicker, J. I., Joyce, R. M., Levine, J. D., Anderson, K. C., Kufe, D. & Avigan, D. Lenalidomide enhances anti-myeloma cellular immunity. *Cancer Immunol Immunother*. 2013; 62(1):39-49.

390. Vuckovic, S., Minnie, S. A., Smith, D., Gartlan, K. H., Watkins, T. S., Markey, K. A., Mukhopadhyay, P., Guillerey, C., Kuns, R. D., Locke, K. R., Pritchard, A. L., Johansson, P. A., Varelias, A., Zhang, P., Huntington, N. D., Waddell, N., Chesi, M., Miles, J. J., Smyth, M. J. & Hill, G. R. Bone marrow transplantation generates T cell-dependent control of myeloma in mice. *J Clin Invest*. 2019; 129(1):106-121.

391. Bidwell, B. N., Slaney, C. Y., Withana, N. P., Forster, S., Cao, Y., Loi, S., Andrews, D., Mikeska, T., Mangan, N. E., Samarajiwa, S. A., de Weerd, N. A., Gould, J., Argani, P., Moller, A., Smyth, M. J., Anderson, R. L., Hertzog, P. J. & Parker, B. S. Silencing of Irf7

pathways in breast cancer cells promotes bone metastasis through immune escape. *Nat Med*. 2012; 18(8):1224-1231.

392. Carbone, E., Neri, P., Mesuraca, M., Fulciniti, M. T., Otsuki, T., Pende, D., Groh, V., Spies, T., Pollio, G., Cosman, D., Catalano, L., Tassone, P., Rotoli, B. & Venuta, S. HLA class I, NKG2D, and natural cytotoxicity receptors regulate multiple myeloma cell recognition by natural killer cells. *Blood*. 2005; 105(1):251-258.

393. Bernal, M., Garrido, P., Jimenez, P., Carretero, R., Almagro, M., Lopez, P., Navarro, P., Garrido, F. & Ruiz-Cabello, F. Changes in activatory and inhibitory natural killer (NK) receptors may induce progression to multiple myeloma: implications for tumor evasion of T and NK cells. *Hum Immunol*. 2009; 70(10):854-857.

394. Perez-Andres, M., Almeida, J., Martin-Ayuso, M., Moro, M. J., Martin-Nunez, G., Galende, J., Borrego, D., Rodriguez, M. J., Ortega, F., Hernandez, J., Moreno, I., Dominguez, M., Mateo, G., San Miguel, J. F. & Orfao, A. Clonal plasma cells from monoclonal gammopathy of undetermined significance, multiple myeloma and plasma cell leukemia show different expression profiles of molecules involved in the interaction with the immunological bone marrow microenvironment. *Leukemia*. 2005; 19(3):449-455.

395. Rosenzweig, M., Connole, M., Glickman, R., Yue, S. P., Noren, B., DeMaria, M. & Johnson, R. P. Induction of cytotoxic T lymphocyte and antibody responses to enhanced green fluorescent protein following transplantation of transduced CD34(+) hematopoietic cells. *Blood*. 2001; 97(7):1951-1959.

396. Castano, A. P., Liu, Q. & Hamblin, M. R. A green fluorescent protein-expressing murine tumour but not its wild-type counterpart is cured by photodynamic therapy. *Br J Cancer*. 2006; 94(3):391-397.

397. Baklaushev, V. P., Kilpelainen, A., Petkov, S., Abakumov, M. A., Grinenko, N. F., Yusubalieva, G. M., Latanova, A. A., Gubskiy, I. L., Zabozlaev, F. G., Starodubova, E. S., Abakumova, T. O., Isaguliants, M. G. & Chekhonin, V. P. Luciferase Expression Allows Bioluminescence Imaging But Imposes Limitations on the Orthotopic Mouse (4T1) Model of Breast Cancer. *Sci Rep*. 2017; 7(1):7715.

398. Neri, P., Ren, L., Azab, A. K., Brentnall, M., Gratton, K., Klimowicz, A. C., Lin, C., Duggan, P., Tassone, P., Mansoor, A., Stewart, D. A., Boise, L. H., Ghobrial, I. M. & Bahlis, N. J. Integrin beta7-mediated regulation of multiple myeloma cell adhesion, migration, and invasion. *Blood*. 2011; 117(23):6202-6213.

399. Aoyama, N., Miyoshi, H., Miyachi, H., Sonoshita, M., Okabe, M. & Taketo, M. M. Transgenic mice that accept Luciferase- or GFP-expressing syngeneic tumor cells at high efficiencies. *Genes Cells*. 2018; 23(7):580-589.

400. Stripecke, R., Carmen Villacres, M., Skelton, D., Satake, N., Halene, S. & Kohn, D. Immune response to green fluorescent protein: implications for gene therapy. *Gene Ther*. 1999; 6(7):1305-1312.

401. Gambotto, A., Dworacki, G., Cicinnati, V., Kenniston, T., Steitz, J., Tuting, T., Robbins, P. D. & DeLeo, A. B. Immunogenicity of enhanced green fluorescent protein (EGFP) in BALB/c mice: identification of an H2-Kd-restricted CTL epitope. *Gene Ther*. 2000; 7(23):2036-2040.

402. Steinbauer, M., Guba, M., Cernaianu, G., Kohl, G., Cetto, M., Kunz-Schughart, L. A., Geissler, E. K., Falk, W. & Jauch, K. W. GFP-transfected tumor cells are useful in examining early metastasis in vivo, but immune reaction precludes long-term tumor development studies in immunocompetent mice. *Clin Exp Metastasis*. 2003; 20(2):135-141.

403. Limberis, M. P., Bell, C. L. & Wilson, J. M. Identification of the murine firefly luciferase-specific CD8 T-cell epitopes. *Gene Ther*. 2009; 16(3):441-447.

404. Han, W. G., Unger, W. W. & Wauben, M. H. Identification of the immunodominant CTL epitope of EGFP in C57BL/6 mice. *Gene Ther*. 2008; 15(9):700-701.

405. Skelton, D., Satake, N. & Kohn, D. B. The enhanced green fluorescent protein (eGFP) is minimally immunogenic in C57BL/6 mice. *Gene Ther*. 2001; 8(23):1813-1814.

406. Denaro, M., Oldmixon, B., Patience, C., Andersson, G. & Down, J. EGFP-transduced EL-4 cells from tumors in C57BL/6 mice. *Gene Ther*. 2001; 8(23):1814-1815.

407. Edinger, M., Cao, Y. A., Verneris, M. R., Bachmann, M. H., Contag, C. H. & Negrin, R. S. Revealing lymphoma growth and the efficacy of immune cell therapies using in vivo bioluminescence imaging. *Blood*. 2003; 101(2):640-648.

408. Shibata, M. A., Shibata, E., Morimoto, J., Eid, N. A., Tanaka, Y., Watanabe, M. & Otsuki, Y. An immunocompetent murine model of metastatic mammary cancer accessible to bioluminescence imaging. *Anticancer Res*. 2009; 29(11):4389-4395.

409. Kim, J. B., Urban, K., Cochran, E., Lee, S., Ang, A., Rice, B., Bata, A., Campbell, K., Coffee, R., Gorodinsky, A., Lu, Z., Zhou, H., Kishimoto, T. K. & Lassota, P. Non-invasive detection of a small number of bioluminescent cancer cells in vivo. *PLoS One*. 2010; 5(2):e9364.

410. Tiffen, J. C., Bailey, C. G., Ng, C., Rasko, J. E. & Holst, J. Luciferase expression and bioluminescence does not affect tumor cell growth in vitro or in vivo. *Mol Cancer*. 2010; 9:299.

411. Oyajobi, B. O., Munoz, S., Kakonen, R., Williams, P. J., Gupta, A., Wideman, C. L., Story, B., Grubbs, B., Armstrong, A., Dougall, W. C., Garrett, I. R. & Mundy, G. R. Detection of myeloma in skeleton of mice by whole-body optical fluorescence imaging. *Mol Cancer Ther*. 2007; 6(6):1701-1708.

412. Mori, Y., Shimizu, N., Dallas, M., Niewolna, M., Story, B., Williams, P. J., Mundy, G. R. & Yoneda, T. Anti-alpha4 integrin antibody suppresses the development of multiple myeloma and associated osteoclastic osteolysis. *Blood*. 2004; 104(7):2149-2154.